ICDIM 2016 - FINAL PROGRAM

Monday, July 11	
9:00 – 9:30	OPENING
9:30 – 10:30	**INVITED SPEAKER** C. Thiel
10:30 – 11:00	**COFFEE BREAK**
11:00 – 12:30	C. Stanek G. Watson R. Ledwaba R. Jackson P. Garcia-Fernandez G. Roma
12:30 – 14:00	**LUNCH BREAK**
14:00 – 15:00	**INVITED SPEAKER** H. Vrielinck
15:00 – 15:45	F.A. Selim K. Krambrock A. Sarkar
15:45 – 16:15	**COFFEE BREAK**
16:15 – 17:45	F. Freytag K. Lengyel K. Veenhuizen A. Suchocki S. Arceiz Casas R. Evarestov
18:00 – 20:30	**COCKTAIL**

Tuesday, July 12	
9:00 – 10:00	**INVITED SPEAKER** M. Moreno
10:00 – 10:30	P. Smet F. Moretti
10:30 – 11:00	**COFFEE BREAK**
11:00 – 12:30	M. Nikl S. Gridin Z. Lucenicova W. Drozdowski A. Gektin S. Nagorny
12:30 – 14:00	**LUNCH BREAK**
14:00 – 15:00	**INVITED SPEAKER** D. Scanlon
15:00 – 15:30	A. Lucid P. Plantevin
15:30 – 16:00	**COFFEE BREAK**
16:00 – 17:00	S. Messerschmidt C. Wickleder J. Joos R. Abashev
17:00 – 17:30	Flash talks for posters
17:30 – 20:00	**POSTER SESSION I** & TROPICAL PARTY

Wednesday, July 13	
9:00 – 10:00	**INVITED SPEAKER** F. Messina
10:00 – 10:30	S. Feofilov M. Peng
10:30 – 11:00	**COFFEE BREAK**
11:00 – 12:15	V.S. Nistor M. Stefan M. Alemany A. Vedda I. Kamenskikh
12:15 – 14:30	**LUNCH BREAK**
14:30 – 18:00	**TOUR IN LYON**
FROM 20:00	DINNER

Thursday, July 14	
9:00 – 10:30	E. Savchenko M. Bazzan E. Friedland V.S. Teodorescu I. Reghioua S. Watanabe
10:30 – 11:00	**COFFEE BREAK**
11:00 – 12:30	A. Vasil'ev M.E. Valerio S. Sanna M. Grinberg A. Sontakke T. Lesniewski
12:30 – 14:00	**LUNCH BREAK**
14:00 – 15:00	**INVITED SPEAKER** D. Carpentier
15:00 – 15:30	N. Yokota R.M. Montereali
15:30 – 16:00	**COFFEE BREAK**
16:00 – 17:00	Y. Zorenko A. Chadwick G. Dosovitskiy A. Maraloiu
17:00– 17:30	Flash talks for posters
17:30 – 20:00	**POSTER SESSION II** & BEER PARTY
AT NIGHT	FIREWORKS !

Friday, July 15	
9:00 – 10:30	A. Lushchik M.-F. Barthe L. Vittadello A. Alessi A. Belsky B. Padlyak
10:30 – 11:00	**COFFEE BREAK**
11:00 – 11:30	O. Dicks L. Kovacs
11:30 – 12:30	**INVITED SPEAKER** P. Heitjans
12:30 – 13:00	**CLOSING**

DETAILED PROGRAM

SUNDAY, July 10

17:00 – 21:00	**Registration**	**Hôtel Résidence Odalys Bioparc** **64 avenue Rockefeller** **69008 Lyon**
18:00 – 21:00	**Welcome Party**	**Hôtel Résidence Odalys Bioparc** **64 avenue Rockefeller** **69008 Lyon**

MONDAY, July 11

8:00 – 18:00		**Registration**	**J.F. CIER building** **8 Avenue Rockefeller** **69008 Lyon**
9:00 – 9:30		**OPENING TALK**	
9:30 – 10:30		**INVITED SPEAKER**	
		Chairman : C. Pedrini	
	Mo-I-1	C. Thiel	Design and characterization of materials for rare-earth quantum memories
10:30 – 11:00		**COFFEE BREAK**	
11:00 – 12:30		**Defects modeling & computational methods**	
		Chairman : R. Evarestov	
	Mo-O-1	C. Stanek	Molecular dynamics simulation of thermal transport in UO_2 with intrinsic defects and fission products
	Mo-O-2	G. Watson	Controlling the localisation of electronic defects using DFT+U with occupation matrix control
	Mo-O-3	R. Ledwaba	Visualization of evolving microstructures in mesoporous and bulk $LiMn_2O_4$ Using amorphization and recrystallization technique
	Mo-O-4	R. Jackson	Computer modeling of double doped $SrAl_2O_4$ for phosphor applications
	Mo-O-5	P. Garcia-Fernandez	Evidence of a Jahn-Teller impurity in a cubic lattice displaying a compressed geometry
	Mo-O-6	G. Roma	First order Raman intensities associated to point defects in silicon carbide from first principles

12:30 – 14:00		**LUNCH BREAK**	
14:00 – 15:00		**INVITED SPEAKER**	
		Chairman : R. Jackson	
	Mo-I-2	H. Vrielinck	Structural properties and transformations of metal-organic frameworks studied using paramagnetic probes
15:00 – 15:45		**Point & extended defects in bulk wide band-gap systems**	
		Chairman : R. Jackson	
	Mo-O-7	F. A. Selim	Hydrogen in insulating oxide $Y_3Al_5O_{12}$ strongly narrows the band gap
	Mo-O-8	K. Krambrock	Identification of Rhenium donor in layered MoS_2 samples
	Mo-O-9	A. Sarkar	Positron annihilation spectroscopic characterization of defects in wide band gap oxide semiconductors
15:45 – 16:15		**COFFEE BREAK**	
16:15 – 17:45		**Point & extended defects in bulk wide band-gap systems**	
		Chairman : C. Stanek	
	Mo-O-10	F. Freytag	Atomic insight to small, strong-coupling hole polarons in lithium niobate by local probing of OH- bonds
	Mo-O-11	K. Lengyel	Incorporation of rare earth ions in $Li_6Y(BO_3)_3$ single crystals
	Mo-O-12	K. Veenhuizen	Dependence of stoichiometry of lithium niobate nanocrystals on different initial lithium to niobium ratios in the synthesis step
	Mo-O-13	A. Suchocki	Spectroscopic properties of $Y_4Al_2O_9$:Ce crystals
	Mo-O-14	S. Arceiz Casas	EPR and DFT investigation of Fe and Fe-Ti doping in $LiNbO_3$
	Mo-O-15	R. Evarestov	Ab initio simulations of interstitial oxygen in corundum
17:45 – 18:00			
18:00 – 20:30		**COCKTAIL**	

TUESDAY, JULY 12

9:00 – 10:00		**INVITED SPEAKER**	

		Chairman : A. Vasil'ev	
	Tu-I-3	M. Moreno	Off-Centre and Jahn-Teller Instabilities in Doped Insulators
10:00 – 10h30		**Scintillation, energy transfer & storage, carrier trapping phenomena**	
		Chairman : A. Vasil'ev	
	Tu-O-1	P. Smet	Optically stimulated detrapping limiting the storage capacity of persistent phosphors
	Tu-O-2	F. Moretti	Consequences of Ca co-doping in $YAlO_3$:Ce scintillating crystals
10:30 – 11:00		**COFFEE BREAK**	
11:00 – 12:30		**Scintillation, energy transfer & storage, carrier trapping phenomena**	
		Chairman : P. Smet	
	Tu-O-3	M. Nikl	Optimization of wide band-gap scintillators using variable charge state of fast emitting rare earth dopants
	Tu-O-4	S. Gridin	$LaBr_3$ with Ce and Sr dopants: picosecond absorption spectroscopy and progress on track modeling
	Tu-O-5	Z. Lucenicova	Delayed recombination in Ce^{3+} doped LuAG:Gd,Ga multicomponent garnet scintillators
	Tu-O-6	W. Drozdowski	A deeper insight into LuYAG:Pr scintillator crystals
	Tu-O-7	A. Gektin	Point defect role in Ca co-doped scintillator NaI:Tl
	Tu-O-8	S. Nagorny	The Quenching Factor for alpha particles in ZnSe scintillating bolometers
12:30 – 14:00		**LUNCH BREAK**	
14:00 – 15:00		**INVITED SPEAKER**	
		Chairman : A. Lushchik	
	Tu-I-4	D. Scanlon	Defect chemistry of emerging materials for photovoltaics
15:00 – 15:30		**Phenomena at surfaces & interfaces**	
		Chairman : A. Lushchik	
	Tu-O-9	A. Lucid	Molecular dynamics study of samarium and gadolinium doped ceria and their interfaces for solid-oxide fuel-cell applications
	Tu-O-10	P. Plantevin	Improved interface passivation in heterojunction solar cells with ion irradiation

15:30 – 16:00		**COFFEE BREAK**	
16:00 – 17:00		**Luminescence of excitons, impurities & defects**	
		Chairman : M. Moreno	
	Tu-O-11	S. Messerschmidt	(Ultra-)fast dynamics of self-trapped excitons in Mg-doped lithium niobate
	Tu-O-12	C. Wickleder	Photoluminescence of self-trapped excitons and colour centres in Eu^{2+}-activated $CsMgX_3$ (X = Cl, Br, I)
	Tu-O-13	J. Joos	Luminescence of Mn in CaZnOS: from energy levels to applications
	Tu-O-14	R. Abashev	Thermoluminescence of anion-deficient corundum and its connection with Ti impurity
17:00 – 17:30		**FLASH TALKS FOR POSTERS**	
17:30 – 20:00		**POSTER SESSION I** (& TROPICAL PARTY)	

WEDNESDAY, JULY 13

9:00 – 10:00		**INVITED SPEAKER**	
		Chairman : S. Nistor	
	We-I-5	F. Messina	Optical spectroscopy and light-induced generation of point defects in SiO_2-based materials
10:00 – 10h30		**Luminescence of excitons, impurities & defects**	
		Chairman : S. Nistor	
	We-O-1	S. Feofilov	Impurity ions spectra in garnets solid solutions: disorder, symmetry of centers and lattice deformation
	We-O-2	M. Peng	Superbroad NIR luminescence from bismuth doped crystals and glasses
10:30 – 11:00		**COFFEE BREAK**	
11:00 – 12:15		**Low dimensional & nano-morphological systems**	
		Chairman : S. Feofilov	
	We-O-3	V. S. Nistor	The main role of extended lattice defects in the localization and interaction of Mn^{2+} ions in cubic ZnS quantum dots

	We-O-4	M. Stefan	Collective magnetism from aggregated Mn^{2+} activating ions in self-assembled cZnS quantum dots at higher doping levels
	We-O-5	M. Alemany	Investigation of point defects in HfO_2 using Positron-Annihilation Spectroscopy: Internal Electric Fields impact
	We-O-6	A. Vedda	Hafnium dioxide luminescent nanoparticles: structure and emission control through doping and thermal treatments
	We-O-7	I. Kamenskikh	Energy transfer and carrier multiplication in silicon nanoparticles embedded in silicon dioxide
12:15 – 14:30		**LUNCH BREAK**	
14:30 – 18:00		**TOUR IN LYON**	
FROM 20:00		**DINNER**	At Bellona Boat

THURSDAY, JULY 14

9:00 – 10:30		**Radiation induced effects & material damage**	
		Chairman : V. Dierolf	
	Th-O-1	E. Savchenko	Radiation-induced defects, energy storage and release in nitrogen solids
	Th-O-2	M. Bazzan	Manipulation of high-energy particle beams by channelling and volume reflection in piezoelectric $LiNbO_3$
	Th-O-3	E. Friedland	Investigation of amorphisation energies of silicon carbide implanted with heavy ions
	Th-O-4	V. S. Teodorescu	Nanoscale segregation of Ge nanoparticles in GeSiO and GeTiO amorphous films by RTA and UV laser pulse annealing
	Th-O-5	I. Reghioua	Study of point defects in as-drawn and irradiated Ge-doped optical fibers using cathodoluminescence
	Th-O-6	S. Watanabe	Optical absorption and properties of emerald
10:30 – 11:00		**COFFEE BREAK**	
11:00 – 12:30		**Luminescence of excitons, impurities & defects**	
		Chairman : M. Nikl	
	Th-O-7	A. Vasil'ev	Excitation mechanisms in activated CsI scintillators:

			comparison of Tl^{+} and In^{+} dopants
	Th-O-8	M. E. Valerio	Luminescence in doped and undoped $CaYAl_3O_7$ produced via the Pechini Method
	Th-O-9	S. Sanna	Structural, electronic and optical properties of intrinsic and extrinsic defects in LiNbO3
	Th-O-10	M. Grinberg	Location of the Tb^{3+} and Eu^{3+}energy levels in Y_2O_2S under high hydrostatic pressure
	Th-O-11	A. Sontakke	Novel defects' luminescence based g-YAB phosphors for high CRI white light generation
	Th-O-12	T. Lesniewski	Optical properties of $K_2(Si,Ge)F_6:Mn^{4+}$ at ambient conditions and high pressure
12:30 – 14:00		**LUNCH BREAK**	
14:00 – 15:00		**INVITED SPEAKER**	
		Chairman : P. Heitjans	
	Th-I-6	D. Carpentier	Topological properties of insulators and semi-metals
15:00 – 15h30		**Application-minded materials & interdisciplinarity**	
		Chairman : P. Heitjans	
	Th-O-13	N. Yokota	In situ XAS study during cycling of Li_2FeSiO_4Li ion battery material
	Th-O-14	R. M. Montereali	Lithium fluoride thin film detectors for low-energy proton beam mapping by photoluminescence of colour centres
15:30 – 16:00		**COFFEE BREAK**	
16:00 – 17:00		**Application-minded materials & interdisciplinarity**	
		Chairman : G. Ledoux	
	Th-O-15	Y. Zorenko	Scintillators based on the Ce^{3+} doped single crystalline films of multicomponent garnets: new trends and new challenges
	Th-O-16	A. Chadwick	An X-Ray Absorption Study of Ball-Milled Lithium Titanate and Tantalate
	Th-O-17	G. Dosovitskiy	Persistent luminescence in powdered and ceramic polycrystalline $Gd_3Al_2Ga_3O_{12}$:Ce
	Th-O-18	A. Maraloiu	Using Two Photon Laser Scanning Microscopy to reveal the fate of USPIO nanoparticles in an atherotic murine model

17:00 – 17:30	**FLASH TALKS FOR POSTERS**	
17:30 – 20:00	**POSTER SESSION II** (& BEER PARTY)	
AT NIGHT	**FIREWORKS**	Fired from Notre-Dame-de Fourvière

FRIDAY, JULY 15

9:00 – 10:30		**Radiation induced effects & material damage**	
		Chairman : A. Vedda	
	Fr-O-1	A. Lushchik	Peculiarities of radiation damage caused by light and heavy ions in wide gap materials
	Fr-O-2	M.-F. Barthe	Identification of vacancy defects in UO_2 using Positron Annihilation Spectroscopy: a theoretical and experimental comparison
	Fr-O-3	L. Vittadello	Photorefractive direct laser writing
	Fr-O-4	A. Alessi	Irradiation temperature effects on the induced point defects in Ge-doped optical fibers.
	Fr-O-5	A. Belsky	Creation of transient defects in ionic crystals in regions with high excitation density
	Fr-O-6	B. Padlyak	Paramagnetic centers in the irradiated borate glasses
10:30 – 11:00		**COFFEE BREAK**	
11:00 – 11:30		**Point & extended defects in bulk wide band-gap systems**	
		Chairman : A. Chadwick	
	Fr-O-7	O. Dicks	Electron and hole traps in a-Al_2O_3
	Fr-O-8	L. Kovacs	OH– defects in rare earth ion doped stoichiometric $LiNbO_3$
11:30 – 12:30		**INVITED SPEAKER**	
		Chairman : A. Chadwick	
	Fr-I-7	P. Heitjans	Mobile Li^+ and F^- Ions in Insulating Materials
12:30 – 13:00		**CLOSING TALK**	

POSTER SESSION I, Tuesday, July 12

Flash talks for posters : #

Tu-P-1	R. Montereali	Subsurface Radiation Induced Defects in Lithium Fluoride Nanocrystals	
Tu-P-2	M. Pfiffer	Characterization of the polishing induced contamination of fused silica optics	#1
Tu-P-3	A. Aramburu	Key role of internal electric fields in the properties of ionic materials containing transition-metal complexes	
Tu-P-4	J. García Lastra	Polaronic motion of self-trapped holes in silver halides	#2
Tu-P-5	A. Gavin	Defect modelling in $LaMnO_3$ for intermediate temperature solid oxide fuel cell cathodes	#3
Tu-P-6	R. Jackson	The study of defects in $CaYAl_3O_7$ through a static computer modelling approach	
Tu-P-7	M. Kaviani Baghbadorani	Intrinsic electron trapping in amorphous hafnium oxide	
Tu-P-8	M. Kaviani Baghbadorani	Hydrogen-induced defects in amorphous hafnium oxide	
Tu-P-9	K. Lengyel	Defect structures of ODR dopants in $LiNbO_3$ crystals	
Tu-P-10	A. Lucid	A polarisable force field for doped lanthanum gallate derived from first principles	
Tu-P-11	M. Valerio	EXAFS simulations in Zn-doped $LiNbO_3$ based on defect calculations	
Tu-P-12	G. Watson	The effect of trivalent cation doping on the structure and reducibility of ceria.	
Tu-P-13	A. Akilbekov	AFM and TEM study of hillock-like defects induced by swift heavy ions on Al_2O_3 surface	
Tu-P-14	A. Akilbekov	Luminescence of $ZnWO_4$ crystals with injected oxygen	
Tu-P-15	J. Botsoa	Study of the formation of vacancy defects into 6H-SiC by Positron Annihilation Spectroscopy and Photoluminescence	
Tu-P-16	N. Cano-Mamani	Optical absorption (AO) and thermoluminescence properties of green tourmaline	
Tu-P-17	A. Joita	Paramagnetic defects produced by high radiation doses in silicon detector material	#4
Tu-P-18	K. Krambrock	Radiation-induced green color in natural wet quartz and its relation with the non-bridging oxygen hole center	#5
Tu-P-19	B. Marczewska	Visualisation of Bragg peak of proton beams in LiF crystals	
Tu-P-20	B. Marczewska	Influence of thermal treatment and bleaching on PL of LiF crystals with radiation induced color centers	
Tu-P-21	S. Santos	Radiation effects on microstructure and EPR signal of yttrium oxide rods	
Tu-P-22	S. Shandarov	Changes in optical absorption induced by sequential exposition to short- and long-wavelength radiation in the BTO:Al crystal	
Tu-P-23	S. Watanabe	Optical absorption, electronic paramagnetic resonance and luminescence spectroscopic for characterization of monticellite	
Tu-P-24	S. Watanabe	TL, EPR and Optical Absorption Properties of Yellow Beryl	
Tu-P-25	S. Gridin	Sensitivity study of transport, rate, and energy deposition parameters in a model of scintillation tracks	

Tu-P-26	K. Hovhannesyan	Optical and radioluminescence studies of LuAG:Ce(Pr) with divalent co-dopants	
Tu-P-27	M. Kucera	Improved scintillation properties of co-doped GAGG:Ce,Mg epitaxial garnet films	#6
Tu-P-28	S. Kurosawa	Bandgap Structure and Temperature Dependence of Rare-Earth-Doped La-GPS Scintillator	
Tu-P-29	I. Romet	Recombination luminescence of copper and silver doped $Li_2B_4O_7$ single crystals	
Tu-P-30	N. Shiran	Energy transfer and scintillation properties of $Y_3(Ga_xAl_{1-x})_5O_{12}$: Ce ceramics	
Tu-P-31	A. Vasilyev	Non-uniformity of excitation distribution in the track for modelling scintillation non-proportionality and decay	
Tu-P-32	G. Ren	Research on the Coloration Problems of CsI(Tl) Crystals	
Tu-P-33	E. Coillet	Structural characterization of thin amorphous oxide layers for Gravitational Wave detection	#7
Tu-P-34	M. Naito	Local structure and thermally induced structural evolution in amorphous Nb-Si thin layers	
Tu-P-35	J. Strand	Hole Trapping in Amorphous HfO_2	
Tu-P-36	O. Toma	Excited-state absorption in erbium-doped ceramic langatate	
Tu-P-37	O. Toma	Excited-state absorption in Er-doped partially disordered calcium lithium niobium gallium garnet	
Tu-P-38	L. Vittadello	Diffraction from Fibonacci gratings fabricated in photorefractive Fe:$LiNbO_3$	
Tu-P-39	A. Bensalah-Ledoux	$ZnAL_2O_4$ powders and films for Ultra-Violet emission	
Tu-P-40	G. Dosovitskiy	$Gd_3Al_2Ga_3O_{12}$:Ce stoichiometry deviation influence on the crystal scintillation properties	
Tu-P-41	L. Li	Red Emission from Pr^{3+} in $K_{1-x}Na_xNbO_3$(0?x?1) for Persistent Luminescence	
Tu-P-42	E. Mihokova	Surface functionalized Zn(Cd)O:Ga-nanoparticles for X-ray induced photodynamic therapy	#8
Tu-P-43	V. Mykhaylyk	Remote micro-thermometry using scintillation sensors	#9
Tu-P-44	A. Ruotolo	Giant negative magnetoresistance in oxygen-deficient Mn-substituted ZnO	
Tu-P-45	Y. Zorenko	Synthesis and luminescence properties of Ce^{3+} and Eu^{2+} doped silicate garnet phosphors for white LED convertors	#10
Tu-P-46	S. Messerschmidt	Carrier self-trapping in iron-doped lithium niobate	
Tu-P-47	G. Laurens	Mechanical stress in nano-size particles	#11
Tu-P-48	S. Biderman	Study of the effect of optical bleaching at selected photon energies on the OA and TL of LiF:Mg,Ti (TLD-100).	
Tu-P-49	K. Kamada	Mg co-doping effects on Ce doped $Y_3(Ga,Al)_5O_{12}$ scintillator	
Tu-P-50	V. Khanin	Influence of Yb-related traps on afterglow properties of garnet scintillators	
Tu-P-51	A. Luchechko	Optical bleaching in YAP single crystals doped with manganese ions (poster presentation)	
Tu-P-52	I. Reghioua	Evolution of GLPC defects in O_2-loaded germanosilicate optical fibers: in-situ cathodo-luminescence study	

Tu-P-53	D. Daurenbekov	Modeling of Defect Formation Processes in Na_2SO_4 Crystal	
Tu-P-54	C. Masedi	Beyond Lithium-Ion Batteries: A Computational Study on Advanced Lithium – Sulphur Battery.	#12
Tu-P-55	M. Matshaba	Amorphisation and Recrystallisation Study of Lithium Intercalation into TiO_2 Nano-Architectures	#13
Tu-P-56	C. Sifi	Ab-initio study of structural properties of Lead Barium sulfide alloys.	

POSTER SESSION II, Thursday, July 14

Flash talks for posters : #

Th-P-1	R. Abashev	On real structure of the profiled anion-deficient corundum	
Th-P-2	H. Asatryan	ESR of 151Eu^{2+} rhombic centers in $Y_3Al_5O_{12}$	
Th-P-3	H. Asatryan	ODMR in gadolinium-containing garnet crystals via Ce^{3+} photoluminescence	
Th-P-4	M. Bazzan	Direct measurement of the Fe-polaron deformation in Fe:$LiNbO_3$	#1
Th-P-5	P. Booker	Ultrafast, mid-infrared spectroscopy of small, strong-coupling polarons and free-carriers in lithium niobate	
Th-P-6	M. Buryi	EPR study of stable Eu^{2+} ions and X-ray induced charge traps creation in ceramic $Lu(Y)_3Al_5O_{12}$:Eu,Mg	
Th-P-7	O. Dicks	Spectroscopic properties of oxygen vacancies in $LaAlO_3$	
Th-P-8	A. Gavin	Investigation of $LaCrO_3$ for development of a p-type transparent conducting oxide	#2
Th-P-9	N. Kozlova	Point defects and phenomenon of dichroism in the lanthanum-gallium silicate group crystals	
Th-P-10	C. Laplante	Defect evolution in irradiated optical fibers	
Th-P-11	M. Oda	First-principles calculation of electronic structures and phonon modes at a Ga vacancy in GaN	#3
Th-P-12	A. Sontakke	Localized point defects in amorphous hosts and its influence on quantum yield of Ln^{3+} luminescence	
Th-P-13	M. Alemany	Characterization of point defects in oxygen sub- and over-stoichiometric HfO_2 by Electron-Energy Loss Spectroscopy	
Th-P-14	L. Nistor	Structure and localization of aggregated Mn^{2+} ions as a separate phase in the mesoporous assembly of cZnS:Mn QDs	
Th-P-15	A. Belsky	Luminescence of ZnO crystal and nanoparticles excited by femtosecond IR, UV and VUV laser pulses	
Th-P-16	D. Avram	Role of defects in shaping the emission of Ln doped CeO_2	
Th-P-17	A. Baran	High pressure and time resolved luminescence spectra of $Ba_2K(PO_3)_5$ doped with Eu^{2+} and Eu^{3+}	
Th-P-18	N. Cano-Mamani	Thermoluminescence and Electron Paramagnetic Resonance of Marambaia Topaz	
Th-P-19	I. Carrasco Ruiz	Tunable emission from silico-carnotite type double silicates doped with Tb^{3+} and Eu^{3+}	#4
Th-P-20	G. Corradi	EPR spectroscopy of Er^{3+} in lithium yttrium borate (LYB) single crystals	
Th-P-21	S. Firstov	IR luminescent centers in gamma-irradiated Bi-doped KCl and SrF_2 crystals	
Th-P-22	B. Gimenez Fernandes	Thermoluminescence (TL) Properties of glass from natural diopside and of Synthetic Diopside Glass	
Th-P-23	B. Gimenez Fernandes	Optical absorption and electron paramagnetic resonance of natural and sinthetic diopside glass	
Th-P-24	N. Gorecka	Luminescent properties of $Ca_9Y(PO_4)_7$ doped with Eu^{3+} and Eu^{2+}	
Th-P-25	L. Ivleva	1.5µm Luminescence of colored BGO crystals	

Th-P-26	J. Joos	Connecting crystal structure and luminescence, the case of $SrAl_2O_4:Eu^{2+}$	
Th-P-27	S. Kato	Dynamics of polarons in $LiNbO_3$-type crystals under continuous-wave laser irradiation	
Th-P-28	O. Lalinsky	Effect of Mg-doping on cathodoluminescence properties of GAGG:Ce single crystalline films	
Th-P-29	S. Mahlik	Optical processes in $YVO_4:Eu^{3+}$ across zircon-to-scheelite phase transition	
Th-P-30	Z. Potucek	Optical absorption and charge transfer processes in vanadium doped $SrTiO_3$ crystals	
Th-P-31	N. Soschin	Point defects in rare earth phosphors of garnet structure	
Th-P-32	J. Ueda	Analysis of carrier trap center in $SrAl_2O_4$-based persistent phosphors by spectroscopy and EPR	
Th-P-33	Y. Zhydachevskii	Optical properties of Ce^{3+}-Yb^{3+} and Bi^{3+}-Yb^{3+} doped YAG down-converting epitaxial layers	
Th-P-34	Y. Zorenko	Comparison of the luminescent properties LuAG:Pr and YAG:Pr crystals, films and nanopowders using synchrotron radiation	#5
Th-P-35	A. Bitam	Analysis of absorption and emission spectra at room temperature of rare earth ions doped in fluoride crystals	
Th-P-36	B. Berzina	Blue luminescence caused by native defect in hBN and AlN	#6
Th-P-37	D. Daurenbekov	Formation of Radiation Defects in Sulfates of Alkali Metals by Low-Energy Electron Excitations	
Th-P-38	J. Jaramillo Gomez	Comparative study of defect related emission in ZnO, ZnO-Cu and ZnO-Al nanocrystals obtained by etching method	
Th-P-39	J. Jaramillo Gomez	Emission Dependent on Stoichiometry of Si-rich-SiNX Films obtained by PECVD	
Th-P-40	I. Kindrat	Intrinsic luminescence of the un-doped borate glasses	
Th-P-41	A. Luchechko	Luminescence properties of $Mg_{1-x}Zn_xGa_2O_4$ solid solution co-doped with Mn^{2+} and Eu^{3+} ions	
Th-P-42	N. Martynyuk	Photoluminescent properties of Mn^{2+} ions in YAP single crystals	
Th-P-43	N. Martynyuk	Temperature and spatial changes of diffusion coloration of $LiNbO_3$ single crystals under redox treatment	
Th-P-44	S. Vasyukov	The Europium diiodide investigation	
Th-P-45	J. Zhong	The Effects of Oxygen Vancancies on Luminescence Properties of $Na_3LuSi_3O_9:Ce^{3+}$	
Th-P-46	F. Ali Sahraoui	Pressure effect on the structural and electronic properties of $BN_{1-x}As_x$	
Th-P-47	A. Maraloiu	Localisation and distribution of the Mn^{2+} dopant ions in nanostructured ZnO films	
Th-P-48	R. Montereali	Subsurface Radiation Induced Defects in Lithium Fluoride Nanocrystals	
Th-P-49	R. Jackson	The study of defects in $CaYAl_3O_7$ through a static computer modelling approach	#7
Th-P-50	M. Valerio	EXAFS simulations in Zn-doped $LiNbO_3$ based on defect calculations	#8
Th-P-51	G. Watson	The effect of trivalent cation doping on the structure and reducibility of ceria.	

Design and characterization of materials for rare-earth quantum memories

C.W. Thiel,[1] R.M. Macfarlane,[1] T. Böttger,[2] R.L. Ahlefeldt,[1] P.J.T. Woodburn,[1] A. Marsh,[1] and R.L. Cone[1]

[1] *Montana State University, Bozeman, MT, USA*
[2] *University of San Francisco, San Francisco, California, USA*

Realization of practical solid-state quantum memories critically depends on identifying materials that offer a demanding combination of physical properties along with massively parallel channel scalability to provide required data rates, for example in secure communication networks. Already, experimental demonstrations and theoretical analysis by groups across the world have shown that rare-earth ions doped into dielectric crystals are one of the most promising candidates to meet all of the requirements for multimode optical quantum information storage protocols.

The phenomenon of spectral hole burning (SHB) of inhomogeneously broadened optical absorption lines in these materials enables spectrally distinct ensembles of ions within the high density environment to be individually manipulated and interrogated, leading to the potential for 100,000 or more multiplexed frequency channels within a single absorption line. To realize these advances, we must continue to improve fundamental understanding and practical control of the physical processes that govern ion-ion, ion-spin, and ion-lattice interactions. At the same time, new knowledge is crucially needed regarding the detailed role of material chemistry and fabrication processes in determining, and sometimes limiting, the properties and consistency of existing materials.

With these motivations, we review the unique properties of rare-earth-doped crystals designed and characterized for solid-state quantum memories and outline active areas of materials research aimed at understanding and optimizing these properties. In particular, we highlight the engineering of lattice defects to manipulate both static and dynamic disorder and the resulting effects on optical coherence, spectral multiplexing capacity, spin-state lifetimes, and other key parameters. Ongoing efforts also focus on a better understanding of the nature and consequences of defects introduced during the growth and sample fabrication processes. Finally, these concepts are applied to specific rare-earth-doped material systems and illustrated by our recent results on quantum memory materials with enhanced properties. The material development and new insights gained into the manipulation of structural and chemical defects for the highest quality crystalline materials that are required for quantum information applications may also be applied to understand and improve materials for traditional luminescence applications such as laser materials, phosphors, and scintillators.

Structural properties and transformations of metal-organic frameworks studied using paramagnetic probes

H. Vrielinck

Ghent University, Department of Solid State Sciences, Electron Magnetic Resonance research group, Krijgslaan 281-S1, B-9000 Gent, Belgium

Metal-organic frameworks (MOFs) are crystalline porous solids, built up from inorganic metal complexes and organic linkers. Since the first reports on such hybrid porous solids in the late 1980's, a wide range of metal and linker combinations was shown to yield stable MOFs. By selection of the building blocks the dimensionality and size of the pores and the distance between the metal nodes can be tuned, tailoring the properties to specific functionality. Many MOFs exhibit a large internal surface, which makes them particularly interesting for heterogeneous catalysis, gas sensing, storage and separation [1]. Other applications of MOFs are based on their potential for drug delivery [2], their tuneable electric [3] and/or optical properties [4].

After a general introduction, this lecture will focus on two structurally related so-called one-dimensional MOFs with channel-like pores. In the first, MIL-47(V) (MIL= Matériaux de l'Institut Lavoisier), [V=O-V=O-…] chains are held together by benzene dicarboxylate linkers. The second, MIL-53(Al), has the same linkers and framework topology, but different metal-inorganic chains: [Al-OH-Al-OH-…]. In spite of these similarities, MIL-53(Al) is more stable in aqueous environments than MIL-47(V). In addition MIL-53(Al) features a remarkably higher framework flexibility: it may switch between an open and a closed pore state when changing temperature and pressure conditions, or upon exposure to certain gases. This property is generally referred to as "breathing". MIL-47(V), on the other hand, is a good catalyst but has a more rigid structure. By doping MIL-53(Al) with catalytically active V^{4+} ions, mixed-metal MOFs are created that may combine the favourable properties of both parent MOFs.

In an attempt to understand the origin of breathing and its consequences for applications, we studied the aforementioned mixed-metal MOFs with electron paramagnetic resonance (EPR). In this study the V^{4+} ions, which have one unpaired electron in the 3d shell, serve as paramagnetic probes. The V^{4+} EPR spectrum allows to determine the location of these ions and to monitor changes in their local environment, and its intensity reveals valence state transformations. The EPR results are correlated with those of X-ray diffraction, X-ray absorption spectroscopy, and infrared spectroscopy studies.

This work is the result of a collaboration between the Electron Magnetic Resonance research group and the Center for Ordered Materials, Organometallics and Catalysis of Ghent University, supported by the Research Foundation - Flanders (FWO).

[1] G. Férey, "Hybrid porous solids: past, present, future", Chem. Soc. Rev., **37**, 191 (2008).
[2] P. Horcajada et al. "Metal-Organic Frameworks in Biomedicine", Chem. Rev., **112**, 1232, (2012)
[3] M. Alvaro et al. "Semiconductor Behavior of a Metal-Organic Framework (MOF)", Chem. Eur. J., **13**, 5106 (2007)
[4] M. D. Allendorf et al. "Luminescent metal–organic frameworks", Chem. Soc. Rev., **38**, 1330 (2009)

Off-Centre and Jahn-Teller Instabilities in Doped Insulators

M. Moreno

Departamento CITIMAC, Universidad de Cantabria, Santander, Spain

This talk explores the origin of structural instabilities in doped insulators through the analysis of available spectroscopic data and results of first principle calculations.

The first part deals with the off-centre instability observed in cubic host lattices doped with Transition Metal (TM) impurities. EPR data and theoretical calculations carried out on the isomorphous CaF_2, SrF_2 and $SrCl_2$ lattices doped with TM cations show that only the monovalent Ni^+ moves off-centre along <100> directions in the three compounds while Ag^{2+} moves off-centre only in $SrCl_2$ and Cu^{2+} is also slightly off-centre in SrF_2. Aside from stressing that the off-centre distortion is *not driven* by the ion size these results also reveal that the Jahn-Teller effect does not occur necessarily under cubic symmetry as it is also in competition with an off-centre instability.

First principle calculations prove that the off-centre motion takes place when the associated force constant at the cubic site becomes negative, allowing impurity displacements up to 1.5 Å. It is shown that the deformation of the electronic density along the distortion coordinate (implying changes in the chemical bonding) induces a negative contribution, K_V, to the total force constant, K, of the ground state, which acts against the normal contribution, K_0, characteristic of rigid ions. As the normal contribution to K increases with the charge of the impurity this explains why the off-centre displacement is helped by the use of open shell monovalent cations and soft host lattices. This pattern is also followed by TM impurities in lattices with rock salt structure. So while Ag^{2+} is on-centre in KCl both Mn^+ and Ni^+ impurities move off-centre. In the same vein Ni^+, Cu^{2+} and Ni^{2+} move off-centre in SrO along <111> directions although Ag^{2+}, Cr^{3+} and Ti^{4+} are found to remain on-centre in the series of cubic oxides. Moreover it is also shown that a *single* Ti^{4+} ion is unable to move off-centre in $BaTiO_3$ as K=11.5eV/Å^2. By contrast a small but negative force constant, K=-0.7eV/ Å^2, is obtained when all Ti^{4+} ions are moved *simultaneously* thus supporting that the ferroelectricity in $BaTiO_3$ at ambient pressure has a cooperative origin.

The second part demonstrates the surprising absence of a Jahn-Teller effect in the *model* system K_2ZnF_4: Cu^{2+}. Although the octahedron surrounding Zn^{2+} in K_2ZnF_4 is practically perfect, there are huge differences with respect to optical and EPR data of the Jahn-Teller system $KZnF_3$: Cu^{2+}. It is shown that they obey to an internal electric field, displaying the tetragonal symmetry of the host lattice, which splits the ground state of the CuF_6^{4-} complex in K_2ZnF_4 by 0.35eV *even if* the complex is perfectly octahedral. This result implies that properties of a TM impurity cannot, in general, be understood considering only the complex formed with nearest anions as they also depend on the internal field, often ignored in the interpretation of spectroscopic data.

Defect Chemistry of Emerging Materials for Photovoltaics

D. O. Scanlon[1,2]

[1] University College London, Kathleen Lonsdale Materials Chemistry, Department of Chemistry, 20 Gordon Street, London WC1H 0AJ, UK.
[2] Diamond Light Source Ltd., Diamond House, Harwell Science and Innovation Campus, Didcot, Oxfordshire OX11 0DE, UK.

As the global demand for energy grows inexorably, photovoltaic (PV) solar energy production is becoming increasingly important. While the majority of the suggested renewable energy routes cannot possibly meet this increasing energy requirement, sunlight, with more than ≈89 PW of energy reaching the Earth's surface per day, can more than meet both current (≈15 TW) and future needs. In this presentation I will examine the defect chemistry of two important components in solar cells, namely transparent conducting oxides (TCOs) and the absorber layers. I will discuss the current issues facing TCO fabrication and outline our current strategies to improve the conductivity and mobility of TCOs. Finally I will discuss the ideal defect chemistry necessary for a high performance solar absorber.

Optical spectroscopy and light-induced generation of point defects in SiO_2-based materials

F. Messina

Dipartimento di Fisica e Chimic, Università degli Studi di Palermo, Italy

Amorphous silicon dioxide (a-SiO_2) has attracted for several decades the scientific interest of scholars working in solid-state physics, as a prototype system to investigate the properties of amorphous insulators. Besides, its extremely large electronic bandgap (9 eV), hence its large transparency to visible and UV light, combined with high chemical and radiation resistance, low cost and non-toxicity, are essential and still unparalleled in several applications. At the most fundamental level, the intrinsic optical properties of a-SiO_2 and related materials depend on the dynamics of excitons generated across the bandgap by the absorption of very short-wavelength UV light, or via multi-photon absorption of intense laser light. However, the presence of localized structural defects typically introduces midgap electronic levels responsible of a variety of phenomena, such as near-UV absorption and photoluminescence, charge dynamics in an otherwise insulating material, or entirely new nonlinear optical properties. Thus, defects may either limit the performance of the material or, in other cases, can be deliberately exploited to improve the properties of SiO_2, for example in optical applications such as optical fibers for telecommunications and sensing. Defects can be either introduced by doping the material with extrinsic chemical elements (e.g. Germanium, rare earths, ..), or can be generated by the very interaction of SiO_2 with laser light through a variety of photochemical processes. In recent times, the interest on SiO_2-based materials has undergone a rebirth due to the introduction of nanostructured forms of SiO_2, such as silica nanoparticles and mesoporous silicas. Indeed, these SiO_2-based nanomaterials are endowed with new properties inherently associated to their nanometric size/structure, opening a variety of new application routes, for instance in sensing and drug delivery. This talk aims to provide an itinerary though the research on SiO_2-related materials, from the fundamental understanding of traditional, bulk SiO_2 to the most recent undergoing research on nanostructured SiO_2-based materials. The focus will be especially on the use of optical spectroscopies and light-matter interactions as tools to unveil and exploit the photo-physics of this fascinating class of amorphous insulators, particularly in the presence of defects.

Topological properties of insulators and semi-metals

D. Carpentier

Univ Lyon, Ens de Lyon, Univ Claude Bernard, CNRS,Laboratoire de Physique, F-69342 Lyon, France

In this talk, I will introduce the notion of topological property characterizing a gapped electronic phase, a so-called topological insulator. This property is the consequence of an inverted order of energy bands in the presence of strong spin orbit. It manifests itself in the appearance of robust surface states which are a the origin of peculiar properties. I will discuss experimental realizations of these topological insulators, in particular in reduced dimensions geometries. More recently, similar topological tools have been used to characterize zero gap semi-conductors, with band crossing points. These phases are reminiscent of the electronic properties of graphene, but possess some unique transport properties.

Mobile Li^+ and F^- Ions in Insulating Materials

P. Heitjans

Leibniz Universität Hannover, Institute of Physical Chemistry and Electrochemistry, Callinst. 3a, 30167 Hannover, Germany

The study of ion motion and transport in solids has gained enormous impetus in recent years, in particular due to the worldwide efforts to make better Li-ion batteries. Besides diffusion of Li^+ as the lightest cation (apart from H^+), conduction via F^- as the lightest monovalent anion also receives increasing attention with respect to solid-state electrochemical devices. In fact, fluoride ion conductors in the solid state, first studied by Faraday in 1834, stood at the very beginning of the research field 'Solid State Ionics' (see [1] for an historic review). Li^+ and F^- movements via defects in various electronically insulating materials have early been studied by the present author and colleagues first by beta-radiation detected nuclear magnetic resonance (β-NMR) using the β-emitters ^{8}Li [2] and ^{20}F [3,4] produced in situ by capture of polarized thermal neutrons [5].

The focus of this talk is on our recent studies by solid-state NMR using stable nuclei, mainly ^{7}Li, ^{6}Li and ^{19}F, as well as by impedance spectroscopy. Materials classes covered are on the one hand defect and interface dominated Li ion conductors [6]. These comprise solid electrolytes and electrode materials for Li ion batteries as well as model substances for fundamentals studies. On the other hand stable and metastable fluoride ion conductors are treated. The latter comprise single phase and composite, binary and ternary alkali earth and transition metal fluorides, which often have been diminuted and/or synthesized by mechanical action in nanocrystalline form [7,8].

For both lithium and fluoride ion conductors it is shown that by structural defect and disorder engineering the mobility can be drastically enhanced.

[1] K. Funke, Sci. Technol. Adv. Mater **14**, 043502 (2013).
[2] P. Heitjans, Solid State Ionics **18/19**, 50 (1986).
[3] M. Grupp et. al., J. Phys. Colloques **37**, C7-538 (1976).
[4] W. Buttler et al., Z. Phys. B **45**, 273 (1982).
[5] *Diffusion in Condensed Matter – Methods, Materials, Models,* P. Heitjans, J. Kärger, Eds. (Springer, Berlin 2005).
[6] P. Heitjans, M. Wilkening, MRS Bull. **34**, 915 (2009).
[7] B. Ruprecht et al., Phys. Chem. Chem. Phys. **11**, 3071 (2009).
[8] A. Düvel et al., J. Phys. C **118** 7117 (2014).

Molecular dynamics simulation of thermal transport in UO_2 with intrinsic defects and fission products

C.R. Stanek[1], M.W.D. Cooper[1], D.A. Andersson[1], X.-Y. Liu[1],

[1]*Materials Science and Technology Division, Los Alamos National Laboratory, P.O. Box 1663, Los Alamos, NM 87545*

The importance of thermal transport in nuclear fuel, and in particular the complexity associated with its decrease during burn up, has motived a wide range of experimental and modeling studies. By better understanding the contribution due to individual defects present during service, it may possible to reduce the uncertainty of thermal transport variation. As such, we performed studies using molecular dynamics simulations of UO_2 thermal conductivity including a representative intrinsic defects and fission products. These calculations employed two sets of empirical potentials: a standard Buckingham type interatomic potential and a recently developed potential that combines the many-body embedded atom potential with Morse-Buckingham pair potentials. Potential parameters for U^{5+} and Zr^{4+} in UO_2 are developed here for the latter potential. The thermal conductivity obtained from molecular dynamics simulations does not consider the spin-phonon scattering mechanism known to be responsible for reduced UO_2 thermal conductivity (compared to similar diamagnetic oxides, e.g. ThO_2). In order to improve the accuracy of the thermal conductivity predictions, they are corrected for this missing mechanism by adding the corresponding relaxation time derived from existing experimental data. Very high defect scattering is predicted for Xe compared to that of La and Zr. Intrinsic uranium defects reduce the thermal conductivity more than oxygen defects. For each defect and fission product, scattering parameters are derived for application in both a Callaway model and the corresponding high-temperature model typically used in fuel performance codes. To validate the modeling results, comparison is made with experimental measurements on single crystal hyper-stoichiometric UO_{2+x} samples and literature values.

Controlling the localisation of electronic defects using DFT+*U* with occupation matrix control.

Graeme W. Watson[1], Jeremy P. Allen[1]

[1]*School of Chemistry and CRANN, Trinity College Dublin, Dublin 2, Ireland*

The correct modelling of localized electronic defects (electrons / holes) has been widely discussed in materials chemistry, particularly for defective systems. For modelling such systems, DFT+*U* has become a widely used approach, adding a correction that penalises electron delocalisation and hence overcoming the Self Interaction Error (SIE) of DFT. However, despite its numerous successes it has criticized for not finding the correct electronic ground states, particularly for *f*-element systems. [1]

This study details a comprehensive approach of occupation matrix control [2] which can be used to guide the electronic relaxation toward required configurations [ref]. We will illustrate the approach with examples of Ti d^1 and Ce f^1 containing systems, with both cubic and general *f*-orbitals included. For d-electron systems the occupation matrix control could be used to guide the electronic defects onto specific sites and into specific orbitals. However, once the constraint was removed the electron could revert to lower energy orbitals, although generally on the site intended. For anatase TiO_2, the method successfully predicts a "split vacancy" to be the lowest energy configuration for an oxygen vacancy rather than the more commonly claimed nearest neighbour structure, in agreement with previous studies. [3] For *f* electrons, once localised within a specific orbital the electronic structure was maintained when the occupation matrix control was removed, allowing different orbital and site occupations to be compared. From a practical viewpoint, this ease of accessing the different local minima highlights the importance of fully assessing *f*-electron localisations. Overall, this method represents a viable approach to the modelling of a range of different electron localisations at a range of different sites and hence accessing the true ground state for electronic defects.

[1] Dorado *et al*., *Phys. Rev. B*, **79**, 235125 (2009); *Phys. Rev. B*, **82**, 035114 (2010); *Phys. Rev. B*, **83**, 035126 (2011).
[2] J.P. Allen and G. W. Watson, *Physical Chemistry Chemical Physics*, **16,** 21016 (2014)
[2] B. J. Morgan and G. W. Watson, *J. Phys. Chem. C*, **114**, 2321 (2010).

Visualization of Evolving Microstructures in Mesoporous and Bulk $LiMn_2O_4$ Using Amorphization and Recrystallization Technique

R.S. Ledwaba[1], D.C. Sayle[2] and P.E. Ngoepe[1]

[1]*Materials Modelling Centre, University of Limpopo, Private Bag x1106, Sovenga 0727, South Africa*
[2] *School of Physical Sciences, University of Kent, Canterbury, CT2 7NZ, United Kingdom*

Nanosizing of spinel $LiMn_2O_4$ has been identified as one of the viable strategies to improve performance of the potential lithium ion battery cathode material [1]. This is due to the capability of nanomaterials to possess properties that differ from those of their bulk material such as superior rate capability and improved capacity retention [2]. Simulated armorphization and recrystallization technique was previously employed to generate nano-architectures of binaries such as MnO_2 [3] and will be used in the current study on the spinel. Microstructures of the resulting models conformed to the spinel polymorph and also indicated the presence of rutile-MnO_2 and layered-Li_2MnO_3 in both the bulk and mesoporous $LiMn_2O_4$. XRD patterns are also presented and compare favourably with measured XRD providing valuable validation of the atomistic models with microstructural features.

[1] Xia H., Luob Z. and Xieb J., *Progress in Natural Science: Materials International,* **22**, 572 (2012)
[2] Feng J., Bao J., Hill A.H. and Bruce P.G., *Angewandte Chemie International Edition,* **50**, 9711 (2008)
[3] Sayle T. X.T, Maphanga R. R., Ngoepe, P. E. and Sayle D. C., *Journal of the American Chemical Society,* **131**, 6161 (2009)

Computer modelling of double doped $SrAl_2O_4$ for phosphor applications

R A Jackson, L A Kavanagh

School of Physical and Geographical Sciences, Keele University, Keele, Staffordshire, UK

$SrAl_2O_4$, when doped with Eu^{2+} and Dy^{3+} ions, is a well-known phosphor material, used widely for applications like emergency signs, which utilise its 'glow in the dark' properties [1]. Computer modelling, based on the description of interionic interactions by effective potentials, has been widely applied to the study of optical materials [2, 3]. However, there are relatively few modelling studies of double doped materials, apart from a recent paper on co-doped $LiNbO_3$ [4].

The procedure adopted for modelling singly doped materials is to calculate the solution energy, which takes into account the full energetics of the doping process, including the formation of any charge compensating defects. Prediction of favoured doping sites and charge compensation mechanisms can then be made on the basis of these energies. The same procedure is adopted for double doping, but from the calculated energy it can be now be determined if the addition of the second dopant ion increases or reduces the net energy required per dopant ion. This can in turn suggest whether double doping is favourable energetically compared with single doping.

In the case of $SrAl_2O_4$, the pure material is initially modelled, and then intrinsic defects formation energies calculated, in order to establish the form of intrinsic disorder in the material. Solution energies for doping with a range of 2+ and 3+ ions are calculated, initially for single ion doping, and then for double doping, focussing on combinations of ions used in phosphor materials. The optimum locations of dopant ions, charge compensation mechanisms and solution energies involved in the doping process, are calculated. Finally, comparisons with experimental results are made, and implications for device design are considered.

[1] J Botterman, JJ Joos, PF Smet, *Physical Review B* **90** (2014) 085147
[2] MVS Rezende, JB Amaral, MEG Valerio, RA Jackson, *Optical Materials* **48** (2015) 105
[3] M Mujaji, J Burrows, RA Jackson, *Journal of Luminescence* **151** (2014) 106
[4] RM Araujo, MEG Valerio, RA Jackson, *Proc. R. Soc. A* **470** (2014) 20140406

Evidence of a Jahn-Teller impurity in a cubic lattice displaying a compressed geometry

P. García-Fernández[1], J. A. Aramburu[1], J. M. García-Lastra[2], and Miguel Moreno[1]

[1] *Departamento de Ciencias de la Tierra y Física de la Materia Condensada, Universidad de Cantabria, Avenida de los Castros s/n, 39005 Santander, Spain*
[2] *Center for Atomic-Scale Materials Design, Department of Physics, Technical University of Denmark, DK-2800 Kongens Lyngby, Denmark*

Spontaneous symmetry-breaking around a defect site leads to interesting quantum phenomena, like tunnelling between various stable wells that, under the correct conditions could serve as the basis for applications like quantum computation [1,2]. Of particular interest is the Jahn-Teller distortion appearing in some transition-metal impurities in cubic lattices that usually involves the elongation of the metal ligand octahedron along one of its axes. For a long time it was believed that this was the case for a nickel-associated defect appearing in $CaO:Ni^{2+}$ after irradiation [3], ascribed to a Ni^{3+} ($3d^7$) ion with a S=1/2 ground state [4]. First principle calculations together with an analysis of experimental data found for $3d^9$ and $3d^7$ ions in cubic oxides prove however that the centre found in irradiated $CaO:Ni^{2+}$ corresponds to Ni^+ under a static Jahn-Teller effect displaying a compressed equilibrium geometry [5]. To our knowledge this is the first genuine Jahn-Teller system (i.e. where exact degeneracy exists at the high-symmetry configuration) exhibiting compressed equilibrium geometry. Moreover, the present calculations [5] demonstrate that the anomalous positive $g_{||}$-shift ($g_{||} - g_0 = 0.065$) measured [3] at T = 20 K obeys to the superposition of $|3z^2\text{-}r^2\rangle$ and $|x^2\text{-}y^2\rangle$ states driven by quantum effects associated with the zero-point motion, a mechanism firstly put forward by O'Brien[6] and that, so far, had no rigorous experimental support. In the present case, that mechanism is shown to be enhanced by the low Jahn-Teller barrier (8.7meV) among equivalent configurations [5]. Finally an analysis of calculated energy barriers for different Jahn-Teller systems [2,5] allows us to explain the singular origin of the compressed geometry present in $CaO:Ni^+$.

[1] Stoneham, A. H. *Physics*, **2**, 34 (2009)
[2] Garcia-Fernandez, P. et al. *Phys. Rev. Lett.*, **104**, 0359 (2010)
[3] Low, W.; Suss, J. T. *Phys. Lett.*, **7**, 310 (1963)
[4] I. B. Bersuker, *The Jahn-Teller Effect*, Cambridge University Press, Cambridge, (2006)
[5] Garcia-Fernandez, P et al. Phys. Chem. Chem. Phys. (submitted)
[6] O'Brien, M. C. M. *Proc. Roy. Soc. London, Ser. A*, **281**, 323 (1964)

First order Raman intensities associated to point defects in silicon carbide from first principles

G. Roma[1]

[1]*CEA, DEN, Service de Recherches de Métallurgie Physique, Université Paris-Saclay, F-91191 Gif sur Yvette, France*

Raman spectroscopy has been increasingly used in the last few years in order to characterise the modifications occurring in materials under (or after) irradiation. One of the most investigated materials using this technique is silicon carbide [1]; however, the interpretation of the spectra is not always an easy task. Features observed in experimental spectra cannot be unambiguously associated with specific meso/nanostructures or point defects. A step towards this goal is a reliable prediction of spectral properties from first principles. Although silicon carbide is a material for which a lot of first principles studies on point defects exist, including localised vibrational modes, no attempt has been made to predict line intensities associated to defect structures. Here we present the calculation of first order Raman spectra of selected point defects in cubic silicon carbide using the linear response approach [2], in particular carbon antisites and coordination defects [3]. We discuss the applicability of the Placzek approximation and size effects, intrinsic to the supercell approach.
Furthermore, we consider the possibility of coupling Raman spectra predictions with the evolution of defect populations under irradiation as obtained by rate theory modelling, providing a proof of concept of the procedure, and discuss the limitations and open questions that still hinder this promising approach.

[1] S. Miro et al., J. Raman Spectroscopy **45**, 481 (2014).
[2] M. Lazzeri and F.Mauri, Phys. Rev. Lett. **90**, 036401 (2003).
[3] T. Liao, N. O. Bedoya-Martínez, and G. Roma, J. Phys. Chem. C **114**, 22691 (2010).

Hydrogen in insulating oxide $Y_3Al_5O_{12}$ strongly narrows the band gap

F. A. Selim[1,2], D. Winarski[1], and C. Persson[3]

[1]*Department of Physics and Astronomy, Bowling Green State University, Bowling Green, OH 43403, USA.*
[2]*Center for Photochemical Sciences, Bowling Green State University, Bowling Green, OH 43403, USA.*
[2] *Department of Physics, University of Oslo, P.O. Box 1048 Blindern, No-0316 Oslo, Norway.*

Hydrogen does not exist as a neutral impurity in semiconductors and insulators; it always gives up an electron becoming positively charged impurity or acquires an electron becoming negatively charged impurity [1]. This has profound effects on the incorporation of hydrogen in the structure and the electronic and structural properties of materials [2,3]. The importance and significance of hydrogen in materials has been revealed theoretically; and hydrogen in semiconductors has been the subject of intense investigation. In this work we show that incorporation of hydrogen in the $Y_3Al_5O_{12}$, yttrium aluminum garnet (YAG) structure has led to significant band gap narrowing (BGN) in $Y_3Al_5O_{12}$ single crystals, an unusual surprising effect for hydrogen incorporation in insulating oxides. This BGN has been confirmed by experimental and theoretical results. Furthermore we show that hydrogen binds to native defects passivating their role as charge carrier traps which has remarkable impact on the oxide properties. Funding was provided by NSF-DMR-1359523. We also acknowledge HPC resources through SNIC and NOTUR in Norway.

[1] C. G. Van de Walle, J. Alloys Compd. **446**, 48 (2007).
[2] C. G. Van de Walle and J. Neugebauer, Nature **423**, 626 (2003).
[3] P. C. Srivastava and U. P. Singh, Bull. Mater. Sci. **19**, 51 (1996).

Identification of Rhenium donor in layered MoS_2 samples

F. D. Brandão, G. M. Ribeiro, and K. Krambrock

[1]*Physics Department, Federal University of Minas Gerais, Belo Horizonte, Brazil*

Rhenium is the dominant impurity in natural bulk MoS_2 samples, a very interesting bidimensional semiconductor material which like graphite may be exfoilated to monolayers with direct energy bandgap in the blue spectral range and promising applications in electronic and optoelectronic devices. Very few is known about Rhenium impurity as for example its incorporation site, site symmetry, valence states and ionization energy levels in MoS_2. In this work we present low temperature electron paramagnetic resonance (EPR) and electrical measurements which clearly identify the Rhenium donor by its characteristic, strong anisotropic hyperfine interaction due to the ^{185}Re and ^{187}Re isotopes both with nuclear spins I = 5/2 resulting in a sextet of hyperfine-split lines. Nuclear quadrupole interaction leads also to forbidden EPR lines. EPR angular dependencies have been measured and analyzed and confirm the incorporation of Re in Mo sites with similar spin Hamiltonian parameters compared with Re impurities in MoO_3. [1]. From resistivity and Hall measurements a ionization level of 59 meV below the conduction band is determined which we associate with the Re donor and which is in accordance with theoretical calculations [2]. From EPR measurements the concentration of Re donors is estimated to be in the range of 10^8 - 10^{12} defects per cm^{-2} for different natural samples. Controversially, in a recent publication about shallow donors in MoS_2 natural bulk samples a single line EPR spectrum has been associated to the Re donor [3] whose origin we also discuss in this contribution.

Acknowledgements : The authors are grateful for financial support to the Brazilian agencies CNPq, Fapemig and CAPES.

[1] R Gazzinelli, O F Schirmer and V Wittwer, ESR and optical absorption of rhenium in MoO_3, J. Phys. C. **10**, 3719 (1977).

[2] K. Dolui, I. Rungger, C. D. Pemmaraju, and S. Sanvito, Possible doping strategies for MoS_2 monolayers: An *ab initio* study, Phys. Rev. B **88**, 075420 (2013).

[3] Nguyen T. Son, Yong-Sung Kim and Erik Janzén, Shallow donor in natural MoS_2, Phys. Stat. Sol. (RRL) **9**, 707 (2015).

Positron annihilation spectroscopic characterization of defects in wide band gap oxide semiconductors

A. Sarkar[1] and D. Sanyal[2]

[1]*Department of Physics, Bangabasi Morning College, 19 R. C. Sarani, Kolkata 700009, India.*
[2]*Variable Energy Cyclotron Centre, 1/AF Bidhannagar, Kolkata 700064, India*

Generation and recovery of defects in wide band gap oxide semiconductors, such as ZnO, TiO_2, SnO_2 etc., is a topic of wide interest. Unambiguous identification of defects present in these oxides is extremely important to explain defect induced modification of photoluminescence, conductivity, magnetism, catalytic efficiency and several others [1,2]. Here, we have employed positron annihilation spectroscopy to understand evolution of defects due to thermal annealing and ion irradiation in ZnO, TiO_2 and SnO_2.

Polycrystalline ZnO samples, annealed at 200-1000 ^oC have been investigated using Doppler broadened electron positron annihilation radiation (511 keV gamma ray) lineshape (DBEPARL) measurements with two HPGe detectors in coincidence [1,3]. Ratio curve [1,3] for each DBEPARL spectrum has been constructed with respect to that of the spectrum of as-supplied (unannealed) and single crystalline ZnO. Two prominent peak-like structures at $p_L \sim 16.8 \times 10^{-3}\ m_oc$ and $\sim 22.6 \times 10^{-3}\ m_oc$ for 1000 ^oC annealed sample can be clearly identified (p_L represents electron momentum along the measuring detector). On the other hand, samples annealed at 400 ^oC or below show prominent dip (ratio less than 1) in nearby p_L values. Detailed analysis of the peak (dip) momentum positions shows that they arise due to more (less) annihilation of positrons with Zn 3p and 3s electrons. So generation and recovery of Zn vacancy defects can be successfully monitored. In this way, hydrogen defects in ion irradiated ZnO single crystal [3], Sn vacancies in ion irradiated SnO_2 [4] have been identified. Further analysis also shows that signatures of O vacancies or their agglomeration with Zn vacancies (Zn-O divacancy) can be understood. Such divacancies provide scope for nitrogen molecules to diffuse in bulk ZnO and can generate shallow acceptor states as is seen in our recent work [5]. The detailed results, analysis and methodology will be presented. We feel that the defect probing methodology we have adopted here can be extended to large family of compound semiconductor systems [6] which can provide immense insight in the direction of technological use of such materials.

[1] S. Dutta et al., J. Appl. Phys. 98 (2005) 053513; S. Dutta et al., Prog. Mater. Sci. **54** (2009) 89.
[2] H. Luitel et al., Nucl. Instrum. Meth. B Proceedings (accepted).
[3] A. Sarkar et al., J. Phys.: Condens. Matter **24** (2012) 325503.
[4] A. Sarkar et al., RSC Adv. **5** (2015) 1148.
[5] D. Sanyal et al., (to be communicated).
[6] S. N. Guin et al., J. Am. Chem. Soc. **136** (2014) 12712.

Atomic insight to small, strong-coupling hole polarons in lithium niobate by local probing of OH^- bonds

Felix Freytag[1], Phillip Booker[1], Gábor Corradi[2], Mirco Imlau[1]

[1] *School of Physics, Osnabrueck University, Barbarastraße 7, 49076 Osnabrueck, Germany*
[2]*Institute for Solid State Physics and Optics, Wigner Research Centre for Physics, Hungarian Academy of Sciences, Konkoly-Thege u. 29-33, 1121 Budapest, Hungary*

There's an increasing attention to determine the structural distortion parameters of small, strong couplig polarons [1] for nonlinear optical processes in polar oxides on the ultrafast time-scale [2]. Even though, a multitude of knowledge has been gathered and a variety of experimental techniques like EPR/NMR measurements were applied, there is still no possibility for direct experimental access to the atomic displacements induced by small, strong-coupling polarons within a continuum and at elevated temperatures.

Here, we use ultrafast mid-infrared pump-probe spectroscopy ($\tau_{Pump} \approx 100$ fs, $\tau_{Probe} \approx 230$ fs) combined with potential landscape modelling to experimentally achieve atomic insight about the lattice distortion caused by small, strong coupling hole polarons at room temperature in near stoichiometric lithium niobate. The dynamic absorption change of the OH^- stretching vibration is applied as a local probe for optically excited small, strong-coupling polarons. We experimentally determine a blue shift of $\Delta\upsilon = 3\ cm^{-1}$ with a single scan absorption precision of ≈ 1 mOD that is explained straightforwardly by a local change of the lattice environment induced by small polaron formation. This explanation is supported by the relaxation dynamic of the shift that corresponds with the decay time-constants ($\tau \approx 1$ ms) of small hole O^- and small bound Nb_{Li}^{4+} polarons measured by pump-probe spectroscopy in the visible and near infrared spectral range. Based on our experimental findings, we are able to determine the lattice distortion induced by small hole polarons by means of modelling the vibrational potential landscape in direction of the $O\text{-}H^-$ bond. For this purpose, a combination of a static Morse potential and a Coulomb potential, given by the atom sites in the lattice, is used. We further take into account the state-of-the-art knowledge of the position of hydrogen [3,4] and the structural data of the crystals lattice [5]. Local changes of the oxygen atoms in the first coordination sphere lead to a different vibrational frequency of the OH^- stretching bond. Hereby we are able to finally determine the polaron induced lattice distortion to $\approx 3\%$ in full accordance with the results of previously reported ab-initio calculations. Financial support by the DFG (IM 37/5-2, INST 190/165-1 FUGG) and DAAD (POL 5719940) is gratefully acknowledged.

[1] Emin, Polarons, Cambridge University Press (2013).
[2] Imlau et al., Applied Physics Reviews **2**, 40606 (2015).
[3] Nahm et al., Applied Physics Letters **78**, 3812 (2001).
[4] Lengyel et al. IOP Conf. Ser.: Mater. Sci. Eng. **15**, 012015 (2010).
[5] Abrahams et al., Journal of Physics and Chemistry of Solids **27**, 997 (1966).

Incorporation of rare earth ions in $Li_6Y(BO_3)_3$ single crystals

K. Lengyel[1], L. Kovács[1], É. Tichy-Rács[1], L. Oláh[1], G. Corradi[1]

[1] *Institute for Solid State Physics and Optics, Wigner Research Centre for Physics, Hungarian Academy of Sciences, Konkoly Thege M. út 29-33, 1121 Budapest, Hungary*

Lithium yttrium borate ($Li_6Y(BO_3)_3$, LYB) has a monoclinic crystal structure with the $P2_1/c$ space group and a wide spectral transparency range up to ultraviolet energies. In addition, rare earth (RE) dopants are easily incorporated at yttrium sites in the crystal lattice, so this material is a good candidate for laser host and scintillation applications.

The spectroscopy of Dy^{3+}, Er^{3+} and Yb^{3+} ions has been investigated in LYB single crystals recently [1-3]. The LYB samples studied were doped with various amounts of RE^{3+} ions and grown by the Czochralski method. Polarized absorption and luminescence spectra were measured at low temperature on samples cut in various crystallographic orientations.

Electronic transitions of the RE^{3+} ions in the 3000–40000 cm^{-1} wavenumber range were successfully identified. Beside the effect of crystal field splitting, a particular transition was also observed in the absorption and luminescence spectra at concentrations of about 1 and 5 mol% Yb, which has been previously assigned to Yb-Yb pairs in heavily doped (22-26 mol%) LYB:Yb samples [4].

For interpreting the spectra results of theoretical modeling of the relaxation of LYB crystal lattice around the incorporated RE^{3+} ions will be discussed using the SIESTA quantum chemical software. In addition, the possibility of the formation of RE^{3+} ion pairs in LYB crystal will be analysed as well.

This work has been supported by the Janos Bolyai research fellowship of the Hungarian Academy of Sciences. We acknowledge the NIIF for awarding access to computing resources based in Budapest and Szeged.

[1] É. Tichy-Rács, I . Romet, L. Kovács, K. Lengyel, G. Corradi, V. Nagirnyi, I. Hajdara, "Optical spectroscopy of $Li_6Y(BO_3)_3$ single crystals doped with dysprosium", 9th LUMDETR, Tartu, 2015.

[2] G. Mandula, Z. Kis, É. Tichy-Rács, K. Komlai, L. Kovács, K. Lengyel, G. Corradi, "Spectroscopic properties of Yb^{3+} ions in $Li_6Y(BO_3)_3$ single crystals", 12th EURODIM, Canterbury, England, 2014.

[3] L. Kovács, G. Corradi, É. Tichy-Rács, Zs. Kis, W. Ryba-Romanowski, A. Strzep, A. Scholle, S. Greulich-Weber, "Incorporation and energy levels of Er^{3+} in lithium yttrium borate (LYB) single crystals", ICDIM, Santa Fe, USA, 2012.

[4] V. Jubera, M. Chavoutier, A. Artemenko, P. Veber, M. Velazquez, A. Garcia, Chem. Phys. Chem. **12** (2011) 1288-1293.

Dependence of stoichiometry of lithium niobate nanocrystals on different initial lithium to niobium ratios in the synthesis step

K. Veenhuizen[1], G. A. Stone[2], B. Knabe[3,4], K. Buse[3,4], and V. Dierolf[1]

[1]*Department of Physics, Lehigh University, 16 Memorial Drive East, Bethlehem, PA 18015, USA*
[2]*Department of Materials Science and Engineering, Pennsylvania State University, Millennium Science Complex, University Park, PA 16802*
[3]*Department of Microsystem Engineering (IMTEK), University of Freiburg, Georges-Köhler-Allee 102, 79110 Freiburg, Germany*
[4]*Fraunhofer Institute for Physical Measurement Techniques IPM, Heidenhofstraße 8, 79110 Freiburg, Germany*

Ferroelectric nanocrystals show promise for application in forming hybridized nonlinear materials with liquid crystals. It is well known that bulk single crystals of lithium niobate ($LiNbO_3$) are most easily grown in a congruent (lithium-deficient) form but can also be grown in a stoichiometric form. This is controlled by the specific growth conditions and the stoichiometric ratio $\rho = M_{Li}/(M_{Li}+M_{Nb})$. This work explored the dependence of the stoichiometry of $LiNbO_3$ nanocrystals on the value of ρ in the synthesis step. Batches of $LiNbO_3$ nanocrystals were synthesized using the sol-gel method described in [1]. The nanocrystals were analyzed via SEM (image below) and Raman spectroscopy to gain information about their size, morphology, stoichiometry, and defect content. In analyzing the stoichiometry, we use previous works that demonstrate that the spectral width of specific Raman modes strongly depend on ρ and can hence be used to determine the $LiNbO_3$ crystal composition [2]. As shown in the graph below, the Raman spectra indeed reveal that the resultant nanocrystal stoichiometry depends on the initial ρ used in the synthesis. A close examination of the Raman spectra further reveal an extra phase which is present for all batches with stoichiometric ratio $\rho \geq 55\%$. Somewhat counterintuitively, this phase is identified by its Raman spectra to be relatively lithium-poor $LiNb_3O_8$ [3]. As a result, we find that high quality, roughly spherical $LiNbO_3$ nanocrystals can only be synthesized at certain initial stoichiometric ratios that avoid the presence of the extra phase.

Graphs: Left, Raman spectra of nanocrystals with different Li/Nb ratios: blue, $LiNbO_3$ dominated, with arrows indicating the $E(TO)_3$ mode; black, $LiNb_3O_8$ dominated, with arrows pointing to Raman modes which are unambiguously assigned to $LiNb_3O_8$ nanocrystals. Right, $E(TO)_3$ spectral width as a function of ρ

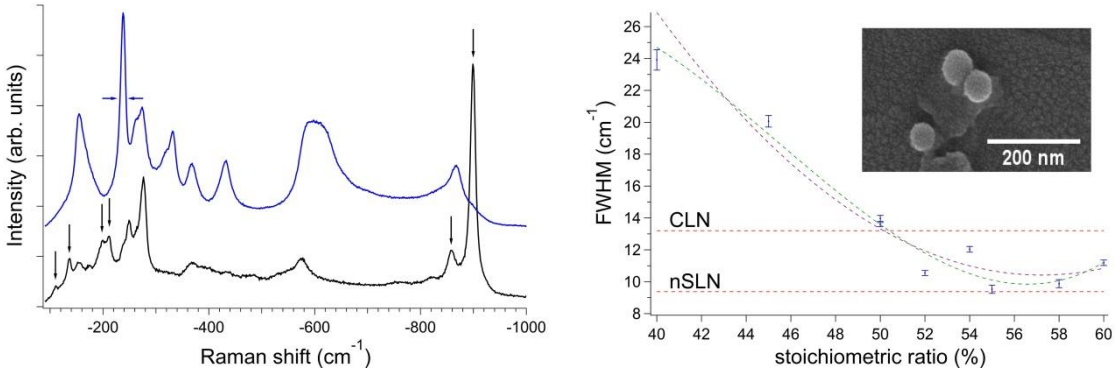

[1] B. Knabe et al., Phys. Status Solidi A **208**(4), 857–862 (2011)
[2] U. Schlarb et al., Appl. Phys. A **56**, 311-315 (1993)
[3] A. Bartasyte et al., J. Phys.: Condens. Matter **25**, 205901 (2013)

Spectroscopic properties of $Y_4Al_2O_9$:Ce crystals

A. Suchocki[1,2], Yongjie Wang[1], M. Ciesielska[3], A. Kaminska[1], Ya. Zhydachevskii[1], S. Turczyński[4], D.A. Pawlak[4], M. Malinowski[5]

[1]*Institute of Physics, Polish Academy of Sciences, Al. Lotników 32/46, 02-668 Warsaw, Poland*
[2] *Institute of Physics, Kazimierz Wielki University, Weyssenhoffa 11, 85-072 Bydgoszcz, Poland*
[2]*Cardinal Stefan Wyszynski University, College of Science, Department of Mathematics and Natural Sciences, Dewajtis 5, 01-815 Warsaw, Poland*
[4] *Institute of Electronic Materials Technology, Wólczynska 133, 01919 Warsaw, Poland*
[5] *Institute of Microelectronics and Optoelectronics, Warsaw University of Technology, ul. Koszykowa 75, 00-662 Warsaw, Poland*

$Y_4Al_2O_9$ crystals, abbreviated here as YAM (monoclinic yttrium aluminate), are difficult to grow in a bulk form by the Czochralski method since they undergo structural phase transition under cooling. However they may be manufactured by the micro-down pulling method. YAM:Ce crystals with various concentrations up to 1% of Ce, grown by this technique were studied in this work.

The material was characterized by various spectroscopic techniques, such as absorption, FTIR, luminescence, luminescence decay kinetics, and photoluminescence excitation. Absorption spectra consist of several bands in the UV region associated with optical transition between 4f and 5d states of Ce^{3+} ions. Luminescence of this material, which appears in a blue spectral region between 430 and 540 nm, undergoes strong temperature quenching, which begins already at temperature of about 20 K. The luminescence quenching is thermally activated with activation energy equal to about 21 meV. We associate this quenching with position of the 5d state of Ce^{3+} close to the bottom of the conduction band. High pressure luminescence experiments, performed in diamond anvil cell confirm this hypothesis. Due to pressure induced increase of the separation energy between the 5d states of Ce^{3+} ions and a bottom of the conduction band the temperature of the luminescence quenching is increased.

The decay kinetics of Ce^{3+} luminescence exhibit two-exponential behaviour. The dominating part of the decay kinetics has decay time of about 20 ns at 4K, and is strongly decreasing with increase of temperature. This component of the decay is associated with the 5d→4f transitions within the Ce^{3+} ions. Much less intense part with a very long decay time in the order of a few hundred nanoseconds is weakly dependent on temperature. Origin of this long decay kinetics is discussed in this work.

FTIR absorption in the spectral region of 4f→4f transitions of Ce^{3+} ions reveals existence of several Ce^{3+}-related centres in this compound, in agreement with its crystallographic structure.

Acknowledgements: The work was partially supported by the Polish National Science Center (project 2015/17/B/ST5/01658).

EPR and DFT investigation of Fe and Fe-Ti doping in LiNbO3.

Sara Arceiz Casas[1], Simone Sana[1], Annamaria Zaltron[2], Giacomo Bettella[2], Gianluca Pozza[2], Cinzia Sada[2], Siegmund Greulich-Weber[1]

[1]*University of Paderborn, Warburger Str. 100, 33098 Paderborn, Germany*
[2]*University of Padova, Via Marzolo 8, 35131 Padova, Italy*

The optical properties of Ti^{4+} indiffused $LiNbO_3$ waveguides are heavily affected by extended and point defects. In particular, even small percentages of unintentional iron doping increase the photorefractive sensitivity of $LiNbO_3$ considerably.
Ti^{4+} is known to stabilize Fe^{2+} impurities against oxidation [1], however, neither the defect complexes formed by Fe and Ti nor the mechanisms leading to the optical degrade are known. As a first step towards the understanding of the photorefractive properties of the waveguides, we investigate isolated Fe and Fe-Ti doped $LiNbO_3$ [2,3] by electron paramagnetic resonance (EPR) and density functional theory (DFT).
Signals originating from different defect centers can be discriminated by EPR in Fe doped and Fe-Ti co-doped samples. Corresponding theoretical models are developed within DFT, showing the structural and electronic properties of the observed defects.

[1] V. Gericke, P. Hertel, E. Krätzig, J. P. Nisius and R. Sommerfeldt, Appl. Phys. B **44**, 155 (1987)
[2] O. F. Schirmer, M. Imlau, C. Merschjann and B. Schoke, J. Phys.: Cond. Matt. **21**, 123201 (2009)
[3] O. F. Schirmer, M. Imlau and C. Merschjann, Phys. Rev. B **83**, 165106 (2011)

Ab initio simulations of interstitial oxygen in corundum

R.A. Evarestov [1,2], Yu.F. Zhukovskii[3], S. Piskunov[3], A. Platonenko[3], E.A. Kotomin[1,3], J. Maier[1]

[1] *Max Planck Institute for Solid State Research, Stuttgart, Germany*
[2] *Dept. of Quantum Chemistry, St. Petersburg University, Russia*
[3] *Institute of Solid State Physics, University of Latvia, Riga, Latvia*

Because of high radiation resistance and wide band gap, Al_2O_3 (corundum) is widely used as an effective detector of ionizing radiation. Its potential applications include also components of breeder blanket and diagnostic windows. Radiation-induced changes in the structural and optical properties of corundum are mainly associated with primary Frenkel defects: neutral and charged interstitial oxygen atoms O_i, as well as oxygen vacancies V_O (*F*-type color centers). Unlike the latter, the former defects are not well studied yet.

In this study, we present the results of periodic *ab initio* simulations on basic properties and mobility of the neutral and charged oxygen interstitials using the CRYSTAL14 computer code. The defect geometry and migration energies, Mulliken atomic charges and the electron density distributions for neutral and charged impurities are compared. The phonon frequencies of perfect and defective corundum crystal, systematized using the symmetry analysis, are considered with a focus on dumbbell vibrational properties.

It has been shown that the neutral and single-charged interstitial ions form dumbbells with a regular oxygen ion displaced from one of the nearest host lattice sites (interatomic distances are 1.40 and 1.87 Å, respectively) [1,2], similar to earlier predicted in irradiated MgO [3]. In turn, the double-charged oxygen interstitial ion tends to occupy a regular lattice site, but not preserving site symmetry. In all the cases, oxygen interstitials form the bonds with regular Al ions in corundum lattice rather than occupy center of octahedron consisting of six nearest O_{reg} ions as one could intuitively expect.

The calculated migration energies along several possible trajectories are compared with available experimental data. In order to get these energies, phenomenological theory of bimolecular reactions was applied, and the interstitial migration energy sought for was fitted to the experimental kinetics of the Frenkel defect recombination in corundum [4]. The results for neutron- and heavy swift ion irradiation of corundum are compared.

[1] A. Platonenko, S. Piskunov, Yu. F. Zhukovskii, and E. A. Kotomin, *IOP Conf. Ser. Mater. Sci. and Eng.* **77**, 012001 (2015)
[2] Yu. F. Zhukovskii, A. Platonenko, S. Piskunov, and E. A. Kotomin, *Nucl. Inst. Meth. B* 2016; DOI: 10.1016/j.nimb.2015.08.087
[3] T. Brudevoll, E. A. Kotomin, and N. E. Christensenet, *Phys. Rev. B* **53**, 7731 (1996).
[4] E. A. Kotomin, V. N. Kuzovkov, A. I. Popov, and R. Vila, *Nucl. Inst. Meth. B* 2016; DOI: 10.1016/j.nimb.2015.08.055

Optically stimulated detrapping limiting the storage capacity of persistent phosphors

Claude Tydtgat[1,2], KatrienW. Meert[1,2], Dirk Poelman[1,2], Philippe F. Smet[1,2]

[1]*Lumilab, Department of Solid State Sciences, Ghent University, Krijgslaan 281-S1, 9000 Gent, Belgium*
[2]*Center for Nano- and Biophotonics (NB-Photonics), Ghent University, B-9000, Belgium*

Persistent phosphors, also called glow-in-the-dark materials, are a specific type of luminescent materials having the unique ability to emit light long after the excitation ended [1]. This is realized by temporarily storing energy in the crystal lattice. Typically a (photo)ionization of the luminescent ion leads to a charge transfer to a trap, which can for instance be a vacancy in the crystal lattice. Ambient heat or pressure can release the trapped charge carrier, after which recombination and light emission can occur.
For many applications in the visible spectrum, such as in emergency signage, the storage capacity of the typically Eu^{2+} based phosphors should further be increased. This would open new application areas, such as glowing road marks[2]. In this work we show that the excitation of the europium center in the blue emitting $Sr_2MgSi_2O_7$:Eu,Dy by near-UV light not only leads to charge trapping, but also to optically stimulated release of previously trapped charges and subsequent luminescence (OSL) [3]. This is substantiated by specific charging-OSL experiments making use of the presence of a thermal barrier for trapping at low temperature in the case of $Sr_2MgSi_2O_7$:Eu,Dy. Furthermore, the optical detrapping is observed to be significantly more important when a larger fraction of the traps is already filled, suggesting OSL is the limiting factor in the storage capacity of persistent phosphors.
The experimental evidence for this particular type of OSL is supported by a model for local trapping in which an additional detrapping rate is introduced, being proportional to the excitation intensity. The characteristics of both the charging and afterglow behaviour can be explained qualitatively [3]. The occurrence of this particular detrapping mechanism is evaluated for other benchmark persistent phosphors.

[1] P. F. Smet et al., "Chapter 274 - Persistent Phosphors," in Handbook on the Physics and Chemistry of Rare Earths, (Elsevier, 2015), pp. 1-108.
[2] J. Botterman and P. F. Smet, "Persistent phosphor $SrAl_2O_4$:Eu,Dy in outdoor conditions: saved by the trap distribution," Optics Express **23**, A868-A881 (2015)
[3] C. Tydtgat et al., "Optically stimulated detrapping during charging of persistent phosphors," Optical Materials Express (submitted) (2016).

Consequences of Ca co-doping in $YAlO_3$:Ce scintillating crystals

F. Moretti[1], K. Hovhannesyan[2], M. Derdzyan[2], A. Petrosyan[2], and C. Dujardin[1]

[1] *Institut Lumière Matière, UMR5306 Université Lyon 1-CNRS, Villeurbanne, France*
[2]*Institute for Physical Research, National Academy of Sciences, 0203 Ashtarak, Armenia*

Research and development in the field of scintillator materials has become very active due to the their use in several applications in high energy physics, medical and quality control imaging, as well as in homeland security areas. New synthesis strategies have been proposed to improve the scintillation performances of the already existing materials in order to better suit the demands of various applications. Among other strategies, co-doping with alkaline earth ions in Ce-doped garnets and silicates has recently become a widely applied method to improve the time-response characteristics and light yield. The observed effects are related to the formation of Ce^{4+} centres which can still participate in the scintillation process by promptly capturing electrons, becoming trivalent and giving rise to the typical Ce^{3+} luminescence. The presence of this additional recombination channel reduces the probability of electron capture by electronic traps, resulting in a reduction of delayed recombination processes which lead to long scintillation decay tails and lower light yields.
In this contribution we will discuss the applicability of Ca co-doping in order to improve the scintillation characteristics of $YAlO_3$:Ce (YAP:Ce) single crystals grown by Bridgman method. Four different Ca concentrations have been considered (from 0 to 500 ppm); the optical properties of these samples have been studied by means of optical absorption (OA), steady state and time resolved photo- (PL) and radio-luminescence (RL). OA data showed a clear increase of the absorption in the UV region as a function of Ca content and related to the Ca-induced Ce^{4+} ion presence in the YAP matrix alongside regular 3+ ones. Steady state PL and RL data evidenced a rather clear decrease in the luminescence intensity. On the other hand, time resolved RL profiles showed a reduction in the weight of long decay components by increasing Ca content as well as a faster Ce^{3+} main decay time. These results are in good agreement with TSL data which show a remarkable reduction in the glow curve intensities. The reduction of the Ce^{3+} decay times was also detected in the case of PL decays, suggesting the possible occurrence of energy transfer phenomena among 3+ and 4+ Ce ions and thus limiting the luminescence efficiency. The results demonstrate the somewhat ambivalent role of Ca in the case of YAP:Ce: the improvement in the overall scintillation decay time is somewhat counterbalanced by the reduction in the luminescence efficiency of the crystals.

This work was performed in the scope of the International Associated Laboratory (CNRS–France & SCS–Armenia) IRMAS and European Union Horizon 2020 Program under grant agreement no. 644260 (INTELUM).

Optimization of wide band-gap scintillators using variable charge state of fast emitting rare earth dopants

M. Nikl

Institute of Physics of the CAS, Cukrovarnická 10, 162 53 Prague, Czech Republic

R&D of fast, efficient and high density single crystal scintillators has been an active field of research for last two decades at least due to demanding applications in high energy physics, medical imaging, security techniques and high-tech industrial applications. It comes out from the studies in literature that it is not only the choice of the appropriate host and doped luminescence center, but also the tailoring and optimization of the initially chosen material system which can provide an ultimate performance and commercially successful new scintillators. So called band-gap engineering and defect engineering strategies have been applied and the success stories were reported in the case of multicomponent garnets [1] and pyrosilicates [2] using the former strategy, while a number of materials was improved using the latter one, mainly by means of codoping, which appears the best controlled instrument to do so. The Sr-codoped $LaBr_3$:Ce [3], Ca or Mg codoped LYSO:Ce [4] and Mg-codoped LuAG:Ce [5] or GGAG:Ce [6] are the most recent examples.

While the mechanism of improvement in $LaBr_3$:Ce,Sr has probably not been yet completely understood, in the other materials mentioned, it is the stabilization of Cerium ion in tetravalent charge state by means of stable divalent codopant which was recognized as a key element improving the scintillation performance. The stable Ce^{4+}, though nonluminescent under direct photo-excitation, it does scintillate at consecutive charge carrier capture in scintillation mechanism providing essentially the same emission pattern as the stable Ce^{3+} center. However, an eventual overlap of charge transfer absorption of Ce^{4+} and emission spectrum of Ce^{3+} must be avoided to prevent reabsorption and nonradiative energy loss processes which degrade scintillation performance.

In this presentation, several selected examples of the above mentioned defect engineering strategy will be described for the Ce^{3+}, Pr^{3+} and Eu^{2+} fast emitting rare ions embedded as active dopants in oxide and fluoride hosts which are frequently used in modern scintillation materials.

[1] K. Kamada, et al, Crystal Growth & Design **11**, 4484 (2011).
[2] A. Suzuki, et al, Appl. Phys. Express, **5**, 102601 (2012).
[3] M. S. Alekhin, et al, Appl. Phys. Lett. **102**, 161915 (2013).
[4] S. Blahuta, et al, IEEE. Trans. Nucl. Sci. **60**, 3134 (2013).
[5] M. Nikl, et al, Crystal Growth Design **14**, 4827 (2014)
[6] K. Kamada, et al, Optical Materials **41**, 63 (2015)

$LaBr_3$ with Ce and Sr dopants: picosecond absorption spectroscopy and progress on track modeling

S. Gridin[1], X. Lu[1], P. Li[1], B. Ucer[1], R. Williams[1], K. Yang[2], P. Menge[2]

[1]*Department of Physics, Wake Forest University, Winston Salem, NC, USA*
[2]*Saint-Gobain Crystals, 17900 Great Lakes Parkway, Hiram, Ohio 44234, USA*

There has been strong recent interest in co-doping of scintillators, promoted particularly by the success of aliovalent co-doping of $LaBr_3$:Ce studied by Yang et al and Alekhin, et al [1, 2]. In this work we investigate the scintillation mechanisms in the $LaBr_3$ system using experiment and modelling. Looking for carrier capture rates, we have conducted picosecond absorption spectroscopy in the near-ultraviolet through mid-infrared spectral range of a set of samples including undoped $LaBr_3$, Ce-doped $LaBr_3$ at several concentrations up to pure $CeBr_3$, and co-doped $LaBr_3$:Ce,Sr (Figure 1).

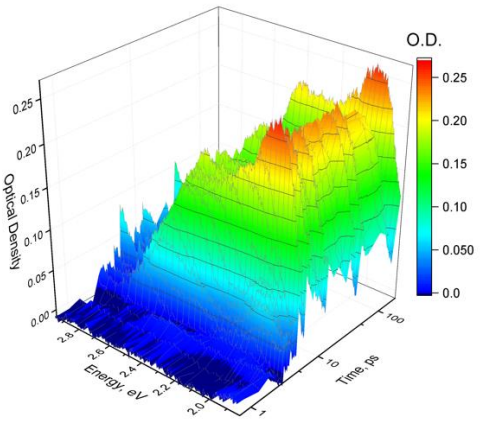

Figure 1. Visible absorption induced in $LaBr_3$:4.4%Ce by excitation with a 300-fs pulse of 4.43 eV light (two-photon absorbed)

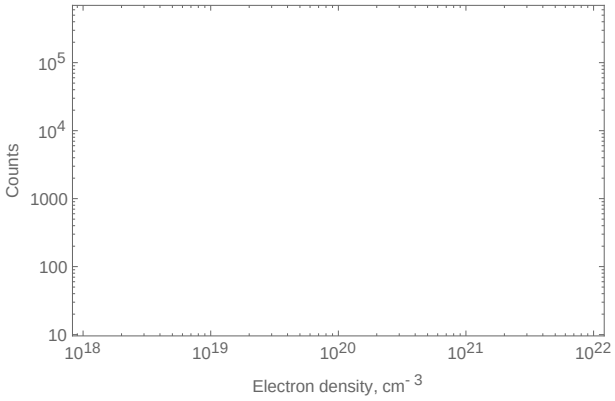

Figure 2. Comparing initial excitation density distributions in a 662-keV electron track for CsI (blue) and $LaBr_3$ (orange) based on Geant4 calculations and an assumed cylindrical track

Simulation of the scintillation processes in the $LaBr_3$ system is done using the transport and rate equation model [3] recently applied for CsI and CsI:Tl scintillators. The model takes into account thermalization of the charge carriers, their diffusion in the crystal, and capture on activator centers and intrinsic defects. Excitation density distribution along the ionization track in $LaBr_3$ is obtained using Geant4 software with 200 eV energy cutoff (Figure 2).

[1] Yang, K., Menge, P. et al, *IEEE NSS/MIC Record*, 308 (2012).
[2] Alekhin, M. S., Biner, D. et al, *J. App. Phys.,* **113** 224904 (2013).
[3] Lu, X., Li, Q. et al, *Phys. Rev. B*, **92,** 115207 (2015).

Delayed recombination in Ce^{3+} doped LuAG:Gd,Ga multicomponent garnet scintillators

Z. Lučeničová[1], M. Kučera[1], M. Hanuš[1], O. Lalinský[2], M. Nikl[3],

[1]*Charles University, Faculty of Mathematics and Physics, Ke Karlovu 5, 12116 Prague 2, Czech Republic*
[2]*Institute of Scientific Instruments, AS CR, Kralovopolska 147, 61264 Brno, Czech Republic*
[3]*Institute of Physics, AS CR, Cukrovarnicka 10, 16000 Prague 6, Czech Republic*

We study the shallow electron traps and their impact on the scintillation properties as scintillation efficiency and timing characteristics of Ce^{3+} doped $(Gd_yLu_{3-y})(Ga_zAl_{5-z})O_{12}$:Ce multicomponent garnets. Highly pure single crystalline films of thickness of 10 - 30 μm were prepared by liquid phase epitaxy with Gd content in the range from y = 0 to 3, and Ga content z = 0 to 3.5. In this research we compare results obtained from cathodoluminescence and photoluminescence decay kinetics.

Firstly, the cathodoluminescence decay kinetics was measured under nanosecond electron beam excitation with pulse width of 50 ns in the temperature range from 100 to 480 K. The decay curves measured in an extended time range and at high dynamical resolution allow to detect simultaneously both the prompt electron-hole 5d-4f(Ce^{3+}) recombination and delayed component which is due to shallow traps. The slow component in decay curves observed in samples with low Gd, and Ga content y,z < 2 can be explained as tunnelling-driven energy transfer process and/or by thermal ionization of Ce^{3+} ($5d_1$) excited state into the conduction band. At higher Gd, Ga concentrations y,z > 2 the delayed component completely disappears and slow part of scintillation response is practically suppressed.

Secondly, the temperature dependence of delayed recombination decay intensity of the same samples was studied in a wide temperature range from 8 to 500 K. These results confirm the presence of quantum tunnelling between the Ce^{3+} excited state and nearby traps. Moreover, any significant thermal ionization of the Ce^{3+} excited $5d_1$ state was not observed up to room temperature.

A Deeper Insight into LuYAG:Pr Scintillator Crystals

W. Drozdowski[1], K. Brylew[1], W. Łachmański[1], A.J. Wojtowicz[1], J. Kisielewski[2], M. Świrkowicz[2], A. Pajączkowska[2], E. Talik[3], M. Szubka[3], J. Kusz[3], A. Guzik[3], K. Balin[4]

[1]*Institute of Physics, Faculty of Physics, Astronomy and Informatics, Nicolaus Copernicus University, Grudziadzka 5, 87-100 Torun, Poland*
[2]*Institute of Electronic Materials Technology, Wolczynska 133, 01-919 Warsaw, Poland*
[3]*Institute of Physics, University of Silesia, Uniwersytecka 4, 40-007 Katowice, Poland*
[4]*A. Chelkowski Institute of Physics and Silesian Center for Education and Interdisciplinary Research, University of Silesia, 75 Pulku Piechoty 1A, 41-500 Chorzow, Poland*

Mixed $(Lu_xY_{1-x})_3Al_5O_{12}$:Pr (LuYAG:Pr) crystals have already been recognized as promising fast and efficient scintillator materials. Compared to their prototype $Lu_3Al_5O_{12}$:Pr (LuAG:Pr) they offer higher light outputs and increased contributions of the prompt component to their scintillation time profiles at an expense of a somewhat lower density [1,2]. Although the mechanism of improvement has more or less been explained, some questions are still open. Therefore, in the current research, we have attempted to acquire some extra knowledge on LuYAG:Pr in the two following fields:

i) To learn more about the internal structure of the Czochralski-grown LuYAG:Pr crystals, we have employed such techniques as X-Ray Photoelectron Spectroscopy (XPS), X-Ray Diffraction (XRD), Time-of-Flight Secondary Ion Mass Spectrometry (ToF-SIMS), and magnetic susceptibility measurements. In particular, concentrations and spatial distributions of the Pr^{3+} ions in the crystals have been determined.

ii) To confirm the role of charge traps in the energy transfer from the LuYAG host to the Pr^{3+} ions and assess its dependence on the Lu-to-Y ratio, we have performed advanced experiments with a coupled X-ray and IR-laser excitation at various temperatures, similar to those on LuAG:Pr [3].

This work has been financed from the funds of the Polish National Science Centre granted on the basis of Decisions no. DEC 2012/05/B/ST5/00324 and DEC 2013/09/N/ST3/01935.

[1] W. Drozdowski, K. Brylew, A.J. Wojtowicz, J. Kisielewski, M. Świrkowicz, T. Łukasiewicz, J.T.M. de Haas, P. Dorenbos, *Optical Materials Express,* **4,** 1207 (2014)

[2] W. Drozdowski, K. Brylew, M.E. Witkowski, A. Drewniak, Z. Masewicz, A.J. Wojtowicz, J. Kisielewski, M. Świrkowicz, *Optical Materials*, in print, doi:10.1016/j.optmat.2016.01.020

[3] W. Drozdowski, P. Dorenbos, R. Drozdowska, A.J.J. Bos, N.R.J. Poolton, M. Tonelli, M. Alshourbagy, *IEEE Transactions on Nuclear Science,* **56,** 320 (2009)

Point defect role in Ca co-doped scintillator NaI:Tl

A. Gektin, S. Vasukov, E. Galenin, N. Shiran, V. Taranyuk

Institute for Scintillation Materials, NAN of Ukraine, 60 Nauka ave., 61001, Kharkov, Ukraine

Last years (recent) studies demonstrated the significant increase in scintillation efficiency as a result of Ca codoping in Ce-doped LSO and LaBr3 crystals [1, 2]. Nevertheless, the origin of this phenomenon is not clear for alkali halides scintillators, in particular for NaI based crystal [3, 4].

Due to the difference of the matrix and dopant cations valency may be supposed the more variable scenario of the luminescence sensitizing. The role of charge compensative vacancies in Ca –doped and Ca, Tl co-doped NaI scintillator is the goal and main subject of this work.

NaI pure, Ca and Tl,Ca crystals were grown from ultra pure raw material for the later absorption, luminescence and scintillation parameters study. It is found that NaI: Ca samples demonstrate the luminescence band with maximum at 385 nm at room temperature, which excited on the tail of fundamental absorption. Even a slight ultraviolet irradiation results in the suppression of emission and the color center creation. The effect is partially reversible, i.e. the color centers annihilate after annealing but without luminescence efficiency restore. It is found that introduced defect behavior is very close both for Ca and Ca,Tl doped crystals. Variation of Tl:Ca rate from 5:1 to 1:5 demonstrates the similar domination of Tl emission and efficient energy transfer from point defects to luminescence centers.

The potential mechanisms of CaI2 centers appearance or transfer from vacancy centers are discussed. Point defects structure (DX like centers [5]) are the subject for discussion as well

[1] Kan Yang; Melcher C.L.; Koschan M.A.; Zhuravleva M., IEEE TNS 58, **3**, 1394 (2011).
[2] M S. Alekhin, D. A. Biner, K. W. Kramer, and P. Dorenbos, J. Appl. Phys., **118,** 213106 (2015).
[3] I. V. Khodyuk, S. A. Messina, T. J. Hayden, E. D. Bourret, G. A. Bizarri, J. Appl. Phys. **118,** 084901 (2015).
[4] K. Yang and P. R. Menge, J. Appl. Phys., **118,** 213106 (2015).
[5] R. Adhikari, Q. Li, R. Williams, A. Burger, and K. Biswas, J. Appl. Phys., **116,** 223703 (2014),

The Quenching Factor for alpha particles in ZnSe scintillating bolometers

S. Nagorny[1], F. Bellini[2,3], L. Cardani[2,3], N. Casali[2,3], I. Dafinei[3], L. Pagnanini[1], L. Pattavina[4], S. Pirro[4], K. Schäffner[1]

[1]*Gran Sasso Science Institute, I-67100 LAquila, Italy*
[2]*Dipartimento di Fisica - Università di Roma La Sapienza, I-00185 Roma - Italy*
[3]*INFN - Sezione di Roma I, I-00185 Roma - Italy*
[4]*INFN - Laboratori Nazionali del Gran Sasso, I-67100 Assergi - Italy*

The cryogenic scintillating bolometers technique is a promising experimental approach for the investigation of the rare nuclear process (neutrinoless double beta decay, rare alpha/beta decays), where both phonon and light channel of the signal allows for an excellent energy resolution and an active particle discrimination. The scintillating bolometer based on ZnSe crystals is used to search for the neutrinoless double beta decay of ^{82}Se within the LUCIFER experiment.
The ZnSe is very attractive material having an anomalous Quenching Factor (QF) behavior: alpha particles produce more light than electrons, i.e. QF > 1, in contrast with other known scintillators for which QF is less than 1. The QF for scintillator is calculated as a ratio of the light yield of alpha particles to that of electrons for the same deposited energy in the detector. Such not standard scintillation behavior still not has proper explanation and theoretical description, although it is very important for the detector performance.
In the framework of the LUCIFER experiment, in order to improve the light yield and the energy resolution a numbers of the ZnSe single crystals were produced and thermally treated in different way after growth. We have established, that after specific thermal treatment (24 hours under argon atmosphere at 900 °C), we can convert the QF into the “normal” mode, where QF < 1. Besides, this type of thermal treatment improves the optical transmittance, however deteriorates the energy resolution.
Our results demonstrate that anomalous QF for alpha particles in ZnSe crystals is a matter of certain type of defect in crystalline structure, and this experimental parameter can be adjusted for various applications via thermal treatment.

Molecular dynamics study of samarium and gadolinium doped ceria and their interfaces for solid-oxide fuel-cell applications

Aoife K. Lucid[1], Graeme W. Watson[1]

[1]*School of Chemistry and CRANN, Trinity College Dublin, Dublin 2, Ireland*

Current solid oxide fuel cells (SOFCs) require temperatures in the region of 1000°C to operate. This is primarily due to the fact that current generation SOFC electrolytes, such as ytrria stabilized zirconia (YSZ), require high temperatures in order for sufficient ionic diffusion of the O^{2-} ions to occur [1]. It has been suggested that replacing YSZ with samarium doped ceria (SDC) or gadolinium doped ceria (GDC) [2] would reduce the operating temperature of SOFCs into the intermediate temperature (IT) range of 600-800°C, thus greatly reducing operating costs and increasing efficiency.

Classical molecular dynamics can be used to investigate ionic conductivity and its limitations in these systems. Here we compare the performance of two interatomic potentials derived for a range of trivalent dopants in ceria from ab initio data, a dipole polarizable ionic model (DIPPIM) and a rigid ion model (RIM) [3]. The DIPPIM allows for polarization effects resulting from induced dipoles whereas the RIM does not. In this study we aim to elucidate whether or not this system can be modelled successfully using a RIM or if a DIPPIM is necessary due to the large polarization effects caused by the presence of O^{2-} ions.

The effect of surfaces and interfaces on the oxide ion conductivity in these materials is essential to their performance as SOFC electrolytes. It has been suggested that the strain which is induced in epitaxial films of these materials can result in enhancements in conductivity. There has been little theoretical investigation into oxide ion conductivity of SDC and GDC at surfaces and interfaces. Here we discuss the effect of low-index surfaces and strained surfaces on the performance of SDC and GDC as oxide ion conductors.

[1] Boudghene et al, *Renew. Sust. Energ. Rev.*, **6**, 433-455 (2002).
[2] Zha et al, *J. Power Sources*, **115**, 44-48 (2003).
[3] Castiglione et al, *J. Phys: Condens. Matter*, **11**, 9009-9024 (1999).

Improved interface passivation in heterojunction solar cells with ion irradiation

O. Plantevin[1], A. Defresne[1,2], P. Roca i Cabarrocas[2]

[1]CSNSM CNRS/IN2P3, Univ. Paris-Sud, Université Paris-Saclay, 91405 Orsay France
[2]LPICM, CNRS, Ecole Polytechnique, Université Paris-Saclay, 91128 Palaiseau, France

Silicon heterojunction (SHJ) technology holds great promise for high-efficiency solar cells production on an industrial scale. So-called HIT (Heterojunction with Intrinsic Thin layer) solar cells have reached record conversion efficiencies of 24.7%, and show above 20% energy conversion efficiency at the industrial production level. These results are due to the appropriate combination of crystalline silicon with different intrinsic and doped hydrogenated amorphous silicon (a-Si:H) thin layers (~10 nm). In particular, the record values for the open-circuit voltage (V_{oc} up to 750 mV) are related to the excellent crystalline silicon surface passivation by hydrogenation of silicon dangling bonds, leading to a reduction of the interface defect density. Several groups have shown that interface passivation represents an actual challenge for SHJ solar cell improvement and may be addressed using hydrogen plasma treatment. We explore an alternative option with ion irradiation for controlled modification of the a-Si:H thin layer and its interface with the crystalline silicon substrate. The effective lifetime of minority carriers, directly correlated with cell efficiency, is obtained via photoconductance, while the competition between radiative and non-radiative recombination centers is probed using photoluminescence spectroscopy [1]. We show that a fine tuning of ion irradiation parameters at low energy and low fluence associated with proper annealing may lead to passivation improvement, as well as improved thermal robustness of the final solar cell. The same method leads to a suppression of the thermal quenching of the photoluminescence, showing further evidence about the amorphous-crystalline interface modification and associated better defects passivation [2].

[1] A. Defresne, O. Plantevin, I.P. Sobkowicz, J. Bourçois, P. Roca i Cabarrocas, *Interface defects in a-Si:H/c-Si heterojunction solar cells*, Nucl. Instr. Meth. Phys. B **365**, 133 (2015), http://dx.doi.org/10.1016/j.nimb.2015.04.009

[2] O. Plantevin, A. Defresne, P. Roca i Cabarrocas, *Suppression of the thermal quenching of photoluminescence in irradiated silicon heterojunction solar cells*, Submitted to phys. stat. sol. (a) on 18/11/2015, Special Issue Amorphous and Nanocrystalline Semiconductors

(Ultra-)fast dynamics of self-trapped excitons in Mg-doped lithium niobate

S. Messerschmidt[1], A. Krampf[1], M. Imlau[1]

[1]*School of Physics, Osnabrueck University, Barbarastraße 7, 49076 Osnabrueck, Germany*

Self-trapped excitons (STEs) have been well-studied in a variety of non-polar materials, e.g. semiconductors. However, there is a lack of knowledge of STEs in polar environments - such as in lithium niobate (LN) - with regard to their formation, lifetime and radiative/non-radiative decay channels. Particularly, nothing is known about the interplay of STEs with small, strong-coupling polarons, that are generated with huge number densities by exposure to (ultra-)short laser pulses and dominate the (non-) linear optical and electrical properties of LN [1]. Here, STEs may either be quenched non-radiatively by the formation (and/or presence) of small polarons or small polaron formation may be strongly preferred in comparison to STE formation. To get insight to these processes, we systematically studied the formation and decay properties of the intrinsic luminescence feature in stoichiometric and Mg-doped LN single crystals within the time regime of 35 fs to 100 ms, i.e. over ten decades of time. STEs are optically generated via band-to-band excitation using (ultra-)short laser pulses in the UV-spectral range of a frequency doubled Ti-Sapphire (pulse duration: 35 fs) or of a YAG:Nd laser (8 ns). The emission features a large Stokes shift centered at about 2.8 eV (at T = 10 K) [2]. It is assumed that the STEs are localized at NbO_6-octahedra [2,3] that is supported by a red-shift of the luminescence peak position with decreasing [Li]/[Nb] ratio, i. e. the crystal composition, due to an increasing disturbance of the NbO_6-octahedron (Nb_{Li}-antisite defect) [2,4,5]. The ultrafast time regime up to about 1 ps highlights the interplay of STE and small polaron formation. We will particularly discuss the onset of ~80 fs of the transient absorption discovered by means of z-scan technique, that strongly limits the time window for STE formation and radiative decay channels. The ultrafast raise of the luminescence signal is inspected by means of up-conversion luminescence spectroscopy with a time resolution of below 50 fs. A model to explain the complex transition of STEs to small polarons is proposed; we furthermore discuss the suppression of luminescence emission by transient small polaron absorption.

Financial support by the DFG (IM 37/5-2, INST 190/165-1 FUGG) is gratefully acknowledged. The authors gratefully acknowledge the **WIGNER Research Centre for Physics** for sample preparation.

[1] Imlau, M. *et al.,* Appl. Phys. Rev. **2** (2015)
[2] Krol, D. M., *et al.,* J. Chem. Phys **73**, 163 (1980);
[3] Blasse, G., J. Phys. Chem. Solids **48** (1968)
[4] Fischer, C., *et al.,*Phys. Stat. Sol. (a) **137**, 247-255 (1993)
[5] Schirmer, O. F., *et al.,* J. Phys. Chem. Solids **52**, 185-200 (1991)

Photoluminescence of self-trapped excitons and colour centres in Eu^{2+}-activated $CsMgX_3$ (X = Cl, Br, I)

C. Wickleder[1], M. Suta[1]

[1]*Inorganic Chemistry, Faculty of Science and Technology, University of Siegen, Germany.*

The photoluminescence properties of self-trapped excitons (STEs) and colour (F) centres are well understood for alkali halides[1] and have an important impact on the performance of high-energy detectors such as scintillators or X-ray storage phosphors. However, their structural appearance as well as the mechanistic details of their interaction with embedded activators such as s^2 ions or the rare earths are often barely understood for more complex halides. Very suitable systems to investigate the dynamics and interactions of such defects are the compounds $CsMgX_3$ (X = Cl, Br, I). Their crystal structure exhibits an intrinsic pseudo one-dimensionality that acts highly stabilizing on the self-trapping of excitons[2-5]. In this contribution, we want to focus on their interaction with Eu^{2+} ions that are normally widely used in LED technology and of which we have intensively investigated the luminescence in these compounds[6-8]. Not only is it possible to prove the luminescence of STEs in $CsMgX_3$ besides the presence of Eu^{2+}, but they also exhibit an energy transfer to the activators. Moreover, it is possible to detect F centres that may even reduce the 4f-4f emitter Eu^{3+} to the 4f-5d emitter Eu^{2+} upon doping into the presented halides.

[1] K. S. Song, R. T. Williams, *Self-trapped Excitons*, Springer Series in Solid State Sciences, **105**, Springer, New York (1993).
[2] Y. Shinozuka, Y. Toyozawa, *J. Phys. Soc. Jpn.*, **46,** 505 (1979).
[3] G. L. McPherson, K. Talluto, *Solid State Commun*., **43** 331 (1982).
[4] C. Andraud, F. Pellé, O. Pilla, B. Blanzat, *Phys. Stat. Sol. (b),* **149**, 759 (1988).
[5] G. L. McPherson, Y. Y. Waguespack, T. C. Vanoy, W. J. Rodriguez, *J. Chem. Phys.*, **92**, 1768 (1990).
[6] M. Suta, P. Larsen, F. Lavoie-Cardinal, C. Wickleder, *J. Lumin.*, **149**, 35, (2014).
[7] M. Suta, C. Wickleder, *J. Mater. Chem. C*, **3**, 5233 (2015).
[8] H. Ramantoanina, F. Cimpoesu, C. Goettel, B. Herden, M. Suta, C. Wickleder, C. Daul, W. Urland, *Inorg. Chem.*, **54**, 8319 (2015).

Luminescence of Mn in CaZnOS: from energy levels to applications

Jonas J. Joos[1], Ang Feng[1], Kurt Lejaeghere[2], Karen Hemelsoet[2], Philippe F. Smet[1]

[1] *LumiLab, Department of Solid State Sciences, Ghent University, Krijgslaan 281/S1, 9000 Gent, Belgium*
[2] *Center for Molecular Modeling (CMM), Ghent University, Technologiepark 903, 9052 Zwijnaarde, Belgium*

Manganese is a well-known optical dopant. It can adapt different charge states of which the divalent, Mn^{2+}, featuring a $3d^5$ electron configuration, and the tetravalent, Mn^{4+}, featuring a $3d^3$ electron configuration are most abundant.
Both charge-states of the Mn defect show efficient luminescence, originating from intraconfigurational 3d transitions, having the emission in the visible spectral range. Excitation of the luminescence can be achieved by directly exciting the $3d^N$ manifold or through a charge-transfer transition.
This study concentrates on the oxysulfide CaZnOS [1]. This polar compound is built of alternating monolayers of ZnS and CaO, and forms a peculiar host for Mn^{2+}. It has been proposed as LED phosphor as well as mechanoluminescent pressure gauge [2, 3]. This material was synthesized by a solid-state reaction and the luminescent properties were characterized in detail by a combination of various experimental techniques.
To get a thorough understanding of the properties this phosphor, the electronic structure of the doped and undoped compound is assessed in detail. First principles calculations within the framework of density functional theory (DFT) are combined with semi-empirical crystal field theoretical (CFT) calculations to obtain the multiplet structure of the $3d^5$ manifold as well as the location of the impurity levels in the single-particle energy gap of the CaZnOS host.

[1] T. Sambrook *et al.*, Inorg. Chem., **46**, 2571 (2007).
[2] C. J. Duan, A. C. A. Delsing, H. T. Hintzen, Chem. Mater. , **21**, 1010 (2009).
[3] J.-C. Zhang *et al.*, Opt. Express, **21**, 12976 (2013).

Thermoluminescence of anion-deficient corundum and its connection with Ti impurity

A.I. Surdo[1,2], R.M. Abashev[1,2], I.I. Milman[2]

[1] *Institute of Industrial Ecology UB RAS, 20 S. Kovalevskaya Str., 620219 Ekaterinburg, Russia*
[2] *Ural Federal University, 19 Mira St., 620002 Ekaterinburg, Russia*

It was found in [1] that the TL response in TLD-500 detectors based on anion-deficient single crystal of corundum (α-$Al_2O_{3-\delta}$) is dose-proportional in the high-temperature peak at 830 K. Where continuous irradiation is used, such response is proportional to a dose up to 2 kGy. In [1], the TL spectrum in the peak at 830 K was also studied to reveal, along with weak luminescence of F^+ centers with $h\nu_{em}$=3.4 eV, intense luminescence with $h\nu_{em}$=4.1 eV whose nature is not known precisely. Similar luminescence was only observed earlier at T≤300 K and was caused by excitons localized at Ti-ions [2]. Besides, preliminary research showed that the TL peak at 830 K is only found in a part of TLD-500 detectors. The proportion of such detectors in the batches studied is not constant and varies between 50% and 80%. The objective of this study is detection in TLD-500 detectors of possible correlations of TL yield in the peak at 830 K with the content of defects of intrinsic and impurity nature.

It has been found that, as Ti concentration (C_{Ti}) in the TLD-500 detectors is increased from the detection threshold of ~7 ppm to 21 ppm, the TL yield in the peak at 830 K decreases to undetectable values. On the other hand, study of samples at constant C_{Ti} and decreasing anion deficiency C_F determined from total concentration of F^+ and F centers shows the TL yield at 830 K to drop essentially as well. Comparative studies of concentration variations of F, F^+ and F_2 centers in samples free of peak and with a TL peak at 830 K were carried out additionally with step-by-step annealing within a range between 300 K and 1400 K. Major inverse changes in concentrations of F and F^+ centers with simultaneous formation of F_2 centers are observed in irradiated samples with a peak in its high-temperature part at 850 ≤ TL ≤ 1000 K. Similar transformation of centers is registered in peak-free irradiated samples, but with changes in concentrations of F, F^+ and F_2 centers smaller by a factor of 5 to 10. Where TLD-500 samples of both types are not pre-irradiated, the above-mentioned changes in concentrations of active centers are not observed.

It can be stated from an analysis of data obtained that the emergence of a TL peak at 830 K is related to the presence of anion vacancies in the samples. The TL yield in this peak decreases to undetectable values with growth of concentration of the Ti impurity to 21 ppm, the impurity being mostly in the charge state Ti^{3+}. No significant correlations of TL yield at 830 K with the content of Ga, Fe, Cr, Ca, Si and Mg impurities in TLD-500 detectors were found.

[1] A.I. Surdo et al., Rad. Meas., in press (2016)
[2] V. B. Mikhailik et al., J. Appl. Phys., **109**, 053116 (2011)

Impurity ions spectra in garnets solid solutions: disorder, symmetry of centers and lattice deformation

S.P. Feofilov[1], A.B. Kulinkin[1], K. Hovhannesyan[2], A. Petrosyan[2]

[1]*Ioffe Institute, St. Petersburg, 194021, Russia*
[2]*Institute for Physical Research, NAS of Armenia, Ashtarak-2, 0203, Armenia*

The inhomogeneous broadening of electronic transitions Zero-Phonon Lines (ZPL) in rare-earth and transition metals impurity ions in solid solutions (mixed crystals) is, usually, much larger than in single-component crystals and comparable to that observed in glasses of similar composition (see e.g. [1]). This broadening is due to structural disorder of the matrix caused by the random distribution of ions in the crystal lattice sites.

We present the results of spectroscopic studies of zero-phonon electronic transitions of Cr^{3+} and Ce^{3+} impurity ions in a series of $Lu_{3x}Y_{3-3x}Al_5O_{12}$ ($0<x<1$) and $Tb_{3z}Y_{3-3z}Al_5O_{12}$ ($0<z<1$) garnet solid solution crystals. The discrete sets of zero-phonon R-lines ($^2E–^4A_2$) of Cr^{3+} ions were observed in fluorescence spectra [2,3]. These R-lines do not experience strong inhomogeneous broadening. This effect is ascribed to high C_{3i} symmetry of $Cr^{3+}(Al^{3+})$ sites that allows only a limited number of non-equivalent Cr^{3+} centers in mixed Lu/Y or Tb/Y environment. Site-selective laser spectroscopy confirms the small number of non-equivalent Cr^{3+} centers existing in garnet solid solutions.

The disordered crystalline system in which impurity ions occupy high–symmetry sites provides a unique opportunity to study locally identical impurity centers inside mixed matrices of different composition. The energies and radiative lifetimes of ^2E states of locally identical Cr^{3+} centers inside the different Lu-Y-Tb Al mixed garnet matrices were studied. The observed dependences on Lu and Tb content are explained by the changes of the lattice parameter that are equivalent to lattice compression occurring under the high hydrostatic pressure or to fully symmetric lattice dilation which cannot be obtained by any other experimental technique. The lattice parameter changes are shown to occur in agreement with Vegard's law.

It was observed that the shifts of the R-lines of particular Cr^{3+} centers due to replacement of cations in the nearest positions and in more distant positions (via lattice compression or dilation) occur in opposite directions. The combination of these two kinds of spectrum modifications determines the Cr^{3+} spectra in solid solution garnets with different x and z.

[1] G.P. Morgan, T.J. Glynn, G.F. Imbusch, J.P. Remeika. J. Chem. Phys. **69**, 4859 (1978).
[2] S. Feofilov, A. Kulinkin, K. Ovanesyan, A. Petrosyan, C. Dujardin. Phys. Chem. Chem. Phys. **16**, 22583 (2014).
[3] S.P. Feofilov, A.B. Kulinkin, K.L. Ovanesyan, A.G. Petrosyan. Solid State Communications **226**, 39 (2016).

Superbroad NIR luminescence from bismuth doped crystals and glasses

Mingying Peng

The China-Germany Research Center for Photonic Materials and Devices, State Key Laboratory of Luminescent Materials and Devices, School of Material Science and Engineering, South China University of Technology, Guangzhou 510640, China

Infrared luminescent materials active in new spectral region of 1000-1600nm are of crucial importance to develop new fiber lasers and optical amplifiers, which could find potential applications such as in medicine, astrophysics, or next generation optical communication system [1-6]. Bismuth doped photonic materials were recently recognized as such a promising candidate which could luminesce in an extremely broad spectral range, that is, from 1000 to 1700nm, or even to 2000nm [1, 3]. In this talk, I am going to present our works on bismuth doped glasses and crystals in last decade, such as the unusual near to mid infrared luminescence at room temperature, the intriguing nature of the infrared luminescence etc [4-6]. In the end, I am going to show my opinion on whether the luminescence is from the intrinsic defects or bismuth itself.

[1] M. Peng, J. Qiu, D. Chen, X. Meng, L. Yang, X. Jiang and C. Zhu, Opt. Lett., **29**, 1998 (2004).
[2] E. Dianov, V. Dvoyrin, V. Mashinsky, A. Umnikov, M. Yashkov and A. Gur'yanovb, Quantum Electron. **35**, 1083 (2005).
[3] R. Cao, M. Peng, L. Wondraczek, and J. Qiu, Opt. Express **20**, 2562 (2012).
[4] J. Zheng, M. Peng, F. Kang, R. Cao, Z. Ma, G. Dong, J. Qiu, and S. Xu, Opt. Express **20**, 22569 (2012).
[5] J. Zheng, L. Tan, L. Wang, M. Peng, and S. Xu, Opt. Express, in press (2016).
[6] Z. Zhao, L. Wang, S. Xu and M. Peng, Opt. Lett., in press (2016).

The main role of extended lattice defects in the localization and interaction of Mn^{2+} ions in cubic ZnS quantum dots

S. V. Nistor, M. Stefan, L. C. Nistor, D. Ghica and I. D. Vlaicu

National Institute of Materials Physics, Atomistilor 105bis, Magurele-Ilfov, 077125 Romania

The properties of ultrasmall (1-3 nm size) cubic ZnS nanocrystals doped with Mn^{2+} ions (cZnS:Mn), known as quantum dots (QDs), have been the subject of intense scrutinity for more than two decades. Essential aspects, such as impurities incorporation in the core of QDs prepared by co-precipitation from solution, the presence of non-cubic lattice distortions at the sites of Mn^{2+} ions substituting the tetrahedrally coordinated Zn^{2+} lattice ions, or the influence of the core and surface localized activating ions on the observed optical and collective magnetism properties raised many unanswered questions. Based on correlated multifrequency electron paramagnetic resonance (MFEPR) and analytical high resolution transmission electron microscopy (HRTEM) investigations of cZnS:Mn QDs of improved crystallinity, self-assembled in mesoporous structures, we found out that the contained stacking lattice defects play an essential role in all these properties [1]. Thus, the Mn^{2+} ions are preferentially incorporated into the QDs core at Zn^{2+} cation lattice sites situated next to a lattice stacking defect, resulting in the presence of a local axial distortion and intense hyperfine forbidden transitions [2]. Such localization is attributed to a newly proposed extended lattice defects assisted (ELDA) mechanism of incorporation, which acts from the initial growth stages and is not limited to larger QDs, as in the case of the trapped dopant model [3] The ELDA mechanism of incorporation, i.e. the trapping of impurity ions at dislocation steps formed by the stacking defects emerging at the QDs surface, also explains the strong decrease in the core incorporation rate of the Mn^{2+} ions with their nominal concentration increase [4]. Quantitative MFEPR measurements show that up to the highest (50,000 ppm) nominal concentration level the Mn^{2+} ions are incorporated in the core and on the surface of cZnS:Mn QDs at isolated sites, in a diluted paramagnetic state characterised by dipolar magnetic interactions, excluding them as a possible source of collective magnetism [5,6].

[1] M. Stefan, S. V. Nistor, D. Ghica, in "*Size Effects in Nanostructures*"; V. Kuncser; L. Miu Eds.; Springer Series in Materials Science, vol. 205, part. 1, Springer: Berlin, Heidelberg, 3-27 (2014);
[2] S.V. Nistor, M. Stefan, L. C. Nistor, et al., *Phys. Rev. B*, 81, 035336 (2010);
[3]. D. J. Norris, A. L. Efros, S. C. Erwin, *Science,* 319, 1776 (2008);
[4] S. V. Nistor, M. Stefan, L. C. Nistor, et al., *J. Phys. Chem. C*, 119, 23781 (2015);
[5] S. V. Nistor, M. Stefan, D. Ghica et al., Phys. Rev. B 83, 045301 (2011);
[6] S. V. Nistor, M. Stefan, L. C. Nistor, et al., *J. Alloys Comp.,* 662, 193 (2016).

Collective magnetism from aggregated Mn^{2+} activating ions in self-assembled cZnS quantum dots at higher doping levels

M. Stefan, S. V. Nistor, L. C. Nistor, V. Kuncser and I. D. Vlaicu

National Institute of Materials Physics, Atomistilor 105bis, 077125 Magurele-Ilfov, Romania

The magnetic properties of cubic ZnS quantum dots (QDs) doped with Mn^{2+} impurity ions (cZnS:Mn) prepared by co-precipitation in a liquid solution, reported so far, are contradictory. While in some cases magnetic ordering was found for nominal Mn^{2+} concentration levels of 2.5 at% and higher [1,2], in other cases a paramagnetic behaviour was reported for concentration levels as high as 15 at% [3,4]. In recent quantitative electron paramagnetic resonance (EPR) studies on 2.9 nm size cZnS:Mn QDs we found out that up to 5 at% nominal impurity concentration the Mn^{2+} ions are incorporated at isolated sites in the core and in the surface layer, in a diluted paramagnetic state characterised by magnetic dipole-dipole interactions [5,6]. It has been suggested that the observed magnetism in such a diluted magnetic semiconductor could be due either to a large concentration of lattice ion vacancies, or to agglomerates of Mn^{2+} ions observed by EPR as a broad, structureless Lorentzian line superposed on the narrow lines of the core and surface localised impurity ions [7]. Here we present the results of a study concerning the structure, localisation and magnetic properties of the agglomerates of Mn^{2+} ions in cZnS:Mn QDs of 2.9 nm average diameter prepared by co-precipitation at several nominal impurity levels in the 0.02 at% to 5 at% range. The investigations were performed by multifrequency EPR, in correlation with analytical scanning high resolution transmission electron microscopy (HRTEM) and magnetometry. They evidence the formation of a Mn^{2+} rich, disordered phase, localised in the interstices and pores of the mesoporous structure of the self-assembled cZnS:Mn QDs, with magnetic properties depending on the doping level. Thus, the dominant magnetic interaction of the aggregated Mn^{2+} ions was found to be of a magnetic dipole-dipole type, with a simple Curie temperature dependence for nominal concentrations of up to 0.2 at%. At higher nominal concentrations the antiferromagnetic coupling between the Mn^{2+} ions becomes dominant, which corresponds to a Curie-Weiss temperature dependence.

[1] I. Sarkar, M. K. Sanyal, S. Biswas et al., *Phys. Rev. B* **78**, 224409 (2007)
[2] Z. H. Wang, D. Y. Geng, D. Li et al, *J. Mat. Res.* **9**, 2376 (2007)
[3] N. Tsuji, H. Kitazawa, G. Kido, *J. Appl. Phys*. **93**, 6957 (2003)
[4] W. Q. Peng, S. C. Qu, G. W. Cong et al., *J. Cryst. Growth* **282**, 179 (2005)
[5] S. V. Nistor, M. Stefan, L. C. Nistor et al., *J. Phys. Chem. C* **119**, 23781 (2015)
[6] S. V. Nistor, M. Stefan, L. C. Nistor et al., *J. Alloys Comp.* **662**, 193 (2016)
[7] M. Stefan, S. V. Nistor, D. Ghica et al., *Phys. Rev. B* **83**, 045301 (2011)

Investigation of point defects in HfO2 using Positron-Annihilation Spectroscopy: Internal Electric Fields impact

A. Chabli[2], M. Alemany[1,3,4], E. Oudot[1,3,5],N. Rochat[3], P. Desgardin[4], F. Bertin[3], M. Gros-Jean[1], M.-F. Barthe[4]

[1] STMicroelectronics, 850 rue Jean Monnet, 38926 Crolles, France.
[2] Univ. Grenoble Alpes, INES, F-73375 Le Bourget du Lac, France, CEA, LITEN, Department of Solar Technologies, F-73375 Le Bourget du Lac, France
[3] Univ. Grenoble Alpes, F-38000 Grenoble, CEA, LETI, MINATEC Campus, F-38054 Grenoble, France
[4] CNRS, CEMHTI UPR3079, Univ. Orléans, F-45071 Orléans, France.
[5]Univ. Grenoble Alpes, Lab. LTM (CEA-LETI/Minatec), 38000 Grenoble, France

The aggressive down scaling of the CMOS devices has required the introduction of numerous new materials and new processes. Thus the most advanced transistor generations, called High-k Metal Gate (HKMG), are based on the use of high-k dielectrics such as HfO2 and metallic layers such as TiN for the gate stack of the CMOS device. The HKMG structure raises new issues for the device performances. Among them the observed shift in the transistor threshold voltage [1] is usually assumed to be related to oxygen vacancies in the HfO2 material [2]. Positron annihilation spectroscopy (PAS) is the most sensitive method for the detection of vacancy defects and is intensively used to characterize such defects in a wide range of materials [3,4] with the possibility to detect them in thin layers using a slow positron beam [5,6]. It should allow to assess their effective role in the HKMG stack behaviours. [4]. However, very few studies are dedicated to high-k dielectrics [7].
In this work, we report on the PAS characterization of point defects in HfO2 layers deposited on a silicon substrate both by Physical Vapour Deposition (PVD) and by Atomic Layer Deposition (ALD) with a layer thickness ranging from 25 to 100 nm. The PAS measurements are performed using a slow positron beam coupled with the Doppler broadening spectrometry (DBS). The results show that DBS can be used on HfO2 layers with a thickness as thin as 25 nm and that PAS measurements are sensitive to the impact of the deposition process type and the post-deposition annealing on the defect concentration. Cathodoluminescence (CL) spectra are obtained at low temperature on the same samples. The intensity evolution of the CL peaks related to the material defects is discussed regarding the the PAS results. In addition, a built-in electrical field induced by charged defects located at the HfO2/Si interface as well as embedded in the HfO2 layer must be taken into account in the PAS data reduction [8]. Both non-contact internal electrical field measurements performed by Corona oxide characterization of semiconductor (COCOS) and internal electrical field simulations using the UTOX software [9] support the PAS finding. These results are an important step in the characterization by PAS of point defects in HfO2 layers used for the microelectronics device developments.

[1] K. Shiraishi, et al., in: "Proc. of SISPAD", 306–313 (2006).
[2] S. Guha and V. Narayanan, Physical Review Letters 98, 196101 (2007).
[3] F. Tuomisto, I. Makkonen, REVIEWS OF MODERN PHYSICS 85/4 1583-1631 (2013)
[4] D.W. Gidley et al., Annual Review of Materials Research 36, 49-79 (2006).
[5] P.E. Lhuillier, et al., Journal of Nuclear Materials 416, 13-17 (2011).
[6] P. Desgardin et al., Applied Surface Science 252, 3231–3236 (2006)
[7] Uedono, et al., Japanese Journal of Applied Physics 46, 3214-3218 (2007).
[8] M. Alemany et al., In International Conference on Frontiers of Characterization and Metrology for Nanoelectronics: 2015, edited by E. M. Secula and D. G. Seiler, Conference Proceedings, 118-121 (2015).
[9] UTOX regroups a series of k.p-Schrodinger-based tools including a KG solver. D. Garetto et al., Proc. Nanotech Conference (2010).

Hafnium dioxide luminescent nanoparticles: structure and emission control through doping and thermal treatments

A.Vedda[1], M. Fasoli[1], R. Lorenzi[1], I. Villa[1], A. Lauria[2], M. Niederberger[2], C. Dujardin[3], F. Moretti[3]

[1]Department of Materials Science, University of Milano-Bicocca, Via R. Cozzi 55, 20125 Milano, Italy.
[2]Laboratory for Multifunctional Materials, Department of Materials, ETH Zürich, Vladimir-Prelog-Weg 5, 8093 Zürich, Switzerland.
[3]Institut Lumière Matière, UMR5306, Université Claude Bernard Lyon1-CNRS, bâtiment Kastler, 10 rue Ada Byron 69622 Villeurbanne CEDEX, France

High density powder phosphors are of great interest in technological fields like imaging and ionizing radiation detection. The powder form is of choice when the material can hardly be synthesized as bulk single crystal by conventional techniques. This is the case of hafnium oxides having a melting point above 2500 °C. Moreover nanoscale dimensions are an important requirement for fabricating nanocomposites, in nanomedicine, and for the realization of optical ceramics. In this last field materials with cubic structure are foreseen since their isotropic optical response allow the minimization of light scattering at grain interfaces.

This work focuses on the synthesis, structural and optical investigation of HfO_2 nanoparticles obtained by non-aqueous sol-gel route. In a first investigation, particular attention was paid to doping with europium and with lutetium. Structure and morphology characterization by XRD, TEM/SEM, elemental analysis, and Raman/IR vibrational spectroscopies confirmed the occurrence of the HfO_2 cubic polymorph for dopant concentrations exceeding a threshold value of nominal 5 mol%, for either Lu^{3+}or Eu^{3+} [1].

The spectroscopic features of Ti^{3+} impurities have been recently analyzed by room temperature radio- and photo-luminescence, time resolved luminescence and scintillation experiments. In addition, we have detected an intrinsic blue emission peaking at 2.5 eV and exhibiting a fast photoluminescence decay time of a few nanoseconds. This emission is due to the presence of surface defects; its intensity, as well as that of an additional band peaking at 2.1 eV, can be varied by thermal treatments that lead to surface modifications and variations of particle dimensions. For temperatures between 500 and 650 °C, tuning of the bands intensities induces a white emission under 3.5 eV excitation. The results demonstrate that the control of intrinsic defects is a potential route to design the optical activity of a material at the nanoscale.

[1] A. Lauria et al., ACS Nano **7**, 7041 (2013).

Energy transfer and carrier multiplication in silicon nanoparticles embedded in silicon dioxide

I. Kamenskikh[1], D. Zhigunov[1], R. Kirkin[1], M. Bykov[1], A. Vasil'ev[2]

[1]*Faculty of Physics of Lomonosov Moscow State University, Leninskie Gory 1(2), Moscow 119991, Russia*
[2]*Skobeltsyn Institute of Nuclear Physics of Lomonosov Moscow State University, Leninskie Gory 1(2), Moscow 119991, Russia*

On the basis of energy band diagram of silicon nanoparticles in silicon dioxide ma-trix the interaction of light with such system is considered: the processes within silicon nanoparticles as well as those including the states of the matrix were analysed. The light absorption as well as impact excitation of nanoparticles by electrons in the oxide were taken into account. The density of states of the nanostructured system was constructed using the densities of states of the constituents with the account for the size of nanoparticles and their concentration. It was demonstrated that the absorption and luminescence quantum yield increase with the excitation energy up to ~ 6 eV is superlinear. Above 6 eV the luminescence yield drops due to the ionization of the nanoparticles. Impact excitation is shown to be the most efficient for the high-energy electrons created in silicon dioxide by VUV-photons.
The results of the simulation are compared with experimental ones obtained on multi-layered structures SiOx/SiO2, produced using PECVD technique.
Financial support of the RF Ministry of Science and Education grant under the agreement RFMEFI61614X0006 is gratefully acknowledged.

Radiation-induced defects, energy storage and release in nitrogen solids

E.Savchenko[1], I. Khyzhniy[1], S. Uyutnov[1], M. Bludov[1], A. Barabashov

G. Gumenchuk[2] and V. Bondybey[2]

[1]*Institute for Low Temperature Physics & Engineering, NASU, Kharkiv 61103, Ukraine*
[2]*Lehrstuhl für Physikalische Chemie II TUM, Garching b. München 85747, Germany*

The intense current interest to nitrogen solids is connected with the potential use of polynitrogen compounds as environment-friendly high energy density materials (HEDM). Second important aspect of interest is related to astrophysical research because nitrogen is one of the most abundant elements in the Universe. Despite a long history of solid N_2 spectroscopy such problems as defect production and defect-induced processes in this model wide band-gap (15.6 eV) insulating material remained almost unexplored until recently with the exception of N radical formation.

Here we present new trends in the study of radiation effects in nitrogen solids with a focus on the defect production, their properties and defect-induced processes. We have created a comprehensive technique that enabled us to detect both neutral and charged defects of both signs. An electron beam of variable energy was used to generate radiation defects and discriminate radiation-induced processes in the bulk and at the surface. Defect production and desorption were monitored using optical and current emission spectroscopy: cathodoluminescence (CL), the developed by our group nonstationary luminescence (NsL), as well as thermally stimulated luminescence (TSL) and exoelectron emission (TSEE) or optically stimulated luminescence (OSL) and exoelectron emission (OSEE) along with measurement of the total desorption yield. Our results show stabilization and accumulation of radiation defects – ionic centres of both signs (N_4^+[1], N_3^+, N_3^-), trapped electrons (up to 10^16 cm^{-3}) and radicals (N, N_3). Desorption of excited atoms in the $^4P_{1/2\text{-}5/2}$ states was detected for the first time. Previously we found desorption of the excited N_2^* molecules [2]. The basis of the processes observed are neutralization reactions: $N_4^+ + e^- \rightarrow N_2^* + N_2 + \Delta E_1$ and $N_3^+ + e^- \rightarrow N_2 + N^* + \Delta E_2$. The key role of N_3^+ center dissociative recombination in generation of point defects – N radicals, is suggested. A high value of N_3 electron affinity E_e (2.76 eV) results in efficient formation of N_3^- centres which are stable with respect to electron detachment. The centres were detected with OSEE technique. The part played by pre-existing and radiation-induced defects in energy storage is discussed.

The interaction of found polynitrogen species with metals and other elements opens up fresh way to low-temperature synthesis of a large family of nitrogen-based compounds.

[1] E.V. Savchenko, I.V. Khyzhniy, S.A. Uyutnov, A.P. Barabashov, G.B. Gumenchuk, M.K. Beyer, A.N. Ponomaryov, and V.E. Bondybey, J. Phys. Chem. A **119** 2475 (2015).

[2] E. Savchenko, I. Khyzhniy, S. Uyutnov, A. Barabashov, G. Gumenchuk, A. Ponomaryov, V. Bondybey, Phys. Stat. Sol. C, **12** 49 (2015).

Manipulation of high-energy particle beams by channelling and volume reflection in piezoelectric $LiNbO_3$

M. Bazzan[1], E. Bagli[2], V. Guidi[2], A. Mazzolari[2], L. Bandiera[2], G. Germogli[2], A. I. Sytov[2], D. De Salvador[1], N. Argiolas[1], A. Carnera[1], A. Berra[3], D. Bolognini[3], D. Lietti[3], M. Prest[3] and E. Vallazza[4]

[1]*Dipartimento di Fisica e Astronomia, Università di Padova, Via Marzolo 8, 35131 Padova, Italy and INFN Laboratori Nazionali di Legnaro, Viale dell'Università 2, 35020 Legnaro, Italy*
[2]*INFN Sezione di Ferrara, Dipartimento di Fisica e Scienze della Terra, Università di Ferrara Via Saragat 1, 44100 Ferrara, Italy*
[3] *Università dell'Insubria, via Valleggio 11, 22100 Como, Italy and INFN Sezione di Milano Bicocca, Piazza della Scienza 3, 20126 Milano, Italy*
[4] *INFN Sezione di Trieste, Via Valerio 2, 34127 Trieste, Italy*

In this talk we report on the feasibility of a device to steer highly energetic (up to hundreds of GeV) charged particle beams, by exploiting their interaction with a polar piezoelectric single crystal. This application is especially meaningful in large-scale circular accelerators such as the Large Hadron Collider (LHC).
Crystal-based steering devices are nowadays produced by mechanically bent single crystals, suitable for deflecting the particle beam by the channelling or volume reflection mechanisms. The same phenomena are here tested on $LiNbO_3$ single crystals. The idea is to take advantage from the pronounced piezoelectric coefficients of $LiNbO_3$ that allow for the realization of devices where the planes curvature can be conveniently tuned by use of properly designed electrodes, as we demonstrate by finite element piezo-elasticity simulations.
To test our idea, we performed some preliminary experiments at the Super Proton Synchrotron (SPS), one of the external lines at CERN, by using mechanically bent $LiNbO_3$ strips that were previously characterized by High Resolution X-Ray Diffraction and Rutherford Backscattering. The obtained results, interpreted with the help of the DYNECHARM++ Monte Carlo code, point out the key role of structural defects [1]. While the channelling efficiency for a proton beam at 400 GeV/c is low compared to other high-perfection crystals such as Si or Ge [2], the volume reflection phenomenon is demonstrated to be robust and exploitable for this kind of application, even using commercial samples which are characterized by a considerable dislocation density of 10^4 cm^{-2}.

[1] E. Bagli et al. Phys. Rev. Lett., **115**, 015503 (2015)
[2] E. Bagli et al., Phys. Rev. Lett., **110**, 175502 (2013)

Investigation of amorphisation energies of silicon carbide implanted with heavy ions

E. Friedland

Physics Department, University of Pretoria, 0002 Pretoria, South Africa

At ion energies with inelastic stopping powers ε_e < 1 keV/nm, irradiation damage is thought to be due to atomic displacements by elastic collisions only. However, it is well known that inelastic processes and non-linear effects can significantly increase or decrease damage efficiencies. The relative importance of these two opposing processes depends on the ion mass. For light ions the amorphisation energy of silicon carbide decreases strongly with increasing inelastic energy transfer, while non-linear effects should become more important with heavy ions and reduce the damage efficiency. To investigate this, damage profiles were obtained from α-particle channelling spectra of 6H-SiC wafers implanted at room temperature with ions in the mass range $84 \leq M \leq 133$, employing the computer code DICADA. Critical damage energies were extracted from the elastic energy transfers obtained from TRIM simulations at the experimentally observed boundary positions of the amorphous zones and compared with the corresponding inelastic energy deposition.

Nanoscale segregation of Ge nanoparticles in GeSiO and GeTiO amorphous films by RTA and UV laser pulse annealing

V.S. Teodorescu[1], A.V. Maraloiu[1], A. Kuncser[1], C. Ghica[1], M.L. Ciurea[1], A.M. Lepadatu[1], I. Stavarache[1], D.N. Scarisoreanu[2], M. Dinescu[2], M-G. Blanchin[3]

[1] National Institute of Materials Physics, 077125, Bucharest-Magurele, Romania
[2] National Institute of Lasers Plasma and Radiation Physics, 077125 Bucharest-Magurele, Romania
[3] ILM- Université Claude Bernard Lyon1, 69622 Villeurbanne Cedex, France

Ge nanocrystals embedded in dielectric oxide matrix are formed by RTA and laser pulse annealing of high Ge content mixed amorphous oxides. These systems have special application in memory devices. Amorphous GeSiO and GeTiO [1] films with different Ge/oxide ratio where produced by magnetron sputtering deposition on Si wafers. In these systems, Ge nanoparticles are formed during annealing by segregation of the Ge atoms via a nucleation and growth processes. The Ge nanoparticles can remain in amorphous state or become crystallized, depending on the temperature and the annealing method. The SiO_2 matrix remains amorphous after annealing, but the TiO_2 matrix crystallizes together with the Ge nanocrystals formation. In the case of GeSiO films, the Ge diffusion near the Si substrate interface is accompanied by an auto-organization effect of the Ge nanoparticles. This reveals the presence of the Ge nanoparticle interaction by a mechanism based on competition between Ge diffusion and segregation. The study of the nanoscale structure was investigated by HRTEM using TEM specimens prepared by cross section (XTEM). Depending of the Ge concentration in the as deposited films, the Ge segregation and the Ge diffusion is sensitive to the electron beam irradiation and the transformations can be followed in situ during the HRTEM observations. These oxide films were laser pulse annealed, using a low laser pulse fluences between 15 to 50 mJ/cm^2 and □□= 266 nm (the forth harmonics radiation of the Nd-YAG laser), The fluence values are less than the melting threshold of these oxide films. Formation of the Ge nanoparticles during laser pulse irradiation shows the presence of a very high diffusivity of the Ge atoms in the laser pulse field, similar to the diffusivity taking place in the liquid state.

[1]. Nanostructuring of GeTiO amorphous films by pulsed laser irradiation , V.S. Teodorescu, C. Ghica, A.V. Maraloiu, M. Vlaicu ,A. Kuncser, M.L. Ciurea, I. Stavarache, A. M Lepadatu, N.D. Scarisoreanu, A. Andrei · V. Ion · M. Dinescu, Beilstein Journal of Nanotechnology, **6** 893 (2015).

Study of point defects in as-drawn and irradiated Ge-doped optical fibers using cathodoluminescence

I. Reghioua[1], A. Alessi[1], D. Di Francesca[1], S. Girard[1], E. Marin[1], A. Morana[1], M. Fanetti[2], L. Martin-Samos[2], N. Richard[3], M. Raine[3], A. Boukenter[1], Y. Ouerdane[1]

[1] *Univ-Lyon, Laboratoire Hubert Curien, UMR CNRS 5516, Saint-Etienne, France*
[2] *Materials Research Laboratory, University of Nova Gorica, Vipavska 11c 5270-Ajdovscina, Slovenija*
[3] *CEA, DAM, DIF, F91297, Arpajon, France*

It is well known that Ge-doped optical fibers are among the most used in the telecommunication domain, due to the ability of the Ge doping in the fiber's core to increase its refractive index allowing the light guiding. Simultaneously, the presence of Ge atoms causes photosensitivity usable for the fiber Bragg grating inscription within the waveguides [1]. Recently, the optical fibers were integrated in harsh nuclear environment for data transfer, sensing, implying to study the point defects generation by different sources of radiations that cause a strong decrease of the fiber transmission. Investigations are today carried out combining both experimental and multiscale simulation methods, the new codes being validated by confrontation with experimental data [2].

We used the cathodoluminescence (CL) technique, which is considered as a powerful measuring mean to characterize both the existing defects before irradiation, and those generated by the probe electron beam (*electron energy ranging from 5 to 20keV, current ~nA*) during the CL measurements. Indeed, the CL allows us to obtain the *in situ* changes of the emission spectra (from 300 to 800 nm) and for various electron flux and fluencies.

For our investigation, we employed a Ge-doped multimode optical fiber allowing to investigate the impact of Ge concentration. In details, we studied the evolution, under electron irradiation, of the emission features of the fiber samples. One was the as-drawn fiber, the second was pre irradiated with an UV cw laser at 244 nm and the last one was irradiated at 9 MGy(SiO_2) -ray dose by using the Brigitte ^{60}Co source of SCK-CEN. Furthermore, taking advantage of the employed experimental set-up, which allows to perform spatially-resolved (<1µm) CL measures, we were able to investigate the emission evolution in the differently doped zones of the fiber. Our data indicate that (i) the CL spectra of our three samples are dominated by the 400 nm emission band related to the Germanium Lone Pair Center (GLPC) [1], (ii) the spatial distributions of this defect differ in the three fibers and (iii) the electron exposure decreases the GLPC concentration in all samples (pristine, UV and γ irradiated). A detailed study of these bleaching kinetics (resolution of ~1s) will be presented at the conference.

[1] Defects in SiO2 and Related Dielectrics: Science and Technology, edited by G. Pacchioni, L. Skuja, and D. L. Griscom (Kluwer Academic, Dordrecht, 2000).
[2] N.Richard, S.Girard, L.Giacomazzi, L.Martin-Samos, D.Di Francesca, C.Marcandella, A.Alessi, P.Paillet, S.Agnello, A.Boukenter, Y.Ouerdane, M.Cannas et R.Boscaino, "Coupled theorical and experimental studies for the radiation hardening of silica-based optical fibers" IEEE TNS **46** 1819 (2014).

Back to Program -- Th-O-6

Optical absorption and properties of emerald

E.E. Cuevas-Arizaca, T.K. Gundu Rao, S. Watanabe

Institute of Physics, University of São Paulo, São Paulo, SP, Brazil

Second to diamond, emerald is the most valued precious stone. It is a silicate mineral called beryl which belongs to ring silicates characterized by hexagonal rings of six SiO_4 tetrahedra. These rings form hollow columns in z-direction which can accommodate impurities. Emerald samples investigated here were acquired at a mine in Nova Lima, State of Minas Gerais, Brazil. They are found incrusted in shales.

The X rays diffraction pattern of the emerald sample compared to the standard one indicates that it is a emerald crystal. Optical measurements show a strong UV absorption (410 nm) plus bands at 625, 820 nm and infrared region. 820 nm absorption band was attributed to Fe^{2+} ion The band at 410 nm is due $^4A_{2g} \rightarrow {}^4T_{2g}$ transition and the band at 625 nm to the transition $^4A_{2g} \rightarrow {}^4T_{1g}$ in Cr^{3+} (Tanabe-Sugano diagram). The 820 nm absorption band is to the transition $^5T_{2g} \rightarrow {}^5E_g$ in due the Fe^{2+} ($3d^6$) ion

The room temperature EPR spectrum of natural emerald exhibits signals at around g equal to 1.992 and at g ~ 4.27. The signal at g = 1.992 is attributed to Fe^{3+} ion in a relatively high symmetry environment experiencing a weak crystal field. The line at g ~ 4.27 arises from an Fe^{3+} ion in a stronger crystal field arising from distortions of the environment.

Excitation mechanisms in activated CsI scintillators: comparison of Tl^+ and In^+ dopants

A. Belsky[1], C. Dujardin[1], A. Gektin[2], S. Gridin[1,3], I. Iskandarova[4], A. Scherbinin[5], N. Shiran[2], A. Vasil'ev[6]

[1] *Institut Lumière Matière, Université Claude Bernard Lyon 1-CNRS, UMR 5306, F-69622 Villeurbanne Cedex, France*
[2] *Institute for Scintillation Materials, 60 Nauki Avenue, 61001 Kharkov, Ukraine*
[3] *Department of Physics, Wake Forest University, Winston Salem, NC, USA*
[4] *Kintech Lab Ltd., 12, 3-ya Khoroshovskaya street, 123298, Moscow, Russia*
[5] *Faculty of Chemistry, Lomonosov Moscow State University, Leninskie Gory 1(3), Moscow 119991, Russia*
[6] *Skobeltsyn Institute of Nuclear Physics, Lomonosov Moscow State University, Leninskie Gory 1(2), Moscow 119991, Russia*

Centers with the same s^2 electronic configuration, like In^+ and Tl^+ in CsI can behave in a different way depending on the position of the levels, strength of electron-phonon coupling, etc. Comparative analysis of luminescent properties of these two emission centers in CsI lattice was done using fluorescence spectroscopy methods. The position of emission bands are about the same for both activators – one UV band around 400-420 nm and two visible ones at 500 nm and 550 nm (560 for CsI:Tl). Nevertheless, the widths of indium induced bands are smaller than of thallium ones, and the excitation spectra are quite different. In case of CsI:In crystals lower energy photons (around 310 nm) excite only low energy emission band (550 nm). Increase of the excitation energy results in appearance of 490 nm emission and then 420 nm one. On the contrary, in case of CsI:Tl crystals, all the three main emission bands are excited around the lowest energy absorption band at 295nm. For higher energies the emission at 400 nm region disappears and only two visible bands (490 nm and 550 nm) are present, which is consistent with other works [1, 2].

In order to investigate the excitation mechanism of these bands we perform calculation of ground and different excited and charge states in these systems using DFT with hybrid exchange-correlation functional. It is shown that due to different hybridization of s^2 states with iodine valence band states in case of In and Tl the minimum of the configurational parabola of charge transfer state Tl^0+h is lower than the minimum of excited Tl^+ parabola, in contrary with the situation in In centers. These calculations could explain the experimental results. The calculations also predict the microscopic structure of excited and ionized states of these centers.

[1] V. Sivasankar and P. W. M. Jacobs, Philos. Mag. Part B, **51,** 479 (1985).
[2] V. Nagirnyi, S. Zazubovich et al, Chem. Phys. Lett., **227,** 533 (1994).

Luminescence in doped and undoped $CaYAl_3O_7$ produced via the Pechini Method

G. F. C. Bispo[1], A. B. Andrade[1], V. C. Teixeira[2], M. E. G. Valerio[1]

[1]*Department of Physics, Federal University of Sergipe, São Cristóvão-SE, Brazil*
[2]*Brazilian Synchrotron Light Laboratory, National Center for Research in Energy and Material, Campinas – SP, Brazil*

$CaYAl_3O_7$ (CYAM), like other Y-containing crystalline matrixes, has been studied as a host for rare earth (RE) ions due to its luminescence properties. Several potential applications have been pointed as sensing structural damage, solid-state light source for white LED's and temperature sensors. In this work, Pechini method was used to produce CYAM undoped and doped with Eu^{3+}, Tb^{3+}, Ce^{3+} and Sm^{3+}in order to produce white light. Thermal analysis results combined with XRD measurements showed that 1000°C/4h is the best condition for the CYAM synthesis. Morphological analyse by scanning electron microscopy (SEM), shown submicrometric particles with irregular shape. Photoluminescence (PL) studies were carried out by exciting samples in a range from near-ultraviolet (NUV) to vacuum ultraviolet (VUV). Furthermore, absorption and excitation spectra measured in the same range allowed a study about changes in band structure caused by doping with different rare earth ions. Undoped CYAM sample showed complex emission spectra related with the presence of F and F+ centres besides self-trapped exciton (STE). The fundamental interband transition was found to be around 8eV. The CYAM:Ce^{3+} sample showed a emission broad band centred at 2.88eV(430nm) related with $^5d_1 \rightarrow {}^2F_{7/2;5/2}$ transitions and in CYAM:Sm^{3+} the typical transitions $^4G_j \rightarrow {}^6H_j$ were observed. For CYAM:Tb^{3+}, $^5D_4 \rightarrow {}^7F_6$, $^5D_4 \rightarrow {}^7F_4$ and $^5D_4 \rightarrow {}^7F_2$ emissions are observed and in CYAM:Eu^{3+}, $^5D_0 \rightarrow {}^7F_2$ emission is more intensity than $^5D_0 \rightarrow {}^7F_1$ emission, both due the low local symmetry in Ca/Y site. In addition, excitation spectra of Ce^{3+} and Tb^{3+}-doped samples present the RE typical transitions besides interband transition of undoped material. Charge transfer band (CTB) localized in 5.32eV and 4.04eV were observed for Sm^{3+} and Eu^{3+}-doped samples, respectively. All these information allowed the proposal of a model including the positions of the energy levels of the dopants as well as the F, F+ and STE transitions.

Acknowledgments: The authors are thankful to CNPq, CAPES, FINEP and FAPITEC-SE funding agencies and to LNLS, CMNano-UFS for the measurements in VUV and the SEM analysis, respectively.

Structural, electronic and optical properties of intrinsic and extrinsic defects in $LiNbO_3$

S. Sanna[1], W. G. Schmidt[1]

[1]*Department Physik, Universität Paderborn, 33095 Paderborn, Germany*

Lithium niobate ($LiNbO_3$) is one of the most prominent optical materials and is vastly employed, among others, for quantum information applications, surface acoustic waves devices, holographic data storage and optical filters. The ferroelectric and optical properties of the material can be modified to a large extent by ion doping. Iron doping is e.g. employed to enhance the photorefractive effect, while with titanium doping it is possible to increase the refractive index [1].

Unfortunately, our knowledge of the doping defect centres at the microscopic level is very poor. Few theoretical investigations are available, and the picture that arises from these works is far from being conclusive. In this work, we present a quantitative microscopic description of intrinsic and extrinsic defects in $LiNbO_3$, including polaronic centres such as $Nb_{Li}^{4+/5+}$, $Fe_{Li}^{2+/3+}$ as well as Ti and Zr related defect centres. Spin-polarized density functional theory with Hubbard corrections is employed to investigate the atomic structure around dopants.

The main intrinsic defects as well as dopants in realistic concentrations are discussed in regard to their structural, electronic, ferroelectric and optical properties. The theoretical models are compared with available experimental results [2], providing clear evidence for the polaronic distortion upon $Nb_{Li}^{4+/5+}$ and $Fe_{Li}^{2+/3+}$ charge transition. The calculated atomic and electronic structures allow for a detailed consideration of the microscopic processes leading to the optical absorption, as well as the extrapolation of data that can be employed in the classic polaronic theory. The change of the optical absorption upon doping with different ions is demonstrated and discussed.

[1] F. Schirmer et al., *Bulk photovoltaic effect of $LiNbO_3$:Fe and its small-polaron-based microscopic interpretation*, Phys. Rev. B **83**, 165106 (2011).

[2] Sanson *et al.*, Polaronic deformation at the $Fe^{2+/3+}$ impurity site in Fe:$LiNbO_3$ crystals, Phys. Rev. B **91**, 094109 (2015).

Location of the Tb^{3+} and Eu^{3+}energy levels in Y_2O_2S under high hydrostatic pressure

M. Behrendt, S. Mahlik, K. Szczodrowski, B. Kukliński, M. Grinberg

Institute of Experimental Physics, University of Gdansk, Wita Stwosza 57, 80-952 Gdańsk, Poland

Although the universal behaviour in the energy of the ground state of $4f^n$ electronic configuration with n can be determined, [1] it is not easy to estimate these energies with respect to the band edges. However when positions of one the Ln^{2+} and one of the Ln^{3+} with respect to the bandedges are known this universal rule allows to predict the positions of the ground states of other ions.

In this contribution it is discussed how unique experimental technique ; the high pressure spectroscopy can be used for determination of the positions of the Ln^{3+} and Ln^{2+} energy levels in the bandgap of the host. We present spectroscopic characterization of $Y_2O_2S:Tb^{3+}$and $Y_2O_2S:Eu^{3+}$. The luminescence, luminescence kinetics and excitation spectra were measured under pressure up to 250 kbar. We found that pressure caused quenching of the Tb^{3+} luminescence from the $^5D_3$ excited level, whereas in the case of Eu^{3+} additional luminescence related to the transitions from the $^5D_3$ state appeared under pressure. These effects were related to decrease of ionization energy of Tb^{3+} and increase of charge transfer energy in Eu^{3+} caused by pressure that induces the rise of the energies of the divalent and threevalent lanthanide ions with respect to the band edges. Analysis of the emission and excitation spectra allowed to estimate the location of the ground states of Tb^{3+} and Eu^{3+} and then all other Ln^{3+} and Ln^{2+} ions in the bandgap of Y_2O_2S host.

[1] P. Dorenbos, *Phys. Rev. B*, **85** 165107 (2012)

Novel defects' luminescence based g-YAB phosphors for high CRI white light generation

Atul D. Sontakke[1], Vinicius F. Guimarães[2], Lauro Maia[3], Pauline Burner[2], M. Salaun[2], Isabelle Gautier-Luneau[2], Alban Ferrier[1], Bruno Viana[1], and Alain Ibanez[2]

[1]*PSL Research University, Chimie-Paristech, CNRS, IRCP, 75005 Paris, France*
[2]*Inst NEEL, CNRS & UGA, F-38042 Grenoble, France*
[3]*Instituto de Física, Universidade Federal de Goiás, Goiânia/GO, Brazil*

In view of the recent lanthanides crisis, several allied industries, primarily phosphors, magnets, etc., are looking for new alternatives for the lanthanide elements [1]. Phosphors top this list owing to its core dependence, and gradually shifting the attention to other paramagnetic centers, such as the *d*-block active ions as in $K_2SiF_6:Mn^{4+}$ and $SrB_4O_7:Bi^{2+}$ commercial phosphors. Certain insulating materials with defects also show broadband visible luminescence that can be useful for phosphor application.

Recently, we observed that the amorphous yttrium aluminoborates (g-YAB) obtained by polymeric precursor (Pechini) method exhibits intense emissions of defect-related luminescence under near UV excitation covering the whole visible range [2]. Figure 1a presents the luminescence spectra of g-YAB powders. Both luminescence intensity and spectral shape show strong dependence on the annealing temperature. Amongst, the 740-750 °C annealed g-YAB reveals intense white luminescence (Fig. 1b). These g-YAB powders exhibit high luminescence quantum yield (*i*-QY) of about 90% (λ_{ex} : 365 nm) and the color rendering index (CRI) of about 94, suggesting their potential for high efficacy, high CRI white light phosphors for solid-state lighting under UV LEDs excitation. Further study on understanding of luminescence mechanism is in progress through detailed investigation of the defects centers present in g-YAB using various spectroscopic techniques.

(a)

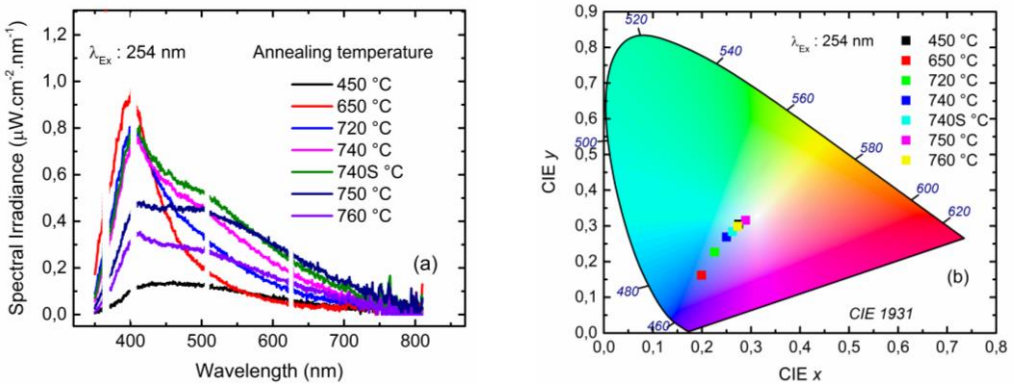

Figure 1: Photoluminescence, and (b) color chromaticity of g-YAB phosphors.

[1] http://www.paristechreview.com/2013/02/12/earth-metals-geostrategy/
[2] V. F. Guimarães, *et al.*, *J. Mater. Chem. C*, **3**, 5795 (2015).

Optical properties of $K_2(Si,Ge)F_6:Mn^{4+}$ at ambient conditions and high pressure

T. Lesniewski[1], S. Mahlik[1], A. Lazarowska[1], B. Kuklinski[1], M. Grinberg[1], Chun-Che Lin[2], Ru-Shi Liu[2,3]

[1] *Institute of Experimental Physics, University of Gdansk, Wita Stwosza 57, 80-952 Gdansk, Poland*
[2] *Department of Chemistry, National Taiwan University, Taipei 106, Taiwan*
[3] *Department of Mechanical Engineering and Graduate Institute of Manufacturing Technology, National Taipei University of Technology, Taipei 106, Taiwan*

In this work we present optical properties of $K_2(Si_{1-x}Ge_x)F_6:Mn^{4+}$ (x=0, 0.25, 0.5, 0.65, 1) at ambient conditions and at high pressure up to 20 GPa. $K_2(Si,Ge)F_6:Mn^{4+}$ is an efficient red phosphor emitting in 610 – 650 nm spectral range which has cubic or hexagonal crystal structure depending on chemical composition. Luminescence excitation and emission spectra as well as luminescence kinetics (TRES) measurements of $K_2(Si,Ge)F_6:Mn^{4+}$ were performed at ambient conditions and high pressure. Luminescence excitation spectra consist of two broad bands attributed to the $^4A_{2g} \rightarrow {}^4T_{2g}$ and $^4A_{2g} \rightarrow {}^4T_{1g}$ transitions. Luminescence emission spectra consist of several lines attributed to the phonon assisted $^2E_g \rightarrow {}^4A_{2g}$ transition. Depending on composition additional line attributed to the $^2E_g \rightarrow {}^4A_{2g}$ zero phonon transition is either present (x=0,5, 0.65) or not present (x=0, 0.25, 1) at ambient conditions.
Under influence of high pressure $^4A_{2g} \rightarrow {}^4T_{2g}$ and $^4A_{2g} \rightarrow {}^4T_{1g}$ excitation bands shift towards shorter wavelengths whereas $^2E_g \rightarrow {}^4A_{2g}$ emission band shifts towards longer wavelengths. The location of excitation and emission peaks allowed us to calculate Racah parameters B, C and crystal field strength parameter Dq as well as their dependence on pressure. This enables full characterisation of electronic structure of Mn^{4+} in $K_2(Si,Ge)F_6$ at ambient conditions and high pressure.
Compressing the materials also induces changes in luminescence spectra which remain present even after decompression, namely appearance (x=0, 0.25) and disappearance (x=0.65) of zero phonon line as well as permanent shift of emission spectra (x=0.5, 0,65). Surprisingly, no permanent pressure induced phase transitions occur in the materials as evidenced by Raman spectra of the decompressed samples. We conclude that changes in emission spectra are a result of local change of structure in the vicinity of Mn^{4+} ions.

In situ Fe K-edge X-Ray Absorption Spectroscopy (XAS) study during cycling of Li_2FeSiO_4 and $Li_{2.2}Fe_{0.9}SiO_4$ Li ion battery materials

Nanami Yokota[1] Alexander W. Brownrigg,[1,2,3] Gavin Mountjoy,[1] Alan V. Chadwick,[1] Wim Bras,[2] Robert A. Armstrong,[4] Peter G. Bruce,[5] Robert Dominko,[6] and Erik M. Kelder[3], Matteo Hogan[1], Maria L. Alfredsson[1]

[1]*School of Physical Sciences, Ingram Building, University of Kent, Canterbury, Kent, CT2 7NH*
[2]*Netherlands Organisation for Scientific Research (NWO), DUBBLE, ESRF Grenoble 38042, France*
[3]*Delft University of Technology, Chemical Engineering, Julianalaan 136, 2628 BL, Delft, The Netherlands*
[4]*School of Chemistry, University of Saint Andrews, Fife KY16 9ST, St Andrews, UK*
[5]*Department of Materials, University of Oxford, Parks Road, Oxford, OX1 3PH, UK*
[6]*Laboratory for Materials Electrochemistry, NIC, Hajdrihova 19, SI-1000, Ljubljana, Slovenia*

X-Ray Absorption Spectroscopy (XAS) is a powerful tool, which can be used to study the atomic local structure as well as oxidation state during battery cycling. Hence, XAS can be used to provide detailed atomic information for improvement of materials design.
Here we present in situ XAS results for Li_2FeSiO_4 and $Li_{2.2}Fe_{0.9}SiO_4$, promising cathode materials for lithium-ion batteries. It provides a low cost solution and is considered as a safe electrode material for future electric transportation, as the Si–O bond provides stability similar to the P – O bond in $LiFePO_4$ compounds. In theory, it is possible to remove two Li ions from Li_2FeSiO_4, by utilizing both Fe^{+2}/Fe^{+3} and the Fe^{+3}/Fe^{+4} redox couples and, thus, producing a higher capacity than 166 $mAhg^{-1}$ for one Li ion. Although capacities greater than 200 $mAhg^{-1}$ it has yet to be clarified whether it was due to Fe^{+4} formation or electrolyte degradation.

The aim was to establish the valence and local structure of Fe during charge and discharge. The valence state changes between Fe^{+2} and Fe^{+3}, with no evidence of Fe^{+4} before the onset of electrolyte degradation. There is a reversible contraction and extension of the Fe–O bond lengths during cycling while the Fe-Si distance remains constant, which underlines the stability of the Li_2FeSiO_4 material. The same observations apply to $Li_{2.2}Fe_{0.9}SiO_4$ cathode material indicating that changing the stoichiometry does not provide any additional structural stability.[1]

[1] A.W. Brownrigg, G. Mountjoy, A.V. Chadwick, M. Alfredsson, W. Bras, J. Billaud, A.R. Armstrong, P.G. Bruce, R. Dominko and E.M. Kelder, J. of Mater. Chem. A, 2015, 3, 7314-7322

Lithium fluoride thin film detectors for low-energy proton beam mapping by photoluminescence of colour centres

R.M. Montereali[1], A. Ampollini[1], L. Picardi[1], C. Ronsivalle[1], F. Bonfigli[1], S. Libera[1], E. Nichelatti[2], M. Piccinini[1], M.A. Vincenti[1]

[1]*ENEA C.R. Frascati, Fusion and Technologies for Nuclear Safety and Security Department, Via E. Fermi 45, 00044 Frascati (Rome), Italy*
[2]*ENEA C.R. Casaccia, Fusion and Technologies for Nuclear Safety and Security Department, Via Anguillarese 301, 00123 S. Maria di Galeria (Rome), Italy*

Luminescence properties of point defects in insulating materials are successfully used for solid state light sources and dosimeters. Among them, broad-band light-emitting F_2 and F_3^+ colour centres (CCs) in lithium fluoride, LiF, are well known for their application in tuneable lasers and radiation imaging detectors [1]. Under blue optical pumping in their overlapping absorption bands, the efficient photoluminescence spans the green-red visible spectral range. Novel LiF thin-film radiation imaging detectors based on the exploitation of the peculiar spectral characteristics of F_2 and F_3^+ defects and of the radiation sensitivity of the LiF material have been proposed and successfully applied for extreme ultraviolet, soft and hard X-ray imaging [1].
Recently, their use has been successfully extended to proton beam advanced diagnostics [2]. Optically transparent LiF thin films thermally evaporated on glass and Si(100) substrates were used for direct imaging of proton beams of energy from 1.4 to 7 MeV produced by a linear accelerator (TOP-IMPLART) under development at ENEA C.R. Frascati. The proton irradiation of LiF films induces the local formation of stable CCs, mainly the primary F centres and the aggregate F_2 and F_3^+ ones.
After exposure of LiF films perpendicularly to the proton beams, their transversal spatial distributions were measured by reading in a conventional optical microscope the latent two-dimensional (2-D) fluorescence images stored in the LiF thin layers by local formation of optically active defects.
Placing a cleaved LiF film so that its top surface is parallel to the direction of the impinging proton beams, the photoluminescence 2-D images of such top surface allowed to directly obtain the depth profile of the energy released by protons, which mainly lose their energy at the end of the path. The measured values of the Bragg peak positions were found in satisfactory agreement with SRIM (The Stopping and Range of Ions in Matter) software simulations, taking into proper account the polycrystalline nature of the LiF films.
These results are very encouraging for dose mapping of proton beams at high spatial resolution with LiF film detectors based on radiation-induced luminescent CCs.

[1] R.M. Montereali, F. Bonfigli, M. Piccinini, E. Nichelatti, M.A. Vincenti,, J. Lumin., **170** 761 (2016).
[2] M. Piccinini, F. Ambrosini, A. Ampollini, L. Picardi, C. Ronsivalle, F. Bonfigli, S. Libera, E. Nichelatti, M.A. Vincenti and R.M. Montereali, App. Phys. Lett., **106** 261108 (2015).

Scintillators based on the Ce^{3+} doped single crystalline films of multicomponent garnets: new trends and new challenges

Yu. Zorenko[1], V. Gorbenko[1,2], T. Zorenko[1], K. Paprocki[1], T. Martin[3], P.-A. Douissard[3], P. Bilski[4], A. Twardak[4], O. Sidletskiy[5], B. Gryniov[5], A. Fedorov[6], V. Laguta[7], J.A. Mares[7], M. Nikl[7], A. Suchocki[1,8], Ya. Zhydachewskii[8]

[1]*Institute of Physics, Kazimierz Wielki University in Bydgoszcz, Bydgoszcz, Poland*
[2]*Electronics Department, Ivan Franko National University of Lviv, Lviv, Ukraine*
[3]*European Synchrotron Radiation Facility, Grenoble, France;*
[4]*Institute of Nuclear Physics, Polish Academy of Science, Krakow, Poland*
[5]*Institute of Scintillation Materials, National Academy of Sciences of Ukraine, Kharkiv, Ukraine*
[6]*SSI Institute for Single Crystals, National Academy of Sciences of Ukraine, Kharkiv, Ukraine*
[7]*Institute of Physics, Academy of Science of Czech Republic, Prague, Czech Republic*
[8]*Institute of Physics, Polish Academy of Science, Warsaw, Poland*

This report presents our latest achievements in the creation and investigation of new types of single crystalline film (SCF) scintillators based on the solid solution of Ce^{3+} doped $A_{3-x}B_xAl_{5-x}Ga_xO_{12}$ (A, B = Gd, Lu,Tb and their combination) multicomponent garnets at x=0÷3.0 and y= 1.5÷3.5, using the liquid phase epitaxy (LPE) method. The development of SCF scintillators with extremely large X ray absorption ability and high light yield (LY) is now a hot research field directed to the creation of screens for X-ray imaging with submicron spatial resolution [1]. For this purpose two novel concepts for creation of SCF scintillators have been proposed recently: 1) engineering „K-edge of X-ray absorption" of scintillator using solid-solution of Gd, Tb and Lu containing compounds [2]; 2) development of complex multilayer scintillators with separate pathway for registration of the optical signal from each film scintillator. We have found that all SCF of the mentioned garnet compounds can be grown both from PbO and BaO based fluxes mainly onto $Gd_3Al_{2.5}Ga_{2.5}O_{12}$ (GAGG) substrates; part of them can be also crystallized onto $Y_3Al_5O_{12}$ (YAG) substrates. The detailed comparison between the luminescent and scintillation properties of $A_{3-x}B_xAl_{5-y}Ga_yO_{12}$:Ce SCF; A=Gd, Lu, Tb, grown from PbO and BaO fluxes, was performed for estimation of the influence of flux related dopants on the optical properties of these SCFs. Taking into account that the SCF scintillators with different content can be grown onto high-quality $Gd_3Al_{2-2.5}Ga_{3-2.5}O_{12}$:Ce substrates as bulk scintillators, we can consider also the LPE-prepared *new types of phoswich detectors* for simultaneous registration of the different components of mixed ionization fluxes. Due to the precise composition engineering of the SCF content and the presence of the efficient $Gd^{3+}\rightarrow Ce^{3+}$, $Tb^{3+}\rightarrow Ce^{3+}$ and $Gd^{3+}\rightarrow Tb^{3+}\rightarrow Ce^{3+}$ energy transfer processes in the mentioned garnet hosts, we have observed strong LY increase in SCFs of selected compositions in comparison with LuAG:Ce SCF counterpart. Namely, we have found that from all the studied SCF compositions at x=0÷3 and y=1.5÷3.5 the best scintillation properties are realized in the $Gd_{1.5}Lu_{1.5}Al_{2.75-2.5}Ga_{2.25-2.5}O_{12}$ and $Tb_{1.5}Gd_{1.5}Al_{2.75-2.5}Ga_{2.25-2.5}O_{12}$ SCFs whose LY under α–particle excitation overcomes by 1.5-1.6 times the LY of the best reference LuAG:Ce SCF sample [3]. The LY of these SCF scintillators is comparable with the LY of high performance $Gd_3Al_{2-2.5}Ga_{3-2.5}O_{12}$:Ce bulk crystals but the decay kinetics of SCF is notably faster due to elimination of various electron traps caused by garnet host defects at low temperature LPE crystallization. The role of Ga^{3+} co-doping in the efficiency improvement of the energy transfer processes in Ce^{3+} doped $A_{3-x}B_xAl_{5-x}Ga_xO_{12}$ (A, B = Gd, Lu,Tb) SCFs will be discussed. We found that the preference in the distribution of Al^{3+} and Ga^{3+} cations in the octahedral and tetrahedral sublattices, respectively, strongly influences the luminescent and scintillation properties of SCF of different garnet compositions.

This work was realized within the Polish NCN 2012/07/B/ST5/02376, Ukrainian F64/44, SL-20F and Czech Science Foundation No. 16-15569S projects.

[1] T. Martin, A. Koch, Journal of Synchrotron Radiation, 13 (2006) 180.
[2] F. Riva, P-.A.Douissard, T. Martin, Y. Zorenko, C. Dujardin, CrystEngComm, 18 (2016) 608.
[3] P.-A. Douissard, T. Martin, F. Riva, Y. Zorenko, et all, Proc. SCINT2015, San-Francisco, 2015.

An X-Ray Absorption Study of Ball-Milled Lithium Titanate and Tantalate

A.V. Chadwick[1], M. Wilkening[2]

[1] *School of Physical Sciences, University of Kent, Canterbury, Kent CT2 7NH, UK*
[2] *Institute for Chemistry and Technology of Materials, Graz University of Technology, Stremayrgasse 9, 8010 Graz, Austria*

High-energy ball-milling is a very convenient and fast method of preparing materials with crystallite sizes in the tens of nanometre regime [1]. This method has been used to produce a wide range of nanomaterials and in particular metal oxides. However, the microstructure of the oxide samples formed is often quite complex, being a mixture of both crystalline and amorphous material. The amorphous phase will not be detected by diffraction techniques but is seen in X-ray absorption spectroscopy (XAS) measurements, a powerful method of studying local atomic structure. A good example of the differences between ball-milled and sol-gel prepared nanomaterials is available from studies of zirconia, ZrO_2. Sol-gel produced 5 nm zirconia gives an XAS scan that is virtually identical to the bulk material, indicating low levels of disorder [2]. In contrast, zirconia ball-milled to 15 nm produced a highly attenuated XAS spectrum, indicative of very high levels of disorder.
Lithium titanate, Li_2TiO_3, and lithium tantalate, $LiTaO_3$, are ternary oxides that are being studied for a range of applications including electrodes for lithium-ion batteries. These oxides in normal bulk form do not have the high lithium ion mobilities required for a practical battery. However, ball-milling can increase the ionic conductivity of both materials be a few orders of magnitude [4, 5]. In this contribution we will report new XAS studies of the local structure of these materials and discuss the results in terms of the enhanced lithium ion mobility.

[1] Heitjans, P. and Indris, S., *J. Phys. Cond. Matter,* **30**, 1257 (2003).
[2] Rush, G.E., Chadwick, A.V., Kosacki, I. and Anderson, H.U., *J. Phys. Chem.,* **104**, 9597 (2000).
[3] Chadwick, A.V., Pooley, M.J., Rammutla, K.E. Savin, S.L.P. and Rougier, A., *J. Phys., Cond. Matter,* **15**, 431 (2003).
[4] Brandstaetter, H., Wohlmuth, D., Bottke, P., Pregartner, V. and Wilkening, M., *Z. Phys. Chem.,* **229**, 1363 (2015).
[5] Wilkening, M., Epp, V., Feldhoff, A. and Heitjans, P., *J. Phys. Chem.,* **112**, 9291 (2008).

Persistent luminescence in powdered and ceramic polycrystalline $Gd_3Al_2Ga_3O_{12}$:Ce

G. Dosovitskiy[1], A. Dosovitskiy[1], A. Fedorov[2], M. Korjik[2,3], V. Mechinsky[3], A. Borisevich[3], E. Tret'jak[4]

[1]*NeoChem, Moscow, Russia*
[2]*Radiation Instruments and New Components, Minsk, Belarus*
[3]*Research Institute for Nuclear Problems, Minsk, Belarus*
[4]*Research Institute for Chemical Problems, Minsk, Belarus*

Scintillator crystals and phosphors based on Ce-activated mixed garnets $RE_3(Al,Ga)_5O_{12}$ get increasing interest recent years, as they allow to tune their luminescent and scintillation properties by varying composition, particularly – Al/Ga ratio in solid solution. There are two mechanisms for that – change of crystal field strength and symmetry around activator ions and shift of Ce^{3+} emitting levels energy relative to the conduction band bottom. Furthermore, separation of genetically linked charge carrier pairs is suppressed in solid solutions, which leads to scintillation light yield increase.

The impressive light yield of 55000 Ph/MeV was obtained for $Gd_3Al_2Ga_3O_{12}$:Ce transparent ceramic[1] and single crystal scintillators[2]. At the same time, garnets with Al/Ga solid solution turned out to be promising materials for phosphors with persistent luminescence. Strong persistent luminescence was observed in $Y_3Al_2Ga_3O_{12}$:Ce,Cr ceramic samples. Moreover, strong persistent luminescence was observed for $Gd_3(Al,Ga)_5O_{12}$:Ce single crystals with different Al/Ga ratio, grown from raw materials of 99,995% or better purity. High level of phosphorescence is a major drawback in application of this material in scintillation detectors, so studying this effect and its minimizing is a mandatory and an important issue for its future application.

In order to define an origin of persistent luminescence in $Gd_3Al_2Ga_3O_{12}$:Ce we have examined spectroscopic properties of powder samples (coprecipitated, annealed at 1000-1600 °C) and ceramics, made of these powders. It was found, that persistent luminescence emerges with increase of material crystallinity. Mechanism of persistent luminescence origin in Ce^{3+} doped mixed gadolinium-aluminium-gallium garnet compounds is discussed.

[1] Z.M. Seeley, N.J.Cherepy, S.A.Payne., J. Cryst. Growth, **379,** 79 (2013).
[2] K. Kamada, S. Kurosawa, P. Prusa et al., Opt. Mater., **36**, 1942 (2014).

Using Two Photon Laser Scanning Microscopy to reveal the fate of USPIO nanoparticles in an atherotic murine model

VA Maraloiu[1], F Appaix[2], A Broisat[3], D Le Guellec[4], VS Teodorescu[5], C Ghezzi[3], B van der Sanden[4], MG Blanchin[1]

[1] *Institut Lumière Matière, UMR 5306 Université Claude Bernard Lyon1- CNRS, Université de Lyon, 69622 Villeurbanne, cedex, France*

[2] *Two-Photon Microscopy Platform, IBiSA-ISdV, Grenoble Institute of Neuroscience INSERM U836, UJF, Grenoble, France*

[3] *Radiopharmaceutiques Biocliniques Lab., Faculté de Médecine, La Tronche, France*

[4] *Clinatec, INSERM UA 01, Grenoble, France*

[5] *Institut de Biologie et Chimie des Protéines, LBTI, UMR 5305, CNRS / University of Lyon 1, Lyon, France*

[6] *National Institute of Materials Physics, Magurele, Bucharest, Romania*

Cardiovascular inflammatory lesions represent a major health issue in Western countries. The lesions are currently examined by Magnetic Resonance Imaging (MRI) of which the resolution and contrast can be improved using **nanosized selective contrast agents.** Atherosclerotic lesions of the mouse's aorta were studied by means of ultrasmall superparamagnetic iron oxide (USPIO) contrast agents having a maghemite (γ-Fe2O3) core and an organic envelop for targeting (P904 agent provided by GUERBET Laboratories, France).

The biolocalization and biotransformation of USPIO nanoparticles were analyzed through a multiscale approach combining **Two Photon Laser Scanning Microscopy** (TPLSM) and **High-Resolution Transmission Electron Microscopy** (HRTEM) at different times after intravenous injection in an atherosclerotic $ApoE^{-/-}$ mouse model.

TPLSM imaging of USPIOs uptake in aorta, kidneys, liver and spleen was performed and showed that some USPIOs were eliminated by kidneys and some accumulated in aorta, liver and spleen. TPLSM was shown to bridge the spatial resolution gap between MRI and electron microscopy since sampling for TEM studies could be monitored from bio-localization of USPIOs in both aortic plaque and spleen by TPLSM. This proved to be especially powerful to characterize the so tiny mouse's aorta. The phagolysosomal processing of the USPIOS in the mouse's aorta was then revealed for the first time at the subcellular level with atomic resolution thanks to TPLSM combined with TEM.

The present study demonstrated the transformation of UPSIOs iron oxide core in ferritin, characterized by combination of HRTEM imaging and SAED in a same phagolysosome. That combination revealed the spatial and structural parentship of maghemite, ferrihydrite and intermediate phases in a same lysosome.

Peculiarities of radiation damage caused by light and heavy ions in wide gap materials

A.Lushchik[1], A.Akilbekov[2], R.Assylbayev[1,2], E.Feldbach[1], K.Mizohata[3], J.Räisänen[3], E.Shablonin[1], E.Vasil'chenko[1]

[1]*Institute of Physics, University of Tartu, Ravila 14c, 50411 Tartu, Estonia*
[2]*L.N. Gumilyov Eurasian National University, Munaitpasov 5, 010008 Astana, Kazakhstan*
[3]*Department of Physics, University of Helsinki, P.O. Box 43, Helsinki, Finland*

Radiation-induced structural defects strongly affect the functionality of many inorganic wide gap materials (WGMs, E_g > 5 eV). Therefore, the understanding of the mechanisms of defect creation as well as promising ways of increasing the radiation resistance of construction and functional WGMs are of fundamental importance. Besides elastic collisions of incident particles with the crystal nuclei (the knock-out mechanism), the decay/recombination of different electronic excitations (EEs) is responsible for the creation of stable Frenkel defects (interstitial-vacancy pairs, i-v) under irradiation of WGMs with high-energy particles. In WGMs with high threshold energy for i-v formation ($E_{iv} > E_g$), the recombination of hot (non-relaxed) electron-hole pairs or the decay of long-lived core EEs cause the radiation damage of materials. The probability of hot e-h recombination significantly increases under irradiation conditions that provide extremely high density of EEs, e.g., in the cylindrical tracks of ~GeV heavy ions.

The present paper is devoted to a comparative study of radiation damage in WGMs caused by 0.23-GeV Xe^{132} ions (DC-60 cyclotron in Astana), 2.38-GeV Bi^{209} ions (UNILAC linear accelerator, GSI, Darmstadt) or 100-keV hydrogen ions (KIIA 500 kV implanter, Helsinki). According to the SRIM code, the used proton fluence (10^{17} cm^{-2}) causes in the irradiated layer (400-500 nm) of MgO target the damage level of ~0.5 dpa, while heavy ions spent more than 95% of their energy on ionization losses (LET > 20 keV/nm, ion range up to 100 μm). Cathodoluminescence spectra were used as a versatile diagnostic tool for radiation resistance of WGMs by applying the electron beam of adjustable energy (2-10 keV) that excited the full proton-irradiated depth of a sample (MgO, Al_2O_3, $MgAl_2O_4$). The stepwise annealing of the radiation-induced optical absorption (incl. vacuum ultraviolet spectral region) and the accompanying thermally stimulated luminescence were measured for several ion-irradiated WGMs.

Similar to neutron-irradiated $MgAl_2O_4$, there are some experimental proofs of the inversion of spinel crystals under irradiation with protons or Xe ions. Irradiation of CaF_2 crystals with Xe or Bi ions results in induced optical absorption at 2-10 eV, a part of which is not caused by X-rays. The ~9.7 eV band is tentatively connected with EEs nearby complex defects. The joint contribution of acoustic shock waves and EE-related mechanisms to ion-induced damage of WGMs as well as specificity of radiation damage (in nano- and macro-scale) in CaF_2 under irradiation by Bi^{209} ions with very high nuclear spin (I = 9/2) and tentatively enhanced track core are considered.

Identification of Vacancy defects in UO2 using Positron Annihilation Spectroscopy: a theoretical and experimental comparison

Y.Ma[1,2], J. Wiktor[2], M. Bertolus[2], G. Jomard[2], P. Desgardin[1], G Carlot[2], P. Garcia[2] and M.-F. Barthe[1]

[1] CEMHTI / CNRS, Université d'Orléans, Site cyclotron, 3A rue de la Férollerie, 45071 Orléans cedex 2, France
[2] DEN/DEC/SESC, CEA Cadarache, 13108 Saint Paul lez Durance, France

Uranium dioxide is currently the most widely used fuel material in fission reactors. During reactor operation, the fission of uranium atoms causes the formation of defects, such as vacancies and vacancy clusters, as well as the creation of fission products, which induce a significant evolution of the fuel physical properties. The vacancies can trap insoluble fission products, in particular fission gases and it is of great importance to understand their role in the early stages of the formation of gas bubbles in UO2. Separate effect experiments and atomic scale modeling can bring invaluable insight into the properties of defects and in the elementary mechanisms involved in the evolution of microstructure of materials which endure irradiation. Positron Annihilation Spectroscopy (PAS) is a nondestructive experimental method that allows studying open volume defects in solids.
In this work, Positron Annihilation Lifetime Spectroscopy (PALS) and Doppler broadening spectroscopy (DBS) have been performed using fast ^{22}Na sources and slow positron beams in UO_2 prepared and irradiated in various conditions. These experimental results are compared to the Positron lifetime and Doppler broadening calculated using two-component density functional theory [1]. Self-consistent calculations of positron characteristics have been carried out for vacancies and vacancy clusters [2], using the implementation of the two-component density functional theory in the ABINIT code.

This work was funded in part by F-Bridge Project which is part of the European Union's Framework Programme 7 and the French PACEN and NEEDS Programmes.

[1] R. M. Nieminen, E. Boronski and L. J. Lantto, Phys. Rev. B **32**,1377 (1985)
[2] J. Wiktor, M.-F. Barthe, G. Jomard *et al*., Phys. Rev. B **90**, 184101 (2014)

Photorefractive Direct Laser Writing

L. Vittadello [1], A. Zaltron[1], N. Argiolas[1,2], M. Bazzan[1,2], N. Rossetto[3], R. Signorini[3]

[1]*Dipartimento di Fisica e Astronomia, Università degli studi di Padova*
[2] *CNISM, sezione di Padova*
[3]*Dipartimento di Scienze Chimiche, Università degli studi di Padova*

Direct laser writing (DLW) is a powerful technology today widely employed in contact - less lithography and in other micro-machining techniques. It consists in scanning the surface or the volume of an optical sample with a focused laser beam with the aid of a computer-controlled translation stage or by deflecting the focused beam by some suitable opto - mechanical system. If the sample is coated with a photo-sensitive material, or the sample itself possesses some kind of photo-sensitivity, it is possible to realize one, two or three dimensional structures with micron-size accuracy by modifying the sample properties at the focal region, where the light intensity is much higher than elsewhere.
We demonstrate [1] a new DLW approach to obtain 1D and 2D optical structures in lithium niobate, based solely on the photorefractive (PR) effect. The idea is to increase the PR sensitivity of the substrate by increasing the concentration of extrinsic defects (in our case Fe). In this way large semi-permanent refractive index changes can be obtained by scanning the sample with a low-power, cw focused light source at visible wavelength. The obvious advantage is therefore that no expensive laser systems are required.
The obtained refractive index changes, characterized using an interferometric technique, are negatives and range from 10^{-4} to 10^{-3} for extraordinary polarization. Moreover, the physics related to the formation of the refractive index modification can be modeled using standard models for photorefractivity, provided that the beam intensity remains below 10^6 W/cm^2.
The proposed method offers interesting advantages in terms of simplicity, versatility and cost effectiveness, making it interesting especially for rapid prototyping of diffractive optical elements such as Fresnel lenses, chirped gratings, coupled waveguide arrays and so on. Some examples of these possibilities are presented.

[1] Vittadello et al.: *Photorefractive Direct Laser Writing* , accepted for publication in Jour. Phys. D (2016).

Irradiation temperature effects on the induced point defects in Ge-doped optical fibers.

A.Alessi[1], I.Reghioua[1], S.Girard[1], S. Agnello[2], D. Di Francesca[1], L.Martin-Samos[3], C. Marcandella[4], N.Richard[4], M. Cannas[2], A.Boukenter[1], Y. Ouerdane[1]

[1] *Univ-Lyon, Laboratoire H. Curien, UMR CNRS 5516, Université Jean Monnet, 18 rue du Pr. Benoît Lauras, 42000 Saint-Etienne, France.*
[2] *Dipartimento di Fisica e Chimica, Università di Palermo, I-90123 Palermo, Italy.*
[3] *CEA, DAM, DIF, F91297, Arpajon, France.*
[4]*Materials Research Laboratory, University of Nova Gorica, Vipavska 11c 5270-Ajdovscina, Slovenija.*

The Ge-doped silica is widely employed in the optical fiber technology [1] and, as consequence different studies were published regarding the radiation induced generation or conversion of the Ge related point defects [1-5]. Despite this research activity various aspects are still unclear [2-4] or slightly investigated [5]. The present study is focused on the irradiation temperature effects on the concentrations and typologies of the radiation induced centers. Indeed, though the thermal stability of different Ge related defects has been investigated [2] a systematic exploration of the impact of changing the temperature during the irradiation is still missing. The understanding of this aspect is relevant for both basic and applicative research. First, it can clarify the point defect generation/evolution mechanisms and the proposed structural models of the various centers. Second, it provides relevant information on the performances of these fibers at the different temperatures encountered by a new generation of fiber sensors and not only at the usual room temperature conditions. For our investigation we performed X-ray irradiation of a two steps multi-mode optical fiber and we employed different experimental techniques such as the electron paramagnetic resonance (EPR) and the confocal microscopy luminescence (CML) to highlight radiation effects. Indeed, we were able to study the paramagnetic and the light emitting defects. Our EPR results evidence that for temperatures higher than 200 °C the radiation induced concentrations of the defects decrease with respect to those measured in samples irradiated at lower temperatures. Simultaneously, our preliminary CML data, recorded under excitation at 442 nm, highlight different emission responses in the red spectral domain for samples irradiated at different temperatures. We underline that this latter result could be very useful to clarify the still unclear origin of some red emissions detected in the irradiated Ge doped silica.

[1] Defects in SiO_2 and Related Dielectrics: Science and Technology edited by G. Pacchioni, L. Skuja, and D. L. Griscom (Kluwer Academic, Dordrecht, 2000).
[2] A. Alessi, S. Agnello, and F. M. Gelardi, Properties and Generation by Irradiation of Germanium Point Defects in Ge-Doped Silica in: Germanium: Properties, Production and Applications, edited by R. V. Germanno. (Nova Science Publishers, New York, 2012), pp. 75–150.
[3] D. L. Griscom, Opt. Mater. Express **1**, 400 (2011).
[4] L. Giacomazzi, L. Martin-Samos, A. Boukenter, Y. Ouerdane, S. Girard, N. Richard, Opt. Mater. Express **5**, 1054 (2015).
[5] K. Awazu, K.-I. Muta, H. Kawazoe, J. Appl. Phys. **74** 2237 (1993).

Creation of transient defects in ionic crystals in regions with high excitation density

A. Belsky[1], C. Dujardin[1], A. Gektin[2], S. Gridin[1,3], I. Kamenskikh[4], N. Shiran[2], A. Vasil'ev[5]

[1] *Institut Lumière Matière, Université Claude Bernard Lyon 1-CNRS, UMR 5306, F-69622 Villeurbanne Cedex, France*
[2] *Institute for Scintillation Materials, 60 Nauki Avenue, 61001 Kharkov, Ukraine*
[3] *Department of Physics, Wake Forest University, Winston Salem, NC, USA*
[4] *Faculty of Physics, Lomonosov Moscow State University, Leninskie Gory 1(2), Moscow 119991, Russia*
[5] *Skobeltsyn Institute of Nuclear Physics, Lomonosov Moscow State University, Leninskie Gory 1(2), Moscow 119991, Russia*

Multiparticle relaxation in regions of high density of electronic excitation produced in insulating crystals by X-ray photons could result in creation of radiation-induced defects. Concentration of carriers in such regions changes when the photon energy exceeds the core level absorption threshold. This transient defect creation route is characterized by the increase of the defect-related luminescence yield just above the threshold. In this presentation we discuss luminescence excitation spectra for some wide-band-gap crystals around the edges of core level absorption. Experimental results for 310 nm luminescence excitation of pure CsI are discussed in details. Two crucial creation mechanisms of nanometer clusters of electronic excitations are analyzed.

The first mechanism is connected mainly with electron cascade and is due to high rate of energy losses for electrons having energy around 100 eV. Such electrons produce excited regions with mean dimension about 10 nm. They are composed of several low energy electronic excitations (e-h pairs with total energy close to forbidden gap E_g). Interaction of these pairs results in the luminescence quenching with decay kinetics similar to quenching of excitons by defects. In the majority of crystals mean thermalization length for holes is smaller than for electrons, and non-uniform distribution of the charge could result in defect creation. This process can be even more dominant for the second mechanism of cluster creation due to Auger cascade of a deep holes created by photons with energy above the core level edge. In crystals with heavy ions there are several core levels for upper 100 eV regions of filled states, and the number of Auger holes created at the same ion or neighbor ions can range from 3 to 6. It results in creation of unstable multicharged ions or several charged ions inside a nanometer cluster and surrounded by few electrons at larger distances. Lifetime of such a cluster is about tens of picoseconds. The strong induced electric field in such a cluster lead to the creation of transient radiation defect. The latter mechanism seems to be the most common one for defect creation under high-energy excitation. It can be treated as modified Varley mechanism, induced by mutual evolution of nanometer multiply charged cluster of excitations.

Paramagnetic centers in the irradiated borate glasses

B. V. Padlyak[1,2], I. I. Kindrat[2], A. Drzewiecki[2]

[1]*Institute of Physical Optics, Sector of Spectroscopy, 23 Dragomanov Str., 79-005, Lviv, Ukraine*
[2]*University of Zielona Góra, Institute of Physics, 4a Szafrana Str., 65-516 Zielona Góra, Poland*

The X-band ($\nu \cong 9.4$ GHz) electron paramagnetic resonance (EPR) spectra of the series borate glasses with LiB_3O_5, SrB_4O_7, CaB_4O_7, $Li_2B_4O_7$, $KLiB_4O_7$, SrB_6O_{10}, and $LiCsB_6O_{10}$ chemical compositions, irradiated by γ - ray (dose 10^7 Gy) and X - ray (dose $1 \div 2 \times 10^4$ R) at room temperature have been investigated and analyzed. The nominally-pure borate glasses of high chemical purity and optical quality were obtained from corresponding polycrystalline compounds by standard glass synthesis using technological conditions described in [1].

The analysis of EPR spectra in the γ - and X - irradiated borate glasses shows presence radiation-induced paramagnetic centers stable at room temperature practically in all investigated glasses. The most intense and well-resolved EPR spectra of the radiation-induced centers have been observed in the Sr-contained borate glasses. Detailed analysis of the observed EPR spectra shows that these spectra belong to the same type of radiation-induced paramagnetic centers, which can be described in the framework of model of the O^- hole centers in borate glass network. The 4-component EPR spectra of the O^- centers are related to the superhyperfine (SHF) structure, caused by interaction of the unpaired electron spin with one nucleus of the ^{11}B magnetic isotope (nuclear spin $I = 3/2$, natural abundance – 80.1 %). In the irradiated borate glasses also were observed weak EPR signals with 7-component SHF structure, which belong to the O^- centers, localized near one nucleus of the ^{10}B isotopes (nuclear spin $I = 3$, natural abundance – 19.9 %). Observed in the irradiated borate glasses unstructured anisotropic EPR signal can be ascribed to the O^- hole centers, localized near non-magnetic isotopes in the glass network. The EPR spectra of anisotropic O^- hole centers without SHF structure were observed previously in the neutron-irradiated $Li_2B_4O_7$ single crystals [2] as well as in the γ - and X - irradiated glasses of the $CaO\text{-}Ga_2O_3\text{-}GeO_2$ system [3].

The features of ESR spectra, electronic and local structure and mechanisms of creation of the radiation-induced centers in the borate glasses with different chemical composition have been discussed in comparison with available referenced data for EPR spectroscopy of the γ -, X -, and neutron-irradiated borate crystals and glasses.

[1] B.V. Padlyak, S.I. Mudry, Y.O. Kulyk, A. Drzewiecki, V.T. Adamiv, Y.V. Burak, I.M. Teslyuk, Mater. Sci. Poland **30** 264 (2012).
[2] Ya.V. Burak, B.V. Padlyak, V.M. Shevel, Nucl. Instr. and Meth. in Phys. Res. B, **191** 633 (2002).
[3] B.V. Padlyak, Radiat Eff. Defects Solids **158,** 411 (2003).

Electron and hole traps in a-Al_2O_3

O. A. Dicks[1], A. L. Shluger[1], P. B. Littlewood[2]

[1] *UCL, Department of Physics and Astronomy, Gower Street, London, WC1E 6BT*
[2] *Argonne National Laboratory, 9700 S. Cass Avenue, Lemont, IL 60439, United States*

Thin films of amorphous Al_2O_3 (a-Al_2O_3) are currently being investigated for use in electronic applications, including charge-trapping memory devices [1,2] . Experimental measurements [3] of charge traps in thin film Al_2O_3 have been performed, but the mechanism for electron trapping has not been established. In order to understand these results we present a comprehensive categorization of intrinsic electron and hole traps in a-Al_2O_3 using DFT calculations with hybrid functionals.

Amorphous structures of Al_2O_3 have been generated through the molecular dynamics (MD) melt-quench method, using a Born-Mayer type potential previously used to generate a-Al_2O_3 structures [4]. These structures have been compared to various x-ray diffraction [5] and NMR studies of amorphous films and are also shown to accurately recreate experimental densities of 2.9-3.2gcm^{-3} [6]. Intrinsic electron and hole trapping has then been investigated using hybrid functional DFT calculations, with hybrid functionals being used to overcome self-interaction error. Both electrons and holes show deep trap states and trapping energies of ~1eV, though the distribution of states is also discussed. We also show that these traps are a result of structural precursors in the amorphous topologies, which can then be used to predict the trap densities in physical films. These results will allow the first step in identification of intrinsic trap states in thin films of Al_2O_3 and greater understanding of amorphous metal oxides.

[1] Goux, L.; Fantini, A.; Kar, G.; Chen, Y.; Jossart, N.; Degraeve, R.; Clima, S.; Govoreanu, B.; Lorenzo, G.; Pourtois, G.; Wouters, D.J.; Kittl, J.A.; Altimime, L.; Jurczak, M.,*VLSI Technology (VLSIT),* 159 (2012)
[2] Ya Li; Yanli Pei; Ruiqin Hu; Zimin Chen; Yiqiang Ni; Jiayong Lin; Yiting Chen; Xiaoke Zhang; Zhen Shen; Jun Liang; Bingfeng Fan; Gang Wang; He Duan, *Electron Devices, IEEE Transactions on* **62,** 1184 (2015)
[3] Zahid, M.B.; Aguado, D.R.; Degraeve, R.; Wang, W.C.; Govoreanu, B.; Toledano-Luque, M.; Afanasev, V.V.; Van Houdt, J., *Electron Devices, IEEE Transactions on* **57**, 2907 (2010)
[4] L. Bläckberg, E. Metsanurk, a. Tamm, A. Aabloo, and M. Klintenberg, Nuclear Instruments and Methods in Physics Research Section A: Accelerators, Spectrometers, Detectors and Associated Equipment, **759**, 10 (2014)
[5] P. Lamparter, R. Kniep, Physica B, **236,** (1997)
[6] B. Ilic, S. Krylov, and H. G. Craighead, Journal of Applied Physics, **108** (2010)

OH^- defects in rare earth ion doped stoichiometric $LiNbO_3$

L. Kovács, Zs. Szaller, L. Oláh, K. Lengyel, G. Dravecz, G. Corradi

Institute for Solid State Physics and Optics, Wigner Research Centre for Physics, Hungarian Academy of Sciences, Budapest, Hungary

Stoichiometric $LiNbO_3$ (SLN) crystals with Li/Nb≈1 possess a number of specific properties not shown by congruent (Li/Nb≈0.945) lithium niobate (CLN) [1]. This comes first of all from the reduced number of intrinsic defects such as antisite Nb (Nb_{Li}) ions and its charge compensating lithium vacancies (V_{Li}).

Rare earth ions (e.g. Nd^{3+}, Er^{3+}, etc.) as laser activators are often introduced to $LiNbO_3$ for practical applications. Their spectroscopic properties in SLN significantly differ from those observed in CLN. The line width of the optical absorption signals are much narrower for SLN than for CLN due to the above mentioned more ordered structure.

It is well-known that the optical damage resistance (ODR) of $LiNbO_3$ can be increased by special dopants like Mg^{2+}, Zn^{2+}, In^{3+}, Sc^{3+}, Hf^{4+}, Zr^{4+}, Sn^{4+}, see e.g. Ref. 1 and references therein. Above a threshold concentration which depends on the crystal stoichiometry and the valence state of the dopants the photorefractive damage can be strongly suppressed. While this concentration is in the range of several (2–7) mole % for CLN it is usually less than 0.1 mole % for nearly stoichiometric $LiNbO_3$ [1]. According to the highly-accepted defect model Nb_{Li} ions disappear and the dopants occupy Nb sites above the threshold.

In the present work several rare earth ion doped SLN crystals (Er^{3+}, Gd^{3+}, Nd^{3+}) have been grown by the high temperature top seeded solution growth (HTTSSG) method. The nominal rare earth ion concentration in the solution was 0.5–1 mole % well above the threshold concentration determined for the ODR ions. It has been assumed that a threshold effect should also occur for rare earth ion doped crystals resulting in the appearance of the dopants on Nb sites. The defect structure induced by the incorporation of rare earth ions in relatively high concentrations into SLN crystals has been probed by measuring the stretching vibration spectrum of hydroxyl ions (OH^-) always present in $LiNbO_3$ grown in air. The obtained results will be discussed based on previous experimental findings and theoretical models.

[1] K. Lengyel, Á. Péter, L. Kovács, G. Corradi, L. Pálfalvi, J. Hebling, M. Unferdorben, G. Dravecz, I. Hajdara, Zs. Szaller, K. Polgár: Growth, defect structure and THz application of stoichiometric lithium niobate, *Applied Physics Reviews* **2** (2015) 040601/1-28.

Subsurface Radiation Induced Defects in Lithium Fluoride Nanocrystals

A.P. Voitovich[1], V.S. Kalinov[1], A.P. Stupak[1], L.P. Runets[1], R.M. Montereali[2], M.A. Vincenti[2]

[1]Institute of Physics, National Academy of Science, Nezavisimosti Prospect 68, 220072 Minsk, Belarus
[2]ENEA C.R. Frascati, Fusion and Technologies for Nuclear Safety and Security Department, Via E. Fermi 45, 00044 Frascati (Rome), Italy

Films, microcrystals and nanocrystals are characterized by a large surface to volume ratio. Therefore, when these objects are exposed to ionizing radiation, it is necessary to take into account specific features of the formation of radiation induced defects in subsurface layers of the samples. In LiF based devices, such as waveguides and nanocrystalline film structures for high spatial resolution data recording, radiation induced defects are also formed in subsurface and surface layers of crystals.

The use of luminescent research methods have allowed to reveal and to classify some surface radiation-induced color centers (SCCs) in nanocrystals of LiF irradiated by gamma rays at 77K. The products of the reactions of these defects with electrons and anions diffusing in nanocrystals (NCs) have been separately determined and allowed to establish surface defects composition (quantities of vacancies and electrons). The presence of the following types of surface CCs has been identified and defined: F_{S1}, F_{S1}^-, F_{S2}^+, F_{S2}, F_{S2}^-, F_{S3}^+ and F_{S3}, where $_S$ stands for surface. It is obtained that the photoluminescence and photoluminescence excitation spectra for SCCs which contain more than one anion vacancy differ from the corresponding spectra for the centers in the bulk crystal. One of the main differences is that the photoluminescence excitation spectra for surface CCs have two (for F_{S2}^+ and F_{S2} centers) or three (for F_{S2}^-, F_{S3}^+ and F_{S3} centers) bands with small variation intensities. The probable reason of photoluminescence excitation spectra splitting is the field asymmetry in the near-surface layer and further experiments are under way to verify and confirm this behavior.

In particular, it has been found that in lithium fluoride NCs diffusion activation energies for anion vacancies and F_2^+ centers are much higher than those in the LiF bulk crystals. Zero-phonon lines in photoluminescence spectra of near-surface layer radiation color centers in LiF NCs have been recorded, and, according with their assignments, the Huang-Rhys parameters for the transitions of these centers have been evaluated in order to compare them with the crystal bulk centers and to connect them with the difference of the electron density distribution in defects.

Characterization of the polishing induced contamination of fused silica optics

M. Pfiffer[1], J.-L. Longuet[2], C. Labrugère[3], E. Fargin[4], B. Bousquet[5], M. Dussauze[6], S. Lambert[2], P. Cormont[1] and J. Néauport[1]

[1] *Commissariat à l'Energie Atomique et aux Energies Alternatives, Centre d'Etudes Scientifiques et Techniques d'Aquitaine, BP2, 33114 Le Barp, France*
[2] *Commissariat à l'Energie Atomique et aux Energies Alternatives, Le Ripault, BP16, 37260 Monts, France*
[3] *Plateforme Aquitaine de Caractérisation des Matériaux, UMS3626, 33608 Pessac, France*
[4] *Institut de Chimie de la Matière Condensée de Bordeaux, 33608 Pessac, France*
[5] *Centre d'Etudes des Laser Intenses et Applications, UMR 5107 CNRS, Université de Bordeaux, CEA, 33405 Talence, France*
[6] *Institut des Sciences Moléculaires, UMR 5255 CNRS, 33405 Talence, France*

One of the most specific features concerning glass polishing is the formation of a thin layer on the surface which is due to chemical reactions between the surface and the polishing slurry. These chemical reactions are responsible for the contamination of the surface by impurities initially contained in the slurry. The aim of the study is to get a better knowledge of contamination depth penetration and concentration on a fused silica polished surface by using various characterization methods. Another goal is to point out that they bring complementary information on the interface composition. The surface characterization was performed by Secondary Ion Mass Spectroscopy (SIMS), Electron Microprobe Analyzer (EMPA), X-Ray Photoelectron Spectroscopy (XPS) and Inductively Coupled Plasma – Optical Emission Spectroscopy (ICP-OES). Samples were prepared using a magnetorheological polishing machine and a cerium-based slurry consequently we focused on cerium and iron contamination. We analysed the depth penetration as well as homogeneity on the surface.

This work confirms that the fused silica polished surface contamination is composed of alkali and metallic elements from the polishing fluid. The cerium and iron penetration and concentration were measured in the surface out of defects. Cerium is embedded at the surface in a 50nm layer and concentrated at 1200ppm in this layer while iron concentration falls down at 30nm. Spatial distribution and homogeneity of the pollution was also studied in the scratches and the bevel using SIMS and EMPA techniques. We evidence that surface defects such as scratches are specific places that hold the pollutants. This overconcentration is also observed in the chamfer. These new insights into the polishing induced contamination of fused silica optics and its repartition have been obtained using various characterization methods. These further techniques were essential to study the pollution induced by polishing and it should be emphasized that none technique could provide alone a complete description.

Key role of internal electric fields in the properties of ionic materials containing transition-metal complexes

J.A. Aramburu[1], J.M. García-Lastra[2], P. García Fernández[1], M. Moreno[1]

[1] *Departamento CITIMAC, Universidad de Cantabria, Santander, Spain*
[2] *Center for Atomic-Scale Materials Design, Technical University of Denmark*

The properties of insulating materials containing a transition metal cation, M, strongly depend on electrons localized on MX_n complexes formed by M and their first neighbors or ligands, X. Traditionally, these properties have been studied using models that only take into account the isolated complex at the right equilibrium geometry. The main goal of this contribution is to show that a quantitative understanding usually requires to go beyond such models, including the electrostatic potential, $V_R(\mathbf{r})$, produced by the rest of ions of the crystal on the electrons confined in the MX_n complex.

In a first step, we study the microscopic origin of the exotic bright blue colour displayed by the Egyptian Blue pigment ($CaCuSi_4O_{10}$) involving square-planar CuO_4^{6-} complexes, the first pigment synthesized by humans, specifically by the Egyptian civilization (~3600 BC) and subsequently used by all Mediterranean cultures. It is stressed that $V_R(\mathbf{r})$ produces a huge red shift of ~1 eV on the highest *d-d* excitation of CuO_4^{6-} in $CaCuSi_4O_{10}$ and the isomorphous Chinese Blue ($BaCuSi_4O_{10}$) but not in $CaCuO_2$ although the Cu^{2+}-O^{2-} distance is the same. This extrinsic red-shift due to $V_R(\mathbf{r})$ is shown to be responsible for the blue colour displayed by $CaCuSi_4O_{10}$ mainly arising from the presence of SiO_4^{4-} tetrahedra in the compound [1].

In a second step, we show that $V_R(\mathbf{r})$ also plays a key role for understanding the optical properties displayed by impurities with sixfold coordination. So, although the metal–ligand distance, R, is the same for both $BaLiF_3$: M^{2+} and $KMgF_3$: M^{2+} (M = Ni, Mn) and both lattices are cubic 10Dq is ~0.2 eV higher for the former that for the latter, a fact due to the different shape of $V_R(\mathbf{r})$ in the two non-isomorphous host lattices.

Along this line, it is stressed that the different colour displayed by ruby, emerald and alexandrite also reflect the distinct shape of $V_R(\mathbf{r})$ and not differences on the Cr^{3+}-O^{2-} distance or covalency [2]. As a salient feature it has been shown that the internal electric field associated with $V_R(\mathbf{r})$ is essentially due only to the first shells of ions surrounding the complex. This internal potential is also behind the distinct optical spectra of C_{4v} and C_{2v} centres involving a close vacancy in MgO: Cr^{3+} [3] or the unusual compressed geometry observed in K_2ZnF_4:Cu^{2+} [3].

Finally, the orbital ordering of pure materials with layered structure (such as K_2CuF_4, La_2CuO_4, Na_3MnF_6, $CuWO_4$ or $Sr_2La_2CuTi_3O_{12}$) has recently been proved to arise mainly from the internal electric field felt by the transition metal complex [4].

[1] P. García-Fernández et al., Inorg. Chem. **54**, 192 (2015)
[2] J. A. Aramburu et al., Phys. Rev. B **85**, 245118 (2012)
[3] P. García-Fernández et al., J. Phys. Chem. Lett. **4**, 2385 (2013)
[4] P. García-Fernández et al., J. Phys. Chem. C **118**, 7554 (2014)

Polaronic motion of self-trapped holes in silver halides

J. M. Garcia-Lastra[1], P. García-Fernández[2], S. Loftager[1], J.A. Aramburu[2], M. Moreno[2],

[1]*Department of Energy Conversion and Storage, Technical University of Denmark. Fysikvej 309, 2800 Kgs. Lyngby, Denmark*

[2] *Departamento de Ciencias de la Tierra y Física de la Materia Condensada, Universidad de Cantabria, Avenida de los Castros s/n, 39005 Santander, Spain*

Self-trapped polarons (STPs) are probably the simplest example of defects in solids. They play a key role for explaining the charge transport in many relevant technologies, like organic light emitting diodes or Li-ion batteries. They are also the basis to explain many attractive phenomena like high-temperature superconductivity in the cuprates or colossal magnetoresistance in manganites.

The self-trapped hole (STH) in AgCl, for its relatively simplicity, represents a model system of STP for which it exists a vast amount of experimental data. EPR and ENDOR studies on silver halides started in 1968, proving the formation of a STH in AgCl, but not in AgBr [1]. Laredo et al. showed that STHs in AgCl become mobile above ~35 K, demonstrating the existence of a dominant mechanism of polaronic hopping, involving an activation energy of 61 $\pm$ 3 meV [2]. Optical absorption transitions associated with the STH in AgCl peaking at 1.2 eV have been measured experimentally [3]. However, their origin has not been clarified yet.

Here we will try to respond, through a Density Functional Theory model, to some fundamental open questions on small polarons in AgCl and AgBr model systems: (i) What is the equilibrium geometry and the contribution of the local distortion to the binding energy of the STH in AgCl? (ii) How much localized is the STH in the $AgCl_6^{4-}$ complex in AgCl? (iii) Why is the STH stable in AgCl, but not in AgBr? (iv) What is the excitation responsible for the band peaked at 1.2 eV in AgCl? (v) By what mechanisms do the small polarons move through the AgCl lattice?

[1] Hohne, M.; Stasiw, M., ESR Detection Of Self-Trapped Holes In AgCl. Physica Status Solidi 1968, **28** (1), 247 (1968)

[2] Laredo, E.; Paul, W. B.; Rowan, L.; Slifkin, L., Interactions Between Self-Trapping And Solute Trapping Of Photocarriers In Pd-Doped AgCl. Physical Review B **27** (4), 2470 (1983)

[3] Marquard.Cl; Williams, R. T.; Kabler, M. N., Hole Self Trapping and Recombination Luminescence in Agl at Low Temperatures. Solid State Communications, **9** (24), 2285 (1971).

Defect modelling in $LaMnO_3$ for intermediate temperature solid oxide fuel cell cathodes

Ailbhe L. Gavin [1], Graeme W. Watson[1]

[1]*School of Chemistry and CRANN, Trinity College Dublin, Dublin*

$LaMnO_3$-based perovskites have been widely studied as the oxygen electrode for high temperature solid oxide fuel cells (SOFCs). Sr-doped $LaMnO_3$ is the conventional cathode material for high temperature operation due to its high electrical conductivity, good activity for the oxygen reduction reaction and compatibility with electrolyte materials[1]. Due to the high costs and accelerated performance degradation associated with SOFCs operating at high temperatures, further research is required to reduce the operating temperature and improve their efficiency. Due to the poor conductivity of the cathode at intermediate temperature (600 – 1000 K), the oxygen reduction reaction is often limited to the interface between the cathode, electrolyte, and the air (the three-phase boundary). To ensure the reaction is not restricted to the three-phase boundary, mixed ionic and electronic conductors, can be used as cathode materials. The ionic and electronic conductivity of $LaMnO_3$ can be improved by introducing lower valence dopants at both the La and Mn sites[2]. Here, we investigate doping with the alkaline earth metals Mg, Ca, Sr and Ba.

The formation energies of defects in $LaMnO_3$ have been calculated using PBEsol + *U*[3]. Oxygen vacancy formation, and its dependence on oxygen partial pressure and chemical potential, in bulk $LaMnO_3$ and at its low index surfaces has been examined. The energies of formation of isolated defects and clustered pairs have been investigated at both La and Mn sites, to establish the most probable site at which they will be introduced, under intermediate temperature SOFC operating conditions. The charge compensation mechanism for the introduction of alkaline earth dopants has been examined by considering both ionic (formation of an oxygen vacancy for every 2 alkaline earth dopants introduced) and electronic compensation (a hole localised at the Mn site for each dopant introduced).

[1] J. A. Kilner and M. Burriel, Annu. Rev. Mater. Res., **44**, 365 – 393 (2014)
[2] L. Gan *et al.*, J. Alloys Compd., **655**, 99 – 105 (2016)
[3] J. P. Perdew *et al.*, Phys. Rev. Lett., **100**, 136406 (2008)

The study of defects in $CaYAl_3O_7$ through a static computer modelling approach

G. F.C. Bispo[1], M. E. G. Valerio[1], R. A. Jackson[2]

[1]*Department of Physics, Federal University of Sergipe, São Cristovão-SE, Brazi*
[2] *School of Physical and Geographical Sciences, University of Keele, Keele, ST5 5BG, England*

$CaYAl_3O_7$ (CYAM) has been studied due its luminescence properties when doped with rare earth ions (RE). Several potential applications have been report as sensing structural damage, solid-state light source for white LED's and temperature sensors. Recently, research discovered a blue luminescence with short lifetime in undoped CYAM possibly caused by the presence of intrinsic defects. CYAM belongs to the melilite family and is represented by a structure with space group P-421m, where the Ca^{2+} and Y^{3+} ions are randomly distributed at the same site in the lattice keeping a composition ratio of 1:1. This shared site is cited as an important factor for luminescence emission mechanisms. The objective of this work was study the intrinsic and extrinsic defects in CYAM host using static computational modelling. This technique is based on energy minimisation with interactions represented by interatomic potentials, and has been used in the study of the defect chemistry of solid state materials. All calculations were performed using the GULP code. The main problem in CYAM modelling is how to model defects given the natural disorder of the Ca/Y crystallographic site. The mean field method is a common approach to model the perfect structure with natural disorder, but for defect modelling it is not advisable. The solution was to build a supercell and distribute Ca^{2+}/Y^{3+} ions randomly, keeping the composition ratio of 1:1. The supercell approach has two important limitations: the computational cost and the number of possible configurations. Those limitations increase dramatically with the supercell size. The strategy was build X-ray diffraction patterns of supercells and compared with CYAM experimental patterns to establish the best configuration to modelling. The potential parameter set was obtained through empirical fitting methods. The defects were modelled using the well-established Mott-Littleton method as well as by incorporation direct into a supercell. The intrinsic defects results showed that Y_{Al} anti-site and O Frenkel were the most probable defects and both were indicated as intrinsic emission centres in undoped CYAM by experimental results. The most probable sites occupied by RE^{3+} were Ca/Y crystallographic site in line with experimental results already reported.

Acknowledgments: we thank CENAPAD-SP, CESUP-RS, CAPES, FINEP and FAPITEC-SE for funding.

Intrinsic electron trapping in amorphous hafnium oxide

Moloud Kaviani[1], Valery V. Afanas'ev[2] and Alexander Shluger[1,3]

[1]*WPI-Advanced Institute for Materials Research, Tohoku University, Sendai, Japan*
[2]*Department of Physics, University of Leuven, Celestijnenlaan 200D, 3001 Leuven, Belgium*
[3]*Department of Physics and Astronomy, University College London, London, UK*

Intrinsic electron localization in non-crystalline materials is usually associated with states near the bottom of conduction band (CB). Recent evidence suggests that in some amorphous oxides intrinsic electron localisation is possible also in deep states, where the effect of local disorder is amplified by polaronic relaxation of amorphous network [1-3]. The experimental results using the exhaustive photo-depopulation spectroscopy suggest the existence of deep electron trapping states in amorphous hafnium oxide (a-HfO_2) structures [4]. To investigate whether these states can be caused by intrinsic electron trapping, we modelled the behaviour of extra electrons in stoichiometric a-HfO_2 structures.

Forty models of a-HfO_2 were produced using classical force fields [5] and *ab-initio* calculations have densities in the range of 9.2-9.9 g cm^{-3}, averaging at 9.6 g cm^{-3}. The electronic structures of these models with one extra electron were then calculated using density functional theory (DFT) with hybrid functional HSE06. In all models, the extra electron is initially partially delocalized at the bottom of CB, but the structure relaxation demonstrates that it can trap spontaneously in a deep state in the band gap. These states are located at ~2.0 eV below the bottom of CB, ranging from 1.0 to 2.7 eV, in good agreement with the experimental data [4]. This energy depends on the a-HfO_2 density and on local environment. Extra electrons are localized typically on two or three Hf ions associated with longer Hf-O bonds or under-coordinated Hf atoms in the structures and induce strong polaronic distortion of the surrounding network. Our results broaden the concept of intrinsic polaron trapping to disordered oxides.

[1] A.-M. El-Sayed, M. B. Watkins, V. V. Afanas'ev and A. L. Shluger, Phys. Rev. B **89** (12), 125201 (2014)
[2] A.-M. El-Sayed, K. Tanimura and A. L. Shluger, J. Phys.: Condens. Matter, **27** (6), 265501 (2015)
[3]. H.-H. Nahm and Y.-S. Kim, NPG Asia Materials **6**, 43 (2014)
[4]. F. Cerbu, O. Madia, V. Afanasiev, et al., ECS Transactions, **64** (8) 17-22 (2014)
[5]. G. Broglia, G. Ori, L. Larcher, and M. Montorsi, Model. Simul. Mater. Sci. Eng., **22** (6), 065006 (2014)

Hydrogen-induced defects in amorphous hafnium oxide

Moloud Kaviani[1], Valery V. Afanas'ev[2] and Alexander Shluger[1,3]

[1]WPI-Advanced Institute for Materials Research, Tohoku University, Sendai, Japan
[2]Department of Physics, University of Leuven, Celestijnenlaan 200D, 3001 Leuven, Belgium
[3]Department of Physics and Astronomy, University College London, London, UK

Hydrogen is ubiquitous in electronic devices due to processing conditions and is known to both passivate the existing and induce new structural defects. Recently it has been demonstrated that atomic hydrogen can break strained Si–O bonds and induce new defects in amorphous SiO_2 [1]. Here we investigate the interaction of atomic H with amorphous hafnium oxide (a-HfO_2). To study the distribution of defect properties, forty defect-free a-HfO_2 structures with average densities of 9.6 g/cm^3 were produced by molecular dynamics simulations using the force field [2] and further optimised using Density Functional Theory (DFT) calculations. DFT with non-local functional was used to model the interaction of hydrogen atoms with strained Hf–O bonds in the a-HfO_2 structures. The calculations show that H atom can break strained Hf–O bonds creating structures which consist of a 5-fold coordinated Hf atom facing a hydroxyl group. This defect introduces a one-electron level at 2.4 eV below the a-HfO_2 conduction gap, ranging from 1.7 to 2.9 eV dependent on the sample density and local environment. An unpaired spin is highly localized on the Hf atoms. These results are discussed in conjunction with the experimental data using the exhaustive photo-depopulation spectroscopy of a-HfO_2 samples to investigate the temperature dependence of deep electron trapping states [3].

[1] A.-M. El-Sayed, Y. Wimmer, W. Goes, et al., Phys. Rev. B **92**(1) 014107 (2015)
[2] G. Broglia, G. Ori, L. Larcher, and M. Montorsi, Model. Simul. Mater. Sci. and Eng., **22** (6)**,** 065006 (2014)
[3] F. Cerbu, O. Madia, V. Afanasiev, et al., ECS Transactions, **64** (8), 17-22 (2014)

Defect structures of ODR dopants in $LiNbO_3$ crystals

K. Lengyel[1], L. Kovács[1], V. Szalay[1]

[1] *Institute for Solid State Physics and Optics, Wigner Research Centre for Physics, Hungarian Academy of Sciences, Konkoly Thege M. út 29-33, 1121 Budapest, Hungary*

The optical damage in $LiNbO_3$, the change of the refractive index induced by high laser intensities, has already been known for a half century [1]. However, the optical damage resistance (ODR) can be increased by improving the stoichiometry (Li/Nb ratio) or using some special dopants [2] (Mg^{2+}, Zn^{2+}, Sc^{3+}, In^{3+}, Hf^{4+}, Zr^{4+}, Sn^{4+}). The ODR effect appears at a threshold concentration which depends on the stoichiometry of $LiNbO_3$ and the valence state of the dopant ion. At the same concentration the antisite niobiums vanish from the $LiNbO_3$ lattice [2], which can be monitored by e.g. the measurement of the characteristic vibration of OH^- ions [3]. For high intensity laser applications $LiNbO_3$ crystals just above the threshold are required. Such samples with good optical quality can be produced only if the incorporation method is known in detail.

The investigation of dopant incorporation into $LiNbO_3$ crystal is usually based on the Li vacancy model. This model has been justified by both experimental and theoretical works (see details in reviews [2, 3]). In the present communication the major energetic results of calculations based on interatomic potentials will be summarized. The importance of the knowledge of the exact defect structure will be shown for the case of OH^- ions in ODR ion doped $LiNbO_3$. The results of calculations for ODR-defect configurations in $LiNbO_3$ using density functional theory along with the supercell method implemented in SIESTA computational code will be presented.

We acknowledge NIIF for awarding us access to resource based in Hungary at Budapest and Szeged.

[1] A. Ashkin, C. D. Boyd, J. M. Dziedzic, R. C. Smith, A. A. Ballman, J. J. Levinstein, K. Nassau, Appl. Phys. Lett. **9** (1966) 72–74.

[2] T. Volk, M. Wöhlecke, Lithium Niobate, Springer Series in Materials Science (2008).

[3] K. Lengyel, Á. Péter, L. Kovács, G. Corradi, L. Pálfalvi, J. Hebling, M. Unferdorben, G. Dravecz, I. Hajdara, Zs. Szaller, K. Polgár, Applied Physics Reviews **2** (2015) 040601/1-28.

A polarisable force field for doped lanthanum gallate derived from first principles

Aoife K. Lucid[1], Douglas J. Temple[1], Graeme W. Watson[1]

[1]*School of Chemistry and CRANN, Trinity College Dublin, Dublin 2, Ireland*

Solid-oxide fuel-cells (SOFCs) are an attractive technology for efficient and clean energy conversion which are applicable to a wide variety of fuels (natural gas, liquefied petroleum gas, methanol and hydrogen).[1] Current generation SOFCs require high operating temperatures in the region of 1000°C. This is primarily due to the high temperatures required by the electrolyte in order for oxide ion diffusion to occur. This high operating temperature contributes greatly to the cost and speed of degradation of these devices. $LaGaO_3$ doped with Sr^{2+} on the A-site and Mg^{2+} on the B-site has been suggested as an alternative electrolyte material which can operate in the intermediate temperature range of 600-800°C.[2]
Here we present the derivation of a doped-$LaGaO_3$ force field, where the dopants are Sr^{2+} on the A-site and Mg^{2+} on the B-site. This force field is known as a dipole-polarisable ion model (DIPPIM).[3] In the DIPPIM polarisation effects resulting from induced dipoles on ions in the system are taken into account. This is important due to the polarisable nature of the O^{2-} ions in doped-$LaGaO_3$. The force field is fitted to force, stress and dipole data obtained from DFT calculations. When fitting to ab initio data as opposed to experimental data details on the potential energy surface which are non-equilibrium can also be accounted for. This increases the number of observables which can be reproduced.

[1] Boudghene et al, *Renew. Sust. Energ. Rev.*, **6**, 433-455 (2002)
[2] Morales et al, *J. Eur. Ceram. Soc.*, **36**, 1-6 (2016)
[3] Castiglione et al, *J. Phys: Condens. Matter*, **11**, 9009-9024 (1999)

EXAFS simulations in Zn-doped LiNbO3 based on defect calculations

M. E. G. Valerio[1], R. A. Jackson[2], F. Bridges[3]

[1]*Physics Department, Federal University of Sergipe, Campus Universitário, São Cristóvão, SE, Brasil*
[2]*School of Physical and Geographical Sciences, Keele University, Keele, Staffordshire, ST5 5BG, UK*
[3]*Univ Calif Santa Cruz, Dept Phys, Santa Cruz, CA 95064 USA*

Lithium niobate, LiNbO3, is an important technological material with good electro-optic, acousto-optic, elasto-optic, piezoelectric and nonlinear properties. EXAFS on Zn-doped $LiNbO_3$ found strong evidences that Zn substitutes primarily at the Li site on highly doped samples. In this work the EXAFS results were revisited using a different approach where the models for simulating the EXAFS results were obtained from the output of defect calculations. The strategy uses the relaxed positions of the ions surrounding the dopants to generate a cluster from where the EXAFS oscillations can be calculated. The defect involves not only the Zn possible substitution at either Li or Nb sites but also the charge compensating defects, when needed. From previous defect modelling, a subset of defects was elected based on the energetic of the defect production in the LiNbO3 lattice. From them, all possible clusters were generated and the simulated EXAFS were computed. The simulated EXAFS were them compared to available EXAFS results in the literature for different Zn concentrations. Based on this comparison different models could be proposed to explain the behaviour of Zn in the LiNbO3 matrix.

The effect of trivalent cation doping on the structure and reducibility of ceria.

Graeme W. Watson[1], Aoife K. Lucid[1], Jeremy P. Allen[1], Patrick R. L. Keating[1]

[1]*School of Chemistry and CRANN, Trinity College Dublin, Dublin 2, Ireland*

CeO_2 has received considerable interest as an electrolyte for intermediate temperature solid oxide fuel cells. [1] Unfortunately, within this temperature range (~600-800°C), CeO_2 displays poor ionic conductivity, while at high temperatures and low oxygen partial pressures Ce^{4+} can be reduced to Ce^{3+}, due to facile oxygen vacancy formation, [2] which results in electronic conductivity. In an attempt to improve the ionic conductivity of CeO_2 aliovalent doping is commonly employed, with trivalent species (e.g. Gd^{3+}, Sm^{3+}) a particular focus due to their creation of charge compensating vacancies which forms an O^{2-} diffusion pathway without the presence of Ce^{3+}. Experimental evidence [3] has corroborated the increased ionic conductivity from trivalent dopants, however a detailed understanding on the effect of the dopant on the electronic structure of CeO_2 and a full exploration of the range of trivalent dopants has been lacking.

This study considers two aspects of trivalent doping using density functional theory simulations: (i) the formation of charge compensating vacancies and their role in O^{2-} conductivity, and (ii) their effect on the reducibility of CeO_2. These aspects are explored for a range of *p*-, *d*- and *f*-block ions. The first part of the study focusses on the position of the dopant ions to the vacancies, as dopant-vacancy association can limit ionic diffusion. The results indicate a clear relationship between the dopant species ionic radius and its position relative to the vacancy. In addition, some rare earth dopants (e.g. Dy, Nd) are found to have low dopant-vacancy association energies, suggestive of better ionic conductivity. The second aspect of the study, which is largely ignored in the literature, shows that the reduction energy correlates with the defect structure, therefore being only indirectly influenced by the ionic radius.

[1] Brett *et al*., *Chem. Soc. Rev.*, **37**, 1568 (2008).
[2] Scanlon *et al*., *J. Phys. Chem. C*, **113**, 11095 (2009).
[3] Fu *et al*., *Int. J. Hydrogen Energy*, **35**, 745 (2010).

AFM and TEM study of hillock-like defects induced by swift heavy ions on Al_2O_3 surface

A. Akilbekov[1], J.H. O'Connell[2], V.A. Skuratov[3], A. Dauletbekova[1], G. Aralbayeva[1]

[1]L.N. Gumilyov Eurasian National University, Astana, Kazakhstan
[2]CHRTEM, NMMU, Port Elizabeth, South Africa
[3]FLNR, JINR, Dubna, Russia

High energy heavy ions induce nanosized hillock-like defects on surface of variety materials including such radiation resistant insulators as aluminium oxide. Most of corresponding experimental data on this material concern on the AFM studies of the hillock parameters as a function of incident electronic stopping power [1,2]. In this report we present and discuss the results of complementary AFM and high resolution XTEM examination of hillock morphology on surface of single crystalline Al_2O_3 irradiated with swift (1.2 - 3 MeV/amu) Xe and Bi ions. It was found that hillocks are crystalline in nature. At the same time the hillocks overlapping may trigger amorphization process in irradiating material.

[1] S. M. Ramos et al., Nucl. Instr. Meth. B, **143** 319 (1998).
[2] V.A. Skuratov et al., Surface and Coating Technology, **196** 56 (2005).

Luminescence of $ZnWO_4$ crystals with injected oxygen

A.Akilbekov[1], V. Lisitsyn[2], Zh. Karipbaev[1], L. Lisitsyna[3], A. Dauletbekova[1], I. Tupitsyna[4], I. Ivanov[5]

[1]*L.N. Gumilyov Eurasian National University,2, Satpayev str., 010008, Astana, Kazakhstan*
[2]*National Research Tomsk Polytechnic University, 30, Lenin ave., 634050, Tomsk, Russia*
[3]*Tomsk State University of Architecture and Civil Engineering, Tomsk, Russia*
[4]*Institute of Scintillation Materials, Kharkiv, Ukraine*
[5]*Astana Branch of Institute of Nuclear Physics, Astana, Kazakhstan*

Results of the study on spectral characteristics of photo- and cathode luminescence of $ZnWO_4$, affected by high-energy oxygen ion irradiation or thermal annealing in the oxygen atmosphere are reported.

Injection of oxygen using ion irradiation with energy of 28 MeV with a fluence up to $10^{15}cm^{-2}$ leads to 2.6 eV efficiency reduction of the $ZnWO_4$ characteristic luminescence and change of the shape of an excitation spectrum. 30 % decline with an increase in the photon energy of 4 to 6.5 eV was observed in the excitation spectrum of the irradiated crystal in comparison with the same non-irradiated crystal. Increase near the edge of the excitation spectrum is sharper than that of the non-irradiated crystal. The decrease in luminescence's effectiveness is explained, most probably, by the change of transmission of the sample during the irradiation [1]. The reason of the change of the form of the spectrum is unknown.

Injection of oxygen using thermal annealing in the oxygen atmosphere at temperature of 900^{o} C during 7-hour period also leads to change of the excitation spectrum. In the excitation spectrum in the range of from 4 to 6.5 eV luminescence efficiency decreases with 5-fold increase of photon energy of excitation while in untreated crystals it is only 30 %. Significant reduction in the efficiency of luminescence excitation with photon energy of excitation in heat treated crystals compared to non-treated crystals can be explained with the decrease of injected oxygen form the surface to the bulk and the concentration of destroyed emissive complexes decreases as well. With increasing energy of the exciting photons in the range of 4 to 6.5 eV decrease of characteristic depth of path rays is observed [2, 3]. It is assumed that the destruction of emitting complexes occurs at a depth where exciting photons penetrated. High energy quanta are absorbed in the areas of the crystal where concentration of the destroyed centers is higher, thus the efficiency of luminescence is lower. Depth of oxygen penetration was estimated as 20 nm during 7-hour treatment of the crystal at 900°C.

[1] V. Lisitsyn , D. Valiev, L. Lisitsyna et al., J. Appl. Spectr. **80** 361 (2013)..
[2] V. Nagirnyi, E. Feldbach, M. Kirm et al., Nucl. Instr. Meth. B., **A486** 395 (2002).
[3] V. Kolobanov V. Mikhailin, I. Shpinkov et al. Proceedings of the 5th International Conference of Inorganic Scintillators and Their Applications, Moscow MSU 648 (1999).

Study of the formation of vacancy defects into 6H-SiC by Positron Annihilation Spectroscopy and Photoluminescence

X. Kerbiriou[1], J.Wiktor[2], J. Botsoa[1], F. Linez[1], G. Jomard[2], M. Bertolus[2], M.-F Barthe[1]

[1]CNRS, CEMHTI UPR3079, Université d'Orléans, Orléans, F-45071, France
[2]CEA, DEN, DEC, Centre de Cadarache, Saint-Paul-lez-Durance, F-13108, France

Silicon carbide (SiC) is an important technological material, thanks to its electronic and physical properties. Due to its high thermal conductivity, high temperature stability, chemical inertness and small neutron capture cross-section, SiC has potential uses in nuclear applications. As a wide-band gap semiconductor, silicon carbide has attracted significant attention as a candidate material for high temperature, high power and high frequency electronic devices. More recently, very interesting results on the properties of some vacancy defects such as $V_{Si}V_C$ [1] and V_CC_{Si} [2] and V_{Si} [3] have demonstrated that it is a key material for next-generation photonic and electronic devices.

Positron Annihilation Spectroscopy (Lifetime Spectroscopy (*PALS*) and Doppler Broadening Spectroscopy (*DBPAS*)) has been used to investigate vacancy defects induced in n-type 6H-SiC under different irradiation conditions (50-keV He^+, 4- and 20-MeV Au^{2+}, 12-MeV H^+)[4][5]. The experimental results obtained have also been analysed with regards to theoretical calculations performed in the two-component density functional theory (TCDFT), and taking into account the full relaxation of defects [6]. From these works, we conclude to the formation of the silicon monovacancy (V_{Si}) or the divacancy ($V_{Si}V_C$) or a larger sized vacancy defect created at high damage doses which is consistent with the ring hexavacancy. Furthermore, the evolution of the irradiation-induced vacancy defect under annealing has been studied for the particular case of 12-MeV proton-irradiated SiC. V_{Si} formed under proton irradiation is found to anneal between 400°C and 700°C with the annealing process involving vacancy migration and formation of V_C+V_{Si} complexes, with a positron lifetime of 235 ps.

Finally, photoluminescence measurements were performed on several samples at different stages (before and after irradiation, and after annealing). Observations of the PL lines assigned to the negatively charged silicon monovacancy [7] and the so-called "UD-2" peaks assigned to the neutral divacancy [8] provide support to the conclusions already made from positron annihilation measurements.

[1] W. F. Koehl, et al, Nature, **479**, 84 (2011).
[2] S. Castelletto et al, Nat. Mater., **13**, 151(2014).
[3] M. Widmann et al, Nat. Mater., **14**, 164 (2015).
[4] X. Kerbiriou et al., Phys. Stat. Sol. C, **4**, 3650 (2007)
[5] F. Linez et al, J. Nucl. Mater., **436**, 150 (2013)
[6] J. Wiktor et al., Phys. Rev. B, **89**, 155203 (2014)
[7] E. Janzén et al., Physica B, **4354**, 404 (2009)
[8] W. E. Carlos et al., Phys. Rev. B **74**, 235201 (2006)

Optical absorption (AO) and thermoluminescence properties of green tourmaline

L.M. Oliveira[1], J.R. Cardoso[2], N.F. Cano[3], S. Watanabe[1]

[1]*Institute of Physics, University of São Paulo, São Paulo, SP, Brazil*
[2]*IPEN – Institute of Research Nuclear and Energy, São Paulo, SP, Brazil*
[2]*Federal University of São Paulo, Santos, SP, Brazil*

Tourmaline is a silicate mineral of chemical formula $XY_3Z_6B_3Si_6(0,OH)_{30}(OH,F)$. Since X can be any of the elements (Na,Ca), Y (Al, Li, Mg, Fe^{2+}, Mn, $Fe3^{+}$) and Z (Al, Fe^{3+}, Mg, Mn, Cr), there are in nature about 12 varieties. Here we investigated properties of green tourmaline.
The green variety of tourmaline presented three peaks in its TL glow curve at 170, 230 and 290 °C. Irradiated with very high dose up to 200 kGy, 190 °C peak grew fast shifting to 190-200 °C so that 230 °C became hidden; 290 °C grew little and was shifted to 320 °C. The 190-200 °C peak grows almost linearly up to 10 Gy and then decreases with doses larger than 120 kGy. Green tourmaline can, therefore be used as detectors of high doses even larger than 120 kGy.
The optical absorption spectrum shows a strong UV absorption band and a band around 700 nm such that a dip is observed around 500 nm typical of green colour. A broad Fe^{2+} band around 116 nm superposed by sharp infra red bands at 1380 and 1420 nm are also observed. Furthermore, four to five infrared lines in the interval of 2120 - 2350 nm are observed.

Acknowledgement: We acknowledgement the important financial support from Fapesp

Paramagnetic defects produced by high radiation doses in silicon detector material

A. C. Joita, S. V. Nistor, I. Pintilie

National Institute of Materials Physics, Atomistilor 105bis, Magurele-Ilfov, 077125 Romania.

Investigations by Q(34GHz)-band electron spin resonance were performed on samples cut from 100 mm diameter/0.3 mm thick wafers of ultrapure, n-type (3–4 kohm.cm), single crystalline silicon grown by floating zone technique, used for making the detectors for collision experiments [1]. Platelets of 10x10 mm^2 of the as-grown and ^{17}O isotope doped material irradiated with up to $1x10^{17}$ cm^{-2} electrons of 3.5 MeV. Anisotropic paramagnetic irradiation point defects could be observed at low temperatures (T < 120K) in the as-irradiated and further thermal annealed samples, only during/after *in-situ* illumination at 1.06 um. Structural models based on spectra parameters and local symmetry are determined for the paramagnetic defects observed in both type of irradiated samples. Changes in the nature and concentration of the paramagnetic point defects as a function of post irradiation annealing temperature up to 300 ^oC are reported and discussed in comparison with previous electrical, transmission electron microscopy and EPR data [2,3] on similar materials.

[1] I. Pintilie G. Lindstroem, A. Junkes, E. Fretwurst, Nucl. Instr. & Meth. in Phys. Res. A **611**, 52 (2009)
[2] R. Radu, I. Pintilie, L. C. Nistor, E. Fretwurst, G. Lindstroem, L. F. Makarenko, J. Appl. Phys. **117**, 164503 (2015)
[3] S. V. Nistor, D. Ghica, I. Pintilie, E. Manaila, Rom. Repts. Phys. **65**, 812 (2013)

Radiation-induced green color in natural wet quartz and its relation with the non-bridging oxygen hole center

T. P. de Andrade, M. V. B. Pinheiro, R. L. Moreira and K. Krambrock

[1]*Physics Department, Federal University of Minas Gerais, Belo Horizonte, Brazil*

In the last years many radiation-induced green quartz from Brazil has entered the gemstone market. Because of its high water content (~3000 ppm) this quartz may be called wet quartz. The green color of this quartz should not be confused with Prasiolith, a special heat-treated Amethyst [1]. The wet quartz originate from hydrothermal geodes in Uruguay and Brazil including the states Rio Grande do Sul, Paraná and Minas Gerais. This quartz is characterized by its high content of molecular water, silanol groups and OH. It is assumed that this quartz has grown very fast at very low temperatures resulting in many different macroscopic defects, not-well developed crystal facets and the inclusion of water. Radiation-induced green color is believed to origin from non-bridging oxygen hole centers although a definitive proof has not been given [2]. In this work optical absorption, infrared absorption, photoluminescence (PL) and low temperature electron paramagnetic resonance (EPR) were used to identify the origin of the green color center. After gamma irradiation the quartz turned green characterized by strong UV absorption and an absorption band in the 600 nm spectral region forming a transmission valley at about 500 nm. In addition a PL band at about 700 nm appears after irradiation. Low-temperature powder and monocystalline EPR measurements reveal paramagnetic resonance signals which may well be associated with a non-bridging oxygen hole center (NBOHC) with spin Hamiltonian parameters similar to such defects observed in fused quartz and fiber optics [3]. The EPR analysis is discussed in detail. The color center may be annealed by heat treatments in between 150-250 ºC and also by strong UV light.

Acknowledgements - The authors are grateful for financial support to the Brazilian agencies CNPq, Fapemig and CAPES.

[1] R. Schultz-Güttler, U. Henn, and C.C. Milisender, Z. Dt. Gemmol. Ges. **57**, 61 (2008).
[2] C. T. Enokihara, PHd Thesis, University of São Paulo, Brazil (2013).
[3] M. Stapelbroek, D. L. Griscom, E. J. Friebele, G. H. Sigel Jr., J. Non-Cryst. Solids 32, 313 (1979); J. C. Lagomacini , D. Bravo, M. León, P. Martín, Á. Ibarra, A. Martín, F. J. López, J. Nucl. Mat. **417**, 802 (2011).

Visualisation of Bragg peak of proton beams in LiF crystals

B. Marczewska, P. Bilski, T. Nowak

Institute of Nuclear Physics, Polish Academy of Sciences, PL-31342 Krakow, Poland

Lithium fluoride (LiF) is one of the most common phosphors routinely used in radiation protection services in many countries. One of many advantages of LiF is radiophotoluminescence which occurs after its irradiation. Radiation creates in LiF color centers, namely F_2 composed of two anion vacancies bounded to two electrons, and F^{3+} consisting of three vacancies connected with two electrons. Excitation of LiF samples with a blue light causes the emission of photoluminescence with two peaks at about 520 nm and about 670 nm. This property of LiF gives the unique occasion to use this material for direct visualisation of the path of radiation, as for example the energy loss of ionizing radiation during its travel through matter, reaching the maximum of energy deposition called Bragg peak, shortly before the energy drops to zero. This phenomenon is exploited in particle therapy of cancer, to concentrate the effect of light ion beams on the tumor being treated while minimizing the effect on the surrounding healthy tissue. The aim of our work was to observe Bragg peaks by the measurement of fluorescence light in LiF crystals excited with a blue light after their previous irradiation with the proton beams of energy from the range 20-58MeV with different doses.

The irradiation was performed at the proton eye radiotherapy facility operating at the Institute of Nuclear Physics Polish Academy of Sciences (IFJ PAN) in Krakow. Transparent LiF bulk crystals grown at IFJ PAN by Czochralski method were cut to cubes with different size (even larger than $1x1x1cm^3$). The fluorescence of LiF crystals was observed by their stimulation with a 460nm light. The range of proton beams in LiF structure for different energies was calculated through Monte Carlo simulations.

Preliminary results showed that LiF crystal, due to its radiophotoluminescence, can be successfully used for visualisation of the radiation paths and to be one of tools exploited for proton beams monitoring.

This work was supported by the National Science Centre, Poland (Contract No. UMO-2015/17/B/ST8/02180).

Influence of thermal treatment and bleaching on PL of LiF crystals with radiation induced color centers

B. Marczewska, P. Bilski, W. Gieszczyk

Institute of Nuclear Physics, Polish Academy of Sciences, PL-31342 Krakow, Poland

Lithium fluoride (LiF) is characterised by a number of advantages among which can be distinguished its good physical and optical qualities and the ability to host different types of color centers (CC) stable at room temperature. Color centers, very common in naturally occurring minerals, may be "artificially" produced by exposing a crystal to ionizing radiation. In LiF, radiation creates color centers or their agglomeration, namely F_2 composed of two anion vacancies bounded to two electrons, and F^{3+} consisting of three vacancies connected with two electrons. The excitation of LiF crystals with a blue light causes photoluminescence emission (PL) with two distinct peaks at about 520 nm and about 670 nm. The main aim of our work was to investigate the influence of optical bleaching or thermal annealing (various wavelengths, temperatures and time duration) on the photoluminescence of LiF crystals previously colorized by irradiation with high doses (kGy) of gamma rays or beta particles.
The investigation was performed on transparent bulk LiF crystals grown by Czochralski method at IFJ PAN using un-doped and Ti and Mg doped LiF as feed material. The crystals were next cut to the plates of $5x5x0.5mm^3$. The batches of LiF samples were annealed at 400^oC and then irradiated with beta or gamma rays. The readouts of PL were done in self-constructed HELIOS reader equipped with 5W blue LEDs for stimulation, a photomultiplier and a set of optical and interference filters enabling the measuring of green (520nm) or red (670nm) emitted light. PL signal was analysed for doped and un-doped LiF crystals in aspect of the radiation dose (number of induced color centers) and further thermal and optical treatment.

This work was supported by the National Science Centre, Poland (Contract No. UMO-2015/17/B/ST8/02180).

Radiation effects on microstructure and EPR signal of yttrium oxide rods

Santos, S. C, Rodrigues Júnior, O, Campos, L.L.

Instituto de Pesquisas Energeticas e Nucleares – IPEN, Av. Prof. Lineu Prestes 2242, Cidade Universitaria, Sao Paulo, Brazil.

Designing nanostructured materials with a high dosimetric efficiency is a great challenge for radiation dosimetry. Yttrium oxide is known as excellent host matrix for rare-earth elements due to its excellent optical, mechanical, chemical, and thermal properties. However, there is a lack of information which correlates microstructural characteristics and performance of material. This work aims to evaluate the radiation effects on microstructure and EPR signal of Y_2O_3 rods produced by colloidal processing followed by sintering at 1600ºC/4h in air. Ceramic rods were exposed to gamma radiation with doses from 1Gy to 50kGy. Microstructural and dosimetric characterizations were performed by XRD, SEM and EPR techniques. Yttrium oxide rods as sintered exhibited dense microstructure (90% theoretical density) and linear EPR dose response behaviour up to 10kGy. These results show that yttrium oxide is a promising material for radiation dosimetry.

Changes in optical absorption induced by sequential exposition to short- and long-wavelength radiation in the BTO:Al crystal

S. Shandarov[1], V. Dyu[1], M. Kisteneva[1], E. Khudyakova[1], S. Smirnov[1], A. Akrestina[1], Yu. Kargin[2]

[1]*State University of Control System and Radioelectronics, 40Lenin Ave, Tomsk 634050, Russia*
[2] *A.A. Baikov Institute of Metallurgy and Materials Science RAS, Moscow 119991, Russia*

Changes in the spectral dependences of the optical absorption induced in the (100)-cut $Bi_{12}TiO_{20}$:Al crystal with a thickness of 6.6 mm as a result of sequential exposition to cw radiation first with the wavelength λ_d = 532 nm and then with the longer wavelength $\lambda_{l,n}$= 588, 633, 655, 658, 663, 700, 780, 871, or 1064 nm are investigated. Our experiments show that after the short-wavelength exposition to radiation with λ_d = 532 nm, the optical absorption in the crystal increases, and in the range 470–1000 nm, yields the spectrum whose form of absorption coefficient $\alpha_d(\lambda)$ is independent of the initial crystal state. The subsequent exposition to longer-wavelength radiation leads to enhanced transmittance of the crystal in the examined spectral range with absorption coefficients $\alpha_{l,n}(\lambda)$, which reaches saturation depending on the employed wavelength $\lambda_{l,n}$. A maximum decrease of the optical absorption in the crystal is observed upon exposure to radiation with the wavelength $\lambda_{l,n}$ = 663 nm. Even though the dependences $\alpha_d(\lambda)$ and $\alpha_{l,n}(\lambda)$ were monotonic, the spectral dependences of the changes in absorption $\Delta\alpha_n(\lambda)= \alpha_d(\lambda)- \alpha_{l,n}(\lambda)$ demonstrated a resonant character.
We interpret the observed spectra of light absorption in terms of model that takes into account the contribution to the absorption from the photoexcitation of electrons from deep donor centres to the conduction band and intrancentre transitions described by three Gaussian curves with maxima at λ_{m1} = 827 nm (quantum energy $\hbar\omega_{m1}$ = 1.5 eV), λ_{m2} = 761 nm ($\hbar\omega_{m2}$ = 1.63 eV), and λ_{m3} = 704 nm ($\hbar\omega_{m3}$ = 1.76 eV). In addition, to account for dependence of an achievable bleaching of the $Bi_{12}TiO_{20}$:Al crystal preliminary darkened by radiation with λ_d = 532 nm on the wavelength $\lambda_{l,n}$ for clarifying one the model based on configuration coordinate diagram for deep-level defects characterized by large lattice relaxation is used.
Finally, we show that the theoretical model under consideration describes experimental results for the $Bi_{12}TiO_{20}$:Al crystal adequately.

This work was supported in part by the State Assignment of the Ministry of Education and Science of the Russian Federation for 2015 and 2016 and R&D under the Project of State Assignment No. 3.878.2014/IK.

Optical absorption, electronic paramagnetic resonance and luminescence spectroscopic for characterization of monticellite

A. Quina, S. Watanabe, T.K. Gundu Rao

Institute of Physics, University of São Paulo, São Paulo, SP, Brazil

The members of the Olivine Group are crystallized with orthorhombic symmetry. The structure consists of independent SiO4 tetrahedral linked by divalent atoms in six-fold coordination. In the (Mg, Fe) olivine there is a complete solid solution between Mg2SiO4 (Forsterite) and Fe2SiO4 (Fayalite). There are also (Fe, Mn) olivine that behave in similar manner. The CaMgSiO4 called of Monticellite is another member of Olivine group.
We acquired a sample as being olivine, but the X-ray fluorescence analysis indicated that it is a montecillite, therefore the whole work is on monticellite. The monticellite sample from Teofilo Otoni's region on the state of Minas Gerais (Brazil) with green colored crystal and its dimensions size of 2 cm x 3 cm x 5 cm.
The EPR spectrum of natural montecillite sample is composed of: (1) An intensive signal around 1000 Gauss with g≃6,3; (2) weak signals around 1500, 1900 and 2200 Gauss; (3) Mn^{2+} hyperfine lines; (4) About seven lines in the magnetic field range from 3753 to 4160 Gauss, some of them due to Ti.
The Optical Absorption spectra taken using several slabs have shown besides UV-band, two bands at 450 and 630 nm in the visible spectrum and a relatively intense band around 1100 Gauss due to Fe^{2+}. The green color of olivine sample is due to 450 and 630 nm wavelength absorption band.
The Termoluminescent curves present three different peaks around 145, 260 and 360 ^{o}C. Deconvolution methods applied on the samples indicated that each TL peak at 149, 266 and 369 ^{o}C have E-values 0,55, 1,55 and 2,25 eV, respectively.

Acknowledgement: To FAPESP for financial support and to CAPES for providing with Visiting Professor fellowship to Dr. T. K. Gundu Rao.

TL, EPR and Optical Absorption Properties of Yellow Beryl

S.E. Fernández-Huaycho[1], Lucas S. Carmo[2], S. Watanabe[2]

[1]*Universidad Nacional de San Agustín, Arequipa, Perú.*
[2]*Institute of Physics, University of São Paulo, São Paulo, SP, Brazil*

Heliodor, yellow beryl, of chemical formula Be3Al2(SiO3)6 is ring silicate minerals. The sample here investigated has its origin in Teófilo Otoni, state of Minas Gerais, Brazil. For TL and EPR measurements a portion of sample was crushed and sieved to retain grain sizes between 75 and 170 μm. Fine grains were used for X rays fluorescence analysis. The TL grow curves for doses up to 1500 Gy presented a peak at 150 °C and very weak peaks at 220 and 325 °C. The TL intensity of 150 ° C peak grows linearly at least up to 1500 Gy . Higher dose behavior will be presented at the meeting.
The EPR spectrum presents only one large signal at g= 2,0 typical of Fe 3+ signal. The absorption spectrum consists of a strong UV absorption for λ < 300 nm and a broad absorption found around 800 nm.
High dose irradiation with 1 and 2 MGy only raises absorption curve upward such that the crystal becomes darker. Under heat treatment above 200 °C, following results were observed; up to 280 - 300 °C no change in yellow colours; above 300°C to 380°C the yellow colour is gradually reduced in intensity such that above 420° C the heliodor becomes uncoloured . The heliodor thus obtained is now irradiated with high dose to recover the yellow colour. The result will be presented at the meeting.

Acknowledgements: To FAPESP for financial support and to CONCYTEC for fellowship that allowed one of us S.E. Fernández-Huaycho to participate in this work.

Sensitivity study of transport, rate, and energy deposition parameters in a model of scintillation tracks

X. Lu[1], R. T. Williams[1], S. Gridin[1], M. R. Mayhugh[2]

[1]*Department of Physics, Wake Forest University, Winston Salem, NC, USA*
[2]*Faceted Development, LLC, 3641 Rawnsdale Road, Shaker Hts., OH, USA*

We have recently published a transport and rate equation model of the scintillation process in CsI applied first to calculating proportionality of the total light yield in the undoped material at 295 and 100 K and for Tl doping at 295K [*Lu et al, Phys. Rev. B 92, 115207 (2015)*]. The model also provides time- and radial space-resolved distributions of the carrier and trap populations and recombination events. There is not much doubt about the applicability of the basic phenomena of diffusion, thermalization, charge separation, trapping, release, nonlinear quenching, and recombination that occur in a scintillation track and are incorporated in the equations of the model, nor the list of material parameters that these processes invoke. These parameters are in principle measureable and/or calculable, but there are over 20 of them, they govern competing processes along the ionization track, and assuring uniqueness for successful combinations can be a concern, particularly for a simple target curve like proportionality. CsI has the advantage that relatively many material parameters have been independently measured, many of the parameters can be fixed or restricted by those auxiliary measurements, and other types of scintillation data than proportionality are available for refining the parameters. For example, the scintillation light pulse itself exhibits decay times of multiple components, relative amplitudes of those components, total light yield, temperature-dependence of all of the above, and dependence on activator concentration, which can be fitted by the same model to determine specific material parameters separately from proportionality fitting [*Lu et al (2016) in progress*]. Given that the physical interactions in a spatially inhomogeneous and time-varying electron track are complex, we have repeatedly found it useful to study the changes in scintillation performance produced by varying each material parameter individually in the context set by the others, and in sequence and logical combination as we will report here. The analysis in this work provides guidance on how adjustments of the parameter values affect the scintillator response. The dependences found are sometimes unexpected and the model provides insight not accessible experimentally, for example how process rates depend on population overlaps and electric field driven movements, both of which vary with excitation density. More conventionally, insight is conveyed on how decay characteristics link to transport characteristics and to electron and hole trapping parameters on activators and defects.

WFU acknowledges support from the NNSA Office of Defense Nuclear Nonproliferation Research and Development (DNN R&D) and LBNL under Venture Contract LB15-V-GammaDetMater-PD2Jf, and from the DHS Domestic Nuclear Detection Office (DNDO), ARI grant 2014-DN-077-ARI077-03. This support does not constitute an express or implied endorsement on the part of the Government.

Optical and radioluminescence studies of LuAG:Ce(Pr) with divalent co-dopants

K. Hovhannesyan[1], M. Derdzyan[1], F. Moretti[2], A. Petrosyan[1], C. Dujardin[2]

[1]*Institute for Physical Research, National Academy of Sciences, 0203 Ashtarak, Armenia*
[2]*Institut Lumière Matière, UMR5306 Université Lyon 1-CNRS, Villeurbanne cédex, France*

Divalent co-doping of LuAG:Ce scintillator is widely applied to improve the time-response parameters and the light yield, relative to LuAG:Ce with no co-doping [1]. The observed effects are due to creation of Ce^{4+} centers which trap excited electrons directly from the conduction band leading to excited Ce^{3+} and their radiative de-excitation. Remarkable decrease of the delayed recombination leading to slow scintillation components is achieved in LuAG:Ce co-doped with Ca [2]. Competition in electron capture between Ce^{4+} and other traps leads to improvement of the radiation hardness as well [2].

Growth of LuAG-based crystals is extended to high concentrations of both activator and divalent co-dopant (Me^{2+}=Ca,Mg) concentrations. Single crystals of LuAG:Ce(0.08-0.15 at%),Me(100-350 ppm) and LuAG:Pr(0.1-0.3 at%),Ca(50-120 ppm) were grown by the vertical Bridgman method. Typical defects originating at high co-dopant concentrations are studied on optical and electron microscopes.

The radioluminescence (X-ray, 30 kV, 30 mA; -70 C) intensity from LuAG:Ce,Me increases with concentration of co-dopants. Besides the wide band of Ce^{3+} at 450-600 nm, a weak band peaking at 310 nm is seen, which is commonly ascribed to "antisite" defects. The intensity of the latter band decreases at higher amounts of Ca or Mg evidencing of decrease in the concentration of these defects. Air-annealing leads to further increase of absorption in the UV associated with Ce^{4+} and to decrease of the Ce^{3+} content (by around 10 %). A strong increase of the Ce^{3+} emission intensity (by around 25 %) is seen in air-annealed sample, relative to as-grown. As expected, both the fast and slow decay components are shortened with increasing the Me^{2+} concentration and after applied air-annealing (down to 28.8 ns for the fast component). Combination of divalent co-doping with air-annealing provides an additional opportunity for studies of involved mechanisms and development of improved crystal compositions.

In LuAG:Pr,Ca, an additional wide absorption band is originated at 200-370 nm the intensity of which increases with Ca concentration and leading to radioluminescence (d-f) intensity decrease, due to re-absorption. A direct interrelation is observed between host luminescence and the concentration of added impurities. Increasing the Ca content leads to shortening of the fast decay (down to 9 ns) and suppression of the slow components.

This work was performed in the scope of the International Associated Laboratory (CNRS–France & SCS–Armenia) IRMAS and European Union Horizon 2020 Program under grant agreement no. 644260 (INTELUM).

[1] M. Nikl, K. Kamada, V. Babin, et al, Cryst. Growth Des., **14** 4827 (2014)
[2] A.G. Petrosyan, K.L. Ovanesyan, M.V. Derdzyan, et al, J. Cryst. Growth, **430,** 46 (2015).

Improved scintillation properties of co-doped GAGG:Ce,Mg epitaxial garnet films

M. Kucera[1], Z. Lucenicova-Onderisinova[1], M. Hanus[1], P. Prusa[2], M. Nikl[2], O. Lalinsky[3]

[1]*Charles University, Faculty of Math. & Physics, Ke Karlovu 5, 12116 Prague, Czech Republic*
[2]*Institute of Physics, ASCR, Cukrovarnicka 10, 16000 Prague, Czech Republic*
[3]*Institute of Scientific Instruments, ASCR, Kralovopolska 147, 61264 Brno, Czech Republic*

Scintillation properties were studied in multicomponent garnet scintillators $(GdLu)_3(GaAl)_5O_{12}:Ce^{3+}$ co-doped by divalent Mg^{2+} ions. The technological breakthrough in the liquid phase epitaxy enabled to grow high purity single crystalline films from the BaO flux with scintillation properties comparable to single crystals [1]. The impact of shallow traps on the light yield and timing characteristics were examined using the decay kinetic techniques under e-beam and alpha-particle excitations. The Mg^{2+} doping stabilizes part of cerium ions in the tetravalent Ce^{4+} state and creates an additional fast radiative pathway. The photoelectron yield of GAGG:Ce,Mg epitaxial films with optimized composition approaches that of the best bulk single crystals measured so far. The films have excellent timing characteristics and the prompt Ce^{3+} (5d-4f) component in the scintillation decay (under alpha-particle or e-beam excitation) was around 60 ns. Depending on Mg co-doping the Ce decay decreases to ~40 ns while the photoelectron yield is only slightly influenced. The slow components in the decays are considerably suppressed: the signal decreases two orders of magnitude within 1 μs after a millisecond e-beam pulse excitation. The cathodoluminescence decay kinetics measured in nano- and millisecond time ranges suggests that the trap centers, which are responsible for "slow light" in the scintillation signal, are completely suppressed in heavily Gd, Ga doped samples and appropriate Mg^{2+} co-doping contributes to even faster scintillation response. The energy transfer processes involving trap states are eliminated in GAGG:Ce,Mg garnet films and the dominant part of scintillation response is due to the prompt recombination of electrons and holes at the Ce^{3+} and/or Ce^{4+} emission centers.

[1] P. Prusa, M. Kucera, J.A. Mares, Z. Onderisinova, M. Hanus, V. Babin, A. Beitlerova, M. Nikl, Crystal Growth & Design, **15,** 3715 (2015).

Bandgap Structure and Temperature Dependence of Rare-Earth-Doped La-GPS Scintillator

S.Kurosawa[1], R. Murakami[2], T. Horiai[2], Y. Shoji[2,3], A. Yamaji[2], Y. Ohashi[2], Y. Yokota[3], K. Kamada[1,3], A. Yoshikawa[1,2,3]

[1]*Institute for Materials Research, Tohoku University, Sendai, Japan*
[2]*New Industry Creation Hatchery Center, Tohoku University, Sendai, Japan*
[3]*C&A Corp., Sendai, Japan*

Recently, the pyrochlore crystals described with a $A_2Si_2O_7$ formula, have been studied as scintillation materials, where the A is rare-earth atoms. Although the crystal size is small, we have developed Ce:(La, Gd)$_2Si_2O_7$ (Ce:La-GPS) scintillator crystals with a good energy resolution (FWHM) of 5% at 662 keV were obtained [1]. Moreover, good scintillation properties are expected to be stable up to 450 K [2], and it can be used for oil well logging.

In this study, we reveal the reason why this material has good light output even at 450 K using some Ce:La-GPS sample with different mount of La-admix grown by micro pulling down method or Czochralski process; We found that the band gap energy of La-GPS was larger than other oxide scintillators such as Ce:Gd_2SiO_5 which is conventional scintillator for oil well logging. The energy between excitation site of Ce^{3+} to the bottom of the conduction band would be larger than Ce:Gd_2SiO_5, and quenching energy can be larger than Ce:Gd_2SiO_5. Moreover, from thermo-luminescence study, small number of trap sites were estimated to be found in this material. Additionally, temperature dependence of scintillation properties were investigated for these samples, and we discuss the relationship between the band and temperature dependence in this paper.

[1] A. Suzuki, S. Kurosawa, and A. Yoshikawa et al., Appl. Phys. Express **5** (2012) 102601.
[2] S. Kurosawa et al. NIMA **772** (2015) 72–75

Recombination luminescence of copper and silver doped $Li_2B_4O_7$ single crystals

I. Romet[1], E. Aleksanyan[1,2], M.G. Brik[1,3,4,5], G. Corradi[6], A. Kotlov[7], V. Nagirnyi[1], K. Polgar[6]

[1]Institute of Physics, University of Tartu, Ravila 14c, 50411 Tartu, Estonia
[2]A. Alikhanyan National Science Laboratory, 2 Br. Alikhanyan Str., 0036 Yerevan, Armenia
[3]College of Science, Chongqing Univeristy of Posts and Telecommunications, 400065 Chongqing, PR China
[4]Institute of Physics, Jan Dlugosz University, Armii Krajowej 13/15, PL-42200 Czestochowa, Poland
[5]Institute of Physics, Polish Academy of Sciences, Al. Lotników 32/46, 02-668 Warsaw, Poland [6]Institute for Solid State Physics and Optics, Wigner Research Centre for Physics, Hungarian Academy of Sciences, Konkoly-Thege M. ut 29-33, H-1121 Budapest, Hungary
[7]Photon Science at DESY, Notkestrasse 85, 22607 Hamburg, Germany

Lithium tetraborate (LTB) has been recognized as a promising tissue-equivalent (Z_{eff}=7.4) material for thermoluminescent dosimetry. Doped with various impurities (e.g., Cu, Ag, and P) it demonstrates an outstanding sensitivity exceeding that of the well-known LiF:Mg,Ti (TLD-100) [1]. The role of particular impurities in recombination luminescence relevant for dosimetry is not well understood. Complex investigations of thermostimulated luminescence (TSL) and radioluminescence properties of $Li_2B_4O_7$, $Li_2B_4O_7$:Cu, $Li_2B_4O_7$:Ag and $Li_2B_4O_7$:Cu,Ag crystals suitable for tissue equivalent dosimetry were carried out in the temperature range 4.2 – 650 K. The TSL, cathodoluminescence and X-ray excited luminescence spectra were compared to those measured under photoexcitation. The emission band at 4.6 eV in LTB:Ag was reliably related to Ag^+ ions based on the comparison of the results of optical spectroscopy studies and first principle calculations. Energy transfer from the relaxed exited state of the Ag^+ ion to the Cu^+ ion in double-doped $Li_2B_4O_7$:Cu,Ag crystals will be demonstrated. It will be shown that thermostimulated recombination takes place mainly at the oxygen sites at low temperatures and at impurity sites at high temperature in irradiated crystals. For the first time, the appearance of the low-temperature TSL peak at 90 K is related to the ionic processes in lithium tetraborate crystals. The appearance of pyroelectric flashes due to the lattice relaxation in the temperature region 90-240 K will be demonstrated and their surface-related nature will be clarified. In accordance with earlier EPR studies we attribute the dosimetric TSL peaks in copper and silver doped lithium tetraborate crystals to electron recombinations with Cu^{2+} and Ag^{2+} centres.

[1] M. Prokic. Radiat. Prot. Dosim., **100**, 265 (2002).

Energy transfer and scintillation properties of $Y_3(Ga_xAl_{1-x})_5O_{12}$: Ce ceramics

N. Shiran, K. Hubenko, O. Voloshina, A. Gektin, V. Baumer, V. Pedash, O. Zelenskaya, Yu. Onufriyev, O. Sidletskiy,

Institute for Scintillation Materials, NAS of Ukraine 60 Nauki Avenue, 61001 Kharkov, Ukraine

In past few decades scintillation ceramics based on compounds with the garnet structure attract increased interest from both scientists and engineers as the main alternative to single crystals in many applications, in particular, in computer tomography.

This work was aimed to study the lattice structure, emission, TSL and scintillation properties as a function of the gallium content in ceramic samples of the cerium-activated mixed yttrium aluminum-gallium garnets $Y_3(Ga_xAl_{1-x})_5O_{12}$ ($x = 0 \div 1$).

Polycrystalline ceramics were synthesized by the solid-state reaction. Commercial powders of Y, Ga and Al oxides were used as starting materials. The activator was introduced in the charge as the cerium oxide CeO_2. The powders were mixed, grained, pressed into a pellet and sintered at 1100–1400^{o}C in argon atmosphere. All samples were identified by XRD patterns as a single garnet phase.

Luminescence, decay kinetics, TSL, afterglow as well as scintillation characteristics were studied for Ce-doped polycrystalline ceramics as compared with single crystals. It was found that luminescence spectra are similar for both cases and typical for Ce^{3+} ions. The increase of the gallium content up to 40% leads to scintillation efficiency enhancement. At that the pellets demonstrate the considerably reducing the decay time and phosphorescence suppression. Study of thermostimulated luminescence of ceramics as compared with crystals showed the reduction of high temperature TL peaks associated with vacancy and antisite defects. Besides, the ceramics advantages are uniformity distribution of activator ion as well as low cost and manufacture simplicity.

These features allow us to consider the ceramic of the cerium-activated yttrium aluminum-gallium garnet as promising materials for scintillation application.

Non-uniformity of excitation distribution in the track for modelling scintillation non-proportionality and decay

A. Belsky[1], C. Dujardin[1], A. Gektin[2], S. Gridin[1,3], A. Vasil'ev[4]

[1] *Institut Lumière Matière, Université Claude Bernard Lyon 1-CNRS, UMR 5306, F-69622 Villeurbanne Cedex, France*
[2] *Institute for Scintillation Materials, NAS of Ukraine, 60 Nayki Avenue, 61001 Kharkov, Ukraine*
[3] *Department of Physics, Wake Forest University, Winston Salem, NC, USA*
[4] *Skobeltsyn Institute of Nuclear Physics, Lomonosov Moscow State University, Leninskie Gory 1(2), 119991, Moscow, Russia*

Method of rate equations can be conveniently used to describe the dynamics of electronic excitations in luminescent materials. It allows reproducing some properties in scintillators, such as emission intensity, luminescence decay, thermoluminescence and others in wide temperature range. The rate equations account for mono-, bi-, and tri-molecular interactions between the excitations, including diffusion terms, channels of radiative and non-radiative relaxation. The method is easy to use for uniform concentration/density distributions. However, spatial distribution of charge carriers in an ionizing particle track is strongly non-uniform. Such non-homogeneous distributions always occur in insulators after interaction with X-rays or γ-photons or other ionizing radiation. To include the non-uniformity in the kinetic equations, one would need to expand the calculation over 3D space, which requires too much of computational time.

We present technique to calculate the non-uniformity of electron densities in the track of ionizing particle. The approach allows to obtain an electron density distribution function for an incident particle of given energy. It accounts also for overlaps between individual tracks. The system of kinetic equations is solved separately for each of the excitation densities in the distribution. The following step is to average the solutions over the corresponding weights of the densities. Initial distribution of excitation densities can be obtained in the simplest case using the convolution of 1D distribution of stopping power $-dE/dx$ along the track with 3D distribution of the coordinates of thermalized excitations produced at each point of the track. A typical excitation density distribution spreads from 10^{10} to 10^{21} excitations per cm^3. Shape of this distribution depends on the ionizing particle energy and temperature. For instance, the maximum of such distribution produced in CsI by high-energy electrons is shifted from 10^{16} to 10^{12} cm^{-3} as the incident electron energy changes from 100 eV to 100 keV.

To test this approach, we chose pure and doped CsI crystals to simulate scintillation non-proportionality and decay kinetics for the excitonic and activator emission. The simulations were found to be in good agreement with the experimental data.

Research on the Coloration Problems of CsI(Tl) Crystals

Guohao Ren*, Xiaofeng Chen, Huanying Li, Yuntao Wu, Jian Shi

Shanghai Institute of Ceramics, CAS, Shanghai 201800, P.R.China

CsI(Tl) single crystal is an excellent scintillation crystal and has been applied in various radiation detection instruments. However, coloration is a very common phenomenon which deteriorate the scintillation properties. In this manuscript, ϕ80x300mm CsI(Tl) crystals were grown with vertical Bridgman method. Based on the coloration, three kinds of CsI(Tl) crystals, colorless, light pink and dark pink were identified. Their transmission spectra, afterglow curves, photoluminescence, X-ray excited luminescence and thermo-stimulated luminescence (TSL) were measured respectively. It was not found any significant difference for their photoluminescence and X-ray excited luminescence. However several optical absorption bands, 356nm,390nm,435nm,460nm,515nm and 560nm were observed in the dark pink CsI(Tl) samples, and its afterglow is strongest among three samples. The TSL curves show one band around 60°C for all three samples, but the strength of the pink and light pink samples are much stronger than the colorless one. Their infrared absorption spectra were measured at room temperature. Even though the three samples present nearly identical absorption wavenumbers, such as 1692, 1651, 1460, 1405, 1338, 1312, 1276, 1260, 1220 cm^{-1}, the intensity ratio of the pink sample to light pink and colorless is equal to 15:3:1. Of these IR absorption bands, part of them were suggested to be caused by CO_3, part of them were suggested from HCO_3 [1,2]. But part of them have not been resolved up till present. These oxygen-containing impurities might be introduced during crystal growth or the raw material processing. Therefore, crystal defects related to oxygen should be responsible for the pink coloration and strong afterglow of CsI(Tl) crystals.

[1] T.N.Trefilova, A.M.Kudin, L.V.Kovaleva, T.A.Charkina, A.I.Mitichkin, L.E.Belenko, Radiation Measurements **33,** 687 (2001).
[2] A.N.Panova, V.I.Goriletsky, T.B.Grinyova,K.V.Shakhova, EL.Vinograd, J.Crystal Growth **198/199** 865 (1999).

Structural characterization of thin amorphous oxide layers for Gravitational Wave detection

E.Coillet[1], V. Martinez[1], M. Granata[2], V. Dolique[2], G. Cagnoli[1,2], A. Mermet[1]

[1]*Institut Lumière Matière, France*
[2]*Laboratoire des Matériaux Avancés, France*

One of the ultimate test of the general relativity theory is the detection of Gravitational Waves (GW). This measurement would give essential information to get a better understanding of the Universe. At present, one of the major sensitivity limitation of the GW detectors comes from the thermal noise of the mirrors coatings. The Braggs mirrors are composed by alternating thin films made of amorphous SiO_2 and TiO_2-doped Ta_2O_5 deposited by Ion Beam Sputtering (IBS) on a fused silica substrate.
In order to reduce the thermal noise, which is directly linked to the mechanical losses of the layers, one solution is to anneal the mirrors at a temperature lower than the glass transition temperature of both materials. This annealing allowing then a structural relaxation of the layers.
The aim of this study is to present the link between the mechanical losses and the evolution of the layers structure at short and medium range order probed by Raman spectroscopy. Raman spectra shown that the IBS-deposited silica glass was similar to densified fused silica. With the annealing, the evolution of spectroscopic signatures reveal a decrease in the glass density with an increase of Si-O-Si angles and a diminution of 3-membered rings population. Those evolutions were correlated with the evolution of the mechanical losses measured at the LMA.
Besides the SiO_2 measurements, a similar study on Ta_2O_5 will be presented. The effects of the titanium oxide doping on the structure of the Ta_2O_5 will also be discussed.

Local structure and thermally induced structural evolution in amorphous Nb-Si thin layers

M. Naito[1],Y. Kobayashi[1], M. Ishimaru[2], L. Bergé[3], L. Dumoulin[3], C. A. Marrache-Kikuchi[3]

[1]*Department of Chemistry, Konan University, Japan*
[2]*Department of Materials Science and Engineering, Kyushu Institute of Technology, Japan*
[3]*CSNSM, Université Paris Sud, France*

Amorphous and crystalline forms of niobium silicides have attracted attention from the scientific and technological point of view because of their diverse physical properties. It has been reported that Nb-Si amorphous alloys can be formed in a wide composition range and exhibit an Anderson-type metal-to-insulator transition as a function of Nb concentration, film thickness or annealing temperature. Furthermore, superconducting behaviour is also observed in this system. For further understanding of such nature in amorphous Nb-Si alloys, a detailed structural description is of importance. In the present study, we synthesized amorphous Nb-Si thin layers using conventional evaporation technique and examined their atomistic structures as well as thermally-induced structural alteration by means of transmission electron microscopy (TEM).

A $Nb_{13}Si_{87}$ thin film with a thickness of approximately 150 nm was deposited on the (001)Si substrate at room temperature by electron beam co-deposition of Nb and Si. The composition and thickness were precisely controlled with a piezo-electric quartz system. A 20nm-thick SiO_2 capping layer was also deposited on the Nb-Si layer to avoid surface oxidation. The as-deposited thin film was annealed in a N_2 atmosphere at 523K for 1h. Cross-sectional TEM samples were prepared by mechanical polishing followed by ion thinning.

Cross-sectional TEM and energy dispersive x-ray spectroscopy revealed the formation of an amorphous $Nb_{13}Si_{87}$ thin layer in the as-deposited sample. After annealing at 523K, no crystallization or significant morphological change are observed in the TEM image, while an additional halo ring appears in the diffraction pattern from the annealed sample. The halo ring is observed at a scattering vector of $20nm^{-1}$, which is in good agreement with the position of the first halo ring from an amorphous Si. Electron diffraction atomic pair-distribution function analysis indicated that a peak associated with the Si-Si inter-atomic distance (r = 0.236nm) is more enhanced in the annealed sample than the as-deposited one. These results suggest that a nanoscale phase separation into Nb-poor and Nb-rich regions takes place at the early stage of the crystallization process of the amorphous $Nb_{13}Si_{87}$ thin layer.

Hole Trapping in amorphous HfO_2

J. Strand[1], A. Shluger[1]

[1]*University College London, Dep. Of Physics and Astronomy, London, United Kingdom*

HfO_2 is a high dielectric constant material which is sometimes used as a gate insulator in field effect transistors. Charge traps within gate dielectrics may have important effects on device performance, and holes are known to exist as shallow traps on 3 coordinated oxygen sites in monoclinic HfO_2 [1]. In this work hole trapping in amorphous HfO_2 is investigated using 25 96-atom cells which were generated by a melt and quench procedure. The trapping has been simulated using hybrid density functional theory approximated within the auxiliary density matrix method (ADMM) [2], which is implemented within the CP2K ab-initio software package [3]. It is found that holes trap more deeply in amorphous HfO_2 than they do in their monoclinic counterpart, with the majority of the spin density trapping on one oxygen atom in the form of a p-state. The one-electron defect levels are found to be, on average, 3.3 eV above the valence band maximum and are associated with a trapping energy of 0.61 eV. It is observed that holes trap on oxygen atoms which are 2 coordinated with respect to hafnium, or alternatively can trap on a 3 coordinated oxygen in some cases. Upon trapping, structural relaxation due to the localisation of charge occurs, which results in an elongation of the O-Hf bonds by up to 0.1 Å.

[1] Ramo, D. Muñoz, et al., *Physical review letters*, **99** 155504 (2007).
[2] Guidon, Manuel, Jurg Hutter, and Joost VandeVondele, *Journal of Chemical Theory and Computation*, **6** 2348 (2010).
[3] VandeVondele, Joost, et al., *Computer Physics Communications*, **167** 103 (2005).

Excited-state absorption in erbium-doped ceramic langatate

O. Toma, S. Georgescu, A. Stefan

National Institute for Laser, Plasma and Radiation Physics, 409 Atomistilor Street, 077125, Magurele, Jud. Ilfov, Romania

Langatate ($La_3Ga_{5.5}Ta_{0.5}O_{14}$ - LGT) is a partially disordered crystal with one of the crystallographic positions shared with equal probability by two different ions (Ga^{3+} and Ta^{5+}). When doped with rare-earth ions, this results in inhomogeneously broadened absorption and luminescence lines. This makes LGT desirable in both phosphor and laser applications: broad absorption lines allow an efficient pumping while broad luminescence lines can be used for tunable emission. Erbium-doped LGT can be used as an upconversion phosphor with emission in green and red [1]. For applications based on upconversion luminescence, the characterization of excited-state absorption processes is very important for the understanding of the upconversion mechanisms and for the prediction of the material's performances.

Excited-state absorption (ESA) spectra of erbium-doped ceramic langatate (Er:LGT) were obtained using a modified pump-probe experimental setup. The samples used in the experiments (Er(3 at.%):LGT) were synthesized using a solid-state reaction method in the shape of light-scattering ceramic pellets 12-mm in diameter and cut to 0.68 mm, 0.38 mm and 0.24 mm thickness.

The ESA spectra were obtained using a pump-probe setup modified to allow a good superposition of the intensity profiles of pump and probe beams. The ESA spectra were then separated from the upconversion-pumped luminescence in the green and red spectral ranges using a numerical method. The calibration of ESA spectra in transparent materials can be a challenging task; in light-scattering ceramic media, this task is still more difficult due to the unknown propagation length of the light in the medium. The ESA spectra were calibrated using ground-state absorption spectra which were previously calibrated using the Judd-Ofelt parameters for Er:LGT found in [2].

The cross-sections of the ESA transitions originating on $^4I_{13/2}$, in the spectral ranges 400 - 900 nm and 1300 - 1800 nm, are presented. This is, to our knowledge, the first ESA measurement performed on ceramic light-scattering samples.

[1] S. Georgescu, O. Toma, A. M. Voiculescu, C. Matei, R. Birjega, L. Petrescu, Physica B, **407** 1124 (2012).
[2] S. Georgescu, A. Stefan, A. M. Voiculescu, O. Toma, J. Lumin., **162**, 168 (2015).

Excited-state absorption in Er-doped partially disordered calcium lithium niobium gallium garnet

O. Toma, S. Georgescu

National Institute for Laser, Plasma and Radiation Physics, 409 Atomistilor Street, 077125, Magurele, Jud. Ilfov, Romania.

The partially disordered calcium lithium niobium gallium garnet (CLNGG) doped with rare-earth ions is an interesting laser material due to its attractive combination of properties: broad absorption and emission lines, comparable with those found in glasses, and good thermal conductivity characteristic to garnets. These properties make it suitable for efficient diode laser pumping and tunable/ultrashort laser emission [1,2].
The excited-state absorption (ESA) processes can play an important role in Er^{3+} laser emission on various transitions: they can populate a laser initial level by upconversion [3] or be a loss mechanism by reabsorption of the laser photons [4].
Bulk crystalline samples of Er:CLNGG of concentrations 2.46 at.% and 5 at.% with respect to Ca^{2+} were grown in our laboratory using the Czochralski method according to the congruent formula $Ca_3Li_{0.275}Nb_{1.775}Ga_{2.95}O_{12}$. The ESA spectra were obtained using a pump–probe method, in a double modulation scheme, with the sample at room temperature. The experimental setup is similar to that described in [5], with a laser diode centered at the wavelength 973 nm (Er^{3+} transition $^4I_{15/2} \rightarrow {}^4I_{13/2}$) as pump source. The main advantage of this pump method is that only the two lowest excited states of Er^{3+} ($^4I_{11/2}$ and $^4I_{13/2}$) are significantly populated and thus the influence of stimulated emission in most of our spectra (except those in the 1300 - 1800 nm range) is negligible.
ESA spectra in the spectral ranges 400 - 900 nm and 1300 - 1800 nm were recorded and calibrated using ground-state absorption spectra. The cross-sections of the ESA transitions originating on the $^4I_{13/2}$ level were found. The $^4I_{11/2}$ level, although directly pumped, was much less populated than $^4I_{13/2}$.

[1] H. H. Yu, H. J. Zhang, Z. P. Wang, J. Y. Wang, Y. G. Yu, Z. B. Shi, X. Y. Zhang, M. H. Jiang, Opt. Express, **17**, 19015 (2009).
[2] J. Ma, G. Q. Xie, W. L. Gao, P. Yuan, L. J. Qian, H. H. Yu, H. J. Zhang, J. Y. Wang, Opt. Lett., **37**, 1376 (2012).
[3] S. Georgescu, O. Toma, C. Florea, C. Naud, J. Lumin., **101**, 87 (2003).
[4] R. Brede, E. Heumann, J. Koetke, T. Danger, G. Huber, B. Chai, Appl. Phys. Lett., **63**, 2030 (1993).
[5] P. LeBoulanger, J.-L. Doualan, S. Girard, J. Margerie, R. Moncorgé, Phys. Rev. B, **60**, 11380 (1999).

Diffraction from Fibonacci gratings fabricated in photorefractive Fe:$LiNbO_3$

L. Vittadello[1], N. Lo Gullo[1,2], L. Dell'Anna[1,2], M. Bazzan[1,2]

[1]*Dipartimento di Fisica e Astronomia, Università degli Studi di Padova*
[2]*CNISM, sezione di Padova*

The study of quasicrystals attracted quite a lot of attention in last years. The diffraction pattern of these structures reveals an intrinsic long range order although they are not translationally invariant, giving rise to a rich and fascinating phenomenology. These properties have stimulated the research of exciting technological applications especially in optics, such as optical dielectric multilayers for resonant transmission [1], solar energy harvesting [2] and nonlinear optics [3].
In 1D, one of the most studied aperiodic structures is the Fibonacci lattice (FL) which can be constructed by arranging, according to a precise sequence, two segments of lengths L and S with $L/S = \tau$, where $\tau = \left(1+\sqrt{5}\right)/2$ is the golden mean. In view of their technological applications but also purely from the fundamental point of view, it is interesting to investigate whether there exists any relation between different FLs characterized by an arbitrary choice of their length ratio $L/S \neq \tau$. We show that it is possible to group the FL into equivalence classes for which the diffraction spectrum is essentially the same up to a proper rescaling [4]. This means that, even if the spectrum is not exactly the same, the most prominent features are shared by all FLs belonging to the same class.
To test our theoretical analysis, we fabricated several 1D Fibonacci gratings using an innovative approach based on Photorefractive Direct Writing of arbitrary optical structures in Fe:$LiNbO_3$ [5]. This technique allows for the realization of complex structures hardly obtainable using standard holographic techniques, in this case a set of Fibonacci gratings with different L/S ratios. The diffraction properties of these gratings are subsequently measured using a specially designed optical diffractometer. The obtained results are in excellent agreement with the theoretical expectations.

[1] Peng, Liu, Huang, Qiu, Wang, Hu, Jiang, Feng, L. Z. Ouyang and J. Zou, Phys. Rev. B., **69,** 165109 (2004).
[2] A. Lin, Y. K. Zhong, S. M. Fu, C. W. Tseng and S. L. Yan, Opt. Expr., **22,** 880 (2014).
[3] Y. W. Lee, F. C. Fan, Y. C. Huang, B. Y. Gu, B. Z. Dong, andM. H. Chou, Opt. Lett., **27,** 2191 (2002).
[4] Lo Gullo et al. arXiv:1601.07499.
[5] Vittadello et al. accepted for publication in Jour. Phys. D. (2016).

$ZnAL_2O_4$ powders and films for Ultra-Violet emission

A.Bensalah-Ledoux[1], C. Le Luyer[1], F. Moretti[1], S. Boudjelal[1], A. Pereira[1] and C. Dujardin[1]

[1]*ILM, UMR5306 CNRS, Université Claude Bernard Lyon 1 Domaine Scientifique de La Doua, Villeurbanne, France*

Zinc Aluminate ($ZnAl_2O_4$) spinels are well known for their applications in optoelectronic devices, catalysis and chemical industry [1-3]. Recently $ZnAl_2O_4$ based phosphors have also been investigated due to their intrinsic UV luminescence for mercury free UV emission devices. [4, 5]

$ZnAl_2O_4$ powders were prepared by solid state reaction using ZnO and αAl_2O_3 as precursors. After mixing, grinding and pressing at 10 tonnes, the pellets were heat treated at 1200°C for 3 hours in air

$ZnAl_2O_4$ films were made using different deposition methods. The $ZnAl_2O_4$ obtained films and powders were analysed by XRD measurements. Radio- luminescence and cathodo-luminescence were also performed on both types of samples.

The $ZnAl_2O_4$ powders prepared via solid State reaction present a high intensity UV cathode and radio-luminescence around 250nm. The ratio between ZnO and αAl_2O_3 was tuned to optimize the luminescence intensity. Surprisingly, no or weak UV luminescence was detected in the case of films even though the required and pure phase was obtained. The UV luminescence in $ZnAl_2O_4$ is likely due to intrinsic defects into the material. However, the origin of these defects is not yet very clear. It has been reported that it might be due to oxygen vacancies [5]. In order to create these defects in the films, different synthesis parameters were modified such as the $ZnO/\alpha Al_2O_3$ molar ratio and the post-deposition annealing temperature and atmosphere. Luminescence measurements obtained on the different films and the powders will be presented and compared.

[1] B.B. Dantas, N.A.S. Nogueira, J.M. Sasaki, N.L. Freitas, R.H.G.A. Kiminami, A.C.F.M. Cost and K.M.S. Viana, *Mater. Sci. Forum*, **660-661**, 52 (2010).
[2] P. Mierczynski, W. Maniukiewicz, D. Gebauer, W.K. Jozwiak and T.P. Maniecki, *kinet.Catal.,* **50**, 228 2009.
[3] T.K. Parya, R.K. Bhattacharyya, S. Banerjee ans U.B. Adhikari, *Ceram. Int*., **36**, 1211 (2010).
[4] H. Kominami, T. Iguchi, Y. Nakanishi and K. Hara, *Journal of Ad. Res. In Phys*., **2**, 1 (2011).
[5] T. Ishinaga, T. Iguchi, H. Kominami, K. Hara, M. Kitaura and A. Ohnishi, *Phys. Status Solidi C*, **12**, 797 (2015).

$Gd_3Al_2Ga_3O_{12}$:Ce stoichiometry deviation influence on the crystal scintillation properties

G. Dosovitskiy[1], O. Buzanov[2], A. Dosovitskiy[1], A. Fedorov[3], L. Grigorjeva[4], M. Korjik[3,5], V. Mechinsky[5], S. Nargėlas[6], G. Tamulaitis[6], A. Vasiliev[2], S. Zazubovich[7], A. Zolotarjovs[4]

[1]*NeoChem, Moscow, Russia*
[2]*Fomos Crystals, Moscow, Russia*
[3]*Radiation Instruments and New Components, Minsk, Belarus*
[4]*Institute of Solid State Physics, University of Latvia, Riga, Latvia*
[5]*Research Institute for Nuclear Problems, Minsk, Belarus*
[6]*Vilnius University, Vilnius, Lithuania*
[7]*Institute of Physics, University of Tartu, Tartu, Estonia*

Mixed garnet $Gd_3Al_2Ga_3O_{12}$:Ce (GAGG:Ce) scintillation crystal has very good prospects to be applied in radiation detectors for medical imaging[1]. The crystal has 1.5-3 times higher light yield as compared with Lu_2SiO_5:Ce and Gd_2SiO_5:Ce scintillation materials, and its luminescence spectrum pretty much fits the SiPM spectral sensitivity. Due to Ga presence in the compound, the temperature of the crystal growth is lower than for orthosilicate crystals. Moreover, the garnet crystal growth technology is the most developed one to produce high quality crystalline materials. However, like all the Gd-based scintillation materials, $Gd_3Al_2Ga_3O_{12}$:Ce contains slow components in the scintillation decay, which time parameters depend on the Ce content in the material. Moreover, this crystal has a sufficient level of phosphorescence, which is practically absent in $Y_3Al_5O_{12}$:Ce. The $Gd_3Al_2Ga_3O_{12}$:Ce is considered a disordered solid solution with random spatial distribution of the Al and Ga ions in the crystal lattice[1]. This leads to a plurality of possible point structure defects in the crystal. Their role in the deterioration of the crystal scintillation properties is not clarified yet.

Thus motivated, we investigated scintillation properties of the set of $Gd_3Al_2Ga_3O_{12}$:Ce single crystals grown by the Czochralski method in argon atmosphere with 0.5-2% oxygen addition atmosphere from an Ir crucible. 5N materials were used to prepare the raw mixture for the crystal growth. One of the problems of Ga-containing crystals is Ga evaporation from the melt, which could cause non-stoichiometry and related defects. We tapped this issue by varying Ga content in the melt and performing post treatment of grown crystals. Samples were evaluated using a wide range of spectroscopic measurements. It was found that a deviation from stoichiometry has a strong impact on scintillation kinetics but does not affect the presence of phosphorescence.

[1] K. Kamada, S. Kurosawa, P. Prusa et al., Opt. Mater., **36,** 1942 (2014).

Red Emission from Pr^{3+} in $K_{1-x}Na_xNbO_3(0\leq x\leq 1)$ for Persistent Luminescence

Liyi Li,[1,2] Daniel Rytz,[3] Yumiko Katayama,[1] Atul D. Sontakke,[1] Mingying Peng,[2] Bruno Viana[1]

[1]*IRCP Chimie ParisTech, 11 rue Pierre et Marie Curie, 75231 Paris Cedex 05, France*
[2]*The China-Germany Research Center for Photonic Materials and Devices, The State Key Laboratory of Luminescent Materials and Devices, School of Materials Science and Engineering, South China University of Technology, Guangzhou 510641, China.*
[3]*Forschungsinstitut für mineralische und metallische Werkstoffe -Edelsteine/Edelmetalle- GmbH (FEE), Struthstr. 2 55743 Idar-Oberstein, Germany.*

Currently, the development of efficient red-emitting persistent phosphor is still an ongoing challenge. In the research of persistent materials in the red range, Pr^{3+} is a good candidate for its transitions between the $^1D_2$ excited state and the ground state $^3H_4$ at 611nm [1]. In this report, we investigated the red-emitting persistent phosphor using Pr^{3+} as the luminescent activator and host lattices containing closed-shell transition metal ions, such as $KNbO_3$. Unfortunately, $KNbO_3$:Pr^{3+} appears to have no persistent luminescence, but the substituted compounds $K_{1-x}Na_xNbO_3$:Pr (x=0, 0.1, 0.3, 0.5, 0.7, 1) on powder samples give more and more persistent luminescence when Na content increases (see Fig. 1). This is in good agreement with the thermoluminescence (TL) glow curves. TL peaks were found to vary with Na content (see fig.2). The peak maxima shift toward higher temperatures with increasing Na content, indicating the formation of deeper traps. In addition, defect with broad emission is observed at low temperature (not shown here). All the optical features will be discussed at the conference.

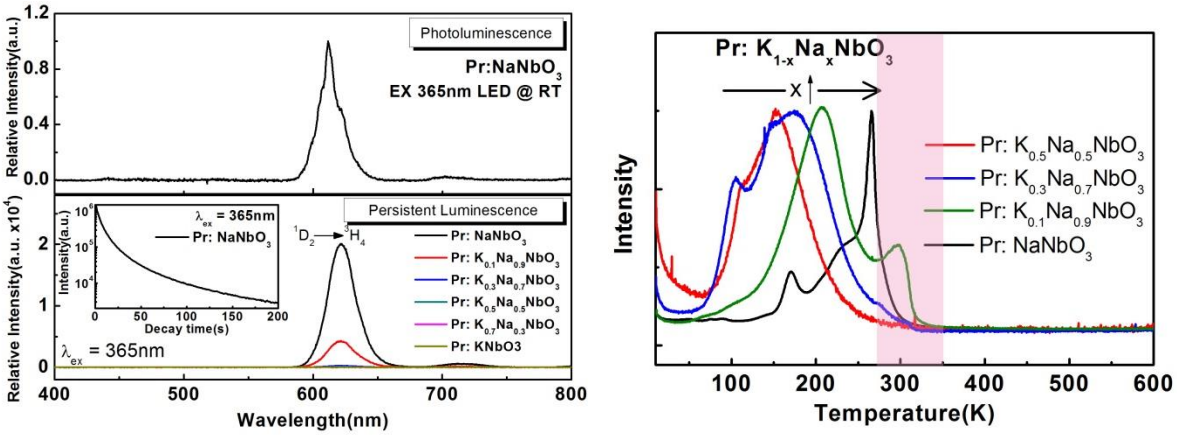

Fig.1 PL spectra of Pr^{3+}-doped $NaNbO_3$ and Persistent spectra of $K_{1-x}Na_xNbO_3$:Pr^{3+} (x=0, 0.1, 0.3, 0.5, 0.7, 1). The inset shows the persistent decay curve of $NaNbO_3$.
Fig.2 Nomalized TL glow curves of $K_xNa_{1-x}NbO_3$:Pr^{3+} (x=0, 0.1, 0.3, 0.5) samples (excitation wavelength, 365nm; heating rate, 10K/min).

[1] P. Boutinaud, L. Sarakha and R. Mahiou, *J. Phys.: Condens. Matter,* **21,** 025901 (2009).

Surface functionalized Zn(Cd)O:Ga-nanoparticles for X-ray induced photodynamic therapy

E. Mihóková[1], L. Procházková[2], R. Dědic[3], V. Čuba[2], I. T. Pelikánová[2], K. Popovich[2], V. Jarý[1], M. Nikl[1]

[1] *Institute of Physics of the CAS, Cukrovarnická 10, 162 53 Prague, Czech Republic*
[2]*Czech Technical University in Prague, Faculty of Nuclear Sciences and Physical Engineering, Břehová 7, 115 19 Prague, Czech Republic*
[3]*Department of Chemical Physics and Optics, Faculty of Mathematics and Physics, Charles University, Ke Karlovu 3, 121 16 Praha 2, Czech Republic*

X-ray induced photodynamic therapy (PDTX) is a modern way of treatment applicable for certain types of cancer. It combines radiotherapy with PDT where simultaneous effect of both can increase efficacy of radiotherapy or allow reduction of the dose administered to a patient. In PDTX [1,2], X-rays induce the scintillation of the nanoparticle that can be localized in a tumor. The scintillation light subsequently excites a photosensitizer, usually a derivate of porphyrin, at its surface. An interaction of photosensitizer with light generates oxygen in its lowest singlet excited state. This singlet oxygen is highly reactive species, it easily oxidizes neighboring molecules causing death of the tumor tissue cells.

We study luminescence and scintillation properties as well as singlet oxygen production of Zn(Cd)O:Ga-nanoparticle-based conjugates with a perspective of their PDTX application. Nanocomposites of Zn(Cd)O:Ga are synthesized by UV photochemical method [3]. Introduction of Cd into ZnO matrix causes a red shift of ZnO:Ga excitonic luminescence [4]. By changing the Cd amount we tune the emission wavelength to match the absorption of protoporphyrin IX (PpIX) in the Soret band around 400 nm. Zn(Cd)O:Ga nanoparicles are coated by SiO_2 layer and conjugated with photosensitive PpIX molecules. We compare luminescence and scintillation properties of silica-coated nanoparticles versus Zn(Cd)O:Ga@SiO_2-PpIX conjugates. We confirm an energy transfer between the nanoparticle and PpIX. We also study the generation of the singlet oxygen by prepared conjugates using two independent methods. In the first, the conjugates suspended in H_2O or D_2O are excited by a laser beam around 400 nm and the singlet oxygen emission around 1275 nm is directly monitored. In the second, we use a reaction of the singlet oxygen with 3'-(p-aminophenyl) fluorescein (APF) chemical probe after X-Ray excitation. Our results suggest that Zn(Cd)O:Ga@SiO_2-PpIX nanoconjugates can be considered as candidates for PDTX application.

[1] A.-L. Bulin, A. Vasil'ev, A. Belsky, D. Amans, G. Ledoux and C. Dujardin, Nanoscale, **7**, 5744 (2015).
[2] P. Retif, S. Pinel, M. Toussaint, C. Frochot, R. Chouikrat, T. Bastogne, M. Barberi-Heyob , Theranostics **5**, 1030 (2015).
[3] L. Procházková, T. Gbur, V. Čuba, V. Jarý, M. Nikl, Opt. Mater. **47**, 67 (2015).
[4] V. Čuba, L. Procházková, J. Bárta, A. Vondrášková, T. Pavelková, E. Mihóková, V. Jarý, M. Nikl, J. Nanopart. Res. **16**, 2686 (2014).

Remote micro-thermometry using scintillation sensors

V. B. Mykhaylyk[1], H. Kraus[2], A.Wagner[1]

[1]*Diamond Light Source Ltd, Harwell Science and Innovation Campus, Didcot, OX11 0DE, United Kingdom*
[2]*Department of Physics, University of Oxford, Keble Road, Oxford OX1 3RH, United Kingdom*

An accurate and reliable measurement of temperature is very important for monitoring chemical, physical and biological processes. For example, knowledge of the precise sample temperature is of high importance in reducing radiation damage to protein crystals during X-ray diffraction experiments using intense synchrotron radiation [1]. Design and construction of the I23 beamline at Diamond Light Source [2], that will permit protein crystallography experiments at lower energy X-rays (3 - 8 keV), prompted the development of new methods compatible with the vacuum environment of such experiments. Therefore, a unique monitoring system is being developed for *in situ* monitoring of the protein sample temperature inside a vacuum chamber of I23 beamline.
Conceptually the method is based on the measurements of the variation of the decay time of a scintillation crystal with temperature. The possibility to have a submicron size sensor in the proximity of the sample under test and the contactless readout of the signal are the main appealing features of such method. The system for temperature monitoring uses the multiphoton counting technique (MPC) pioneered at Oxford University [2]. It comprises a scintillator, an excitation source, an optical system, a photodetector, DAQ and software for data analysis. The scintillations are excited by ultraviolet LED while the detector is integrated in a high-performance optical system used for visualisation of protein crystals. This viewing system collects and conveys the scintillation light to the photodetector. The key to the success of MPC is the fast digitization-based DAQ and analysis software package. The latest version of electronics takes advantage of an on-board FPGA, substantially reducing the space and manufacturing cost. Initial testing could demonstrate the feasibility of this technique to measure temperature changes over the 20-100 K range. The results of the test of the temperature monitoring system with several types of scintillation sensors will be presented and discussed.

[1] A. Meents et al., *Proc. Natl. Acad. Sci. USA,* **107**, 1094 (2010).
[2] A. Wagner et al. *Acta Cryst. D***72,** (2016) *accepted.*
[3] H. Kraus et al., *Nucl. Instr. Meth. Phys. Res. A*, **553**, 522 (2005).

Giant negative magnetoresistance in oxygen-deficient Mn-substituted ZnO

X. L. Wang[1], Q. Shao[1], R. Lortz[2], J. N. Wang[2], A. Ruotolo[1]

[1]*Department of Physics and Materials Science, City University of Hong Kong, Kowloon, Hong Kong, SAR China*
[2]*Department of Physics, Hong Kong University of Science and Technology, Kowloon, Hong Kong, SAR China*

Magnetic thin films change their resistance under the application of a magnetic field. This magnetoresistive effect can be engineered to become *giant* by resorting to metallic multilayer devices [1,2]. An alternative route is the magnetically induced metal-insulator transition shown by strongly correlated semiconductors like mixed-valence manganites [3]. Yet, the application of these materials is limited by the difficulty and cost of fabrication. We here show that a negative magnetoresistance as large as several hundreds percent can be induced in simple zinc oxide (ZnO) doped with manganese (Mn) [4]. This anomalous effect was found to appear in oxygen-deficient films and to increase with the concentration of dopant. By combining magnetoresistive measurements with magneto-photoluminescence, we demonstrate that the effect can be explained as the result of a magnetically induced transition from hopping-type to metallic-type band conduction where the activation energy is caused by the *sp-d* exchange interaction.

The study was carried out on films of $Zn_{1-x}Mn_xO$ with x = 0 (pure ZnO), 0.02, 0.04 and 0.08 grown by pulsed laser deposition on sapphire substrates. Oxygen vacancies (V_O's) were introduced in the films by increasing the temperature of the substrate and decreasing the oxygen partial pressure during growth. A detailed characterization of our films showed that all the Mn is in valence 2+, therefore Mn-O-Mn double-exchange interaction can be ruled out [5]. As the temperature is reduced, the resistivity of the films increases with distinct signatures of a transition from band- to hopping-conduction. A sharp decrease of resistance of the Mn-substituted films was measured when an external magnetic field was applied The change of resistivity was found to increase with the concentration of Mn.

Since ZnO is a transparent semiconductor, the magnetic activation of electrons to the band conduction can be probed by resorting to magneto-photoluminescence measurements. In fact, V_O's are optically active defect centers that can form mono centric or pair exciton complexes at low temperatures. In our films, the oxygen vacancies form deep-level *F*-centres, where electrons are localized when the temperature is reduced. Electrons can hop between Mn-V_O complexes under the application of an electric field. An applied magnetic field reactivates the electrons in the conduction band, resulting in a sharp drop of resistivity.

[1] M. N. Baibich et al., Phys. Rev. Lett., **61**, 2472 (1988).
[2] G. Binasch et al., Phys. Rev. B **39**, 4828 (1989).
[3] A.-M. Haghiri-Gosnet et al., J. Phys. D: Appl. Phys. **36**, R127 (2003).
[4] X. L. Wang et al., Sci. Rep. **5**, 9221 (2015).
[5] Q. Shao, J. Appl. Phys. **115**, 153902 (2014).

Synthesis and luminescence properties of Ce^{3+} and Eu^{2+} doped silicate garnet phosphors for white LED convertors

N. Khaidukov[1], Yu. Zorenko[2], T. Zorenko[2], K. Paprocki[2],
M. Batentschuk[3], I. Levchuk[3], R. Van Deun[4]

[1]*Kurnakov Institute of General and Inorganic Chemistry, Russian Academy of Science, 119991Moscow, Russia*
[2]*Institute of Physics, Kazimierz Wielki University in Bydgoszcz, 85090 Bydgoszcz, Poland*
[3]*Institute of Materials for Energy and ElectronicTechnology (i-IMEET), Department of Materials Science and Engineering VI, University of Erlangen-Nuremberg, 91058 Erlangen, Germany*
[4] *L3 – Luminescent Lanthanide Lab, Department of Inorganic and Physical Chemistry, Ghent University, 9000 Gent, Belgium*

The work is devoted to development of phosphors based on the singly and doubly Ce^{3+} and Eu^{2+} doped solid solutions of $\{Ca_2R\}[Mg,Sc,Al,Ga]_2(Ga,Al,Si)_3O_{12}$, R= Y, Gd, Lu silicate garnets, which can be used for producing high power white LEDs (WLEDs) having high color rendering index and low correlated color temperature values. At present the development of such phosphors is a very important problem taking into account that only ceramic phosphors based on yellow emitting YAG:Ce garnet are now accessible for manufacturing high power WLED under near UV and blue LED excitations.

In this presentation we report the first results on the crystallization of monophasic ceramic of Ce^{3+} doped $Ca_2YSc_2GaSi_2O_{12}$, $Ca_2LuSc_2GaSi_2O_{12}$, $Ca_2GdSc_2GaSi_2O_{12}$, $Ca_2YSc_2AlSi_2O_{12}$ and $Ca_2YMgScSi_3O_{12}$ garnets as well as Eu^{2+}/Eu^{3+} doped $Ca_3Sc_2Si_3O_{12}$, $Ca_2YSc_2AlSi_2O_{12}$, $Ca_2YSc_2GaSi_2O_{12}$ and $Ca_2YMgScGaSi_2O_{12}$ garnets, synthesized by using a high temperature hydrothermal method , high-energy ball milling technique and high temperature solid-state reaction method. The structural analyzes of the ceramics were performed using XRD measurements and scanning electron microscopy. Chemical compositions were determined using an EDX microanalyzer.

The luminescent properties of the silicate garnet phosphors depending on the cation content were examined by recording cathodoluminescence spectra, photoluminescence (PL) emission and excitation spectra as well as PL decay kinetic. The obtained spectroscopic data were systematized in correlation with the structural features of the garnet hosts resulting in parameters of the crystal field strength around the Eu^{2+} and Ce^{3+} ions. Energy transfer between the garnet host and Ce^{3+}, Eu^{2+} and Eu^{3+} was also investigated. We have observed some trends in variations of the spectroscopic properties of Ce^{3+}, Eu^{2+} and Eu^{3+} doped garnets which can be suitable for the development of white convertors based on the compounds under study.

In summary, detailed spectroscopic research of $\{Ca_2R\}[Mg,Sc,Al,Ga]_2(Ga,Al,Si)_3O_{12}$, R= Y, Gd, Lu silicate garnets having dodecahedral sites for simultaneous localization of Ce^{3+}, Eu^{2+} and Eu^{3+} ions can open new perspectives for designing single-phase phosphors with blue, green and red components, which can be excited by near UV and blue LEDs.

This work was realized within the NANOLUX 2014 # 286 project in the ERA NET Rus Plus S&T program.

Carrier self-trapping in iron-doped lithium niobate

S. Messerschmidt[1], A. Krampf[1], T. Nörenberg[1], M. Imlau[1],
L. Vittadello[2], M. Bazzan[2]

[1]*School of Physics, Osnabrueck University, Barbarastraße 7, 49076 Osnabrueck, Germany*
[2]*Dipartimento di Fisica e Astronomia, Università di Padova, Via Marzolo 8, 35131 Padova, Italy*

Iron doped lithium niobate, $LiNbO_3$:Fe (LN:Fe), is a prototype material for studying the bulk photovoltaic effect (BPVE) and related nonlinear optical phenomena with the photorefractive effect being the most prominent one. Recently, Schirmer et al. [1,2,3] proposed a microscopic interpretation of the BPVE based on the phenomenon of carrier self-trapping. In this view, the BVPE results from the interplay between the optical transfer of small strong-coupling polarons from Fe_{Li}^{2+} defect centres to next-neighbouring Nb^{5+} atoms of the regular lattice, and low-mobility small-polaron hopping transport in the dark, that is the subject of the present work. Already in 2005, Herth et al. studied hopping and recombination of optically generated, Nb_{Li}^{4+} electron polarons in presence of extrinsic Fe_{Li}-defect centres by means of transient absorption spectroscopy [4]. It was shown that O^- hole polarons give rise to a green-induced blue-light absorption and Fe_{Li}^{3+} acts as intermediate trapping centre within Nb_{Li}^{4+}-O^- recombination.

In this study we repeated those measurements in the unexplored temperature range between 100 and 300K using an improved setup with the possibility of simultaneous detection in the UV, VIS and NIR spectral range. Moreover, we exploited the spectral features of the absorption cross-section of small polarons, as determined by Merschjann et al. [5], to test quantitatively our models deducing the time evolution of the number densities for the involved polaron species.

Remarkably, our study uncovers a temporal offset between the blue- and near-infrared absorption features, particularly at temperatures below 250 K, that is in contradiction with the commonly accepted Nb_{Li}^{4+}-O^- recombination path via Fe_{Li}^{3+}. We show that an additional X-centre must be considered with (i) an absorption feature in the blue-green spectral range, (ii) a ms-lifetime comparable to the one of Nb_{Li}^{4+} polarons and (iii) under the condition of charge conservation. Potential candidates are discussed: transient Nb_{Li}^{4+}:Nb_{Nb}^{4+}-bipolarons, self-trapped Nb_{Nb}^{4+}-O^--excitons or Fe_{Li}^{2+} within differently distorted lattice environments.

1. Schirmer, O. F. *et al.,* Phys. Rev. B **83** (2011)
2. Sanson, A. *et al.,* Phys. Rev. B **91** (2015)
3. Imlau, M. *et al.,* Appl. Phys. Rev. **2** (2015)
4. Herth, P. *et al.,* Phys. Rev. Lett. **95** (2005)
5. Merschjann, C. *et al.,* J. Phys.: Condens. Matter **21** (2009)

Mechanical stress in nano-size particles

G. Laurens[1], G. Ledoux[1], J. Lam[1], A. Chemin[1], C. Martinet[1], A. Cornet[1], K. Lebbou[1], C. Dujardin[1], F. Chaput[2], B. Gökce[3], S. Barcikowski[3], and D. Amans[1].

[1]*Institut Lumière Matière, UMR5306 Université Lyon 1-CNRS, Université de Lyon, F-69622 Villeurbanne cedex, France*
[2]*Laboratoire de Chimie, UMR5182 Université Lyon 1 - CNRS - ENS Lyon, Université de Lyon, F-69364 Lyon, France.*
[3]*Technical Chemistry I, University of Duisburg-Essen and Center for Nanointegration Duisburg-Essen CENIDE, Universitaetsstrasse 7, 45141 Essen, Germany*

When doped with Cr^{3+} the corundum phase (α) of alumina (Al_2O_3) is called ruby (α-Al_2O_3:Cr^{3+}). Known for its value as a gemstone, ruby also shows interesting optical properties such as the pressure dependence of its R fluorescence lines which is commonly used as a continuous pressure sensor [1]. In order to check the validity of Laplace-Young pressure conjecture on small particles ruby is a candidate of choice. Additionally there is a growing need of smaller sensors for testing pressure on smaller systems and with a better colloidal stability. Synthesis of α-Al_2O_3 nanoparticles, with an average size larger than 30 nm, has been reported previously [2]. But no evidence of α-Al_2O_3 nanoparticles with sizes smaller than 10 nm has been reported. In general, the laser ablation of an Al target in water leads to ϒ-Al_2O_3, which is considered the thermodynamically stable polymorph for particle sizes smaller than 10 nm [3].
Using 2-[2-(2-methoxyethoxy)ethoxy] acetic acid (MEEAA) [4], we have successfully synthesized highly reproducible monodisperse luminescent nano-ruby. The obtained size distribution shows little dependence on the laser source, with about 4 nm median size, and less than 1 nm standard deviation. In this work, we measure the pressure dependence of the Cr^{3+} luminescence and show that for pressures under 11 GPa, the shift of the R1 line in the nanoparticles is identical to the one observed in bulk ruby. The inner pressure of the nano-rubies is then directly measured from their own luminescence. If Laplace-Young pressure conjecture was relevant for solid matter, we should measure a luminescence shift, compared to bulk rubies, for the as-produced 4 nm ones. However, this is not the case. The surface energies can drive the thermodynamic stable phase for nanoparticles, as depicted by Mc Hale et al., but this change definitively does not correspond to a pressure induced shift in the phase diagram.

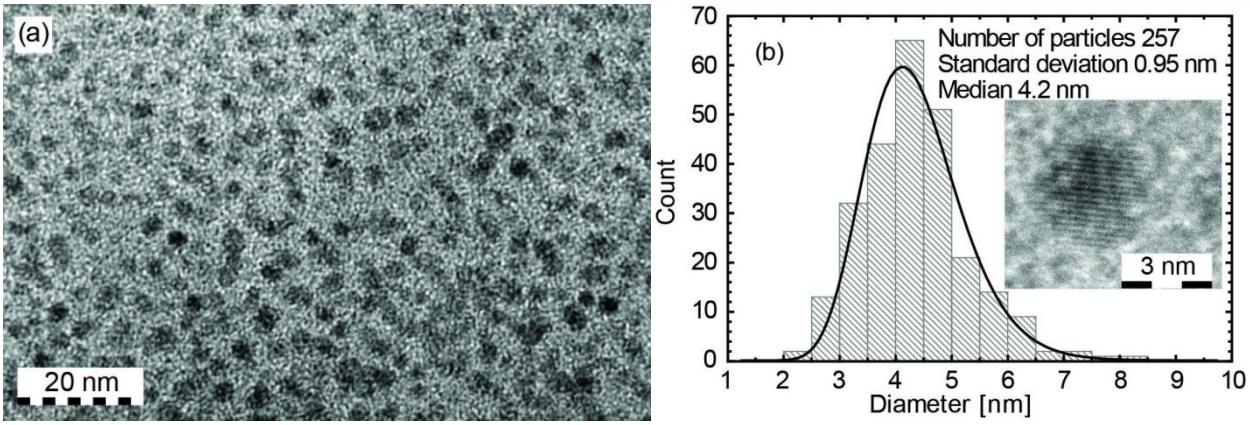

Figure : (a) Typical TEM picture and (b) size distribution

[1] R. Forman, S. Block, J. Barnett, and GJ. Piermari, Science **176**, 284 (1972).
[2] C. L. Sajti, R. Sattari, B. N. Chichkov, and S. Barcikowski, J.Phys. Chem. C **114**, 2421 (2010).
[3] J. McHale, A. Auroux, A. Perrotta, and A. Navrotsky, Science **277**, 788 (1997).
[4] D. Amans, C. Malaterre, M. Diouf, C. Mancini, F. Chaput, G. Ledoux, G. Breton, Y. Guillin, C. Dujardin, K. Masenelli-Varlot, and P. Perriat, J. Phys. Chem. C **115**, 5131 (2011).

Study of the effect of optical bleaching at selected photon energies on the OA and TL of LiF:Mg,Ti (TLD-100)

L.Oster[1], S.Druzhyna[2], G.Reshes[1], I.Eliyahu[3], Y.S.Horowitz[4], S.Biderman[5]

[1]Physics Unit, Sami Shamoon College of Engineering, Beersheva, Israel
[2]Nuclear Engineering Unit, Ben Gurion University of the Negev, Beer Sheva, Israel
[3]Soreq Nuclear Research Center, Yavneh, Israel
[4]Physics Department, Ben Gurion University of the Negev, Beer Sheva, Israel
[5]Nuclear Research Center-Negev, Beer Sheva, Israel

A previous investigation has demonstrated an alternate analysis of the optical absorption (OA) spectrum of LiF:Mg,Ti. The spectra in the vicinity of 4 eV can be fitted over a wide range of levels of dose by two OA bands at 3.8 eV and 4.3 eV rather than a broad band at 4.0 eV (associated with peak 5 in the glow curve) and an additional band at 4.45 eV of unknown identity. The increased intensity of the 4.3 eV band relative to the 3.8 eV band at high levels of dose suggests that it is associated with the electron-hole (e-h) configuration giving rise to peak 5 whereas the 3.8 eV band arises from the e-only configuration. Preliminary kinetic simulations of the effect of 5.08 eV (F band) photon bleaching on the OA spectrum have interpreted the results by invoking V_3-V_k transformation as a hole-production-mechanism but have been inconclusive concerning the e-h/e-only interpretation.

Samples of TLD-100 (3 x 3 x 0.89 mm^3) were irradiated with 4 MeV alpha particles and ^{137}Cs gamma rays. Glow curve readout was carried out at a heating rate of $1^oC\ s^{-1}$ and deconvolution was carried out with first order peak shapes based on ancillary thermal and optical excitation which isolate peaks 4 and 5. The OA spectra were deconvoluted using a commercial "Peak-Fit" non-linear curve fitting program from Jandel Scientific. Optical bleaching was carried out at 3.8 eV, 4.3 eV, 5.08 eV and 5.45 eV using a 300 W Xenon lamp attached to an Oriel 1/8 m monochromator with a bandwidth of 5 nm.

Several observations are worthy of note. (i) All the bands decrease or are largely unaffected following the bleach except for the 5.45 eV band which always increases. (ii) The ratio of the decrease of the 4.3 eV band to the decrease of the 3.8 eV band increases continuously from a value of 1.48 at 3.8 eV to a value of 3.14 at 5.45 eV.(iii) The bleach decreases peak 5 and peak 5a intensity by 40% and 33 % respectively whereas peak 4 increases by 22%.

The increase in peak 4 (associated with a h-only configuration) can be explained by transformation of the e-h to the h-only configuration by direct removal of the electron from the e-h configuration. The increase of the 5.45 eV band is due to a far stronger electron recombination probability compared to the hole recombination probability. Kinetic simulations will attempt to unravel the mystery of the dependence of the 4.3/3.8 ratio on photon energy.

Mg co-doping effects on Ce doped $Y_3(Ga,Al)_5O_{12}$ scintillator

Kei Kamada[1,2], Shunsuke Kurosawa[1,3], Yuui Yokota[1],Yuji Ohashi[3], Akira Yoshikawa[1,2,3]

[1]*Tohoku University, New Industry Creation Hatchery Center*
[2] *C&A corporation*
[3]*Tohoku University, Institute for Material Research*

Scintillator materials combined with photodetectors are used to detect high energy photons and accelerated particles in medical imaging techniques, high energy and nuclear physics detectors, high-tech industrial applications and most recently also in the advanced homeland security related techniques. In these applications, highlight yield, high stopping power, fast decay time without slower decay components, low cost and high radiation resistivity and low cost are required for scintillator materials. Recently improvement of scintillation performance by co-doping with alkali earth AE^{2+} ions in Ce activated garnet scintillators such as $Y_3Al_5O_{12}$ (YAG), $Lu_3Al_5O_{12}$ (LuAG) and $Gd_3Ga_3Al_2O_{12}$ (GAGG) were reported [1]. In these materials charge transfer absorption of Ce^{4+} was clearly observed in the near UV range below 350 nm and Mg co-doping caused acceleration of the scintillation decay time and increase of light yield. In this study, Mg co-doping effects on optical and scintillation properties of $Y_3(Ga,Al)_5O_{12}$ were investigated.

Mg 200 ppm and non co-doped Ce0.5% doped $Y_3Ga_xAl_{5-x}O_{12}$ (YGGAG) (x=0, 1, 2, 3, 4) was successfully grown by the micro-pulling down method (Fig.1). Charge transfer absorption of Ce^{4+} below 350 nm was investigated in the Mg co-doped crystals. Scintillation decay time was accelerated in all of the Mg co-doping crystals (Fig.2). Details of chemical composition analysis, optical and luminescence properties will be reported in my presentation.

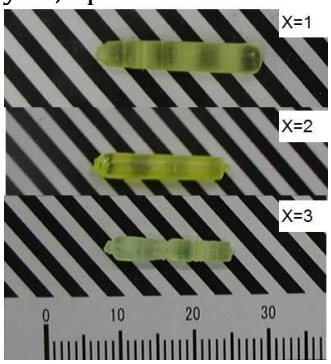

Fig.1 Example photographs of the grown YGGAG crystals

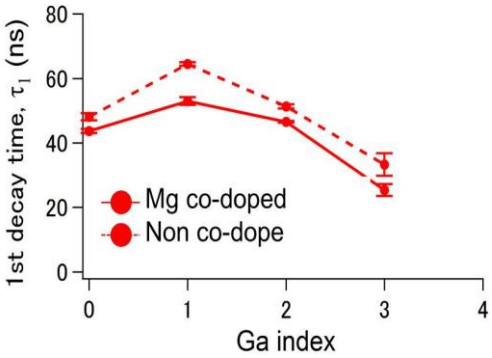

Fig.2 Decay time of 1st decay component in the Mg and non co-doped Ce:YGGAG

[1] A. Nagura,et al, Japan.J. App. Phy., **54** 04DH1 (2015).

Influence of Yb-related traps on afterglow properties of garnet scintillators

V.Khanin[1,2], C. Ronda[2], P.A. Rodnyi[1]

[1]*Peter the Great St. Petersburg Polytechnic University, St. Petersburg, Russia*
[2]*Philips Research, Eindhoven, the Netherlands*

In the search for new efficient scintillators for medical and industrial applications, cerium-doped oxide garnets have been investigated extensively during recent years. $Y_3Al_5O_{12}$:Ce and $Lu_3Al_5O_{12}$:Ce were shown to have relatively low light yields (< 30 ph/KeV [*1*]), whereas more than 60 ph/KeV can be expected from calculations. Relatively high light yields were found in mixed oxide garnets (e.g. (Y,Gd)-garnets and Gd_3(Ga,Al)-garnets [*2*]). However, many of the mixed oxide garnets as well as YAG:Ce and LuAG:Ce are characterized by a multi-exponential decay and severe afterglow [*3*]. The afterglow is due to trapping of either electrons or holes.
Here we study Thermally Stimulated Luminescence (TSL) of mixed oxide garnet ceramics containing Yb impurity as it is expected to be present even in high purity starting materials, based on its chemical similarity with the starting materials.
Additionally, afterglow curves in the 10^{-3}-10^5 sec range after X-ray excitation were measured. Changes in TSL curves were correlated to changes in afterglow curves.
The trap parameters of the Yb-related defects are discussed.
Oxide garnet ceramics of $(Y,Gd)_3Al_5O_{12}$:0.2%Ce with Y:Gd ratios 3:0, 2.85:0.15, 2.75:0.25, 2.25:0.75 and 1.8:1.2 co-doped with 50 ppm of Yb_2O_3 were prepared at Philips Research Eindhoven by conventional “mix and fire” synthesis techniques with rare-earth- (RE-) and aluminium oxides as starting materials.
TSL measurements were conducted after 50 kV, 10mA, 5 min of X-ray irradiation at liquid nitrogen temperature with a heating rate of 0.25 K/s up to 550 K. Afterglow was measured after 2 or 6 seconds of irradiation with 120kV, 20mA from an X-ray tube.

[1] Moszynski M., et al. Nucl. Instrum. Methods Phys. Res A, **345**, 461 (1994).
[2] Kamada K., et al. J. Phys. D Appl. Phys., **44**, 505104 (2011).
[3] Mihokova E., et al. Rad. Meas., **56**, 98 (2013).

Optical bleaching in YAP single crystals doped with manganese ions

A. Luchechko[1], Ya. Zhydachevskii[2,3], *M. Glowacki[2],* S. Ubizskii[3], *M. Berkowski[2], A. Suchocki[2,4]*

[1]Ivan Franko National University of Lviv, Lviv, Ukraine
[2]Institute of Physics, Polish Academy of Sciences, Warsaw, Poland
[3] Lviv Polytechnic National University, Lviv, Ukraine
[4]Institute of Physics, University of Bydgoszcz, Bydgoszcz, Poland

The luminescence characteristic of YAP crystals have been extensively studied, because of this perovskite doped with manganese ions was proposed as new dosimetric material with good thermally stimulated luminescence (TSL) properties. The TSL characteristics of YAP: Mn are sensitive to doping level, crystal grown conditions and thermochemical treatment. The OSL is an alternative technique for not only to measure the signal of the deep traps without the sample heating, but also use this signal for dosimetry. The aim of this work was to study the bleaching characteristic of TSL and possibility of the continues-wave optical stimulation (CW-OSL) of YAP: Mn single crystals.

The Mn-doped $YAlO_3$ single crystals were grown by Czochralski method in the Institute of Physics of the Polish Academy of Sciences. The manganese doping concentration was 0.02, 0.035 and 0.05 wt.% in the melt with respect to yttrium. The TSL investigations were carried out in the temperature range from 300 to 550 K. The Xe-lamp and monochromator was used for the light stimulation. The OSL measurements were performed at room temperature using a spectrofluorometer CM2203. Irradiation of the crystals with X-rays was performed using a X-ray tube with Cu anticathode.

After X-ray excitation of the YAP: Mn crystals at 300 K, the TSL curve shows a weak peak at 370 K and an intense dosimetric peak at about 450-470 K. Exposure of the YAP:Mn crystal by blue-green light after previous excitation with X-ray photons leads to the appearance of OSL and a significant decrease in the TSL light sum stored in 450 K peak. In this case, thermally and optically-stimulated emission in green spectral region (at 530 nm) appears as a result of the electron-hole recombination process. More long-wavelength illumination has less effect to this peak intensity.

The correlation between the bleaching of TSL and OSL signal, in particular the study of sequential reading of the OSL and TSL signals has been carried out. The dependencies of the OSL signal from the stimulation time, activator concentration and duration of X-rays irradiation will be presented. The possible mechanisms of the TSL and OSL processes in YAP:Mn are discussed.

The work was partially supported by the EU within the European Regional Development Fund through the Innovative Economy grant (POIG.01.01.02-00-108/09) and by the NATO SfP Project NUKR.SFPP 984649.

Evolution of GLPC defects in O_2-loaded germanosilicate optical fibers: *in-situ* cathodo-luminescence study

D. Di Francesca[1], I. Reghioua[1], S. Girard[1], S. Agnello[2], A. Alessi[1], L. Martin-Samos[3], M. Fanetti[3], N. Richard[4], M. Raine[4], A. Boukenter[1], F.M. Gelardi[2], Y. Ouerdane[1]

[1] *Univ-Lyon, Laboratoire Hubert Curien, UMR CNRS 5516, Saint-Etienne, France*
[2] *Dipartimento di Fisica e Chimica, Università di Palermo, I-90123 Palermo, Italy*
[3] *Materials Research Laboratory, University of Nova Gorica, Vipavska 11c 5270-Ajdovscina, Slovenija*
[4] *CEA, DAM, DIF, F91297, Arpajon, France*

Cathodo-Luminescence (CL) is a powerful experimental technique to investigate the evolution of luminescent defects with irradiation in dielectric materials. We demonstrated in a previous work [1] that the radiation response of Ge-doped Optical Fibers (OFs) depends strongly on the initial concentration of oxygen-deficient center, called Germanium Lone Pair Centers (GLPC, lone pair localized on a twofold coordinate Ge atom), which are precursors of other radiation induced Ge-related defects (Ge(1) and Ge(2)). An O_2-loading treatment is able to remove up to 98% of native GLPC and improve the Radiation Induced Attenuation (RIA) by a factor 3 around 350 nm. In this spectral range the main radiation induced absorbing defect should be the Ge(1) (an electron trapped on a tetra-coordinated Ge atom), which, however, is not detected in the irradiated O_2-loaded sample by Electron Paramagnetic Resonance (EPR). Therefore, the relatively high RIA levels of the O_2-loaded samples were initially attributed to generation of oxygen-excess-related defects and, eventually, to the restoring of GLPC.
The current investigation exploits the well-known emission band of GLPC, [2] around 400 nm, to monitor the evolution of GLPC with the electron fluence. Such luminescence is generated by a sharp electron beam which also represents the source of the radiation dose. The results show that in the O_2-loaded OFs the intensity of the GLPC luminescence grows with the irradiation. In contrast, the opposite evolution can be observed in the same OF type which were not pre-treated in O_2. The employed experimental system also allows measuring GLPC CL with micrometric spatial resolution and obtaining 2D cartographies of the fiber transverse cross-section. After a sufficiently long irradiation, the concentration of GLPC approaches a stable level in each region of the OF for both the O_2 loaded and unloaded samples. Remarkably enough, the shapes of the CL intensity cartographies of the irradiated O_2–loaded and unloaded OFs are very similar. On the basis of this phenomenology, we conclude that at high fluences the GLPC concentration may depend mainly on the Ge-doping concentration, whereas the initial concentration of GLPC, which is a production related parameter, impacts the radiation response of the material by either promoting or forbidding the radiation induced mechanism that converts GLPC in Ge(1) and Ge(2).

[1] D. Di Francesca *et al.*, "O_2-loading treatment of Ge-doped silica fibers: a radiation hardening process," J. Lightwave tech., 2016, accepted for publication.
[2] V. B. Neustruev, "Colour centres in germanosilicate glass and optical fiber," *J. Phys. Condens. Matter*, **6**, 6901 (1994)

Modeling of Defect Formation Processes in Na_2SO_4 Crystal

D.H. Daurenbekov, Zh.M. Salikhodzha, T.N. Nurakhmetov, K.A. Kuterbekov, A.M. Zhunusbekov, A.Zh. Kainarbay

L.N. Gumilyov Eurasian National University, Munaitpasov str., 13, Astana, Kazakhstan

It is known that interest to the investigation of formation of radiation defects in sulfates of alkaline metals is caused by their use as thermoluminescent dosimeters. For example, sodium sulfate crystals doped with the rare earth element dysprosium are used as thermoluminescent dosimeters [1]. The anion complex SO_4^{-2} in the alkali metal sulfates has perfect tetrahedral structure. The analysis of theoretical and experimental investigations [2-4] shows that in the irradiated sulfates of alkaline and alkaline-earth metals such defects as SO_4^-, SO_4^{-3}, $SO_3^- v_a^+ e^-$ and O_3^- are formed. SO_4^--center is a hole center formed by ionization of the anionic complex SO_4^{-2} . SO_4^{-3}-center is an electronic center formed by the capture of a single electron by the anionic complex and stable only at low temperatures. The stable electronic center $SO_3^- v_a^+ e^-$ is a product of decay of excited anionic complex. A rather unstable O_3^- – center is formed by the reaction $O^0 + O^0 \rightarrow O_2^0$ and $O_2^0 + O^- \rightarrow O_3^-$. Therefore, the processes of radiation defect formation in sulfates of alkaline and alkaline-earth metals are caused by the decay of the anionic complex. The report will present the results of semi-empirical quantum-chemical method PM7 obtained using the software package MOPAC 2012 (Molecular Orbital PACkage) developed for simulation of the processes of defect formation in crystal.

[1] Rowlands A.P., Tyagi A.K., Karali T., Townsend P.D., Radiat. Prot. Dosim. **100** 55 (2002).
[2] Kityk I.V., Andrievskii B.V. and Yuvchenco V.O. Phys. Stat. Sol. (b). **182** 79. (1994)
[3] Danby R.J., Boas J.F., Calvert R.L., Pilbrow J. J. Phys.C: Solid State Phys., **15** 2483 (1982)
[4] Byberg I.R. J. Chem. Phys. **84, II**, 6083 (1986)

Beyond Lithium-Ion Batteries: A Computational Study on Advanced Lithium – Sulphur Battery

[1,2] M.C. Masedi, [2] H.M. Sithole and [1] P.E. Ngoepe

[1]Materials Modelling Centre, University of Limpopo, Private Bag x1106, Sovenga 0727, South Africa.
[2] CSIR, Meraka Institute, Meiring Naude, Brummeria, P. O. Box 395, Pretoria 0001, South Africa.

Rechargeable lithium−sulfur (Li−S) batteries hold great potential for high-performance energy storage systems because they have a high theoretical specific energy, low cost, and are eco-friendly [1].

This work shows a study on stability, structural and electronic properties of discharge products formed in Li-S battery (Li_2S) using different kinds of computational techniques. *ab intio* method was employed to generated structural parameters which compare well with experimental results [2]. The elastic properties and phonon agreed with experimental work and suggested that the structure is stable [3]. GULP_code was used to successfully derive Buckingham potential models.

The potential models were employed and validated during molecular dynamics calculations producing same melting temperature as experimental study. Cluster expansion technique was later used to improve Li_2S material by introducing selenium and forming Li_2S-Se structure which has potential to offer higher theoretical specific energy and remedies the challenges that Li-S battery encounters. Cluster expansion generated new stable phases of Li_2S-Se system while and Monte Carlo simulations which allow varying of concentrations and temperature successfully determined the temperature of the system mixing.

[1] J.Nelson, J. Am. Chem. Soc.,**134**, 6337−6343 (2012)
[2] P. E. Blöchl, Phys. Rev. B **50**, 17953 (1994)
[3] Bertheville J Phys. Cond Matt **10**, 2155 -2169 (1998)

Amorphisation and Recrystallisation Study of Lithium Intercalation into TiO_2 Nano-Architectures

.

M. G. Matshaba[1], D. C. Sayle[2] and P. E. Ngoepe[1],

[1] *Materials Modelling Centre, University of Limpopo, Private Bag x1106, Sovenga 0727, South Africa*
[2] *School of Physical Sciences, University of Kent, Canterbury, CT27NZ, United Kingdom*

Titanium dioxide is playing an increasingly signif-icant role in easing environmental and energy concerns [1,2]. Its rich variety of polymorphic crystal structures has facilitated a wide range of applications such as photo-catalysis [3], photo-splitting of water [4], photoelectrochromic devices [5], insulators in metal oxide [6], semiconductors devices [7], dye sensitized solar cells (DSSCs) (energy conversions) [8], rechargeable lithium batteries (electrochemical storage) [9]. The complex structural aspects in nano TiO_2, are elucidated by microscopic visualization and quantification of the microstructure for electrode materials, since cell performance and various aging mechanisms depend strongly on the appearance and changes in the microstructure. Recent studies on MnO_2 have demonstrated that amorphisation recrystallisation simulation method can adequately generate various nanostructures, for Li-ion battery compounds. The method was also previously employed to produce nano-TiO_2. In the current study, the approach is used to study lithiated nano- porous, sheet and bulk structures for TiO_2 which have been extensively studied experimentally, as mentioned above. Molecular graphic images showing microstructural features, including voids and channels have accommodated lithium's during lithiation and delithiationas. Preliminary lithiation of TiO_2 will be considered, where concentration profiles of different ions are shown in the structures, together with radial distribution functions.

[1] Diebold, U. The Surface Science of Titanium Dioxide. Surf. Sci. Rep., **48**, 53 – 229 (2003).
[2] Tong, H.; Ouyang, S.; Bi Y.; Umezawa, N.; Oshikiri, M.; Ye, J. Nano-photocatalytic materials: possibilities and challenges. Adv. Mater., **24**, 229 – 251, (2012).
[3] Fujishima, A.; Honda, K. Electrochemical photolysis of water at a semiconductor electrode. Nature 1972, 238, 37 - 38. [4] Z. Y. Wang, S. Z. Liu, G. Chen and D. G. Xia, Electrochem. Solid-State Lett., **10** A77 (2007).
[4] Gratzel, M. Photoelectrochemical Cells. Nature 2001, 414, 338 - 344. [6] T. X. T. Sayle, R.R. Maphanga, P. E. Ngoepe and D. C. Sayle, J. Am. Chem. Soc, **131**, 6161 (2009).
[5] Pichot, F.; Ferrere, S.; Pitts, R. J.; Gregg, B. A. Flexible Solid-State Photoelectrochromic Windows. J. Electrochem. Soc., **146** (11), 4324 – 4326 (1999).
[6] Qingjiang, L.; Khiat, A.; Salaoru, I.; Papavassiliou, C.; Hui X.; Prodromakis, T. Memory Ompedance in TiO2 based Metal-Insulator-Metal Devices. Sci. Rep., **4522**, 1 – 6 (2013)**.**
[7] McFarland, E. W.; Tang, J. A photovoltaic device structure based on internal electro emission. nature, **421**, 616 - 618 (2003)
[8] Susanti, D.; Nafi, M.; Purwaningsih, H.; Fajarin, R.; Kusuma, G. E. The Preparation of Dye Sensitized Solar Cell (DSSC) from TiO2 and Tamarillo Extract. Procedia Chem., **9**, 3 – 10, (2014).
[9] Bruce, P. G.; Scrosati, B.; Tarascon, J-M. Nanomaterials for Rechargeable Lithium Batteries. Angew. Chem. Int. Ed., **47** (16), 2930 – 2946 (2008).

Ab-initio study of structural properties of Lead Barium sulfide alloys.

C. Sifi, F. Chouit, M. Slimani, H. Meradji and S.Guemid.

Laboratoire de Physique des Rayonnements, Département de Physique, Faculté des Sciences, Université de Annaba, Algeria

The ab-initio full potential linearized augmented plane wave (FP-LAPW) method within density func¬tional theory was applied to study the structural, and thermodynamic properties of PbS , BaS and Pb1-xBaxS ternary alloys. We use both Perdew–Burke–Ernzerhof (PBE) GGA and Engel–Vosko generalized gradient approximations of the exchange-correlation energy that are based on the optimization of total energy and corresponding potential, respectively. Our investigation of the effect of composition on the lattice constant, bulk modulus and ionicity for ternary alloys shows almost nonlinear dependence on the composition. Besides, a regular-solution model is used to investigate the thermodynamic stability of the alloys, which mainly indicates a phase miscibility gap. The thermal properties are also investigated in this work.

On real structure of the profiled anion-deficient corundum

V.I. Maksimov[1], R.M. Abashev[2], V.I. Sokolov[1], A.I. Surdo[2], E.N. Yushkova[1]

[1] *Institute of Metal Physics UB RAS, 18 S. Kovalevskaya Str., 620990 Ekaterinburg, Russia*
[2] *Institute of Industrial Ecology UB RAS, 20 S. Kovalevskaya Str., 620219 Ekaterinburg, Russia*

Profiled anion-deficient single crystals of corundum (α-$Al_2O_{3-\delta}$) grown by Stepanov's method under reducing conditions are widely used for the manufacture of radiation detectors of the type TLD-500 and Al_2O_3:C. In the present work two types of these single crystals were investigated by scattering of thermal neutrons (λ=1.57 Å) at *T*=300 K. The first type (or α-$Al_2O_{3-\delta}$) as grown crystal was with a concentration of anion vacancies ~10^{17} cm^{-3}. The second type obtained by the same synthesis was annealed at T=1970 K for 70 hours in oxygen atmosphere to restore the "natural" structure state of corundum or α-Al_2O_3. In it concentration of anion vacancies was less than 10^{12} cm^{-3}. The neutronographic research was carried out on D7b multichannel diffractometer (IVV-2M reactor, Zarechny, Sverdlovsk region, Russia).

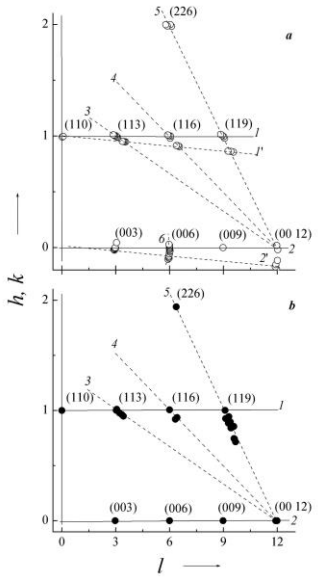

Fig.1. Projections of reciprocal lattice of α-$Al_2O_{3-\delta}$ (a) and α-Al_2O_3 (b) on the (100) plane refined in neutronographic experiment: 1, 2 – knot lines of the "main" lattice; 1', 2' – knot lines of the lattice of "twins"; 3, 4, 5 – lines, along which

Real structure of as grown α-$Al_2O_{3-\delta}$ crystal is characterized by existence of single massive crystallite of corundum structure in presence of large numbers of small fragments, with full volume of them being in commensurability with the volume of the main crystal block. These microfragments, almost of all, are deformed and irregular strains are seemed to be concentrated in their volumes. In full, neutron scattering picture obtained on fragmented part allows to suppose that anion vacancies, being concentrated mostly in fragments, result in the highest vacancies content on the boundaries of the fragments. As it seen from fig.1a, striking fragmentation may be formed by twinning. Data obtained on annealing crystal show suppression of fragmentation indications, whereas very weak reflections of superstructure corresponding to wave vectors q = (1/9 1/9 0) $2\pi/a$ + (0 0 1/3) $2\pi/c$ and their second and third harmonics appear. The most pronounced points of this superstructure are situated along straight lines connecting "main structure" knots containing places of the "twinning" knots in reciprocal space (fig1b). These results are under discussion, with possible displacements of Al-ions surrounding individual extra O-vacancy being taken into quality-level consideration.

ESR of $^{151}Eu^{2+}$ rhombic centers in $Y_3Al_5O_{12}$

V.A. Vazhenin[1], A.P. Potapov[1], H.R. Asatryan[2], Yu. A. Uspenskaya[2], K.L. Hovhannesyan[3], A.G. Petrosyan[3]

[1]Ural Federal University, 19 Mira Street, Yekaterinburg, 620002 Russia
[2]Ioffe Physical-Technical Institute, Politekhnicheskaya ul. 26, St.Petersburg, 194021 Russia
[3]Institute for Physical Research, NAS RA, Ashtarak-2, 0203 Armenia

The electron paramagnetic resonance (ESR) of Eu^{2+} ions (electron spin S=7/2) in single crystals of yttrium aluminum garnet ($Y_3Al_5O_{12}$) was for the first time reported in [1, 2]. Due to absence in [2] of superfine structure on many of the ESR signals, there were difficulties in ascribing them to definite transitions of Eu^{2+}. In the present work $Y_3Al_5O_{12}$ single crystals doped with europium enriched to 97.5 % of ^{151}Eu (nuclear spin I=5/2) were grown by the vertical Bridgman method under reducing atmosphere. HfO_2 or SiO_2 were added to the melts to stabilize sufficiently high concentrations of Eu^{2+}. The obtained ^{151}Eu:$Y_3Al_5O_{12}$ crystals, dark-blue in color, demonstrated (as in [2]) a spectrum of six equivalent and variously oriented Eu^{2+} centers, but showing now well-resolved superfine structures on a bigger number of transitions (see the Figure). No noticeable difference has been observed in experimental spectra of crystals co-doped with either Si^{4+} or Hf^{4+}.

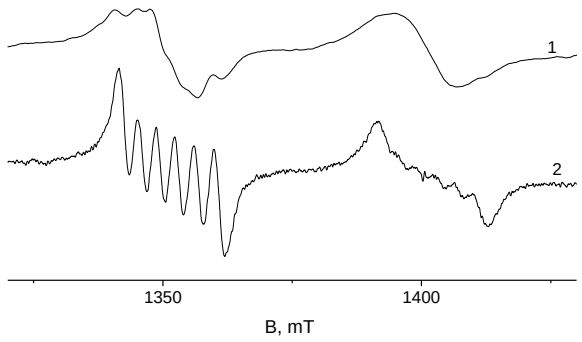

Fig. ESR spectra of two electron transitions: the upper along the field - 3↔4 (B||Z||C_2), the lower - 5↔6 (B||Y||C_2) in crystals with natural abundance of europium isotopes (curve 1) and enriched with ^{151}Eu (curve 2).

Close values of b_{20} and b_{22} parameters of the spin hamiltonian (≈9000 MHz) is a typical peculiarity of Eu^{2+} centers in $Y_3Al_5O_{12}$. Due to this, the energy level scheme in B||X orientation is almost symmetrical and the energy level schemes in B||Z and B||Y orientations are bound to each other by a turn around the magnetic field axis. For this reason the signals shown on the Figure (as well as other B||C_2 linked transitions) turn to be close neighbours. It is established that the observed superfine structure is described by practically isotropic parameter (≈100 MHz) of the superfine interaction, while no influence of the nuclear quadrupole interaction is found.

The research was made possible in part by the Ministry of Education and Science of the Russian Federation. This work is supported also by the RFBR grant № 5-52-05040 Arm_a and grant № 15RF-003 of the State Committee of Science of Armenia.

[1] H.R. Asatryan, A.A. Mirzakhanyan. Fizika Tverdogo Tela (in Russian). 1991, Vol. 33, pp.1899-1900.
[2] A.P. Potapov, H.R. Asatryan, Yu.A. Uspenskaya, V.A. Vazhenin, A.G. Petrosyan, A.V. Fokin. Book of abstracts. XVI International Feofilov Simposium, Saint Petersburg, 9-13 November 2015, p. 185.

ODMR in gadolinium-containing garnet crystals via Ce^{3+} photoluminescence

H.R. Asatryan[1], N G. Romanov[1], A.S. Gurin[1], Yu.A. Uspenskaya[1], A.G. Badalyan[1], P.G. Baranov[1], A.G. Petrosyan[2], H. Wieczorek[3], and C. Ronda[3]

[1]*Ioffe Physical-Technical Institute, Politekhnicheskaya ul. 26, St. Petersburg, 194021 Russia*
[2] *Institute for Physical Research, NAS RA, Ashtarak-2, 0203 Armenia*
[3] *Philips Research, High Tech Campus 34, 5656 AE, Eindhoven, The Netherlands*

Ce^{3+}-doped garnet crystals are used as high-performance scintillators in many fields, including positron emission tomography imaging and high energy physics. In recent years, the high potential of Ce-doped gadolinium based garnets [1], which have extremely high photon gain, a high density and a high stopping power, was recognized.

In this paper, we report results of a study of Ce-Gd co-doped single crystals of $Y_3Al_5O_{12}$ and cerium doped $Lu_{1-x}Gd_xAl_5O_{12}$ by means of optically detected magnetic resonance (ODMR). 35 GHz ODMR was recorded at a temperature of 1.8 - 2 K via PL intensity of Ce^{3+} excited by a 405 nm semiconductor laser followed by a quarter-wave plate.

It was shown that ODMR of Ce^{3+} in the ground state in $Y_3Al_5O_{12}$ crystals can be observed by monitoring the Ce^{3+} photoluminescence (PL) intensity. We have proved that the effect is due to selective PL excitation from one of two Ce^{3+} ground state spin sublevels under circularly polarised excitation. Due to the Boltzmann population distribution between spin sublevels the PL intensity increases under σ^+ and decreases under σ^+ polarized excitation thus allowing monitoring the electron spin polarization of the Ce^{3+} ground state. EPR transitions that tend to equalize the populations of the levels in resonance can therefore be detected via PL intensity.

In cerium doped $Y_3Al_5O_{12}$ crystals containing small concentration (< 0.1%) of gadolinium new ODMR signals have been found in addition to Ce^{3+} ODMR. They correspond to the ground state EPR of Gd^{3+}. In $Lu_{2.75}Gd_{0.25}Al_5O_{12}$ and $Lu_{2.875}Gd_{0.125}Al_5O_{12}$ crystals only ODMR of Gd^{3+} was observed via Ce^{3+} PL. This demonstrates the impact of the Gd^{3+} spin polarization on the spin polarization of Ce^{3+}, which appears due to cross-relaxation between the Ce^{3+} (effective electron spin S=½) and Gd^{3+} (S=7/2) spin systems. Strong forbidden EPR-transitions have been observed in Gd^{3+} ODMR spectra recorded by monitoring Ce^{3+} emission intensity and additional ODMR lines, which can be ascribed to Gd^{3+} pairs, have been found.

This work has been supported by Russian Science Foundation under Agreement № 14-12-00859 and Philips.

[1] V. Bachmann, C. Ronda, A. Meijerink, Chem. Mater., **21**, 2077-2084. (2009)

Direct measurement of the Fe-polaron deformation in Fe:$LiNbO_3$

M. Bazzan, A. Sanson, A. Zaltron, N. Argiolas and C. Sada

Università di Padova, Dipartimento di Fisica e Astronomia Via Marzolo 8, 35131 Padova, Italy

In this talk, some recent experimental results on the structural characterization of the Fe small polarons in iron doped lithium niobate will be discussed. On one hand, High Resolution X-rays Diffraction shows a bulk average strain appearing in the crystal as a consequence of the reduction process Fe^{3+} -> Fe^{2+}. It will be shown that this effect has to be attributed to strain dipoles located at the Fe centers, with a magnitude dependent on the charge state of the Fe ion [1].

These findings are definitely confirmed using X-Ray Absorption Fine Structure Spectroscopy at the Fe edge: upon oxidation or reduction the oxygen cage surrounding the Fe impurity is more or less compressed with respect to the regular $LiNbO_3$ structure [2].

Those results give a quantitative picture of the polaronic lattice deformation associated to the localization of an electronic charge at the Fe impurity.

[1] M. V. Ciampolillo, A. Zaltron, M. Bazzan, N. Argiolas, C. Sada, and M. Bianconi, *Lithium niobate crystals doped with iron by thermal diffusion: Relation between lattice deformation and reduction degree*, Journal of Applied Physics **107** (2010) 084108.

[2] A. Sanson, A. Zaltron, N. Argiolas, C. Sada, and M. Bazzan, *Polaronic deformation at the $Fe^{2+/3+}$ impurity site in Fe:$LiNbO_3$ crystals*, Physical Review B **91** (2015) 094109.

Ultrafast, mid-infrared spectroscopy of small, strong-coupling polarons and free-carriers in lithium niobate

P. Booker[1], F. Freytag[1], M. Imlau[1]

[1] *School of Physics, Osnabrueck University, Barbarastraße 7, 49076 Osnabrueck, Germany*

The formation dynamics of small, strong-coupling $Nb^{4+}{}_{Nb}$ polarons has been subject of recent research activities [1,2] and revealed onset and formation times of $\tau_{onset} \sim 90$ fs and $\tau_{formation} \sim 100$ fs, respectively, in the visible spectral range. As a remarkable result, a contribution of free-carrier absorption was not observed and needed even to be ruled out for the description and analysis of the experimentally determined formation dynamics. The lack of free-carrier absorption prior to carrier-phonon relaxation may be attributed to the fact that the photon energy of the probing pulse is insensitive to the free-carrier absorption cross section σ_{FC} [3]. For a proper analysis, it therefore becomes necessary to inspect the ultrafast optical response in the mid-infrared spectral range, as well, which is the topic of this work.

We applied time-resolved mid-infrared pump-probe-spectroscopy ($\tau_{probe} \sim 230$ fs) to determine formation time and amplitude of the transient absorption change over a broad spectral range in the mid-infrared. Ultrashort, single laser pulses ($\tau_{pump} \sim 100$fs) with photon energy in the blue-green spectral range (2.5 eV) served for the generation of a large carrier density by means of two-photon, band-to-band absorption (TPA, $\beta \sim 5.6$ mm/GW). The anchor of our study are time-resolved results obtained with a narrow probe wavelength at $\lambda_{probe} = 2000$ nm that is used to verify both onset and formation time predominantly attributed to small, strong-coupling $Nb_{Nb}{}^{4+}$ polarons in the sub-picosecond time regime. The saturation amplitude of the induced absorption change is tantamount with a value of the absorption cross section of about $\sigma \sim 10^{22}\,m^{-2}$ in the MIR and a polaron density of about $N_P \sim 10^{22}$. Thus, the absorption cross section is reduced with respect to the maximum value in the near-infrared spectral range. This result can be explained and modeled straightforwardly by the spectral features of small, strong-coupling polarons and is verified in full accordance with the predictions of our previous results [4]. In the second step, the transients are studied for probing wavelengths up to 6.000 nm. We discuss the results in a comprehensive picture taking free carrier absorption into account and present an approach for modeling the spectral behavior of transients from the UV/VIS to MIR.

Financial support by the DFG (IM 37/5-2, INST 190/165-1 FUGG) is gratefully acknowledged. We gratefully acknowledge the WIGNER Research Centre for Physics for sample preparation.

[1] Badorreck et al., Optical Material Express **5**, pp. 2829-2741 (2015).
[2] Qiu et al., Phys. State Sol. **2**, pp. 232-235 (2005).
[3] Beyer et al., Appl. Phys. **B83**, pp. 527-530 (2006).
[4] Merschjann et al., J. Phys.: Condens. Matter **21** (2009).

EPR study of stable Eu^{2+} ions and X-ray induced charge traps creation in ceramic $Lu(Y)_3Al_5O_{12}$:Eu,Mg

M. Buryi[1], V. Laguta[1], M. Nikl[1], J. Li[2], Y.B. Pan[2]

[1]*Institute of Physics CAS, Cukrovarnicka 10, 162 00 Prague, Czech Republic*
[2]*Key Laboratory of Transparent Opto-functional Inorganic Materials, Shanghai Institute of Ceramics, Chinese Academy of Sciences, 200050 Shanghai, P.R. China*

For very long time lutetium and yttrium garnets (Lu(Y)AG) doped with various activation ions (see e.g., [1,2]) are serving as effective scintillating materials finding application in different fields of science, medicine and industry. They go through improvements all the time in search of better scintillating abilities, for instance, by restricting charge trapping defects formation. The present work deals with the ceramic garnets: as grown YAG:Eu,Mg, YAG:Eu,Mg annealed in air and as grown LuAG:Eu,Mg. Remarkably that in the as grown YAG some small part of the initial europium content has embedded into the yttrium position as stable Eu^{2+} ions, which are paramagnetic and thus detectable in EPR.

Annealing in air obviously evokes charge transfer process of the kind $Eu^{2+} \rightarrow Eu^{3+} + e^-$ as afterwards EPR spectra do not contain any traces of the Eu^{2+} resonances. The spectra measured in LuAG:Eu do not reveal the Eu^{2+} resonance at all. The presence of the divalent europium ions will require special compensation mechanism. It would be the following $Eu_Y^- + Mg_Y^- + V_O^{2+}$. To the best of our knowledge there are no reliable data in literature proving the Eu^{2+} ions existence in lutetium and yttrium garnets. Moreover no works have been dedicated to the EPR study of the ions yet.

X-ray irradiation does not affect the Eu^{2+} ions in the as grown YAG, however, it is responsible for the charge trapping processes. In the as grown YAG:Eu,Mg only the signal from O^- defect, shallow hole trap, appears in EPR spectra after the irradiation at liquid nitrogen temperature (LNT). In the annealed one, the two types of the O^- center, deep and shallow hole traps, occur after the irradiation at room temperature (RT) and LNT, respectively. On the contrary, the LuAG:Eu,Mg exhibits the property of both shallow the electron and the hole traps creation once been irradiated at LNT. Corresponding spectral parameters of the newly observed centers have been determined and their thermal stability was studied.

[1] Y. Zorenko, T. Zorenko, V. Gorbenko, B. Pavlyk, V. Laguta, M. Nikl, V. Kolobanov, D. Spassky, Radiat. Meas. **45** (2010) 419–421
[2] Ch. Hu, Sh. Liu, M. Fasoli, A. Vedda, M. Nikl, Xi. Feng, Yu. Pan, Phys. Status Solidi RRL **9** (2015) 245–249.

Spectroscopic properties of oxygen vacancies in $LaAlO_3$

O. A. Dicks[1], A. L. Shluger[1], P. V. Sushko[2], P. B. Littlewood[3]

[1] *UCL, Department of Physics and Astronomy, Gower Street, London, WC1E 6BT*
[2] *Pacific Northwest National Laboratory, PO Box 999, Richland, WA 99352, USA*
[3] *Argonne National Laboratory, 9700 S. Cass Avenue, Lemont, IL 60439, USA*

Oxygen vacancies in $LaAlO_3$ (LAO) play an important role in the formation of the 2-dimensional electron gas observed at the $LaAlO_3/SrTiO_3$ interface and affect the performance of MOSFETs using LAO as a gate dielectric. However, their spectroscopic properties are still poorly understood, which hampers their experimental identification. We present[(1)] predicted absorption spectra and electron spin resonance (ESR) parameters of oxygen vacancies in LAO, calculated using periodic and embedded cluster models and Density Functional Theory (DFT) and time-dependent DFT (TDDFT). The structure, charge distribution, and spectroscopic properties of the neutral (V_O^0) and charged (V_O^+ and V_O^{2+}) oxygen vacancies in cubic and rhombohedral $LaAlO_3$ have all been investigated.

The absorption spectra calculated using TDDFT, as implemented in the Gaussian09[(2)] code, show that the highest intensity optical transitions have onsets at 3.5 and 4.2 eV for V_O^0 and 3.6 eV for V_O^+ in rhombohedral LAO and 3.3 and 4.0 eV for V_O^0 and 3.4 eV for V_O^+ in cubic LAO, respectively. These transitions are from the vacancy state to perturbed states in the conduction band, and from studying the molecular orbitals involved in the transitions, due to the D_{4h} point symmetry of the vacancy, all transitions are from A_{1g} to E_u states.

The calculations of ESR parameters we present can also be directly compared to experimental studies of the V_O^+ defect. We calculated an isotropic g-value of 2.004026, and due to the hyperfine splitting of the Al ions, we predict a signal broadening of 3mT.
These results may further facilitate the experimental identification of oxygen vacancies in LAO and help to establish their role at the LAO/STO interfaces and in nanodevices using LAO.

[1] O. A. Dicks, A. L. Shluger, P. V. Sushko, P. B. Littlewood, *Physical Review B*, submitted
[2] M. J. Frisch et al., Gaussian 09, Gaussian, Inc., Wallingford CT, **2009**.

Investigation of $LaCrO_3$ for development of a *p*-type transparent conducting oxide

Ailbhe L. Gavin [1], Graeme W. Watson[1]

[1]*School of Chemistry and CRANN, Trinity College Dublin, Dublin*

Transparent conducting oxides (TCOs) have a wide variety of applications in optoelectronics, including photovoltaic cells and flat panel displays. TCO materials possess a band gap of greater than 3 eV, allowing them to transmit visible light, and conductivity greater than 1000 S cm^{-1}, with carrier concentrations in the region of 10^{20}-10^{21} cm^{-3}. Currently only *n*-type materials, such as Sn-doped In_2O_3 and Al-doped ZnO, exhibit high electronic conductivity and optical transparency required for use in these devices. Transparent electronics is a prospective application of TCOs, but a suitable *p*-type material with properties to match those of the *n*-type materials is required in order to produce pn junctions. Doped $LaCrO_3$ has recently been suggested as a potential *p*-type TCO. Sr doping is reported to effectively dope holes into the top of the valence band, resulting in *p*-type conductivity [1]. Thin films of Sr-doped $LaCrO_3$ were shown to exhibit an increase in conductivity, from 1.2 to 54 S cm^{-1} with increase in Sr content from 4 to 50%., and hole concentrations of 10^{20} to 10^{21} cm^{-3} were observed.

Defect analysis of pure $LaCrO_3$ and $LaCrO_3$ containing Sr defects has been carried out using PBEsol + *U* calculations [2]. All possible intrinsic and extrinsic defects have been assessed, in order to investigate the improvement in electronic conductivity and optical properties that have been observed experimentally when $LaCrO_3$ is doped with Sr. The electronic structure, origin of the charge carriers, and defect stabilities have been examined, by calculating formation energies and transition levels for each defect. The chemical potential dependence of defect formation has been investigated, allowing the potential of Sr-doped $LaCrO_3$ as a *p*-type TCO to be assessed.

[1] Zhang *et al*., Adv. Mater, **27**, 5191-5195 (2015)
[2] J. P. Perdew *et al.*, Phys. Rev. Lett., 2008, **100**, 136406

Point defects and phenomenon of dichroism in the lanthanum-gallium silicate group crystals

N. Kozlova[1] , O. Buzanov[2], Ev. Zabelina[1], A. Kozlova[1], M.Bykova[1], Zh. Goreeva[1]

[1]NUST MIS&S, Moscow, Russia
[2]"Fomos-Materials" Company Limited, Moscow, Russia

Langasite (LGS, $La_3Ga_5SiO_{14}$), langatate (LGT, $La_3Ga_{5,5}Ta_{0,5}O_{14}$) and catangasite $Ca_3TaGa_3Si_2O_{14}$ (CTGS) are crystals with calcium-gallogermanate structure. In consequence of the unique combination of piezoelectric, thermal, luminescent and nonlinear optical properties these crystals are expected to satisfy requirements for various applications including laser media or parametric quantum oscillators. The presence of point defects and their associations, in particular, color centers, in the crystals hinders their application. Different research groups develop the models of point defects in LGS and LGT [1-3]. But still these models are incomplete and contradictory.

Here we present the results of our studies of the optical characteristics of these crystals depending on their composition, orientation and growth conditions. All investigated crystals were grown in "Fomos-Materials" Company Limited using Czochralski method in Ir crucibles, growth atmosphere – Ar or Ar with O_2. Optical transmission, 90° scattering and diffuse reflection spectra were measured using UV-Vis-Nir spectrophotometer «Cary-5000» with UMA (Agilent Technologies).

The growth atmosphere significantly influences the coloration and, as a consequence transmission spectra of these crystals [4]. Colorless crystals are obtained in Ar atmosphere, while colored crystals – with addition of oxygen. In transmission spectra in visible and UV spectral regions we observed three absorption bands in the colored crystals (290, 380 and 490 nm) and only one band in the colorless crystals (290 nm). Also in transmission spectra of all investigated samples there are two bands in near infra-red region - 1850 and 2920 nm.

We observed anisotropy of transmission spectra of samples. However for the samples, which were cut in the direction parallel to axis Z we also observed phenomenon of dichroism. This effect occurs in some crystals with specific structure when naturally polarized or p-, s-polarized light passes along directions perpendicular to the optical axis, and may be caused by the symmetry of the crystals' structure or by the anisotropy of color centers.

In order to determine origin of the defects we studied light scattering and diffuse reflection spectra of the single crystals in the spectral region of 250 ÷ 800 nm.

[1] T. Taishi, T. Hayashi, N. Bamba, Y. Ohno, I. Yonenaga, W. Hoshikawa, Physica B: Condensed Matter **401-402** (2007) 437-440.

[2] A.V. Butashin, V.A. Fedorov, V.F. Mescheriakov, V.S. Mironov, L.G. Shilin, O.A. Busanov, A.N. Zabelin, S.A. Sakharov NCCG-2008. Book of abstracts, Moscow, 2008.

[3] G.M. Kuz'micheva, I.A. Kaurova, V.B. Rybakov, S.S. Khasanov, A. Cousson, O. Zaharko, E.N. Domoroshchina, A.B. Dubovskii, Cryst. Res. Technol. **47-2** (2012) 131-138.

[4] O.A. Buzanov, N.S. Kozlova, E.V. Zabelina, Crystallography Reports **52-4** (2007) 691-696.

Defect evolution in irradiated optical fibers

C. Laplante[1], G. Gelinas[1], C. Brosseau[1], É. Haddad[2], F. Rosei[3], D. Barba[3], F. Schiettekatte[1]

[1] *Regroupement Québécois sur les matériaux de pointe, Département de physique, Université de Montréal, Québec, Canada*
[2] *MPB Communications Inc. Pointe-Claire, Québec, Canada*
[3] *INRS- Énergie Matériaux Télécommunications, Varennes, Québec, Canada*

Fiber Bragg gratings (FBG) are used as optical sensors for real-time temperature and mechanical stress measurements in space vehicles and engine turbines, but their performance and durability degrade rapidly in harsh environment. To simulate the effects of cosmic radiation on FBG, optical fibers are irradiated using 5 MeV protons from an accelerator. These FBG are characterized by absorbance measurement in the UV-visible spectral range, showing the generation of defects after proton bombardment. These defects are investigated after thermal annealing conducted at different temperatures in order to identify their evolution and the effect of thermal diffusion on the FBG performances.

First-principles calculation of electronic structures and phonon modes at a Ga vacancy in GaN

T. Tsujio, M. Oda and Y. Shinozuka

Faculty of Systems Engineering, Wakayama University, Sakaedani 930, Wakayama, 640-8510, Japan

Killer centers are certain deep-level defects in semiconductors that act as a nonradiative recombination center, limiting the efficiency of light emitting devices. The multiphonon process is considered to be a serious issue in light emitting devices, because it involves the conversion of electronic energy to phonon energy, which is considered to be a trigger for defect reactions, known as phonon-kick mechanism [1].

In the previous work [2], using a model configuration coordinate diagram we have simulated the time evolution of the electron-lattice coupling mode, and a series of nonradiative carrier captures by a deep-level defect in a semiconductor. If the lattice relaxation energy is of the order of the band gap, a series of coherent (athermal) electron and hole captures by a defect is shown to be possible for high carrier densities, which results in an inflation in the induced lattice vibration, which in turn enhances a defect reaction.

Although this feedback inflation process has been shown to be a possible mechanism for degradation mechanisms, the parameters on actual defects and the relation between a defect level and localized phonon modes have not been clarified. In this study, using the first-principles scheme based on density functional theory we calculate the electronic structures and phonon modes at a Ga vacancy in GaN. We adopt GaN 2×2×2 supercell for a basic model and introduce a Ga vacancy in it. Comparing the calculated phonon-frequency density of states without defect and those with a Ga vacancy, we find there are localized phonon modes near above the both acoustic and optical bulk phonon bands. From the phonon mode analysis, we find these localized modes contain an asymmetric mode in which one of the four N atoms around a Ga vacancy strongly oscillates. We calculate the change of the electronic structures as a function of this symmetry breaking mode. It is revealed that the defect level oscillates in the band gap synchronously with this mode. These results indicate that abovementioned phonon-kick mechanism is possible in GaN based devices. The results on other localized phonon modes are also discussed.

[1] Y. Shinozuka in "*Materials and Reliability Handbook for Semiconductor Optical and Electron Devices*" Ed. by O. Ueda and S. Pearton (Springer, 2012) Chapter 10.

[2] Y. Shinozuka, M. Wakita, and K. Suzuki, Jpn. J. Appl. Phys. **51** (2012) 11PC03.

Localized point defects in amorphous hosts and its influence on quantum yield of Ln^{3+} luminescence

Atul D. Sontakke[1,2] and Setsuhisa Tanabe[1]

[1]*Graduate School of Human and Environmental Studies, Kyoto University, Kyoto 606-8501, Japan*
[2]*PSL Research University, Chimie-ParisTech, CNRS, IRCP, 75005 Paris, France*

Amorphous materials, such as glasses lack in long-range periodicity and exhibit a random network structure with large free volume. Such disordered network favours for the presence of several point defects in the network, *i.e.* non-bridging oxygens, wrong bonds, dangling bonds, etc [1]. These point defects create Gaussian type localized defects states below the conduction band [1]. Figure 1 shows the absorption profile of amorphous borate glass showing defects' absorption inside the bandgap region.

The localized defects, in association with the Urbach tail, which is a characteristic of amorphous materials, bring an extended band tailing of the fundamental absorption inside the bandgap region [2]. In Ce^{3+} doped borate glass, the excitation energy for Ce^{3+} 4*f*-5*d* transition overlaps with the host's band tail absorption (inset of Fig. 1), causing a finite loss of excitation pump energy. We observed that this hosts' intrinsic absorption loss causes about 20% reduction in the external luminescence quantum yield (QY) of the Ce^{3+} doped borate glass. A similar reduction in QY is evident in Tb^{3+} doped borate glass under 372 nm excitation ($^7F_6 \rightarrow {}^5D_3$). In this work, we present a detailed investigation on defects absorption in oxide glasses and its influence on dopant's luminescence properties, as well as a methodology of its quantitative analysis is discussed.

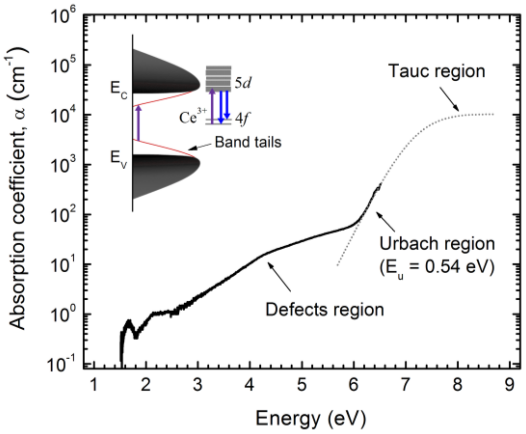

Figure 1: Log plot of the experimental absorption coefficient (solid line) of borate glass. Inset: Host glass band tail schematic and Ce^{3+} $4f \rightarrow 5d$ transitions in studied borate glass.

[1] K. Tanaka, *J. Non-Cryst. Solids*, **389** (2004) 35.

[2] A. D. Dontakke, J. Ueda, S. Tanabe, *J. Lumin*, **170** (2016) 785.

Characterization of point defects in oxygen sub- and over-stoichiometric HfO_2 by Electron-Energy Loss Spectroscopy

M. Alemany[1,3,4], A. Chabli[2], N. Bernier[3], V. Delaye[3], F. Pierre[3], E. Martinez[3], N. Vaxelaire[3], F. Bertin[3], M. Gros-Jean[1], M.-F. Barthe[4]

[1] *STMicroelectronics, 850 rue Jean Monnet, 38926 Crolles, France.*
[2] *Univ. Grenoble Alpes, INES, F-73375 Le Bourget du Lac, France, CEA, LITEN, Department of Solar Technologies, F-73375 Le Bourget du Lac, France.*
[3] *Univ. Grenoble Alpes, F-38000 Grenoble, France, CEA, LETI, MINATEC Campus, F-38054 Grenoble, France.*
[4] *CNRS, CEMHTI UPR3079, Univ. Orléans, F-45071 Orléans, France*.

Oxygen vacancies in high-k oxides for microelectronics applications, are foreseen to have detrimental effects in the case of high-k metal gate MOS transistors [1] and beneficial ones in the case of resistive random-access memories [2]. In this context techniques capable to characterize defects in ultra-thin (<100 nm) oxide layers are required. $Hf0_2$ layers thoroughly characterized in terms of morphology and stoichiometry are used as reference samples to develop a reliable methodology for the characterization of these point defects by combining two characterization techniques: electron energy loss spectroscopy in transmission electron microscopy (EELS-TEM) [2,3,4] and positron annihilation spectroscopy (PAS) [5]. While PAS is used as a reference method by providing the type and density of the defects, EELS-TEM is the only one to allow analysis at the device level.

In this paper we will report on the results obtained using EELS-TEM on 10 to 100 nm thick HfO_2 layers grown by atomic layer deposition (ALD) and physical vapour deposition (PVD). The expected increase of vacancies concentration in annealed TiN-capped samples is also investigated. The samples are characterized by RBS and XPS to determine the stoichiometry and by XRD, TEM and/or SEM to assess the crystallographic morphology. The wide range of the measured O/Hf ratio - from 3 for the PVD layers to 1.9 for the 10 nm thick ALD films – allows to study both over- and sub-stoichiometric materials. The PVD-grown layers afford a complex morphology with two sublayers of amorphous and polycrystalline materials as observed by XRD and TEM. In contrast ALD layers are fully polycrystalline. These layers have been analysed by EELS-TEM, measuring the oxygen K-edge (O-K) on lamella prepared both by focussed ion beam (FIB) and Tripod© mechanical polishing. The signal to noise has been significantly enhanced by using a dual EELS mode coupled with a specific averaging of the detector signal.

No specific impact of the sample preparation on the EELS-TEM results is observed. The effect of the sample stoichiometry on the O-K EELS-TEM spectra will be discussed taking into account the morphological and crystalline particular properties of the samples.

[1] K. Shiraishi, et al., in: "Proc. of SISPAD", 306–313 (2006).
[2] P. Calka, et al. Nanotechnology **24**, 085706 (2013).
[3] T. Mizoguchi et al. Journal of Physics Condensed Matter **21**, 104212 (2009).
[4] J.H. Jang et al. Journal of Applied Physics, **109,2**, 023718 (2011).
[5] A. Uedono, et al., Japanese Journal of Applied Physics **46**, 3214-3218 (2007).

Structure and localization of aggregated Mn^{2+} ions as a separate phase in the mesoporous assembly of cZnS:Mn QDs

L. C. Nistor, S. V. Nistor, M. Stefan and I. D. Vlaicu

National Institute of Materials Physics, Atomistilor 105bis, Magurele-Ilfov, 077125 Romania

The cubic ZnS quantum dots (QDs) doped with Mn^{2+} impurity ions (cZnS:Mn) prepared by co-precipitation in a liquid solution, have been intensely investigated in the last two decades, especially for expected new properties, in particular as a diluted ferromagnetic semiconductor nanomaterial [1]. However, according to quantitative electron paramagnetic resonance (EPR) studies on 2.9 nm size cZnS:Mn QDs doped with up to 5 at% nominal impurity concentration, the Mn^{2+} ions are incorporated at isolated sites in the core and in the surface layer, in a diluted paramagnetic state characterized by magnetic dipole-dipole interactions [2,3]. Therefore ferromagnetism, previously reported for nominal Mn^{2+} concentration levels of 2.5 at% and higher [4,5], could be due either to a large concentration of lattice ions vacancies, or to agglomerates of Mn^{2+} ions. While large concentrations of vacancies were not evidenced by EPR, the agglomerates of Mn^{2+} ions are observed as a broad, structureless Lorentzian line superposed on the narrow lines of the core and surface localised impurity ions [6]. Therefore we decided to investigate by analytical high resolution transmission electron microscopy the very little known structure and localization of the agglomerates of Mn^{2+} ions in the mesoporous structure of the self-assembled cZnS:Mn QDs of 2.9 nm size prepared by co-precipitation at high nominal impurity levels were, according to EPR and magnetometry data, the magnetic properties of Mn^{2+} agglomerates change from paramagnetic to antiferromagnetic states. Our investigation evidences the formation of a Mn^{2+} rich, disordered phase, localised in the interstices and pores of the mesoporous structure of the self-assembled cZnS:Mn QDs. This phase contains, besides manganese, large amounts of oxygen and zinc, suggesting the presence of Mn-O and/or Mn-Zn-O type compounds, the change in its magnetic properties being related to an increase in the local concentration of the Mn^{2+} ions with the increase in the nominal impurity concentration level.

[1] T. Dietl, Nat. Materials **9**, 965 (2010).
[2] S. V. Nistor, M. Stefan, L. C. Nistor, et al., *J. Phys. Chem. C*, **119**, 23781 (2015).
[3] S. V. Nistor, M. Stefan, L. C. Nistor, et al., *J. Alloys Comp.,* **662**, 193 (2016).
[4] I. Sarkar, M. K. Sanyal, S. Biswas et al., Phys. Rev. B **78**, 224409 (2007).
[5] Z. H. Wang, D. Y. Geng, D. Li, et al, J. Mat. Res. **9**, 2376 (2007)
[6] M. Stefan, S. V. Nistor, D. Ghica et al., *Phys. Rev. B* **83**, 045301 (2011)

Luminescence of ZnO crystal and nanoparticles excited by femtosecond IR, UV and VUV laser pulses

A.Belsky[1], P.Martin[2], M.Dumergue[4], S.Petit[2], D.Descamps[2], A.Vasil'ev[3]

[1] *Institut Lumière Matière, UMR 5306, CNRS-Université Lyon 1, 69621 Villeurbanne, France*
[2] *Centre Lasers Intenses et Applications (CELIA), UMR 5107, Université de Bordeaux-CNRS-CEA, 33405 Talence, France*
[3] *Skobeltsyn Institute of Nuclear Physics, Lomonosov Moscow State University, Leninskie gory, 1(2), Moscow 119991, Russia*
[4] *ELI-HU, H-6728 Szeged, Tisza Lajos krt. 85-87, Hungary*

We present results on time resolved photo-luminescence induced by photons with different excitation conditions (photon energy, pulse duration, fluence) of ZnO (E_g=3.4 eV) single crystal (MC) and nanoparticles (NP). Samples were excited by femtosecond IR (1.55 eV,), UV (4.65 eV, third harmonic) and VUV pulses (15-50 eV, high order harmonics generation) of Ti-Sapphire laser. The excitation fluence and the sample temperature in the range 13-300 K were controlled.

Under UV excitation at low temperatures the emission spectra show all emission bands originated from different states: free exciton Fx, bound exciton Dx, Dx phonon replica, TES state and Ax band.

Under IR excitation at all temperatures the emission spectra show that Fx emission is not detected, only emissions associated with Dx states (at low temperatures) and Ax band are observed.

This difference between UV and IR excitation is explained by the supposition that Dx excitons can be created under IR excitation without preliminary formation of Fx state. One of the possibilities is the sequential creation of electrons and holes by ionizing of different defects, e.g. oxygen V_O and zinc V_{Zn} vacancies with levels within the band gap of the ZnO. Depending on the level position, a carrier creation process can be one- or two-photon process. However, we need three photons to produce sequentially an electron and a hole (one one-photon and one two-photon process). In this sequential process non-correlated electrons and holes are produced and then these carriers are captured by a defect with production of Dx state. On the contrary, UV photon creates a correlated electron-hole pair which form Fx state. Some of these free excitons decay radiatively with emission corresponding to Fx band, whereas other can be captured by defect with production of Dx state. Therefore Fx and Dx bands coexist under VUV excitation.

The luminescence decay kinetics of the excitonic emissions (Dx, Fx, and Dx phonon replica) were measured at different temperatures. The dynamics of Fx and Dx excitons are discussed depending on the excitation formation mode, energy, density, temperature and system size. Excitation by VUV photons demonstrate also the effect of the electronic relaxation on decay kinetics

Role of defects in shaping the emission of Ln doped CeO_2

Daniel Avram[1], Bogdan Cojocaru[2], Mihaela Florea[2], Ioana Porosnicu[1], Vasile Parvulescu[2] and Carmen Tiseanu[1]

[1]*National Institute for Laser, Plasma and Radiation Physics, P.O.Box MG-36, RO 76900, Bucharest-Magurele, Romania*
[2]*University of Bucharest, Faculty of Chemistry, Department of Organic Chemistry, Biochemistry and Catalysis, 4–12 Regina Elisabeta Bvd., Bucharest, Romania*

We present the latest results of our group on optical down-/ up-conversion and X-ray excited luminescence properties and mechanisms of lanthanide (Ln) ions (Ln: Sm, Eu, Dy, Ho, Er, Tm, Yb) doped CeO_2 nanoparticles. The aliovalent substitution of tetravalent Ce by trivalent Ln generates oxygen vacancies which interact with the trivalent dopants in either nearest-neighbour or next nearest neighbour modes [1]. By use of time-gated site selective emission spectroscopy, the fingerprint emission, excitation and decay characteristic of each Ln- vacancy associate type are identified. Ceria properties (cation local symmetry, phonon energy, low lying O^{2-} - Ce^{4+} charge-transition, oxygen vacancies as main defects) as well as Ln type and concentration are found to essentially define the emission properties and mechanism of Ln in CeO_2 under both optical and X-ray excitation modes.[1, 2]

Acknowledgements : The authors acknowledge the Romanian National Authority for Scientific Research (CNCS-UEFISCDI), project number PN-II-ID-PCE-2011-3-0534.

[1] D. Avram, M. Sanchez-Dominguez, B. Cojocaru, M. Florea, V. Parvulescu, C. Tiseanu, J. Phys. Chem. C **119**(28), 16303-16313 (2015).
[2] D. Avram, A. Urda, B. Cojocaru, I. Tiseanu, M. Florea, C. Tiseanu, Phys. Chem. Chem. Phys. **17**(46), 30988-30992 (2015)

High pressure and time resolved luminescence spectra of $Ba_2K(PO_3)_5$ doped with Eu^{2+} and Eu^{3+}

A. Baran[1], S. Mahlik[1], M. Grinberg[1], A. Watras[2], R. Pązik[2], P. Dereń[2]

[1] *Institute of Experimental Physics, University of Gdansk, Wita Stwosza 57, 80-952 Gdansk, Poland*

[2] *Institute of Low Temperature and Structure Research, Polish Academy of Sciences, 2 Okólna Street, 50-422 Wroclaw, Poland*

Barium potassium phosphate ($Ba_2K(PO_3)_5$) doped with europium belongs to the hosts able to accommodate both Eu^{3+} and Eu^{2+} ions, which make it useful for white light emitting diodes (WLEDs) based on UV chip technology.

In this work effects of pressure and temperature on the luminescence of Eu^{2+} and Eu^{3+}-doped $Ba_2K(PO_3)_5$ are presented. The luminescence spectra and luminescence decays were measured as a function of temperature and pressure. Depending on the excitation wavelength phosphor shows different luminescence spectra. The emission color was bluish green, when only Eu^{2+} was excited, reddish orange when only Eu^{3+} was excited or white over simultaneous excitation of both ions. At room temperature under excitation with near UV light, the luminescence spectrum consists of broad emission band peaking at 480 nm due to the $4f^65d^1 \rightarrow 4f^7$ ($^8S_{7/2}$) transitions of Eu^{2+} and several sharp lines between 580 and 710 nm region, ascribed to the $^5D_0 \rightarrow {}^7F_J$ (J = 0, 1, 2, 3 and 4) transitions in Eu^{3+}. At low temperatures, we observed three different bands related to the $4f^65d^1 \rightarrow 4f^7$ transitions in different Eu sites (at 415 nm (A), 450 nm (B) and 505 nm (C)): two Eu sites substituting for Ba^{2+} and one Eu site substituting for K^+.

Under fixed excitation wavelength the effect of increasing of the intensity of Eu^{2+} emission with respect to Eu^{3+} emission was observed for temperature range 5 – 100 K. The nonradiative intersystem crossing was responsible for decreasing of the relative intensity of the Eu^{2+} luminescence for temperature range 150 – 500 K and causes decreasing of the Eu^{2+} to Eu^{3+} luminescence intensity ratio for temperature higher than 150 K. Luminescence decays were measured for selected temperatures and pressures. At 10 K the decays of Eu^{3+} luminescence were single–exponential, with time constant being 3.6 ms. When temperature increases all emissions decay faster and become multiexponential. Decay times slightly decreased with increasing pressure. In the range of 10 – 400 K the decays of $4f^65d \rightarrow 4f^7$ emission in the Eu^{2+} were single–exponential, with time constant being 0.65 μs, 0.62 μs and 0.35 μs for A, B and C emission bands, respectively, and did not depend on temperature. At higher temperatures (from 400 K to 500 K) the luminescence decays become shorter and non–exponential, as the result of thermal quenching. When pressure increases all emissions decay faster.

Thermoluminescence and Electron Paramagnetic Resonance of Marambaia Topaz

K.M. Sato[1],T.K Gundu Rao[1], N.F. Cano[2], S. Watanabe[1]

[1]*University of São Paulo, São Paulo, SP, Brazil*
[2]*Federal University of São Paulo, Santos, SP, Brazil*

Since 1960´s it is known that one variety of uncolored topaz can acquire blue color irradiating it with about 2 MGy radiation and then heat treated at around 280 °C. In Brazil this variety is known as Marambaia Topaz (MT) since it is found in Marambaia, state of Minas Gerais.
For the present work it was sold to us about 15 fragments of MT of 15x15x5 mm^3 size.
Lamina 0.7mm x 0.7mm x 0.1mm with polished faces have been prepared for optical absorption (OA) measurements. Natural, 120 kGy and 2 MGy irradiated with gamma rays presented a small absorption band at 350 nm and 1400 nm although the overall crystal absorption coefficient grew with the dose. This means that these MT samples are not colorable.
The glow curves of MT samples irradiated with high doses larger than 500 Gy presented peaks at 130, 200 and 380 °C. For dose below 500 Gy, for example, for 50, 120, 200 and 300 Gy peaks at 140, 250 and 350 °C have been observed.
Why such TL behavior? No answer was found yet. Anyway , the peak around 250 °C is the prominent one. The TL response as function of dose from low to 50 kGy is not a regularly growing curve since between 3.5 and 6.0 kGy, the angular coefficient lowers a little, but after 6.0 Gy it becomes equal to that from o to 3.5 kGy.
In the region of 10 to 50 kGy the TL response is still growing, therefore, MT can be used for high dose dosimetry.
The EPR spectrum has shown a large signal around g=2.0 typical of Fe^{3+}. High doses irradiations did not add new signals, however the intensity of g=2.0 signal grew from 100 (a.u) for natural sample to 200 (a.u) for 30 to 40 kGy irradiation.

Acknowledgements: We are thankful to FAPESP for financial support and to CAPES for Visiting Professor Fellowship to Dr. T.K. Gundu Rao and to CNPq for scholarship to K.M. Sato.

Tunable emission from silico-carnotite type double silicates doped with Tb^{3+} and Eu^{3+}

I. Carrasco, F. Piccinelli, M. Bettinelli.

Luminescent Materials Laboratory, Dept. of Biotechnology, University of Verona, Strada Le Grazie 15, 37134 Verona, Italy.

Double silicates with the silico-carnotite orthorhombic structure and co-doped with Tb^{3+} and Eu^{3+}, have been prepared by solid-state reaction. Room temperature luminescence spectra and decay kinetics have been measured and analysed. Upon UV excitation at 378 nm, the emission colour varies from red to pinkish, depending on the doping level. The resulting colour can be adjusted by controlling the Tb^{3+}/Eu^{3+} concentration ratio. Control of the doping leads to close-to-white emission in some of the analysed samples upon excitation in the wavelength region useful for LED lighting.

EPR spectroscopy of Er^{3+} in lithium yttrium borate (LYB) single crystals

Sara Arceiz Casas[1], Gábor Corradi[2], László Kovács[2], Éva Tichy-Rács[2], Krisztián Lengyel[2], Andreas Scholle[1], Sigmund Greulich-Weber[1]

[1] *Paderborn University, Warburger Str. 100, 33098 Paderborn, Germany*
[2]*Institute for Solid State Physics and Optics, Wigner Research Centre for Physics, Hungarian Academy of Sciences, Konkoly-Thege u. 29-33, 1121 Budapest, Hungary*

Lithium yttrium borate $Li_6Y(BO_3)_3$ having a monoclinic crystal structure belonging to the P21/c space group is an excellent nonlinear optical material with a wide UV range of transparency. Due to the easy incorporation of rare earth ions at Y sites it is also a prospective laser host and scintillator material. Er^{3+} ions are especially interesting for their ~1500 nm emission suitable for optical communication systems. Diode-pumped 1594 nm laser performance has already been realized in Er and Yb co-doped LYB [1]. Concerning the optical spectroscopic properties of Er^{3+} in LYB some results at RT [2, 3] and a preliminary study of absorption spectra at 2K [4] have been reported, but a detailed analysis has not yet been published. Apart from a preliminary announcement [5] we are not aware of EPR studies in LYB:Er. Here low temperature single-crystal EPR and ancillary optical absorption results characterising the $^4I_{15/2}$ ground state and its splitting in the low symmetry crystal field are presented.

LYB crystals doped with 0.05 or 1 mol% Er were grown by the Czochralski method [6]. EPR and polarized absorption spectra were measured at low temperature on samples cut perpendicular to the crystallographic twofold symmetry axis b. Angular dependent EPR spectra near 10K have been taken for the magnetic field in four crystallographic planes required for a full and unambiguous determination of the g-tensor and the hyperfine-tensor of the ^{167}Er isotope. The temperature dependence of the EPR line intensity showed an Orbach-type relaxation with an activation energy between ΔE= 54 cm^{-1} and 78 cm^{-1} depending on the orientation of the magnetic field.

The low temperature absorption spectrum recorded near 80K revealed crystal field splitting with the first two excited Stark sublevels at (46±1) cm^{-1} and (77±1) cm^{-1} from the ground state. Comparison with EPR results indicates that both levels may participate in the Orbach-type spin-lattice relaxation.

[1] Y W Zhao, Y F Lin, Y J Chen, X H Gong, Z D Luo, Y D Huang, *Appl. Phys. B* **90** (2008) 461.
[2] Yuwei Zhao, Xinghong Gong, Yanfu Lin, Zundu Luo, Yidong Huang, *Materials Letters* **60** (2006) 418-421.
[3] Y W Zhao, X H Gong, Y J Chen, L X Huang, Y F Lin, G Zhang, Q G Tan, Z D Luo, Y D Huang, *Appl. Phys. B* **88** (2007) 51-55.
[4] A P Skvortsov, N K Poletaev, K Polgár, Á Péter, *Technical Physics Letters*, **39** (2013) 424-426.
[5] L Kovács, G Corradi, É. Tichy-Rács, Zs Kis, W Ryba-Romanowski, A Strzep, A Scholle, S Greulich-Weber, ICDIM 2012, Santa-Fe, NM, USA, abstract p.108
[6] Á Péter, K Polgár, M Tóth, *J. Cryst. Growth*, **346** (2012) 69-74.

IR luminescent centres in gamma-irradiated Bi-doped KCl and SrF_2 crystals

S.V. Firstov[1], M. Zhao[2,3], L. Su[2], Q.H. Yang[3], L.D. Iskhakova[1], E.G. Firstova[1], S.V. Alyshev[1], K.E. Riumkin[1] and E.M. Dianov[1]

[1]*Fiber Optics Research Center, Russian Academy of Sciences, Russia*
[2]*Key Laboratory of Transparent and Opto-functional Inorganic Materials, Shanghai Institute of Ceramics, Chinese Academy of Sciences, China*
[3]*School of Materials Science and Engineering, Shanghai University, China*

Unusual near infrared luminescence and lasing in spectral regions of 1400–1500 nm and 855–965 nm was demonstrated in alkaline-earth fluoride crystals doped with Tl or Pb [1, 2]. It was shown that laser active centers in these crystals are Tl^0(l) and Pb^+(l) complexes consisting of an ion (Tl^0 or Pb^+) next to an anion vacancy. It was revealed that active IR centres could also be formed in materials doped with bismuth as well as thallium and lead [3]. Now, bismuth-doped materials are of great interest as promising gain media for new lasers and amplifiers. However, the nature of the active centers responsible for the lasing and IR luminescence is still unclear. In this regard, an investigation of crystalline hosts containing Bi is a possible way toward discovery of the nature of the active center.

We report an investigation of the luminescent properties of Bi-doped KCl and SrF_2 crystals grown by vertical Bridgman technique. The bismuth concentration in the crystals was ~0.01-0.1 at.%. The prepared crystals were irradiated by γ-radiation (dose ~20 Gy) using a ^{60}Co-source.

The X-ray diffraction patterns of the crystals were measured and analyzed. As a result, the structural parameters of the prepared crystals were determined. We did not observe any absorption and emission bands in the pristine Bi-doped KCl crystals whereas the 240-nm absorption and red emission bands attributed to Bi^{2+} ion was found in the pristine Bi-doped SrF_2 crystal. It was demonstrated that the optical IR centres in SrF_2 and KCl doped with bismuth can be produced by γ-irradiation. We measured emission and excitation spectra of the NIR luminescence in the irradiated crystals (Fig. 1 a, b).

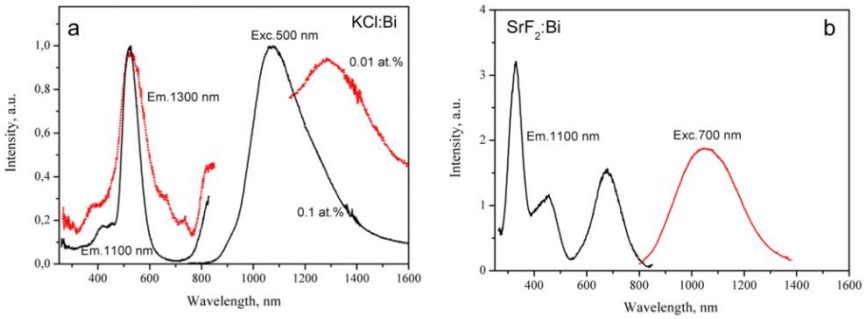

Fig. 1. a) Emission (exc. 500 nm) and excitation (em. 1100 and 1300 nm) spectra of the irradiated KCl:Bi (0.1 and 0.01 at.%); b) emission (exc. 700 nm) and excitation (em. 1100 nm) spectra of the irradiated SrF_2:Bi.

The analysis of the obtained experimental data showed that the structure of the Bi-related optical center is similar to one of the Tl- or Pb-related laser active center. Taking into account same electron configuration of Bi^{2+}, Pb^+ and Tl^0, we suggest that the optical center responsible for the IR luminescence is Bi^{2+} ion next to an anion vacancy.

This research was supported by Russian Foundation for Basic Research (Grant no. 15-52-53127).

[1] G. Horsch, H. J. Paus, Opt. Comm. **60,** 69 (1986).
[2] W. Gelleilmann, F. Loty, Opt. Comm., **39,** 391 (1981).
[3] E.M. Dianov, Light: Science & Applications, **1,** 12 (2012).

Thermoluminescence (TL) Properties of glass from natural diopside and of Synthetic Diopside Glass

Bruno G. Fernandes[1,2], Shigueo Watanabe[1], Douglas Gouvêa[2], Angelo F.Padilha [2]

[1]Institute of Physics, University of São Paulo, Brazil
[2]Department of Metallurgical and Materials Engineering, Polytechnic School, University of São Paulo, Brazil

The diopside (hederabergite) minerals form a complete solid solution series between $CaMgSi_2O_6$ and $CaFeSi_2O_6$. Although Al does not take part in the minerals it is found in most of them. Cr and Mn are also a common impurity, of course, besides Na and K. The diopside belongs to a large PYROXENE GROUP, which is a chain silicate.
In the present work a glass was produced starting with a natural diopside and using devitrification method. A glass is in principle an amorphous solid and as such does not present thermoluminescence except after irradiation with gamma doses of larger than 400 Gy. The glow curve present peaks at 130,210 and 315^{o}C. This third peak that has almost zero height at 400-500Gy growns fast with the dose. Its height that is about 14 (a.u) for 5 kGy dose, reaches 83 (a.u) at 40 kGy while peaks 1 and 2 grow very little.
Starting with reagent grade oxide components of a pure diopside, the mixture is heated in an alumina crucible to 1550 ˚C, temperature at which the mixture becomes a liquid. After about two hours the temperature of the melt is lowered to room temperature in minutes resulting in a glass. The X ray diffraction measurement indicated that it is in fact a diopside glass. The glow curves of this synthetic diopside glass irradiated with gamma rays with doses larger than 400 Gy are now just one very broad peak around 220^o.
The outstanding result is that the peak intensity is now almost 250 times that of the glass of natural diopside mineral. We will carry out later the deconvolution of this broad peak expecting several components. In sequence a artificial diopside glass was produced adding 1,56 (mol%) of Aluminum. Again very broad TL peak resulted around 220^{o}C, however, the peak height reduced from 2500 a.u to 2200 a.u meaning that Al is a reducer of TL behavior.
Then we produced synthetic diopside glass doped with 0,1% 1,0% and 2,0% Ag. We had in mind producing nanoparticles of Ag, but because very high temperature involved it did not result in nanoparticles. As to the TL behavior for two lower concentrations of Ag glow curves peaking at 160 and 330-350^{o}C have been observed. The second peak in glass with 1,0% Ag being three times larger than that in a glass with 0.1% Ag.
It is, however, interesting that doping with 2% Ag, the glass obtained presented just one peak around 135-170^{o}C. Discussion on this work will be present at the conference.

Acknowledgements: We are thankful to FAPESP for financial support.

Optical absorption and electron paramagnetic resonance of natural and synthetic diopside glass

Bruno G. Fernandes[1,2], Shigueo Watanabe[1],T. k. Gundu Rao[1], Douglas Gouvêa[2], Angelo F.Padilha [2]

[1]*Institute of Physics, University of São Paulo, Brazil*
[2]*Department of Metallurgical and Materials Engineering, Polytechnic School, University of São Paulo, Brazil*

Using natural diopside mineral, glass sample was produced by divetrification method. Then synthetic glass of diopside starting with reagent grades of oxides components. Glass doped with 1.56 (w%) of Al, as well as, glass doped 0,1%, 1% and 2% Ag have also been produced. Laminal with 1,5 mm thickness were prepared for optical absorption measurements, with tens of kGy gamma irradiation.

The glass of natural diopside presented on optical absorption spectra with strong UV absorption and a broad absorption band centered at 1000 nm giving rise to green colour to the glass. Pure and Al doped synthetic glasses have shown UV and 8000nm absorption bands, but no colouration was observed Doping with Ag still UV absorption is oberseved but a strong and continued absorption took place beyond 600nm leaving the glass coloured with blue-violet.

The EPR spectra of different diopside glasse are as it follows.

1- Of natural diopside consists of a strong signal around 1600 Gauss due to Fe3+- ions.
2- Of a pure synthetic glass, besides Fe3+- signal at 1600 Gauss, a strong F+- center signal is observed,
3- 3) of 1% doped glass presented a F+- center signal around g=2,0 as in a pure synthetic glass, signals around 2200-2300 Gauss are observe due to the interaction between F+- center and Ag-ions,
4- The glass in 3) now irradiated with 30 kGy gamma-ray presented a Fe3+- signal plus a strong F+- center signal and weak signals at 3600-3700 Gauss due to the interaction Ag-ions and F+- center.

Acknowledgement: thanks are due to

1- Fapesp for financial support
2- Capes for visiting Professor Fellowship to Dr. T. K. Gundu Rao

Luminescent properties of $Ca_9Y(PO_4)_7$ doped with Eu^{3+} and Eu^{2+}

N. Gorecka, K. Szczodrowski, J. Barzowska, M. Grinberg

Institute of Experimental Physics, University of Gdansk, Wita Stwosza 57, 80-952 Gdansk, Poland

The main goal of the research was to investigate the spectral properties of the europium doped phosphate ($Ca_9Y(PO_4)_7$) which belongs to whitlockite-like family of phosphate minerals. Due to the presence of two different cations in the studied matrix (Ca^{2+} and Y^{3+}) that are available for europium substitution [2] the synthesis parameters were selected for incorporation of europium ions (1% mol) into the calcium sites (Sample 1), yttrium sites (sample 2) and equally into the calcium (0.5% mol) and yttrium (0.5% mol) sites (sample 3).
The single phase phosphors were obtained using Pechini synthesis method. The method is based on a mixing of positive ions in a solution, controlled transformation of the solution into a polymer gel, removal of the polymer matrix and calcination of an oxide precursor with a high degree of homogeneity. A two-step strategy of synthesis was applied. This strategy involved an initial annealing of mixture of reagents under inert gas atmosphere and then, after cooling and grinding the product, the reduction - under hydrogen/nitrogen atmosphere. The phase composition analysis as well as spectroscopic measurements of products, were performed to characterize the obtained phosphors. The XRD patterns show, that we obtained the 100% pure $Ca_9Y(PO_4)_7$ in all cases. Emission spectra of materials obtained after first step of the synthesis consist of narrow bands, which are characteristic for $^5D_0 \rightarrow ^7F_J$ transitions in Eu^{3+} ion. However in 450 nm-550 nm spectral range we can also see a broad band originating from europium ion on +2 oxidation states. The emission spectra of materials, which were obtained after reduction process, are characterized by the intensive, broad band attributed to the d-f transitions in Eu^{2+} and very weak line at 619 nm attribute to the europium 3+ ion [1,3]. The time resolved emission spectrum measurement were carried out to confirm the transition nature.

[1] O.Liu, Y.Liu, Z.Yang, X.Li, Y.Han,Spectrochemica Acta Part A 87 (2012) 190-193
[2] Y.Lu, C.H.Huang, T.M.Chen, J.H.Lin, Y.R.Ma, J.L.Chen, C.C.Hsu, C.L.Chen, C.L.Dong, T.S. Chan, Chemical Physics Letters 515 (2011) 245-248
[3] B.Wang, Y.Lin , H.Ju, Journal of Alloys and Compounds 584 (2014) 167-170

1.5μm Luminescence of colored BGO crystals

L.I. Ivleva[1], E.E. Dunaeva[1], T.V. Chukhlovina[1], S.E. Sverchkov[1], V.V. Koltashev[2], S.V. Firstov[2], E.M. Dianov[2]

[1]General Physics Institute Russian Academy of Sciences
[2] Fiber Optics Research Center of the Russian Academy of Sciences

Recently, it was estimated that "red" $Bi_4Ge_3O_{12}$ (BGO) crystals may be useful in amplifier for signals in 1280-1320 nm and 1420-1520 nm spectral ranges of silica fiber. The "red" BGO samples have been grown by Vertical Bridgman method and shown a significant emission around 1490 nm under 808 nm laser diodes excitation [1, 2]. The red crystals were obtained from BGO+2mol.%H_2O raw material mixture. Nevertheless, the nature of the coloration of BGO crystals is not clear up to now. In our work we investigated the ways to obtain "red" BGO by additional thermal treatment of as-grown Czochralski crystals. Micromorphology, absorption and luminescence spectra for the crystals annealed under different conditions were studied.

The optically homogeneous colorless BGO crystals were grown under Czochralsky crystallization conditions along [100] and [111] directions. As a rule, segregation of structural inhomogeneities was observed in top part of the crystal grown from the stoichiometric composition. The mass losses of the melt were $1x10^{-3}$ g/cm^{2}h because of Bi_2O_3 evaporation during growth process. Optimal bulk crystallization rate was 0.7 cm^3/h. In our experiments influence of annealing of BGO crystals turns out to be strongly dependent on temperature, the ambient atmosphere and chemical nature of substances being in contact with the crystal. For example, annealing of the crystal in vacuum in graphite crucible results in appearance of additional absorption peaks in spectral range 300- 2000nm. The samples became pink ("red") color. At the same time, the more obvious transformations in surface morphology takes place at temperature interval 850-900 C. Annealing process in contact with Pt or Ir in vacuum at 850C results in thermal etching of sample surface forming dendritic structure. The crystals remain colorless. On the contrary, annealing under increased temperature leads to disappearance of dendritic images. In these conditions precipitates of bismuth oxide can be segregated at dislocations, arranging dark points. The surface micromorphology is similar chemical etching image. In comparison with vacuum thermal treatment of BGO samples in the air atmosphere have no so remarkable influence on micromorphology and the optical properties of the material. Differences in the surface optical spectra, obtained for various conditions, prove the participation of diffusion in the annealing process. Differences in diffusion coefficients of main components can leads to local redistribution of stoichiometry without changes in the total composition. Nevertheless, this redistribution can produce significant modification of optical and other characteristics. Transmission spectra in the transparency range, IR luminescence spectra and excitation spectra of IR luminescence were measured for as-grown and annealed samples. The vacuum annealed samples appear clear bands in the absorption spectra (calculated from transmission spectra) near the short-wavelength absorption edge: 365, 455 and 520 nm. IR luminescence was recorded well-separated peaks at 1030 and 1500 nm in the "red" samples. For these luminescence peaks excitation spectra were measured: for 1030nm – narrow band with a maximum at 370 nm, 1500 nm – band at 450 nm with a wing at 530 nm.

[1] P.Yu, L.Su, H. Zhao, J. Xu, *Journal of Luminescence*, **154** 520-524 (2014)
[2] P.Yu, L.Su, H. Zhao, et.al., *Optical Materials,* **33** 831-834 (2011)

Connecting crystal structure and luminescence, the case of SrAl2O4:Eu2+

Jonas J. Joos, Jonas Botterman, Dirk Poelman, P. F. Smet

LumiLab, Department of Solid State Sciences, Ghent University, Krijgslaan 281-S1, 9000 Gent, Belgium
Center for Nano- and Biophotonics (NB Photonics), Ghent University, St-Pietersnieuwstraat 41, 9000 Gent, Belgium

Photoluminescent materials or phosphors are ubiquitous in today's technology driven society, for example in LEDs, scintillators or safety signalling. These inorganic materials are composed of a host crystal doped with one or multiple metal ions, activating the luminescence [1]. The luminescence of the metal ion is often strongly dependent on the crystal structure of the host compound.

Upon co-doping with Dy^{3+}, $SrAl_2O_4:Eu^{2+}$ is well-known because of its persistent luminescence, i.e. it shows an extremely long lasting green afterglow. Although frequently used in safety signalling and all kinds of gadgets, the origin of the persistent luminescence is not yet fully explained [2]. More specifically, a second, blue emission band occurs at low temperature. It has been shown that this emission band is of importance in explaining the trapping and detrapping mechanism behind the persistent luminescence in this material. Different conflicting explanations for the occurrence of the blue emission are available in literature [3].

In this work, empirical models relating the luminescence of lanthanide ions with structural parameters of the host are applied to explain the peculiar luminescence in Eu^{2+} doped $SrAl_2O_4$ [3, 4]. It is shown that the blue and green emission bands originate from europium ions substituting two non-equivalent Sr sites inside the host crystal, even if both sites are rather similar.

[1] P. F. Smet, A. B. Parmentier, D. Poelman, J. Electrochem. Soc. (2011), **158**, R37-54.
[2] K. Van den Eeckhout, P. F. Smet D. Poelman, Materials (2010), **3**, 2536-2566.
[3] J. Botterman, J. J. Joos, P. F. Smet, Phys. Rev. B (2014), **90**, 085147.
[4] J. J. Joos, D. Poelman, P. F. Smet, Phys. Chem. Chem. Phys. (2015), **17**, 19058-19078.

Dynamics of polarons in $LiNbO_3$-type crystals under continuous-wave laser irradiation

Susumu KATO[1], Sunao KURIMURA[2], Norikatsu MIO[3]

[1]*National Institute of Advanced Industrial Science and Technology (AIST), Central 2, 1-1-1 Umezono, Tsukuba, Ibaraki 305-8568, Japan*
[2]*Advanced Materials Laboratory, National Institute for Materials Science, 1-1 Namiki, Tsukuba, Ibaraki 305-0044, Japan*
[3]*Photon Science Center, University of Tokyo, 2-11-16 Yayoi, Bunkyo-ku, Tokyo 113-8656, Japan*

$LiNbO_3$ and $LiTaO_3$ crystals are especially useful for green second-harmonic generation of continuous-wave light because of the high nonlinearity. However, laser-induced catastrophic breakdown and damage in nonlinear crystals limit output laser power in high-average-power lasers, where the breakdown threshold intensities of green light for $LiTaO_3$ are in the order of several tens of MW/cm^2 [1]. We proposed that one of the causes of the breakdown is a light-induced heating by the accumulated polarons [2].

It is well known that polarons have large absorption cross sections and stretched-exponential decays in LiNbO3-type crystals [3]. The dynamics of polarons, however, is not yet completely clear. Using a rate-equation model based on the polaron kinetics which included the relaxation between free and bound polarons, we attempted to the stretched-exponential decay in $LiNbO_3$ [4]. In the rate-equation model, the transport of polarons was not considered.

In this paper, we investigate the heating by the light-induced polaron transport and absorption in LiNbO3-type crystals under continuous-wave laser irradiation using a theoretical model, which consists of a transport equation coupled with the rate-equation model.

[1] S. Kurimura, H. H. Lim, and N. E. Yu, "Green-Suppressed Quasi-Phase-Matched Optical Parametric Oscillation," in Advanced Solid-State Lasers Congress, G. Huber and P. Moulton, eds., OSA Technical Digest (online) (Optical Society of America, 2013), paper ATu4A.8.
[2] S. Kato, S. Kurimura, H. H. Lim, N. Mio, Opt. Mater. **40**, 10 (2015).
[3] M. Imlau, H. Badorreck, and C. Merschjann, Appl. Phys. Rev. **2**, 040606(2015) and reference therein.
[4] S. Kato, S. Kurimura, and N. Mio, Opt. Mater. Express **6**, 396–401 (2016).

Effect of Mg-doping on cathodoluminescence properties of GAGG:Ce single crystalline films

O. Lalinský[1], P. Schauer[1], M. Kučera[2], Z. Lučeničová[2], M. Hanuš[2]

[1]*Institute of Scientific Instruments of the CAS, Královopolská 147, 612 64 Brno, Czech Republic*
[2]*Charles University, Faculty of Mathematics and Physics, 121 16 Prague, Czech Republic*

Cerium activated single crystals of gadolinium aluminum gallium garnet (GAGG:Ce) are prospective scintillation materials thanks to their high light yield of 50-60 kPh/MeV [1], and fast luminescence decay with a short decay time of 50-80 ns [2].
However, such decay time can be still too high, for example, for special SEM applications where the very fast e-beam scanning is required. Thus, new materials with faster decay have to be found.
For this purpose, Mg-doped specimens of the GAGG:Ce multicomponent epitaxial films with different concentration of Mg were grown from lead-free BaO-B_2O_3-BaF_2 flux. These films were excited by an electron beam with energy of 10 keV using a specialized CL apparatus [3]. As a result, CL spectra and CL intensity decays were measured in the temperature range between 100 and 500 K. Moreover, thermoluminescence glows were obtained.
One of the results was the decreasing decay time for the increasing Mg content. For the highest content of Mg, the decay time was under 29 ns. Thus, Mg-doped GAGG:Ce single crystalline films are perspective scintillators especially for applications, where very fast response is required.

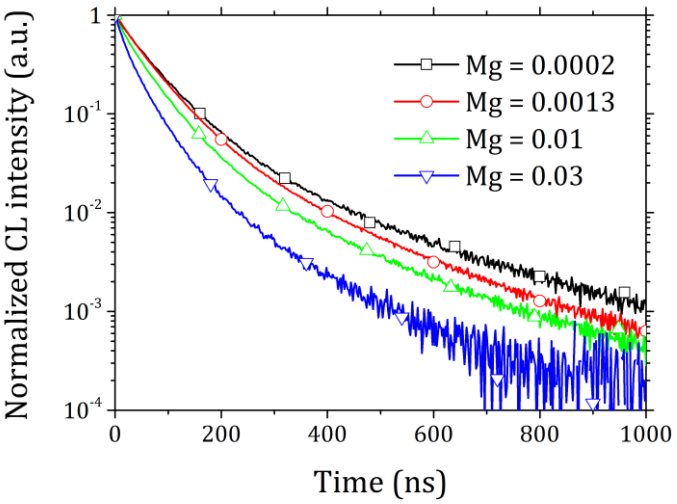

Fig. 1: CL decay characteristics of $(Ce_{0.03}Gd_{2.2}Lu_{0.8})(Al_{2.5-x}Ga_{2.5}Mg_x)O_{12}$ single crystalline films. Values of parameter x are shown in the graph legend. Electron pulses were 50 ns long.

Acknowledgements: The research was supported by Czech Science Foundation (project, GA16-05631S) by Ministry of Education, Youth and Sports of the Czech Republic (project LO1212). The research infrastructure was funded by Ministry of Education, Youth and Sports of the Czech Republic and European Commission (project CZ.1.05/2.1.00/01.0017).

[1] K. Kamada, T. Yanagida, T. Endo, et al., J. Cryst. Growth, **352,** 88 (2012).
[2] M. Kucera, Z. Onderisinova, J. Bok, et al., J. Lumin., **169**, 674 (2016).
[3] J. Bok, P. Schauer, Rev. Sci. Instrum., **82**, 113109 (2011).

Optical processes in $YVO_4:Eu^{3+}$ across zircon-to-scheelite phase transition

Sebastian Mahlik[1*], Agata Lazarowska[1], Karol Szczodrowski[1], Marek Grinberg[1*], Enrico Cavalli[2], Philippe Boutinaud[3]

[1]*Institute of Experimental Physics, University of Gdansk, Wita Stwosza 57, 80-952 Gdańsk, Poland*
[2]*Department of Chemistry, Università di Parma, Parma, Italy*
[3]*Clermont Université, ENSCCF, Institut de Chimie de Clermont-Ferrand, BP 10448, F-63000 Clermont-Ferrand*

The luminescence processes across zircon-to-scheelite phase transition in undoped YVO_4 and Eu^{3+}-doped YVO_4 are investigated by measuring the Raman, excitation and emission spectra and decay characteristics of the compounds with respect to high hydrostatic pressure up to 200 kbar. The scheelite polymorphs obtained after releasing the high pressure show no luminescence when undoped, even down to 10K, but when activated with Eu^{3+} exhibits the characteristic scheelite-related Eu^{3+} emission but with low intensity. This emission is produced upon UV excitation in zircon inclusions that remain after the pressure treatment.

Optical absorption and charge transfer processes in vanadium doped $SrTiO_3$ crystals

Z. Potůček[1], A. P. Skvortsov[2], K. Dragounová[3], Z. Bryknar[3], A. Dejneka[1], V. A. Trepakov[1,2]

[1]*Institute of Physics AS CR, Na Slovance 2, Praha 8, Czech Republic, CZ-182 21*
[2]*Ioffe Institute of the RAS, Polytekhnicheskaya 26, St. Petersburg, Russia, RU-194021*
[3]*Faculty of Nuclear Sciences and Physical Engineering, Czech Technical University in Prague, Trojanova 13, Praha 2, Czech Republic, CZ-120 00*

Strontium titanate ($SrTiO_3$) is the model representative of highly polarizable ABO_3 perovskite-type oxides. They are applied in a wide range of components in various devices due to their exceptional functional properties that can be tailored even by very low amount of suitable admixtures. In this context study of $SrTiO_3$ crystals doped by polyvalent transition metal ions is very desirable because even in the case of their common contamination during growth process these impurities strongly influence the whole range of their physical properties such as optical absorption or charge transport in the crystals. Recently we have found photoluminescence in the slightly vanadium doped $SrTiO_3$ crystals that at low temperatures consisted of a pronounced zero-phonon line near 1157 nm accompanied by well developed vibrational sidebands. We suppose that this near infrared emission originates from the $^1T_{2g} \rightarrow {}^3T_{1g}$ transitions of octahedrally coordinated $V^{3+}(3d^2)$ ions substituted for Ti^{4+} ions. Moreover we have noticed the marked decrease in intensity of this photoluminescence at low temperatures during steady-state excitation by visible lines of Ar-Kr laser.
To elucidate observed photochromic behaviour of the V^{3+} centres we performed on slightly vanadium doped $SrTiO_3$ single crystal a current study of optical absorption and sensitization spectra of photoluminescence with zero-phonon line near 1157 nm in the visible and near infrared spectral region at temperatures between 4.2 and 300 K. In addition to vanadium atoms the inspection of impurity content in the crystal carried out by the PIXE method also revealed the presence of comparable amount of Fe atoms. The optical absorption of the slightly yellow-brown tinted crystal below the $SrTiO_3$ absorption edge was dominated by features previously attributed to Fe centres in $SrTiO_3$:Fe crystals. The contribution of the absorption bands corresponding to transitions from the ground state $^3T_1(^3F)$ to the excited states $^3T_2(^3F)$, $^3T_1(^3P)$, and $^3A_2(^3F)$ of V^{3+} centres that were detected in the excitation spectra of their photoluminescence was very weak. Sensitization spectra of photoluminescence with zero-phonon line near 1157 nm shoved that charge conversion of V^{3+} centres to V^{4+} and/or V^{2+} centers resulting in dependence of their photoluminescence intensity on the history of crystal illumination and cooling occurs in the case of exposure in the spectral region of absorption attributed to Fe centres. The possible models of energy levels and electron transitions in the $SrTiO_3$:V crystal suggested for explanation of the observed photochromic behaviour of V^{3+} centres will be presented.

Point defects in rare earth phosphors of garnet structure

N.Soschin[1], V.Bolshukhin[1], V.Ulasyuk[2]

[1]*SRC «Luminophore», Fryazino, Russia*
[2]*Corp. «ELTAN LTD», Fryazino, Russia*

Rare earth aluminate phosphors (REA) of garnet structure and $(\sum Lu)_3Al_2Al_3O_{12}$ stoichiometric formula, where ∑Lu=Y, Gd, Lu, Tb, Ce, belong to the cubic system and 1a 3d group. They are widely used in modern semiconductor lighting engineering as part of reemitting converters of white LEDs and an in X-ray computed tomography as effective multi-element scintillators, due to a number of their excellent parameters:
- high quantum yield under photoexcitation η≤0,98, as well as considerable energy yield ɣ=20-22% at energies of X-ray quanta ranging from E_1=18 keV to E_2=120 keV;
- very short duration of afterglow (τ_1=2 ms when activated with Tb^{+3} ion and τ_2=64 ns when activated with Ce^{+3} ion);
- insignificant temperature influence on the glow due to the compactness of the cubic crystal lattice and its small parameter d=12.001 Å.

Garnet structure phosphors have three types of structural units, of which the dodecahedral ones, where lanthanides ΣLu=Y, Gd, Tb, Ce are placed, have a coordination number KU=8, while the octahedral ones containing elements of subgroup IIIa, have KU=6. In coordination tetrahedra of $[AlO_4]$ KU=4.

In the process of REA synthesis by techniques of solid-phase nanosynthesis at T=1600°C, or sol-gel technology at T=1400°C, point defects are formed in the bulk and on the surface of the REA grains. We study them by photo-, cathode-, and x-ray luminescence methods.

One of the most common defects is a node placement of Ba^{2+} impurity in the cation sublattice of REA, which takes place due to the presence of fluoride mineralizers of BaF_2 or SrF_2 type in solid-phase nanosynthesis by the reaction $2BaF_2 + Al_2O_3(Y_2O_3) \rightarrow (Bay)^1 + BaAl_2O_4$, where a defect of the Ba^{2+} ion, housed in the constitutional node Lu^{3+} of the cation sublattice, is recorded as Bay. This point defect compensates a deficiency of positive charge by modifying the chemical composition of the nearest tetrahedron $[AlO_4]$ to $\rightarrow[AlO_3F]$, wherein the O^{2-} ion is partially replaced by fluorine ion F^{1-}. The barium point center hardly shows itself in the emission spectra, but it is clearly visible when measuring the duration of the Tb^{3+} ion afterglow due to the appearance of the second exponent τ_e=10 ms, as well as an increase in the attenuation of the Ce^{+3} ion to τ=100 ns. In the process of high-temperature synthesis dissociation of oxygenic tetrahedra $[AlO_4]$ is possible with formation of a vacancy according to the $[AlO_4]T\rightarrow[AlO_3V_0]$ scheme, manifested by an increase of optical absorption of the REA in the visible range.

An absolutely unusual phenomenon is antistructural defects formed in the process of implantation of a lanthanide Lu^{3+} ion into the octahedral (KU=6) nodes of the anion sublattice of REA. The close crystal-chemical radii of the Lu^{3+} ion (a=0,80 Å) and the replaced Me^{3+} node allow to form such nodes as Lu_{Al} or Lu_{Ga} even at low synthesis temperatures. A typical manifestation of antistructural nature is a split of the radiative Gaussian in the spectrum of $(Y, Lu, Ce)_3(Al, Lu)_2[AlO_4]_3$ phosphors (Fig. 1).

In order to reduce the influence of the detected point defects we propose preparative methods of their removal.

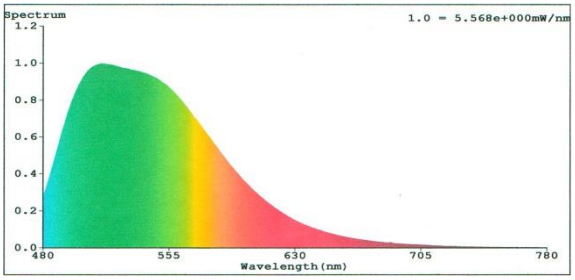

Analysis of carrier trap center in $SrAl_2O_4$-based persistent phosphors by spectroscopy and EPR

J. Ueda[1], S. Tanabe[1]

[1]*Graduate School of Human and Environmental Studies, Kyoto University, Japan*

The $SrAl_2O_4:Eu^{2+}$-Dy^{3+} developed by Matsuzawa *et al.*[1] shows the brightest and longest persistent luminescence among all the afterglow materials ever reported. After their discovery, many researchers have discussed the mechanisms in the $SrAl_2O_4:Eu^{2+}$-Dy^{3+} persistent phosphor. However, the details of carrier transport path and trap centers are not yet clear. In this study, the persistent mechanism and the carrier trap centers were investigated by photoluminescence, persistent luminescence, thermoluminescence, photoconductivity, electron paramagnetic resonance (EPR) measurements and vacuum referred binding energy (VRBE) diagram.

$SrAl_2O_4$ ceramics doped with various Ln^{3+} ions (Eu^{2+}, Eu^{3+}, Ce^{3+}, Eu^{2+}-Dy^{3+}, Eu^{2+}-Nd^{3+}, Dy^{3+}, Nd^{3+}) were prepared by solid-state reaction at 1500 °C. The optical and optoelectronic properties of the obtained samples were analyzed.

Fig. 1 shows the photoluminescence (PL) and PL excitation (PLE) spectra of the $SrAl_2O_4:Ce^{3+}$-Na^+ and Eu^{3+}-Na^+. Na^+ in Sr^{2+} site is a charge compensator for Ln^{3+} in Sr^{2+} site. In the excitation spectrum of $SrAl_2O_4:Ce^{3+}$, the split five 5d bands in the range between 200 nm and 350 nm and the host exciton band at around 181 nm were observed. For the $SrAl_2O_4:Eu^{3+}$, the charge transfer (CT) band of Eu^{3+} was observed at 299 nm. Accoridng the mothod presented by Dorenbos [2], the VRBE diagram was constructed using the obtained energies as shown in Fig. 2. The persistent luminescent mechanism will be discussed using the constructed VRBE diagram and EPR analysis in the presentation.

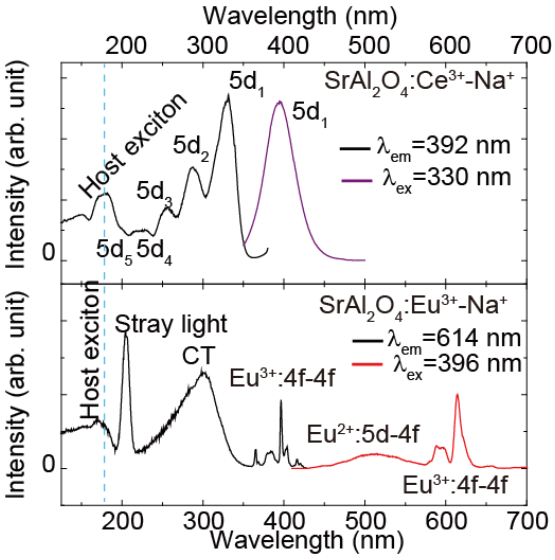

Fig. 1. PL/PLE spectra of $SrAl_2O_4:Ce^{3+}$, $:Eu^{3+}$

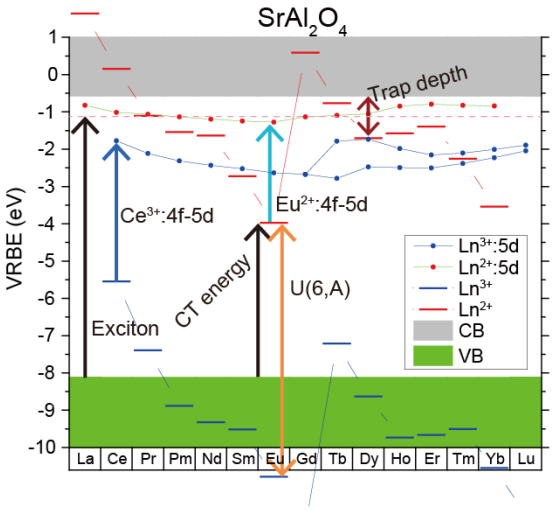

Fig. 2. VRBE diagram of $SrAl_2O_4$

[1] T. Matsuzawa,Y. Aoki,N. Takeuchi,Y. Murayama. *J. Electrochem. Soc.*, **143**, 2670 (1996).
[2] P. Dorenbos. *Phys. Rev. B,* **87**, 035118 (2013).

Optical properties of Ce^{3+}-Yb^{3+} and Bi^{3+}-Yb^{3+} doped YAG down-converting epitaxial layers

Ya. Zhydachevskii[1,2], I.I. Syvorotka[3], A. Wierzbicka[1], A. Suchocki[1,4]

[1] *Institute of Physics of the Polish Academy of Sciences, Al. Lotników 32/46, Warsaw 02-668, Poland*
[2] *Lviv Polytechnic National University, 12 Bandera, Lviv 79013, Ukraine*
[3] *Scientific Research Company "Carat", 202 Stryjska, Lviv 79031,Ukraine*
[4] *Institute of Physics, University of Bydgoszcz, Weyssenhoffa 11, Bydgoszcz 85-072, Poland*

A possibility of the broadband down-conversion in Yb^{3+}-doped oxides using a co-doping with Bi^{3+} or Ce^{3+} ions was shown recently [1-4]. These materials exhibit an efficient broadband quantum cutting of UV-blue light and its conversion into near IR light that can be used for enhancement of efficiency of silicon solar cells by the way of solar spectrum modification.
In the present work, results of optical absorption, photoluminescence and X-ray diffraction measurements of the single crystalline yttrium aluminum garnet (YAG) layers doubly doped with Ce^{3+}-Yb^{3+} or Bi^{3+}-Yb^{3+} ions are reported. The performed studies have aimed to get better insight in to the energy transfer processes in the Ce^{3+}-Yb^{3+} or Bi^{3+}-Yb^{3+} doped garnet of highest optical and structural quality that is ensured by the liquid phase epitaxy (LPE) technique.
The epitaxial films of correspondingly doped YAG were grown by standard LPE method on (111)-oriented YAG substrates in Scientific Research Company "Carat" (Lviv, Ukraine). As a solvent, a mixture of high purity bismuth oxide (Bi_2O_3, 5N) and boron oxide (B_2O_3, 5N) has been used. Series of defect-free, mirror-like and transparent correspondingly doped YAG films with thickness from 10 to 50 μm were grown.
X-ray diffraction measurements confirm high quality and homogeneity of studied films in particular films with a thickness up to about 30 μm. The optical absorption and photoluminescence results revealing presence of Ce^{3+}, Bi^{3+} and Yb^{3+} ions in the studied films and the excitation energy transfer from Ce^{3+} to Yb^{3+} ions and from Bi^{3+} to Yb^{3+} ions are discussed in comparison with literature data on this subject.

Acknowledgements: The work was supported by the Polish National Science Center (project 2015/17/B/ST5/01658).

[1] W. Xian-Tao, Z. Jiang-Bo, et al., *Chin. Phys. B,* **19,** 077804 (2010)
[2] X.Y. Huang, Q.Y. Zhang, *J. Appl. Phys.,* **107,** 063505 (2010).
[3] J. Zhou, Yu Teng, S. Ye, X. Liu, J. Qiu, *Opt. Mater.,* **33,** 153–158 (2010).
[4] Ya. Zhydachevskii**,** L. Lipińska, M. Baran, M. Berkowski, A. Suchocki, A. Reszka, *Mat. Chem. Phys.* **143** 622–628 (2014).

Comparison of the luminescent properties $Lu_3Al_5O_{12}$:Pr and $Y_3Al_5O_{12}$:Pr crystals, films and nanopowders under synchrotron radiation excitation

Yu. Zorenko[1], T. Zorenko[1], E. Zych[3], V. Gorbenko[1,3], S. Nizankovskiy[4], T. Voznyak[3]

[1]*Institute of Physics, Kazimierz Wielki University in Bydgoszcz, 85090 Bydgoszcz, Poland*
[2]*Department of Chemistry, Wroclaw University, 50-383 Wroclaw, Poland*
[3]*Electronics Department, Ivan Franko National University of Lviv, 79017 Lviv, Ukraine*
[4] *Institute for Single Crystals NAS of Ukraine, 61001 Kharkiv, Ukraine*

Pr-doped $A_3Al_5O_{12}$ (A= Lu, Y) garnets, apart from their applications as scintillators in single crystal (SC) form [1], attract also an attention as single crystalline film (SCF) screens for 2D/3D microimaging based on the X-ray or synchrotron (SR) radiation [2] as well as ceramic [3] and nanopowder (NP) phosphors. Properties of these materials in the different crystalline forms are strongly influenced by the differences in the methods and conditions of their preparation.

The aim of our report is to compare the luminescent properties of $Y_3Al_5O_{12}$:Pr (YAG) and $Lu_3Al_5O_{12}$:Pr (LuAG:Pr) SC, SCF and NPs using SR excitation. The SCs of these garnets were grown by the Czochralski method under Ar atmosphere at temperatures around 2000^{o}C. The SCFs were crystalized by the liquid phase epitaxy (LPE) method from melt-solutions based on the PbO-B_2O_2 flux in air atmosphere onto YAG substrates at temperatures 960-1020^{0}C. The NPs of these compounds were prepared by the solid state reaction using the Pechini method at temperatures below 1000^{o}C.

Luminescent and scintillation properties of the YAG:Pr and LuAG:Pr SCF and ceramic were recently compared with those of reference SC using the traditional spectral methods (absorption, cathode- and photoluminescence and light yield (LY) measurements under excitation by α–particles) [3, 4]. We found that the emission spectra and decay kinetic of YAG:Pr and LuAG:Pr SCF due to the $5d^1$-$4f^2$ transition of Pr^{3+} ions are notable different in comparison with SC counterparts due to: (i) the presence of Y_{Al}/Lu_{Al} antisite defects as emission centers in UV range and trapping centers as well in the case of SCs, growth from the melt at high temperatures; (iii) the influence of Pb^{2+} flux related dopants in the case of LuAG:Pr and YAG:Pr SCF, grown from PbO based flux at significantly lower temperatures.

Using the time-resolved luminescent spectroscopy of YAG:Pr and LuAG:Pr SC, SCF and NP under excitation by SR at Superlumi station at HASYLAB at DESY at 10 and 300 K, we exactly determined the positions of the Pr^{3+} 5d energy levels in YAG and LuAG hosts and estimated the differences in the energies of creation of excitons bound with the isolated Pr^{3+} ions in LuAG:Pr and YAG:Pr SCFs and dipole Pr-Lu_{Al}/Y_{Al} ADs centers in SC counterparts. We found the notable differences in the emission, excitation spectra and luminescence decay kinetics of YAG:Pr and LuAG:Pr SC, NP and SCF caused by the involving of the antisite defects and oxygen vacancies in SC and on the boundaries of NP and Pb^{2+} flux related dopant in SCFs in the excitation processes of Pr^{3+} luminescence in LuAG and YAG hosts. We found also the significant difference in the structure of emission centers in the main volume and on the boundaries of NP grains. These differences are caused by presence of the significantly larger concentration Y_{Al}/Lu_{Al} antisite defects, oxygen vacancies, Pr^{3+} ions and their aggregates on the boundaries of NP grains in comparison with NP core.

This work was realized within the Polish NCN 2012/07/B/ST5/02376 and Ukrainian PN 01-05-15 and SL-20F projects.

[1] A. Yoshikawa, V. Chani, M. Nikl, Acta Physica Polonika A, **124** 250 (2013).

[2] T. Martin, P-A. Douissard, M. Couchaud, A. Cecilia, et al., IEEE Trans. Nucl. Sci. **57** 1335 (2010).
[3] Y. Shen, X. Feng, V. Babin, M. Nikl, A. Vedda, F. Moretti, et al. Ceramics Internat., **39** 5985 (2013).
[4] V. Gorbenko, Yu. Zorenko, V. Savchyn, T. Zorenko, et all, Radiation Measurements, **45** 461 (2010).

Analysis of absorption and emission spectra at room temperature of rare earth ions doped in fluoride crystals

A.Bitam[1,2], S.Khiari2

[1] *University Centre of Tamanrasset, Algeria, adel.bitam@gmail.com*
[2] *Laboratory of Laser Physics, Optical Spectroscopy and Optoelectronics (LAPLASO), University Badji Mokhtar, Annaba, BP 12, 23000 Annaba, Algeria, diafma@yahoo.fr*

The present work reported a Judd-Ofelt analysis of spectroscopic and lasers parameters of Er^{3+} ions in crystal hosts. Rare earth-doped fluoride single crystals are considered to be an important class of optical device materials due, mainly, to their low phonon energies. They play a very significant role in the development of laser amplifiers for optical communications. Among the rare earth, trivalent erbium ions Er^{3+} have potential for laser applications due to a large number of available energy levels in the visible and near infrared domains.
We have studied the optical properties of Er^{3+} doped BaF_2 single crystals. Room temperature absorption spectra were recorded in order to investigate spectroscopic properties by using the Judd-Ofelt (JO) analysis. The emission spectra, associated to $^4S_{3/2}$, $^2H_{11/2}$ and $^4F_{9/2}$ to $^4I_{15/2}$ level, have been also registered between 530 and 700 nm. They have been calibrated in emission cross-sections using the usual Fuchtbauer-Ladenburg formula.
Key words: Rare-earth, laser amplifier, Judd-Ofelt analysis, emission cross-section, fluorescence lifetime, absorption spectra.

Blue luminescence caused by native defect in hBN and AlN

B. Berzina, V. Korsaks, L. Trinkler

Institute of Solid State Physics, University of Latvia, 8 Kengaraga Str., LV-1063, Riga, Latvia

Wide band gap materials aluminium nitride (AlN) and hexagonal boron nitride (hBN) have attracted interest of many investigators during the last decades due to their optical properties based on presence of strong exciton luminescence allowing creation of light emitters in the far UV spectral region. Defect induced luminescence is not so profoundly studied. In AlN the main native defect induced luminescence bands are situated at 400 nm and 480 nm being related to oxygen induced defects, whereas in hBN the more intensive luminescence is at 320 nm, which can be presumably referred to carbon impurities. In hBN a weak fine-structured luminescence appears at longer wavelengths above the 320 nm usually assigned to different types of nitrogen vacancies v_N.

Our spectral investigation of variously structured AlN and hBN materials with nano-size and bulk structure have shown that in both materials there is a weak luminescence within the blue spectral region (BL) and its intensity increases considerably when sample is put into vacuum in comparison with that observed when sample is surrounded by air. As a result the materials present properties for sensing of oxygen gas that stimulates interest to spectral investigation of BL.

Spectral studies of the BL for a number of hBN powders of various origin and different average grain size (60 nm, 3 mkm, 5 mkm, 10 mkm) were performed. The photoluminescence (PL) and its excitation (PLE) spectra were studied within the temperature range from room temperature (RT) down to 8 K. The PL kinetics and optically stimulated luminescence (OSL) were studied at RT. It was found that in hBN a wide phonon-structured luminescence at 400 nm appears under excitation either through exciton processes or directly by absorption of UV light covering two wide defect-induced excitation bands at 270 nm and 340 nm. The experimental results obtained allowed proposition of two mechanisms responsible for the 400 nm luminescence. One of them is the intra-center mechanism when light absorption and following emission occur within one and the same luminescent defect. The other one is tunneling recombination mechanism when luminescent defect is interacting with another exited defect forming together a donor-acceptor pair. The most probable candidates of the defects, which are responsible for the BL could be referred to F-center type defects, which are present in material as native defects or created by recombination of an electron with a nitrogen vacancy.

In AlN nanopowder the 420 nm luminescence characteristics are very close to those observed for the BL in hBN allowing suggestion that the same luminescent centers and mechanisms are responsible for the BL formation.

Formation of Radiation Defects in Sulfates of Alkali Metals by Low-Energy Electron Excitations

D.H. Daurenbekov, T.N. Nurakhmetov, K.A. Kuterbekov, Zh.M. Salikhodzha, A.M. Zhunusbekov, A.Zh. Kainarbay, K. Bekmyrza

L.N. Gumilyov Eurasian National University, Munaitpasova str., 13. Astana, Kazakhstan

Sulfates of alkali metals (SAM) are widegap dielectrics. Investigations of K_2SO_4 crystals showed that separated electron-hole pairs and excitons are formed at photon energies of 9eV. The anionic complex SO_4^{2-} plays a special role in the generation of electron excitations in sulfates. The electron configuration of the ground state of the sulfate anion has the form ….$2(a_1)^2(2t_2)^6(1e)^4(3t_2)^6(1t_1)^6$, determining the energy state of the valence band [1]. Unfilled antibinding $3a_1^*$ and $4t_2^*$ orbitals of the anion SO_4^{2-} are in the bottom part of the conduction band. The upper part of the zone is formed from free *S*-states of the cation. Based on the measurements of the reflection spectra of Na_2SO_4, K_2SO_4 and $CaSO_4$ [1] the detected reflection bands were referred to two groups of transitions. The first group of bands at 5.1 eV, 6.8 eV and 10.5 eV is associated with electron transitions from the molecular orbitals $1t_1$, $3t_2$, $1e$, $2t_2$ of SO_4^{2-}anion to the conduction band of the matrix formed by *S*-states of the cation. The second group of bands at 4.4 eV, 6.2 eV and 9.8 eV is referred to intra molecular transitions from the molecular orbitals $1t_1$, $3t_2$, $1e$, $2t_2$ to $3a_1^*$ and $4t_2^*$ orbitals of SO_4^{2-} ion. In irradiated by high-energy photons with energies 5.1 eV and 6.8 eV and 10.5 eV SAM separated electron-hole pairs must be formed. In the case of excitation of SAM, when intracenter transfer of electrons in SO_4^{2-} ion occurs, molecular excitons with an energy of 4.4 eV, 6.2 eV and 9.8 eV must be formed. As a result of localization of free electrons and holes electron-hole capture centers are formed. In the decay of molecular excitons, defects may be created or intrinsic radiation may be emitted. We studied formation of defects in $LiKSO_4$, $LiNaSO_4$ and $KNaSO_4$ crystals when they were excited by photons with energies 4.0-10.5 eV. In $KNaSO_4$ and $LiNaSO_4$ crystals irradiated by X-rays and 6-6.2 eV photons at 80 K, identical peaks of thermally stimulated luminescence (TSL) are formed. Appearance of TSL peaks in $KNaSO_4$ and $LiNaSO_4$ crystals irradiated by 6-6.2 eV photons indicates generation of electron-hole capture centers. The spectra of the main TSL peaks after irradiation by equal numbers of photons from 5 to 11 eV in $LiKSO_4$ crystal were studied. TSL peaks at 165 K, 185 K, 220 K and at 80 K in $LiKSO_4$ are formed at photon energies 6.0 eV, 7.4 eV, 9.0eV, 9.8 eV and 10.5 eV. Thus, we assume that radiation defects or electron-hole capture centers in SAM irradiated by 6.2-6.0eV photons are created as a result of localization of electrons and holes or the decay of molecular exciton $(SO_4^{2-})^*$.

[1] V.G. Sholokh, N.I. Aleshkevich, A.I. Komyak, *Zhurnal Prikladnoi Spektroskopii.,* **42** 400 (1985)

Comparative study of defect related emission in ZnO, ZnO-Cu and ZnO-Al nanocrystals obtained by etching method

Brahim El Filali[1], Juan Antonio Jaramillo Gomez[1] and T. V. Torchynska[2]

[1]UPIITA-Instituto Politécnico Nacional, México D.F.07738, México.
[2]ESFM-Instituto Politécnico Nacional, México D.F.07738, México.

Photoluminescence (PL) spectra of ZnO ZnO-Cu and ZnO-Al nanocrystals (NCs) grown by the electrochemical method have been investigated. Photoluminescence (PL) spectra present at least four Gaussian shape PL bands centered at 3.10-3.14, 2.60-2.70, 2.45 and 2.05 eV. The former one around 3.10-3.14 eV, is identified as the near band edge (NBE) emission related to the free exciton or bound exciton emission and/or their LO phonon replicas. The PL spectra in all samples ZnO, ZnO-Cu and ZnO-Al, grown by electrochemical method, are similar, but the PL intensity of defect related emission is higher in the ZnO-Cu nanocrystals prepared electrochemically in comparison with ZnO.
Defect related PL bands have been investigated using the variation of temperature (Fig.1) and the intensity of excitation light with the aim to separate the overlapped 2.05, 2.45 and 2.60 eV PL bands. Finally the nature of the defects responsible for the 2.05, 2.45 and 2.60 eV PL bands has been discussed.

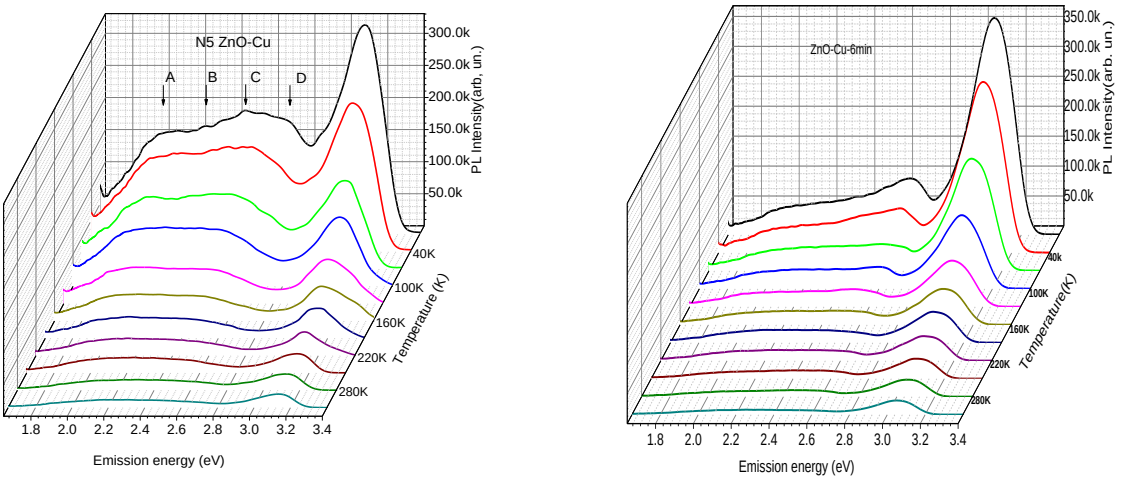

a) b)

Figure 1. PL spectra of ZnO-Cu-3min (a) and ZnO Cu-6min (b) NCs measured in the temperature range 10–300 K.

Emission Dependent on Stoichiometry of Si-rich-SiN_X films obtained by PECVD

T.V. Torchynska[1], J.A. Jaramillo Gomez[2], J.L. Casas Espinola[1], J. A. Bentosa Gutiérrez[2], L. Khomenkova[3] and A. Slaoui[4]

[1]*Instituto Politécnico Nacional, ESFM, México DF, 07738, México*
[2]*National Polytechnic Institute, UPIITA, México DF, 07340, México*
[3] *V. Lashkaryov Institute of Semiconductor Physics at NASU, Ukraine*
[4]*ICube, 23 rue du Loess, BP 20 CR, 67037 Strasbourg Cedex 2, France*

Bandgap engineering of Si-based materials through the control of the distribution of Si nanocrystals (Si-NCs) offered future applications of Si-based nanostructured materials in optoelectronics as low-cost, miniaturized, and CMOS-compatible, light-emitting, solar cell and photovoltaic devices. Present work deals with the study of Si-rich silicon nitride films, which were grown by the plasma enhanced CVD technique on silicon substrates. The film stoichiometry was controlled via variation of NH3/SiH4 ratio from R=0.45 up to 1.0. Thermal treatment was performed at 1100°C for 30 min in nitrogen flow to form Si-NCs.

To control structural and optical properties of the films the Raman scattering, X-ray diffraction (XRD), Transmission electron microscopy (TEM), Atomic force microscope (AFM) and photoluminescence (PL) methods were used. The evolutions of PL spectra with the temperature of measurements from 20 to 300 K, as well as with the change of the excitation light quanta and excitation power densities, were studied aiming the determination of the types of optical transitions.

The PL spectra were found to be complex and the shape and magnitude of PL spectra depends on silicon nitride stoichiometry. To study the defect and Si nanocrystals related PL bands two different PL excitation wavelengths (325 nm and 532 nm) were used. The increase of gas ratio from R=0.63 to R=1 results in the shift of PL peak position from 1.6 eV up to 2.7 eV. Analysis of the temperature dependence of PL spectra revealed the presence of several PL components with the maxima at 2.9-3.0 eV, 2.5-2.7 eV, 1.9-2.2 eV, 1.8-1.9 eV and 1.6-1.7eV. The peak position of the former three PL components unchanged with the decrease of temperature of the measurements. This allows describing all these components to the defects of silicon nitride host. At the same time, PL band peaked at 1.8-1.9 eV or 1.6-1.7 eV in different samples showed high-energy shift with sample cooling and can be ascribed to the exciton recombination inside Si-ncs. The presence of these latter was confirmed by Raman scattering spectra and TEM images. The nature of light emitting defects in silicon nitride, the mechanism of photoluminescence excitation and the way for the optimization of optical properties are discussed.

Intrinsic luminescence of the un-doped borate glasses

I.I. Kindrat[1], B.V. Padlyak[1,2], A. Drzewiecki[1]

[1]*University of Zielona Góra, Institute of Physics, 4a Szafrana Str., 65-516 Zielona Góra, Poland*
[2]*Institute of Physical Optics, Sector of Spectroscopy, 23 Dragomanov Str., 79-005 Lviv, Ukraine*

The intrinsic luminescence of the series borate glasses with $Li_2B_4O_7$, LiB_3O_5, $LiKB_4O_7$, CaB_4O_7, and $LiCaBO_3$ chemical compositions have been investigated and analysed at room temperature. The un-doped nominally-pure borate glasses of high chemical purity and optical quality were obtained from corresponding polycrystalline compounds by standard glass synthesis technology according to [1]. Optical absorption spectra show that the investigated un-doped borate glasses are high transparent in the 330 – 2500 nm spectral region.

Upon UV excitation all investigated borate glasses exhibit broad intrinsic luminescence emission band with maximum in the 460 – 480 nm (2.6 – 2.7 eV) spectral range. This band slightly depends on glass composition and characterises by large half-width that equals about 140 nm (0.74 eV or 6000 cm^{-1}). Time-resolved luminescence shows that broad band of intrinsic luminescence consist of two components: weaker short-lived with maximum about 440 nm (2.8 eV) and stronger long-lived with maximum about 490 nm (2.5 eV). Luminescence decay curves of observed emission bands are slightly non-exponential with mean lifetimes, which equal about few ns and hundred μs for fast and slow components, respectively.

Excitation spectra show that intrinsic luminescence are efficiently exited in the 260 – 270 nm (4.6 – 4.7 eV) spectral range. It should be noted that intrinsic luminescence in borate glasses is quite intensive and clearly reveals also in rare-earth doped borate glasses as previously reported in [2,3]. Additionally, the fast intrinsic luminescence is exited about 380 nm (3.2 eV) that well correlates with band-gap energy of investigated glasses obtained by the Urbach analysis of absorption edge.

Basing on obtained results the recombination mechanism of intrinsic luminescence in the borate glasses is proposed. In particular, the fast emission most likely arises from the recombination of electron–hole pairs and/or self-trapped excitons (STEs). The slow intrinsic luminescence can be associated with recombination of electrons and holes released from traps at room temperature.

[1] B.V. Padlyak, S.I. Mudry, Y.O. Kulyk, A. Drzewiecki, V.T. Adamiv, Y.V. Burak, I.M. Teslyuk, Mater. Sci. Poland, **30,** 264 (2012).
[2] I.I. Kindrat, B.V. Padlyak, A. Drzewiecki, J. Lumin., **166,** 264 (2015).
[3] I.I. Kindrat, B.V. Padlyak, S. Mahlik, B. Kukliński, Y.O. Kulyk, Opt. Mater., in press, (2016).

Luminescence properties of $Mg_{1-x}Zn_xGa_2O_4$ solid solution co-doped with Mn^{2+} and Eu^{3+} ions

A. Luchechko, *O. Kravets, L. Kostyk, O. Tsvetkova*

Ivan Franko National University of Lviv, Faculty of Electronics, Tarnavskogo Str. 107, Lviv 79017, Ukraine

The $ZnGa_2O_4$ and $MgGa_2O_4$ phosphors have attracted much attention because of possible application in vacuum cathode-ray tubes, field emission displays, thin film electroluminescence displays [1]. $MgGa_2O_4$ and $ZnGa_2O_4$ spinels doped with Eu^{3+} ions have bright luminescence in orange-red spectral region. Manganese doped gallate spinels exhibit strong emission in green spectral region with a maximum around 505 nm [2]. Solid solutions of Mg-Zn gallate spinel give a possibility to change relative intensity of emission bands in different spectral regions [3].

In this work, solid solution samples of $Mg_{1-x}Zn_xGa_2O_4$ ($x = 0 \div 1.0$) doped with constant concentration of 0.05 mol.% Mn^{2+} and 4 mol.% Eu^{3+} ions have been synthesized via high temperature solid state reaction method at ~1200 °C. X-ray diffraction measurements of all obtained samples show single-phase nature with spinel structure. The photoluminescence properties of the ceramics were investigated at 300 K with spectrofluorometer CM2203.

The excitation spectra of $Mg_{1-x}Zn_xGa_2O_4$ show similar behaviour in 230-280 nm spectral region at 430 nm registration that belongs to host luminescence of native defects. Excitation spectra of Mn^{2+} ions registered at 505 nm is similar to the excitation of host emission, but has a long-wavelength tail to 320 nm. A broad charge transfer band was found peaking around 280 nm on the excitation spectra of Eu^{3+} ions registered at 617 nm for all investigated samples ($x = 0 \div 1.0$). Sharp excitation lines that correspond to f-f transitions of Eu^{3+} ions were also found.

The luminescence spectra of $Mg_{1-x}Zn_xGa_2O_4$ samples excited with 240 nm wavelength show two emission bands with maximum around 430 and 505 nm. The 430 nm luminescence band corresponds to emission of host defects. The strongest host luminescence was found in the sample with $x = 0.25$. The luminescence around 505 nm is related to Mn^{2+} ions. The emission of matrix and Mn^{2+} ions excited with 280 nm are an order weaker than at 240 nm excitation. Sharp lines in 570-650 nm spectral range that correspond to $^5D_0 \rightarrow {}^7F_j$ transitions of Eu^{3+} ions were found at 280 and 393 nm excitations.

Influence of excitation wavelength and composition of $Mg_{1-x}Zn_xGa_2O_4$ solid solutions on the relative intensity of host, Mn^{2+} and Eu^{3+} emission as well as the possible mechanisms of energy transfer are under discussion.

[1] M. Yu et al., Material Letters, **56**, 1007 (2002).
[2] A. Luchechko et al., Radiation Measurements, 2015, Article in press.
[3] Bin-Siang Tsai et al., J. of Alloys and Compounds, **407**, 289-293 (2006).

Photoluminescent properties of Mn^{2+} ions in YAP single crystals

N. Martynyuk[1], Ya. Zhydachevskii[1,2], *M. Glowacki[2]*, S. Ubizskii[1], *M. Berkowski[2], A. Suchocki[2,3]*

[1] Lviv Polytechnic National University, 12 Bandera, Lviv 79013, Ukraine
[2] Institute of Physics of the Polish Academy of Sciences, Al. Lotników 32/46, Warsaw 02-668, Poland
[3] Institute of Physics, University of Bydgoszcz, Weyssenhoffa 11, Bydgoszcz 85-072, Poland

Mn^{2+}-doped $YAlO_3$ (YAP) crystals are of interest as a storage phosphor applicable for thermoluminescent (TL) dosimetry of ionizing radiation [1, 2]. The material have the main TL peak at 200 °C with the green emission near 530 nm caused by Mn^{2+} ions ($3d^5$ electronic configuration) in strongly distorted dodecahedral coordination (Y^{3+} sites in YAP structure) [3].

In spite of the application potential of YAP:Mn^{2+} crystals as TL phosphor, the luminescent properties of Mn^{2+} ions in YAP remain scanty studied. In particular, the Mn^{2+} photoluminescence decay time in YAP was not reported yet.

The studied YAP:Mn^{2+} single crystals were grown by Czochralski method in the Institute of Physics of the Polish Academy of Sciences. In order to stabilize manganese ions in desired 2+ oxidation state and to reduce concentration of Mn^{4+} ions emitting in red, a codoping with Si^{4+} or Hf^{4+} ions was used.

The photoluminescence (PL) and photoluminescence excitation (PLE) spectra of YAP:Mn^{2+} crystals were measured. It was found that the Mn^{2+} photoluminescence decay at room temperature, beside a component with $\tau \sim 3.5$ ms, has also a short decay component(s) with a decay time of μs and ns scale. In order to establish nature of the short decay, the time-resolved PL and PLE spectra were obtained.

Acknowledgements: The work was partially supported by the EU within the European Regional Development Fund through the Innovative Economy grant (POIG.01.01.02-00-108/09) and by the NATO SfP Project NUKR.SFPP 984649.

[1] Ya. Zhydachevskii et al., Mn-doped $YAlO_3$ crystal: a new potential TLD phosphor, *Nucl. Instr. Meth. Phys. Res.,* **227** 545-550 (2005).
[2] Ya. Zhydachevskii et al., Characterization of $YAlO_3$:Mn^{2+} thermoluminescent detectors, *Radiat. Meas.,* **45** 516-518 (2010).
[3] M.A. Noginov et al., Spectroscopic studies of Mn^{3+} and Mn^{2+} ions in $YAlO_3$, *J. Opt. Soc. Am. (B),* **16** 475-483 (1999).

Temperature and spatial changes of diffusion coloration of $LiNbO_3$ single crystals under redox treatment

U. Yakhnevych[1], D. Sugak[1,2], I. Syvorotka[2], O. Buryy[1], I. Solskii[2], N. Martynyuk[1], Yu. Suhak[3], S. Ubizskii[1]

[1] *Lviv Polytechnic National University, Lviv, Ukraine*
[2] *Scientific Research Company "Carat", Lviv, Ukraine*
[3] *Clausthal University of Technology, Goslar, Germany*

The work is dedicated to the determination of peculiarities of optical properties changes in the lithium niobate (LN) crystal volume caused by isochronous annealing in H_2 and subsequent annealing of the reduced samples in air. All samples for investigations were cut from the optical quality congruent LN crystals, produced at SRC "Carat". The dimensions of the samples treated in reducing and oxidizing atmospheres were 7(X)×15(Y)×32(Z) mm. The reduction was carried out in the ampoules filled by H_2 for 1 hour at temperatures 673, 773, 873, 973 K. For the investigations of the influence of the subsequent oxidation treatment five samples were annealed in hydrogen at 1 hour and T = 873 K. Annealing in air was carried out for 1 hour at temperatures 673, 773, 798, 823, 873 K. For the investigations of the spatial distribution of optical absorption the 1 mm-thick plates were cut from the central part of each annealed crystal in mutually perpendicular directions. Their absorption spectra were measured in different crystallographic directions (X, Y, Z) by UV3600 Shimadzu spectrophotometer in the 300…800 nm region with the specially designed device allows scanning of the light beam with 150 μm step through the aperture with 100 μm in diameter.

After annealing in H_2 at T = 673 K the samples have got the dark-brown coloration and after annealing at higher temperatures they looks as non-transparent The intensity of coloration cut plates from sample is maximal near the surfaces contacted with the annealing atmosphere, and decreases in direction to crystal center. The changes of the coloration along the 'surface – center' direction were characterized by additional absorption ΔK induced by the treatment, in each point of scanning. Generally, for main crystallographic directions the spectra of ΔK can be represented by a superposition of three bands with maxima at 350…410, 500…520 and 700…750 nm. The relative contribution of these bands in absorption spectrum differs depending on the depth as well as on the temperature of annealing.

The high-temperature annealing in air of LN samples, previously annealed in H_2, leads to discoloration of the crystals. After heating to 673 K the transparent region with thickness about 100 μm appears near the crystal surface. The discoloration process is more intensive at temperatures 773…823 K and at T = 873 K all samples become practically transparent. The spatial dependencies of the ΔK changes caused by oxidizing annealing have got the maxima probably caused by the non-uniformity of the initial coloration after previous annealing in H_2. The observed coloration/discoloration processes are essentially anisotropic, i.e. the changes of additional absorption depend on the crystallographic direction of diffusion process. The obtained spatial distributions of the optical absorption were described by the mathematical model taking into account both the diffusion and the defects recharging processes.

The Europium diiodide investigation

S. Vasyukov[1], A. Gektin[1], E. Galenin[1]

[1] *Institute for Scintillation Materials, NAS of Ukraine, 60 Nayki Avenue, 61001 Kharkov, Ukraine*

Last years trend to heavy Eu doped scintillators (like SrI2…) lead to the wide spread of the data. It relates both to scintillation performance deviation from 2% to 5-6% energy resolution and some differences in luminescence. We suppose that Eu state in the crystal host, association with different defects and dopant purity can play the crucial role in the final scintillator performance. This work devoted to study of EuI2 luminescence peculiarities for crystals, powder and/or granules depending on material purity and treatment.

The key data demonstrate (see fig.) two main peaks of luminescence (A – 440-450 nm and B – about 510 nm). Peak A has complex structure and consist of few peaks associated with Eu2+ ions d-f energy transfer in different local environment. Peak B corresponds to different structure defects. Three main features have to be notes as result: I) It was found that rate between peaks move to the peak A with EuI2 purity increase. II) Mechanical treatment (defects introduction to lattice) lead to the peak B intensity increase and significant quenching of the main emission efficiency. III) It is shown that short wave emission could be partly restored by the sample annealing.

Luminescence decay kinetics reveal some additional for the later separation of EuI2 materials. Monoexponential decay time (400 ns) is typical for the initial and annealed EuI2. In case of mechanical treatment, the Eu2+ emission has non-exponential component (200 and 1000 ns). Peak B emission consists of two parts: rise time and monoexponential (500 ns). It is shown that some energy transfer realization between peaks (centers) take a place in crystals.

Nevertheless the structure of peaks is the subject for additional studies we can conclude that luminescence parameters of EuI2 crystal reflect the difference between initial materials and could be used as criteria for EuI2 raw material selection for scintillator development.

The Effects of Oxygen Vacancies on Luminescence Properties of $Na_3LuSi_3O_9:Ce^{3+}$

Jianbang Zhou[1], Jiuping Zhong[1], Hongbin Liang[1], Qiang Su[1], Jingyuan Guo[2], Qiang Tang[2], Federico Moretti[3], Christophe Dujardin[3]

[1] *State Key Laboratory of Optoelectronic Materials and Technologies, School of Chemistry and Chemical Engineering, Sun Yat-sen University, Guangzhou 510275, China*
[2] *School of Physics, Sun Yat-sen University, Guangzhou 510275, China*
[3] *Institut Lumière Matière, UMR5306 Université Lyon 1 - CNRS, Villeurbanne 69622, France*

In order to study the effects of oxygen vacancies on the luminescence properties of $Na_3LuSi_3O_9:Ce^{3+}$, $Na_3LuSi_3O_9:Ce^{3+}$ phosphors were prepared with a high temperature solid-state reaction method under different atmosphere (air, CO reducing atmosphere and recalcined in air). It was found that the synthesis atmosphere had obvious influence on the diffuse reflectance, photoluminescence and decay curves of $Na_3LuSi_3O_9:Ce^{3+}$. The luminescence intensity and peak position of excitation and emission spectra showed a regular change when the atmosphere changed. UV-visible excitation and emission spectra of $Na_3LuSi_3O_9$: Ce^{3+} samples prepared with different raw materials (CeO_2 and $Ce(NO_3)_3{\cdot}6H_2O$) in air showed that cerium doped in $Na_3LuSi_3O_9$ had strong self-reduction ability. $Na_3Lu_{0.99}Ce_{0.01}Si_3O_9$ prepared in CO and recalcined in air both showed an intensive emission band centered at about 250 nm at 15 K, but this band disappeared when the sample was prepared in air. And it was observed that the decreasing of oxygen vacancies can quicken the photoluminescence decay of $Na_3LuSi_3O_9:Ce^{3+}$. The emission bands of Ce^{3+} and oxygen vacancies were determined under X-ray radiation. At last, the presence of oxygen vacancies was confirmed by thermoluminescence spectra and excitation spectra of Zr^{4+} codoped $Na_3Lu_{0.995}Ce_{0.005}Si_3O_9$. The results showed that $Na_3LuSi_3O_9:Ce^{3+}$ prepared in CO atmosphere showed the highest PL and XEL intensity due to oxygen vacancies' luminescence and the energy transfer from oxygen vacancies to Ce^{3+}. It was proved that the reduction of Ce^{4+} to Ce^{3+} could promote the formation of the oxygen vacancies.

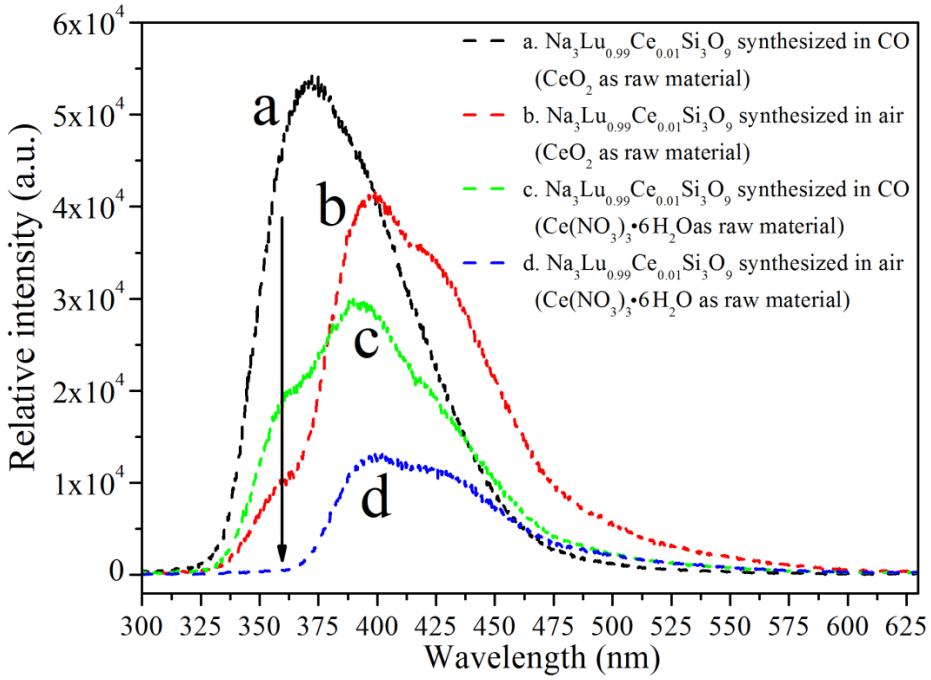

Fig. 1 X-ray excited luminescence spectra of $Na_3Lu_{0.99}Ce_{0.01}Si_3O_9$.

Pressure effect on the structural and electronic properties of $BN_{1-x}As_x$

F. Ali Sahraoui[1], S. Zerroug[1,2] and K. Beldjoudi[1]

[1]*Laboratoire d'Optoélectronique et Composants, Département de Physique,Université Setif 1, Sétif 19000, Algeria.*

[2] *Faculté des sciences de la nature et de la vie, Université Abderrahmane Mira, Bejaia 06000, Algeria*

We have performed a first-principle study of structural and electronic properties of ternary alloy $BN_{1-x}As_x$ (X= 0, 0.03, 0.06) by employing the full potential linearized augmented plane wave (FP-LAPW) method within GGA and mBJ approximations. The calculated equilibrium structural parameters are in excellent agreement with available experimental and theoretical results. The calculated value of fundamental gap using mBJ is very close to the experimental data. The pressure effect and concentration X of As on the structural parameters and energy gaps are also investigated.

Localisation and distribution of the Mn^{2+} dopant ions in nanostructured ZnO films

D. Ghica[1], M. Stefan[1], S. V. Nistor[1], A. V. Maraloiu[1], R. Plugaru[2]

[1] *National Institute of Materials Physics, Magurele-Ilfov, Romania*
[2] *National Institute for R & D in Microtechnologies, Bucharest, Romania*

The magnetic and electrical properties of the nanostructured ZnO films are affected by the non-random impurities distribution due to segregation at grain boundaries, extended defects or interfaces. In order to control these properties it is essential to determine the distribution and localisation of the incorporated impurity ions. We have recently shown [1] that the electron paramagnetic resonance (EPR) spectroscopy provides a simple, statistically relevant and non-destructive method for the quantitative evaluation of the distribution of the paramagnetic impurities in nanostructured films.
We present here the result of EPR and advanced analytical transmission electron microscopy investigations of two ZnO films doped with different Mn concentrations, deposited by the sol-gel technique on Si substrates. The lower concentration of Mn^{2+} in the 0.1 at% Mn doped ZnO film allowed the accurate determination of the Mn^{2+} ions localisation at isolated tetrahedrally coordinated Zn^{2+} sites in both crystalline ZnO nano-grains and surrounding disordered ZnO [2,3], as well as at six-fold coordinated sites in the inter-grain region. In the 5 at% Mn doped ZnO film a much smaller proportion of the Mn^{2+} dopant was found in isolated sites, the main amount being aggregated in a secondary phase as an insular-like distribution between the ZnO nano-grains. Annealing at 600 ^{o}C induced changes in the Mn^{2+} ions distribution, reflecting the increase of the ZnO crystallization degree, better observed in the lightly doped sample. The distribution and localisation of the isolated Mn^{2+} ions in the nano-ZnO films deposited by sol-gel are compared with those evaluated in the case of the nano-ZnO films deposited by magnetron sputtering.

[1] D. Ghica, M. Stefan, C. Ghica, G. E. Stan, *ACS Appl. Mater. Interfaces* ***6***,14231 (2014)
[2] S. V. Nistor, L. C. Nistor, M. Stefan, D. Ghica, Gh. Aldica, J. N. Barascu, *Cryst. Growth Des.* **11**, 5030 (2011)
[3] M. Stefan, S. V. Nistor, D. Ghica, *Cryst. Growth Des*. **13**, 1350 (2013)